Universidad de la República
Programa de Desarrollo de Ciencias Básicas
Area biología
Sub-área Neurociencias

Tesis de doctorado

Estudio de la señalización a través del receptor P2X₇ en astrocitos y motoneuronas: implicancias para la Esclerosis Lateral Amiotrófica.

Mariana Mandi Gandelman

Orientador: Dr. Luis Barbeito
Institut Pasteur Montevideo, Montevideo, Uruguay.

Co-orientador: Joe Beckman, PhD
Linus Pauling Insitute, Oregon State University, Oregon, USA

Índice

Índice de Tablas y figuras

Lista de Abreviaturas

ADP – Adenosín difosfato
AKT – proteína quinasa B
AMP – Adenosín monofosfato
ATP – Adenosín trifosfato
BBG – Azul de coomassie
BzATP – Benzoyl Adenosín trifosfato
COX-2 – ciclo-oxigenasa 2
EAE – Encefalitis autoinmune experimental
ELA – Esclerosis lateral amiotrófica
ELAE - Esclerosis lateral amiotrófica esporádica
ELAF - Esclerosis lateral amiotrófica familiar
E-NTPDasa - difosfohidrolasas de nucleósidos trifosfato extracelular
E-NPP - pirofosfatasa de nucleótidos extracelular
ecto-5'-NT - 5'-nucleotidasa extracelular
ERON - especies reactivas del oxígeno y del nitrógeno
FGF-1 - factor de crecimiento fibroblástico 1
HSP90 – proteína de shock térmico de 90 kilodalton
IL1b – interleukina 1 beta
JNK - quinasas c-Jun N-terminal
LPS – lipopolisacárido bacteriano
MAPK - proteína quinasas activadas por mitógenos
NADPH oxidasa - nicotinamida adenina dinucleótido fosfato-oxidasa
NF-kB – factor nuclear potenciador de las cadenas ligeras kappa de las células B activadas
NMDG+ - N-methyl-d-glucamina
NO – óxido nítrico
NOS – sintasa de óxido nítrico
$O_2^{\bullet-}$- superóxido
ONOO – peroxinitrito
$P2X_7^{-/-}$ - delección del gen que expresa $P2X_7$
SOD1 – superóxido dismutasa tipo 1
$SOD1^{G93A}$ – superóxido dismutasa tipo 1 con mutación glicina a alanina en posición 93

RESUMEN

Las motoneuronas y los astrocitos interactúan íntimamente a nivel morfológico y funcional. Las motoneuronas son la población celular afectada durante la Esclerosis Lateral Amiotrófica (ELA), llevando a una rápida parálisis muscular y defunción del paciente. En respuesta al daño inicial en las motoneuronas los astrocitos disminuyen sus actividades tróficas y surgen nuevas actividades neurotóxicas, contribuyendo a la progresión de la enfermedad. Por lo tanto, el diálogo intercelular entre astrocitos y motoneuronas es un elemento crítico en la expansión y amplificación de la inflamación y muerte celular.

En el sistema nervioso, el Adenosín tri-fostato (ATP) es un neurotransmisor y molécula mensajera extracelular, activando múltiples receptores de membrana en neuronas y células gliales. En respuesta al daño y la inflamación del sistema nervioso los niveles de ATP extracelular aumentan por su fuga desde células necróticas y su liberación regulada a partir de células funcionales. La señalización a través del receptor $P2X_7$ se desregula durante la patología en el sistema nervioso, su expresión aumenta y altos niveles de ATP extracelular causan su activación sostenida. La activación de $P2X_7$ es capaz de promover la respuesta inflamatoria y la muerte en múltiples tipos celulares, sin embargo sus efectos en astrocitos y motoneuronas y las consecuencias para el diálogo entre estos dos tipos celulares no son conocidos.

En él presente trabajo de tesis contribuimos al conocimiento del rol del receptor $P2X_7$ durante la patología en el sistema nervioso, a través del estudio de su activación en astrocitos y motoneuronas espinales aisladas y en modelos animales de ELA.

Encontramos que la activación de $P2X_7$ en astrocitos provocó estrés nitro-oxidativo, determinando su transición a un fenotipo activado. En consecuencia, los astrocitos iniciaron la liberación de un factor (aún no identificado) capaz de inducir muerte de

motoneuronas. En los astrocitos derivados del modelo animal de ELA SOD1^{G93A} encontramos una desregulación basal en la señalización por ATP extracelular, que promueve su proliferación y es responsable de su toxicidad hacia motoneuronas. En motoneuronas encontramos que la activación de P2X$_7$ resulta en la apoptósis y estudiamos los mecanismos y vías implicadas. Encontramos que la activación de P2X$_7$ lleva a la muerte mediante la vía de peroxinitrito/FAS previamente involucrada en la muerte de motoneuronas en modelos animales y pacientes de ELA. Por último, investigamos el potencial de un inhibidor de P2X$_7$ administrado de forma sistémica de retrasar o atenuar la enfermedad en modelos animales de ELA.

Los hallazgos comunicados en la presente tesis constituyen una contribución original al conocimiento del papel del receptor P2X$_7$ en astrocitos, motoneuronas y en el diálogo entre estos dos tipos celulares que contribuye a la patogénesis y progresión de la muerte de motoneuronas en la ELA.

INTRODUCCIÓN

El ATP como molécula de señalización en el sistema nervioso

El ATP es reconocido como la molécula principal del metabolismo energético, sin embargo, en una serie de estudios seminales en los años 70 se demostró que los nucleótidos constituyen moléculas de señalización extracelular. Inicialmente, se describió al ATP como un neurotransmisor en el sistema nervioso autónomo, luego también descubriéndose su rol en fibras motoras y en neuronas del sistema nervioso central (Burnstock 1972; Burnstock 2006). Una acumulación rápida del conocimiento evidenció la complejidad de los efectos de la señalización por nucleótidos extracelulares, también denominada señalización purinérgica y se propuso que múltiples receptores deberían estar implicados. Actualmente sabemos que el ATP, el ADP y la adenosina señalizan a través de los receptores P1 (también conocidos como A) y P2. Ambos son expresados en un gran número de tipos celulares, durante el desarrollo y la vida adulta y controlan procesos fisiológicos complejos con alto nivel de eficiencia. Los receptores P2 son activados principalmente por ATP y los P1 responden a la adenosina. Los receptores a ATP tipo P2 se subclasifican en dos grandes grupos, ionotrópicos P2X y metabotrópicos P2Y (Por una revisión extensa sobre los receptores purinérgicos ver Geoffrey Burnstock, 2014; Volonté, Apolloni, Skaper, & Burnstock, 2012).

Actualmente se conocen 8 receptores de tipo P2Y, caracterizados por estar acoplados a proteína G. Algunos de ellos no son sensibles al ATP, activándose en respuesta a ADP o UDP. Los receptores de tipo P2X son 7 y constituyen canales iónicos permeables a cationes ($Ca^{2+}>Na^{2+}>K^+$). La unión de 3 moléculas de ATP a la porción extracelular del receptor es necesaria para su activación. Los receptores P2X1-7 están formados por tres subunidades proteicas y pueden ser homoméricos o heteroméricos (Nicke *et al.* 1998; Barrera *et al.* 2005; North RA, 2002). La alta heterogeneidad en la familia de receptores P2X se refleja en los variados perfiles

funcionales y farmacológicos; la cinética de activación, inactivación y desactivación es ampliamente variable. En ésta tesis nos focalizaremos en las consecuencias de la activación del subtipo $P2X_7$ ($rP2X_7$).

En el sistema nervioso no sólo las neuronas son capaces de señalizar por ATP extracelular, sino que también se ha encontrado en astrocitos, microglía, oligodendrocitos, células endoteliales y pericitos. La señalización por ATP es capaz de mediar neurotransmisión rápida excitatoria y en neuronas centrales y periféricas (Sperglagh e Iles, 2014). El ATP también es coliberado con otros neurotransmisores como la noradrenalina y el ácido gama aminobutírico (GABA) (Burnstock 2014). En astrocitos, el ATP es el mensajero extracelular responsable de mediar las ondas de calcio, capaces de sincronizar sus acciones y modular la actividad neuronal. Clásicamente, las ondas de calcio se expanden a través de los canales de uniones gap o de hendidura, que conectan células adyacentes. Sin embargo, en los últimos años se ha descubierto que su propagación también es posible entre astrocitos no adyacentes mediante la liberación de ATP al medio extracelular. Su difusión y la activación de receptores purinérgicos resulta en un aumento del calcio intracelular (que es movilizado en respuesta a IP3 del retículo endoplásmico), llevando a la liberación de más ATP. Éste mecanismo amplifica y expande la onda de calcio a través de un sistema de retroalimentación positiva (Guthrie *et al.* 1999). Las ondas de calcio cumplen importantes roles, como ser la regulación de la transmisión sináptica tanto excitatoria como inhibitoria, controlan el flujo sanguíneo cerebral y la tasa respiratoria e influencian los cambios de actividad dependientes del estado, como el sueño o la memoria (Scemes y Giaume 2006).

Aumento del ATP extracelular durante procesos patológicos en el sistema nervioso

Actuando a través de los receptores purinérgicos el ATP cumple importantes roles en la comunicación intercelular durante el funcionamiento normal y durante la patología del sistema nervioso. Durante la inflamación e injuria los niveles de ATP

aumentan y la expresión de receptores es alterada por lo que la señalización por ATP cambia de su típico rol homeostático y es capaz de controlar el ambiente proinflamatorio y proapoptótico (Burnstock 2015; Apolloni *et al.* 2009). Los niveles de ATP extracelular pueden aumentar por su derrame a partir de células necróticas, por su liberación regulada, o por la disminución en su degradación extracelular. La liberación regulada de ATP es ejecutada por exocitosis dependiente de calcio, a través de transportadores ABC (ATP binding cassette), por canales de panexina, hemicanales de conexina, y a través del receptor $P2X_7$ (Kang et al, 2008; Suadicani et al, 2012; Burnstock 2015).

En astrocitos, una de las vías de liberación de ATP son los canales de panexina1 (Suadicani *et al.* 2012). Éstos canales se forman a través de la oligomerización de 6 proteínas transmembrana de Panexina 1 y se caracterizan por ser voltaje dependientes, mecanosensitivos y permeables a moléculas relativamente grandes cómo ser el ATP. Los canales de panexina1 son actualmente reconocidos como el sustrato molecular de funciones previamente adjudicadas a los hemicanales de conexina 43 y del poro de $P2X_7$. Los canales de panexina1 no sólo son conducto para la liberación de ATP, sino que también son modulados por ATP. La apertura del canal puede ser regulada tanto por receptores P2X como P2Y, y su cierre es determinanado por la unión del ATP a la panexina1, estableciendo un mecanismo de control de la concentración de ATP extracelular por feedback negativo. De acuerdo con esto, la concentración de potasio extracelular y de calcio intracelular son capaces de regular la activación y desactivación de los canales de panexina1 (Suadicani *et al.* 2012; Dahl 2015).

Adicionalmente, los astrocitos son capaces de liberar ATP a través de hemicanales de conexina 43, tanto en condiciones fisiológicas como patológicas (Kang et al. 2008; Giaume et al. 2013). La activación de estos canales determina la liberación de ATP, NAD^+, glutatión y prostaglandina E_2 entre otros mediadores de señalización parácrina (Chever *et al.* 2014; Cherian *et al.* 2005; Rana and Dringen 2007; Stout *et al.* 2002; Bruzzone *et al.* 2001). Los hemicanales de conexina 43 son activados

frente a estímulos inflamatorios, demostrando una vía directa por la cuál el ATP podría ser liberado durante la patología (Retamal *et al.* 2015; Bennett *et al.* 2012).

La concentración de ATP extracelular no depende únicamente de la cantidad liberada, sino de un fino balance entre su liberación, recaptación y degradación extracelular. Las células en cultivo ejemplifican este fenómeno de manera simple. La concentración de ATP hace un pico frente al estimulo mecánico determinado por el cambio de medio y posteriormente llega a un valor de reposo dictado por el equilibro entre su liberación e hidrólisis enzimática (Lazarowski *et al.* 2000).

Los astrocitos liberan ATP en respuesta a múltiples estímulos, incluyendo los agonistas de receptores de aminoácidos excitatorios NMDA, AMPA y kainato (Queiroz *et al.* 1997), estímulos mecánicos (Guthrie *et al.* 1999), óxido nítrico (NO) (Bal-Price *et al.* 2002), interferón-gamma (Verderio and Matteoli 2001) y ATP (Anderson *et al.* 2004). La mayoría de estos estímulos causan un aumento del calcio intracelular que lleva a la liberación de ATP. El aumento de calcio multifactorial durante la patología podría entonces disparar la salida de altas concentraciones de ATP observada en estos casos.

En el sistema nervioso se ha visto un gran aumento en el ATP extracelular en la zona de penumbra de una contusión espinal (Fig.1) (Wang *et al.* 2004) y de isquemia aguda (Phillis *et al.* 1993; Melani *et al.* 2005). La inflamación sistémica es capaz de provocar el aumento de ATP extracelular en el cerebro; una inyección intravenosa de lipopolisacárido bacteriano provoca el aumento de ATP en el hipotálamo, donde es capaz de modular la respuesta febril (Gourine *et al.* 2007).
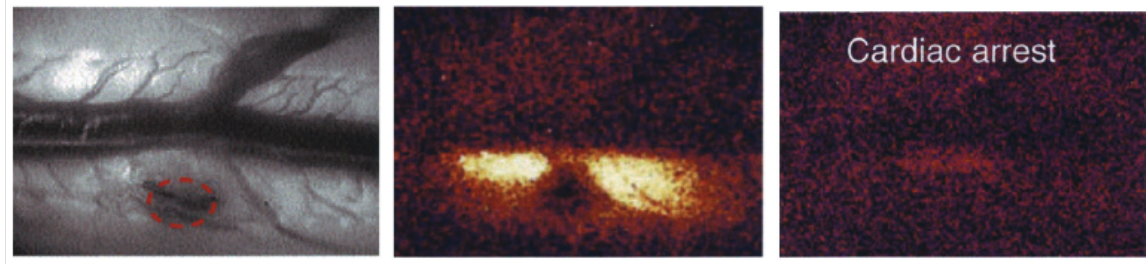
Fig.1. ATP extracelular luego de contusión de médula espinal.
La detección del ATP es posible mediante la cuantificación de la luz emitida por la enzima luciferasa de manera dependiente del ATP. Se observa como 6 horas post-lesión (cuadro izquierdo, círculo rojo) existe un gran incremento en el ATP en el área peri-traumática (cuadro central). La liberación de ATP es un proceso activo mediado por células vitales, ya que la inducción de paro cardíaco en el animal lo detuvo completamente. En la zona directa del trauma no fue encontrada una elevación en el ATP extracelular, probablemente debido a que el registro sólo puedo ser comenzado 10 minutos después de establecida la lesión y la imposibilidad de mantener la producción de ATP en las células necróticas de esta área. Modificado de Wang et al. 2004.

El metabolismo extracelular de ATP y la señalización por ADP y adenosina

La señalización purinérgica es altamente específica, existiendo numerosos niveles de control. Existen mecanismos regulatorios que controlan su liberación, la cantidad, ubicación y tipo de receptores y su degradación y recaptación hacia el interior de la célula. La liberación de ATP al medio extracelular es la etapa crítica para el inicio de la señalización a través de receptores tipo P2X, mientras que su degradación por enzimas extracelulares determina la culminación de este proceso y el inicio de la señalización a través de receptores P2Y específicamente activados por ADP y receptores P1 a adenosina. Las enzimas de degradación extracelular de nucleótidos constituyen un sistema altamente organizado para la regulación de la señalización mediada por nucleótidos, controlando la tasa, cantidad, lugar y momento de degradación nucleotídica y formación de nucleósidos.

En el medio extracelular los nucleótidos son hidrolizados por una batería de enzimas que se encuentran insertadas en la membrana plasmática y que poseen su sitio catalítico hacia el medio extracelular, aunque también se han visto casos donde pueden ser secretadas (Yegutkin *et al.* 2003). Las enzimas de la familias de las E-NTPDasas (ectodifosfohidrolasas de nucleósidos trifosfato, que incluye CD39 y CD39L1) y E-NPP (pirofosfatasa de ectonucleótidos o fosfodiesterasa) son capaces de hidrolizar ATP y ADP produciendo ADP, AMP o adenosina. La ecto-5'-NT (ecto-5'-nucleotidasa, también conocida como CD73) y la fosfatasa alcalina producen adenosina (Yegutkin 2014; Zimmermann *et al.* 1998) . En la figura 1 se esquematiza y resume la función de cada una de éstas enzimas.

Un importante nivel de regulación de los niveles de ATP es determinado por diferencias en la expresión temporal y regional de las enzimas responsables de su hidrólisis. En astrocitos de hipocampo, corteza y fcerebelo se han encontrado importantes diferencias regionales en la tasa de interconversión de los distintos nucleótidos (Wink *et al.* 2003; Wink *et al.* 2006). En el sistema nervioso se ha observado un aumento en la expresión y actividad de ecto-nucleotidasas en episodios de isquemia aguda y luego de una herida cortante en el córtex cerebral (Braun *et al.* 1997; Nedeljkovic *et al.* 2006; Bjelobaba *et al.* 2011).

Un ejemplo de la importancia crítica de la regulación de la degradación del ATP son los gliomas. Las células de estos tumores cerebrales presentan disminuida la capacidad de degradar ATP extracelularmente. Altos niveles de ATP se acumulan en el medio extracelular, estimulando la proliferación de las células transformadas e induciendo la muerte del tejido nervioso circundante, permitiendo la expansión del tumor (Morrone *et al.* 2006; Braganhol *et al.* 2013)

La maquinaria para la liberación, señalización y degradación del ATP son la base para procesos de señalización complejos, requiriendo una combinatoria precisa de eventos. Esto se evidencia en la regulación de la migración de la microglía en respuesta al daño en el sistema nervioso. El ATP y el ADP constituyen potentes

quimiotácticos para la microglía (Honda *et al.* 2001; Davalos *et al.* 2005; Haynes *et al.* 2006). Sin embargo, un trabajo reciente ha mostrado que la degradación del ATP por la ectonucleotidasa CD39 y la señalización simultánea a través de receptores P2 y P1 microgliales son necesarios para inducir la quimiotaxis al sitio de la herida (Färber *et al.* 2008). Éste fenómeno demuestra el importante rol de las ectonucleotidasas en la regulación de la señalización purinérgica.

La adenosina señaliza a través de receptores tipo P1, induciendo una respuesta antiinflamatoria en variados tejidos, por lo que se considera cardioprotectora y neuroprotectora. En casos de isquemia cerebral y epilepsia, la adenosina es capaz de activar astrocitos y microglía de una manera pro-regenerativa y protectora. La adenosina puede ser transportada al interior celular a través de transportadores de nucleósidos o degradada a hipoxantina mediante la acción de enzimas extracelulares, terminado así la cascada de señalización que comenzó en el momento de la liberación de ATP (Daré *et al.* 2007).
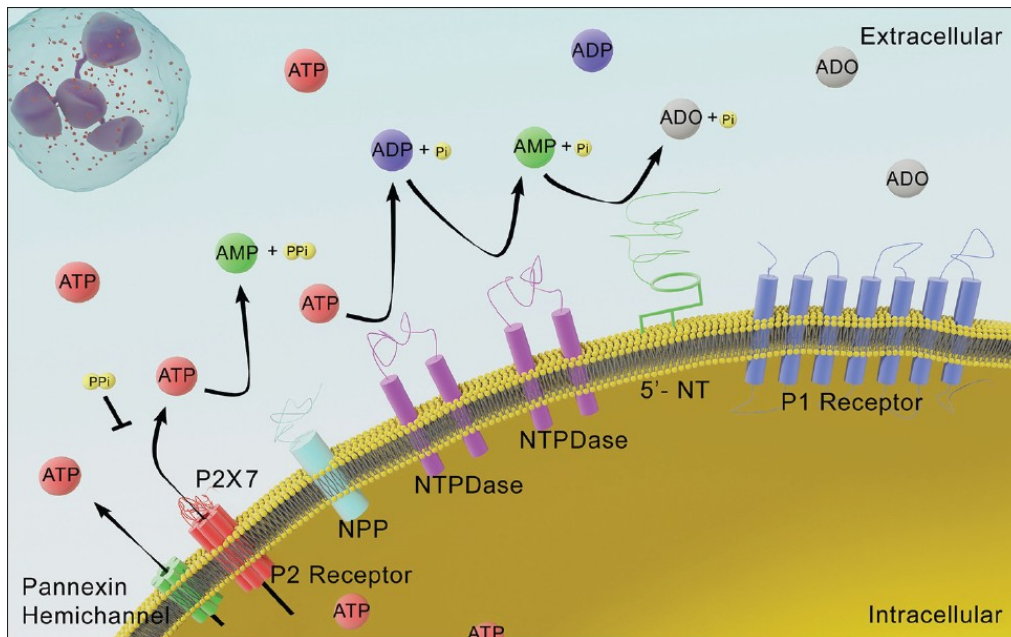
Fig. 2. Metabolismo y señalización extracelular del ATP.

Tanto los canales de panexina, de conexina 43 (no presentes en la figura) como el receptor $P2X_7$ median la liberación de ATP al medio extracelular. El ATP señaliza por los receptores P2 y/o es degradado extracelularmente a ADP y AMP por enzimas de la familia de las E-NTPDasas (ectodifosfohidrolasas de nucleósidos trifosfato, en violeta) o las E-NPP (pirofosfatasa de ectonucleótidos o fosfodiesterasa, en celeste). La ecto-5'-NT (ecto-5'-nucleotidasa (en verde) y la AP (fosfatasa alcalina, no mostrada) catalizan la degradación del nucleótido a adenosina, capaz de señalizar por receptores P1. Figura de (Morandini *et al.* 2014).

El receptor $P2X_7$

Presente en células de linaje hematopoyético así como en astrocitos y neuronas (Fig. 3), el receptor $P2X_7$ es un canal catiónico activado por ATP extracelular que posee múltiples funciones fisiológicas como durante la patología. $P2X_7$ funciona como un trímero, con tres sitios de unión al ATP en la interfase entre las tres subunidades. La unión de al menos 2 moléculas de ATP determina su activación, causando una corriente catiónica entrante, caracterizada por el influjo de calcio y sodio y eflujo de potasio. En comparación con otros receptores purinérgicos el receptor $P2X_7$ no se desensibiliza rápidamente, permitiendo su estimulación persistente y repetitiva. Su activación prolongada o repetida y la ocupación del tercer sitio de unión a ATP determinan una permeabilidad a moléculas de mayor peso molecular (hasta 800kDa) como los fluoróforos catiónicos NMDG+ y Yo-Pro-1+ a través del reclutamiento de los canales de panexina (Geoffrey Burnstock 2014). Éste fenómeno es descrito en mayor profundidad en la página 8. Una vez abiertos, los canales de panexina son capaces de liberar ATP, glutamato e IL1-b al medio extracelular, mediando la señalización intracelular pro-apoptótica que lleva a la muerte celular (Burnstock 2014; Volonté *et al.* 2012). Otro nivel de complejidad y versatilidad en la señalización por $P2X_7$ es agregado por las variantes de éste receptor, originadas por clivaje alternativo de ARN mensajero y polimorfismos de núcleotido simple (Burnstock 2014; Suadicani *et al.* 2012; Dahl 2015).
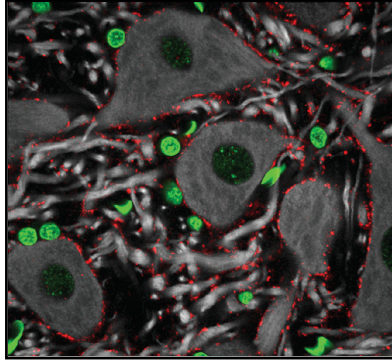
Fig. 3.. Motoneuronas espinales de ratas adultas expresan P2X$_7$. Inmunofluorescencia visualizada con microscopía de dos fotones. Las motoneuronas fueron marcadas con MAP-2 (blanco), P2X7 (rojo) y contratinción con sytox (verde). Modificado de (Wang *et al.* 2004)

La principal función de P2X$_7$ fuera del sistema nervioso es la modulación de la producción de citoquinas durante la respuesta inflamatoria. De hecho, el receptor P2X$_7$ es un importante elemento regulador del inflamasoma, proporcionando el estímulo externo para la modificación post-translacional y siguiente liberación de la citoquina proinflamatoria IL1-b. En el sistema nervioso la activación del receptor P2X$_7$ lleva a la liberación de neurotransmisores, en particular del glutamato, al medio extracelular, tanto en neuronas como en astrocitos, durante el funcionamiento normal y la patología (Kim and Kang 2011; Burnstock 2014).

Los estudios realizados en ratones knockout para P2X$_7$ evidencian su importante rol en la inflamación y en la comunicación extracelular. Estos ratones presentan respuestas inflamatorias deprimidas, causadas por una disminución o desaparición de la liberación de IL1-b y otras citoquinas que resulta en a la activación incompleta de las células inmunes (Solle *et al.* 2001; Labasi *et al.* 2002). En astrocitos de ratones knockout para P2X$_7$ la propagación de ondas de calcio mediadas por ATP, esenciales para la comunicación de redes astrocitarias, se encuentra profundamente disminuida (Suadicani *et al.* 2006).

El rol del receptor P2X$_7$ durante las patologías del sistema nervioso recientemente ha cobrado importancia, y a pesar de que su participación en el aspecto microglial de la neuroinflamación se encuentra ampliamente documentada, sus acciones a

nivel de otras células nerviosas no se conocen en profundidad. En la tabla 1 se resumen los principales hallazgos encontrados hasta el momento que implican al receptor $P2X_7$ en enfermedades del sistema nervioso. El rol de la señalización purinérgica en la ELA se aborda en detalle en la próxima sección. Se ha observado una notable reducción de la activación glial y muerte neuronal mediante la inhibición de receptores P2X durante la isquemia, trauma espinal y cerebral e inflamación y degeneración inducida por la inyección de ATP y LPS in vivo (ver referencias en tabla 1). También se evidenció una disminución en la cicatriz glial y una mejora en el desempeño motor. En modelos de patología aguda la neuroprotección por inhibidores de $P2X_7$ ha resultado exitosa. En modelos de enfermedades neurodegenerativas donde existe un proceso degenerativo e inflamatorio sostenido en el tiempo aún no existe un consenso sobre los resultados de esta estrategia. Sin embargo, recientemente Matute y colaboradores (2007) mostraron en un modelo animal de encefalomielitis autoinmune experimental que la inhibición del receptor $P2X_7$ durante 20 días lleva a una notable mejoría en los parámetros motores, asociado a niveles sorprendentemente disminuidos de demielinización (Ver Tabla 1).

Enfermedad	Rol del receptor P2X$_7$	Referencias
Neurodegeneración crónica		
Enfermedad de Alzheimer	P2X$_7$ media la activación proinflamatoria de la microglía en varios modelos de Enfermedad de Alzheimer	Parvathenani et al. 2003; Ryu and McLarnon 2008; Delarasse et al. 2011;
	P2X$_7$ bloquea la actividad de la α-secretasa/Estimula la activación de la α-secretasa	León-Otegui et al. 2011;
	Inhibición de P2X$_7$ in vivo reduce las placas amiloides	Díaz-Hernández et al. 2009
	Aumento en la expresión de P2X$_7$ en la microglía del córtex cerebral en un modelo animal de Enfermedad de Alzheimer	Lee et al. 2011
Enfermedad de Parkinson	La activación de P2X$_7$ media la necrosis de las células dopaminérgicas SN4741	Jun et al. 2007
	La expresión de P2X$_7$ en astrocitos se encuentra aumentada en el modelo de rotenona	Gao et al. 2011
Enfermedad de Huntington	Antagonistas de P2X$_7$ previenen la muerte neuronal en modelos animales	Díaz-Hernández et al. 2009
Esclerosis múltiple	Los ratones P2X$_7^{-/-}$ son suceptibles al daño en el modelo de Encefalitis autoinmune experimental (EAE)	Chen and Brosnan 2006; Witting et al. 2006
	P2X$_7$ media el daño excitotóxico a los oligodendrocitos y su inhibición alivia el daño neurológico en el modelo de EAE	Matute et al. 2007; Domercq et al. 2010
	Variantes con ganancia de función de P2X$_7$ identificadas en la Esclerosis múltiple	Oyanguren-Desez et al. 2011
Insultos agudos		

Epilepsia	Aumento de la señalización purinérgica en status epiléptico	Avignone et al. 2008
	Los ratones $P2X_7^{-/-}$ y el silenciamiento de la expresión de panexina1 aumentan la suceptibilidad a las convulsiones evocadas por pilocarpina	Kim and Kang 2011; Santiago et al. 2011
	Los antagonistas de $P2X_7$ y el silenciamiento de panexina1 bloquean la inducción de status epiléptico por ácido kaínico	Engel et al. 2012
	Antagonistas de $P2X_7$ previenen la apoptosis de los astrocitos en status epiléptico	Kim et al. 2009
Isquemia	La expresión de $P2X_7$ se encuentra elevada en microglía yneuronas de diferentes modelos in vivo e in vitro	F Cavaliere, Dinkel, and Reymann 2005; Fabio Cavaliere et al. 2004; Franke et al. 2004
	Antagonistas de $P2X_7$ reducen el tamaño del infarto y el daño a las neuronas luego de una isquemia focal transitoria	Le Feuvre et al. 2003; Melani et al. 2005; Arbeloa et al. 2012
	El bloqueo de $P2X_7$ disminuye el daño a oligodendrocitos y a los axones luego de isquemia en la materia blanca	Domercq et al. 2010
Trauma	Inhibición de $P2X_7$ mejora la recuperación luego de una injuria en la médula espinal	Wang et al. 2004; Peng et al. 2009

Tabla 1. Principales evidencias de la participación del receptor $P2X_7$ en la neurodegeneración crónica e insultos agudos en el sistema nervioso.

El daño nitro-oxidativo y su inducción por la activación del receptor P2X$_7$.

Anteriormente considerado una consecuencia inespecífica de las etapas tardías de las enfermedades, ahora sabemos que el daño oxidativo es una característica temprana y común de numerosas enfermedades degenerativas, incluyendo la ELA, la enfermedad de Alzheimer y enfermedad de Parkinson. El daño por radicales libres se inicia tempranamente y es acumulativo, por lo que contribuye a la cascada de eventos que desatan la enfermedad luego de años en latencia. El daño a las proteínas, ADN y lípidos contribuye a la agregación de proteínas, alteraciones metabólicas e inflamación características de las enfermedades degenerativas (Pacher *et al.* 2007; Beckman 2002)

El daño nitro-oxidativo es ejecutado por las especies reactivas del oxígeno y del nitrógeno (ERONs), moléculas que poseen un electrón desapareado y por lo tanto son altamente reactivas. Todas las células normalmente producen el radical superóxido (O2•-) y el NO, que no son intrínsecamente dañinos. En macrófagos y neutrófilos son cruciales para luchar contra bacterias y virus. Adicionalmente, el NO es una importante molécula de señalización implicada en el funcionamiento fisiológico del organismo (Ignarro *et al.* 1987b; Ignarro *et al.* 1987a). Sin embargo, en células dónde los sistemas de detoxificación de ERONs se encuentran saturados, por una disminución en su producción o por un aumento en los ERONs, sobreviene el daño molecular.

Las mismas concentraciones de NO relevantes para la señalización celular también pueden iniciar y amplificar el daño oxidativo a través de su reacción con el superóxido, produciendo peroxinitrito (ONOO-) (Beckman *et al.* 1990). Las motoneuronas son un claro ejemplo de este fenómeno. Nuestro laboratorio ha mostrado que el NO en concentraciones fisiológicas promueve la supervivencia de motoneuronas, sin embargo las mismas concentraciones causan su muerte en condiciones patológicas que estimulan la producción de superóxido en

motoneuronas o astrocitos y por lo tanto resultan en la formación de peroxinitrito (Estevez et al, 1998).

El superóxido es mantenido a niveles extremadamente bajos en las células a través de la actividad de la enzima SOD, que cataliza su conversión a oxígeno y peróxido de hidrógeno con una alta eficiencia. Aumentos simultáneos en tiempo y espacio de superóxido y NO son la base para la rápida formación del peroxinitrito. En los astrocitos, posibles fuentes de superóxido podrían incluir los productos de reacción de la enzima NADPH oxidasa, la xantina oxidasa y la NOS desacoplada, metales de transición, el retículo endoplásmico a través del sistema citocromo p450 y el núcleo y la mitocondria a través de la cadena de transporte electrónico. El óxido nítrico es producido por varios subtipos de óxido nítrico sintasas, incluyendo la neuronal, endotelial y la forma inducible (Pacher *et al.* 2007).

El peroxinitrito es capaz de oxidar moléculas biológicas, incluyendo lípidos, ADN y proteínas. Los radicales derivados de estas reacciones son altamente reactivos y modifican tirosinas, formando nitrotirosina, que es capaz de modificar drásticamente la función y estructura de las moléculas, ejerciendo así sus acciones citotóxicas (Ischiropoulos *et al.* 1992; Beckman *et al.* 1994). En la figura 2 se esquematiza el proceso de formación del peroxinirito y sus consecuencias.

La generación de especies reactivas del oxígeno y nitrógeno (ERONs) por la activación de $P2X_7$ se encuentra ampliamente documentada en macrófagos y microglía (Suh *et al.* 2001; Cruz *et al.* 2006). La activación de NADPH oxidasa es el principal responsable, aunque evidencias recientes señalan que la mitocondria también podría ser fuente de ERONs (Moore et al, 2009). En astrocitos se ha visto que el ATP extracelular es capaz de activar la enzima NADPH oxidasa, sin embargo, se desconoce si el receptor $P2X_7$ se encuentra implicado (Abramov *et al.* 2005). En microglía aislada del modelo animal de ELA $SOD1^{G93A}$, la actividad NADPH oxidasa se encuentra basalmente aumentada y la estimulación del receptor $P2X_7$ lleva a un gran aumento de su actividad y consecuente producción superóxido, en

comparación con la microglía no transgénica dónde el aumento es limitado (Apolloni *et al.* 2013b). De acuerdo con esto, recientemente se ha descrito que la enzima SOD1 es capaz de inactivar a la NADPH oxidasa cuando el ambiente celular es oxidante, regulando la producción de ERONs. Sin embargo la SOD1 mutada pierde su capacidad de inactivar a la NADPH oxidasa de manera que esta enzima continúa produciendo superóxido (Harraz et al., 2008).
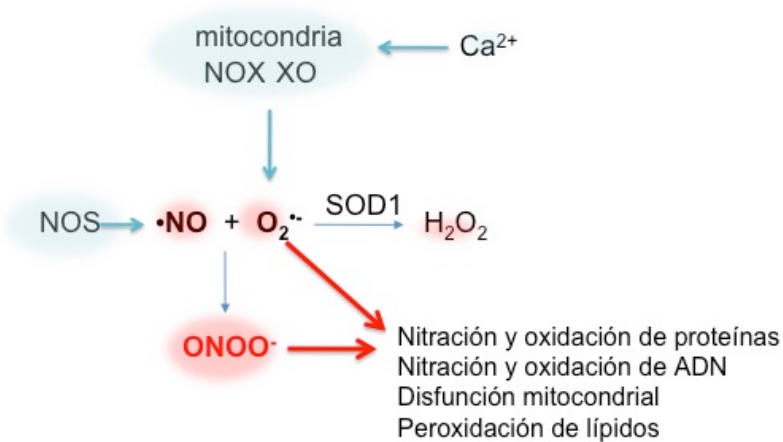
Fig. 4. Interacción y reacciones del NO, O$_2$$^{\bullet-}$, peroxinitrito (ONOO$^-$). Cuando el superóxido y el óxido nítrico se encuentran presentes simultáneamente en tiempo y espacio pueden reaccionar formando peroxinitrito. Tanto el superóxido como el peroxinitrito son capaces de causar daño nitro-oxidativo, alterando proteínas, lípidos y ADN. Modificado de (Pacher et al., 2007).

La Esclerosis Lateral Amiotrófica

La ELA, también conocida como enfermedad de Lou Gehrig, es una enfermedad neurodegenerativa que lleva a la muerte del paciente entre los 3 a 5 años del diagnóstico inicial. Se caracteriza por la muerte selectiva de las motoneuronas de la corteza motora, tronco cerebral y médula espinal, por lo que el paciente muestra síntomas progresivos de espasticidad, hiperreflexia, debilidad y parálisis muscular. En gran parte de los pacientes de ELA, el fallecimiento es causado por parálisis diafragmática. A pesar de grades avances en el conocimiento, la etiología de la ELA

es aún desconocida. Sin embargo se plantean numerosas hipótesis que involucran al estrés oxidativo, excitotoxicidad, disfunción mitocondrial, anormalidades del citoesqueleto, mal plegamiento y agregación de proteínas, autoinmunidad, alteración del soporte trófico y exposición a tóxicos ambientales (Rowland and Shneider 2001; Mancuso and Navarro 2015).

La enfermedad se presenta en su forma esporádica (ELAE) o familiar (ELAF). En la primera, que comprende el 90% de los casos, no existe un componente genético hereditario conocido. En la forma familiar el 10% de los pacientes presentan mutaciones en la enzima SOD1 (Rosen *et al.* 1993). El descubrimiento de mutaciones en la enzima SOD1 y las pronunciadas similitudes patológicas y clínicas entre pacientes con ELAE y ELAF han permitido la generación de animales transgénicos como modelo de la enfermedad (Rosen *et al.* 1993; Gurney *et al.* 1994). Nuestro laboratorio cuenta con colonias de ratas y ratones que sobre-expresan la SOD1 humana mutada (SOD1G93A). Estos animales desarrollan una enfermedad de impactante similitud a la ELAF. La enfermedad se manifiesta alrededor de los tres meses de vida mediante debilidad muscular y progresa a lo largo de un mes, cuando los animales alcanzan la muerte clínica (Rosen *et al.* 1993; Gurney *et al.* 1994).

El descubrimiento de las mutaciones en la SOD1 inmediatamente implicó al estrés oxidativo en la etiología de la ELA. Debido a que el knockout completo del gen que codifica para la SOD1 no produce una enfermedad de las motoneuronas, se postula que su toxicidad no se debería a la pérdida de actividad dismutasa sino a la ganancia de una nueva actividad tóxica (Beckman *et al.* 1993; Reaume *et al.* 1996). Un ejemplo de éste fenómeno es la aparición de anomalías en la interacción de la SOD1G93A con la enzima NADPH oxidasa, resultado en el aumento en los niveles de superóxido, como se detalló en la página 21. De acuerdo con ésto, se observa una elevada inmunorreactividad para nitrotirosina en las médulas espinales de modelos animales y pacientes de ELA (Beal *et al.* 1997; Ferrante *et al.* 1997; Abe *et al.* 1995).

El rol de las células no neuronales y la inflamación en la ELA

24

En pacientes y modelos animales de ELA se observa una pronunciada gliosis reactiva rodeando a las motoneuronas en degeneración. La activación de los astrocitos fue considerada tradicionalmente como una respuesta inespecífica al daño en el tejido nervioso, por ser un rasgo común de numerosas condiciones patológicas. Sin embargo, actualmente se reconoce que la activación de los astrocitos es un fenómeno multifacético que cumple un papel activo y protagónico en múltiples patologías, incluyendo la ELA (Phatnani and Maniatis 2015; Vargas and Johnson 2010). La combinación de las actividades tróficas y/o pro-inflamatorias de los astrocitos activados son altamente dependientes del ambiente y eventos de señalización extracelular a los que se encuentran expuestos, y por lo tanto altamente susceptibles a cambios en la microglía, neuronas, oligodendrocitos, células endoteliales e inmunes. Los principales hallazgos en la alteración del diálogo entre las células gliales y las motoneuronas en la ELA se resumen en la figura 5.

La activación de los astrocitos determina profundas alteraciones funcionales en el sistema nervioso. Los astrocitos activados son altamente proliferativos, exhiben alteraciones morfológicas y expresión génica diferencial (Barbeito *et al.* 2004). Ésto puede resultar en actividades beneficiosas para el tejido, como ser el aislamiento de la zona afectada del tejido sano circundante y la producción de factores proregenerativos. En contraste, en la mayoría de las enfermedades neurodegenerativas donde existe una activación crónica, progresiva y compleja sus actividades proinflamatorias aumentan y las restauradoras se ven reducidas. En consecuencia, el transporte de glutamato perisináptico se alteraría, la barrera hematoencefálica perdería su continuidad y la microglía y células T serían reclutadas a la región, entre otros (Philips and Robberecht 2011; Vargas and Johnson 2010). La movilización de residuos celulares hacia las zonas perivasculares para facilitar su salida del tejido nervioso se enlentece, por la pérdida de eficiencia del sistema glinfático, propiciando la acumulación de proteínas dañadas (Xie *et al.* 2013; Nedergaard 2013). Específicamente, los astrocitos regulan el volúmen del espacio intersticial a través de sus poros de Aquaporina, regulando así el tránsito

extracelular hacia la zona perivascular. Éste nuevo sistema ha sido descubierto en los últimos 5 años, y su potencial relevancia en la fisiología normal y la patología del sistema lo convierten en uno de los principales roles de los astrocitos descritos hasta el momento.

En los últimos años se ha acumulado amplia evidencia que argumenta a favor de un rol de las células no neuronales en la muerte de motoneuronas en la ELA, principalmente mediante la creación de ratones transgénicos que expresan la SOD1 mutada selectivamente en los distintos tipos celulares. Los ratones que expresan la SOD1 mutada únicamente en motoneuronas o únicamente en astrocitos no desarrollan la enfermedad, indicando que la interacción entre estos dos tipos celulares es crucial para el establecimiento de la enfermedad (Gong *et al.* 2000; Pramatarova *et al.* 2001; Lino *et al.* 2002; Yamanaka *et al.* 2008a). La expresión de SOD1 mutada en las motoneuronas tendría un rol disparador de la enfermedad, ya que un decremento específico en su expresión en motoneuronas es capaz de postergar el inicio pero no logra enlentecer el progreso (Miller *et al.* 2005; Ralph *et al.* 2005). Los astrocitos y la microglía activada en respuesta a la degeneración de neuronas tendrían un rol determinante en la progresión de la enfermedad, amplificando y profundizando el daño. Una reducción en los niveles de expresión de SOD1 mutada en microglía o en astrocitos es capaz de enlentecer la progresión de la enfermedad, sin embargo el inicio permanece incambiado (Yamanaka *et al.* 2008b).

En la ELA, la actividad tóxica de los astrocitos podría ejercer un efecto de selección sobre las motoneuronas dañadas, llevando a las más vulnerables a la apoptosis. Los mecanismos específicos por los cuáles los astrocitos son capaces de inducir la muerte de motoneuronas no son conocidos. La reducción de la expresión de transportadores de glutamato, incremento en su producción de radicales libres y citoquinas pro-inflamatorias, la depleción de antioxidantes y disfunción mitocondrial se postulan como algunos de los mecanismos por los cuales los astrocitos podrían modular la supervivencia de las motoneuronas en la ELA

(Howland *et al.* 2002; Cassina *et al.* 2008; Yamanaka *et al.* 2008b; Vargas and Johnson 2010).

Nuestro grupo de investigación ha establecido modelos de co-cultivos de astrocitos y motoneuronas que permiten evaluar su interacción. La previa activación de los astrocitos con lipopolisacárido bacteriano, FGF-1 (factor de crecimiento fibroblástico-1) o peroxinitrito determina una reducción en el número de motoneuronas sobrevivientes (Cassina *et al.* 2002; Pehar *et al.* 2004; Cassina *et al.* 2005). A su vez, nuestro laboratorio ha mostrado que los astrocitos SOD1G93A en condiciones basales presentan un fenotipo que determina la muerte de motoneuronas (Vargas *et al.* 2006). La producción de uno o más factor difusibles aún no caracterizados serían los responsables (Hedlund and Isacson 2008; Nagai *et al.* 2007). La mutación en la SOD1 determina que los astrocitos adquieran un fenotipo inflamatorio, pero múltiples mecanismos, dependientes o no de la SOD1 mutada podrían coexistir. Esto se evidencia en el hecho de que los astrocitos aislados de pacientes afectados por ELA esporádica, que no producen SOD1 mutada, también son capaces de determinar la muerte de las motoneuronas en cocultivo (Re *et al.* 2014).

En modelos animales y en pacientes de ELA se han encontrado cambios en la expresión de mediadores proinflamatorios así como antiinflamatorios (Henkel *et al.* 2009; Meissner *et al.* 2010; Beers *et al.* 2011; Peters *et al.* 2015). A pesar de que los astrocitos no son células del sistema inmune también contribuyen a la respuesta inflamatoria nerviosa. De hecho, los astrocitos derivados de pacientes con ELAE o ELAF un incremento en la expresión de 22 factores del complemento, quimioquinas y citoquinas. Los niveles de NO aumentan, NF-kB es activada, así como las vías de MAPK, JNK y AKT (Haidet-Phillips *et al.* 2011). La tabla 1 detalla los principales fármacos que han sido ensayados en modelos animales y en pacientes de ELA cuya principal función es la modulación de la inflamación. A pesar de que varios fármacos mostraron resultados alentadores en modelos animales de ELA, éstos resultados no han podido ser trasladados a pacientes con ELA. Sin embargo, esto no refleja

necesariamente su falta de potencial en la ELA, sino que muestra la dificultad en la translación de terapias del laboratorio hacia los pacientes. La gran heterogeneidad de la enfermedad en humanos, su diagnóstico tardío y la subdosificación de fármacos son las principales barreras para la experimentación en pacientes.
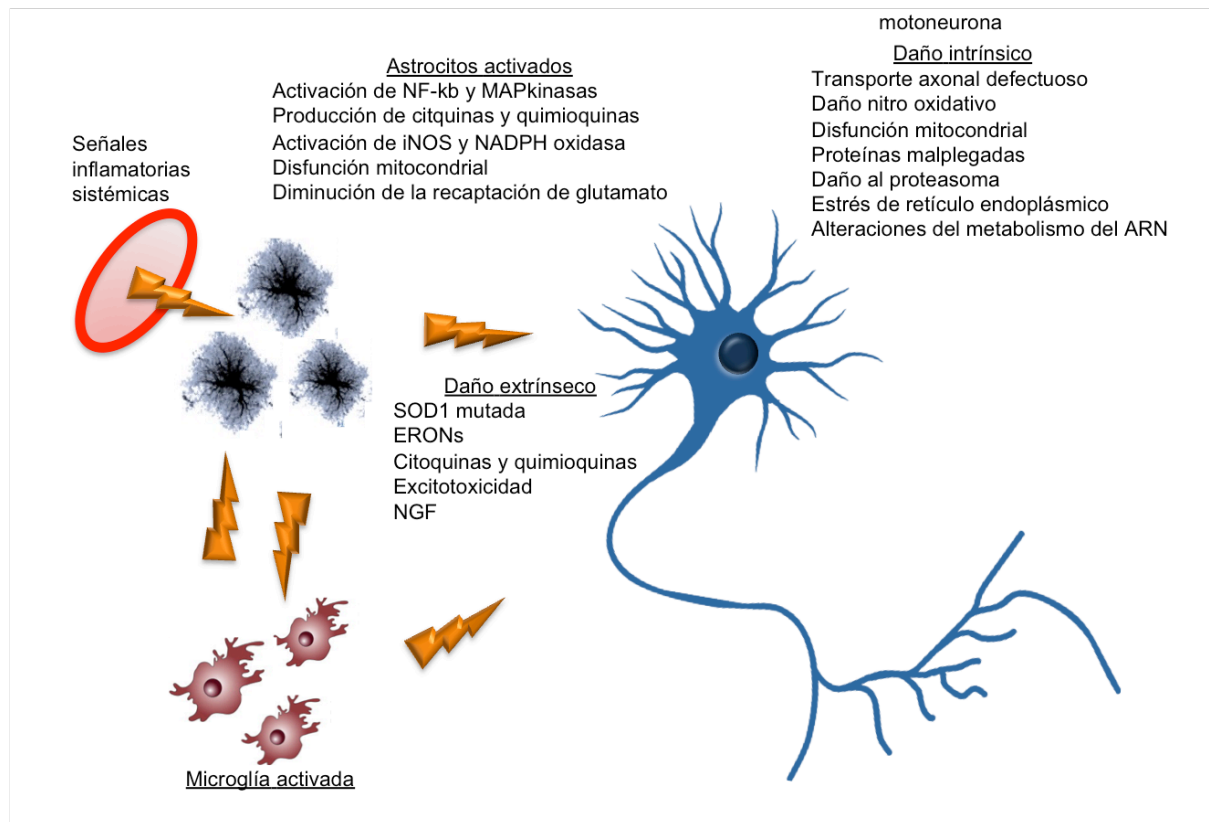
Fig. 5. Alteraciones en la interacción entre las células gliales y las motoneuronas en la ELA. Las motoneuronas de pacientes y modelos animales de ELA manifiestan daño intrínseco en múltiples niveles. Ésto determina una alteración de su interacción con la glia circundante, resultando en su activación. Los astrocitos y la microglía activados causan daño extrínseco a las motoneuronas, amplificando y expandendo el proceso patológico.

Fármaco	Función	Resultados
Minociclina	Reduce la habilidad de las células T de contactar la microglía. Previene la activación proinflamatoria de la microglía.	Protección en modelos animales. Avanzó a experimentación en humanos con resultados perjudiciales.
Taliomida y lanaliomide	Modulan la producción de citoquinas proinflamatorias	Protección en modelos animales. Taliomida avanzó a experimentación en humanos. No mostró beneficios.
Celecoxib	Antiinflamatorio no esteroideo Inhibidor de COX-2, reduce la produccion de prostaglandinas inflamatorias	Protección en modelos animales. Avanzó a experimentación en humanos. No mostró beneficios.
Rofecoxib y creatinina	Rofecoxib es un antiinflamatorio no esteroideo Inhibidor de COX-2. Creatinina ayuda a mitigar sus efectos secundarios.	Protección en modelos animales.
sulindac	Antiinflamatorio no esteroideo inhibidor de COX2	Protección en modelos animales.
pioglitazone	Antiinflamatorio agonista de PPAR-G utilizado en diabéticos.	Protección en modelos animales. Avanzó a experimentación en humanos. No mostró beneficios.

Tabla 2. Fármacos antiiflamatorios ensayados en modelos animales y en pacientes de ELA. A pesar de que múltiples fármacos han mostrado efectos beneficiosos en modelos animales, éstos no han podido ser trasladados con éxito a pacientes con ELA. Para una revisión en este tema, ver Rizzo et al. 2014.

La señalización por ATP en la ELA

Dadas las características patológicas de la ELA, que incluyen excitotoxicidad, inflamación, estrés oxidativo y disfunción mitocondrial entre otros, varios grupos de investigación se han avocado a estudiar el posible rol de la señalización purinérgica y el receptor $P2X_7$ en ésta enfermedad. La tabla 3 detalla los hallazgos hasta el día de

hoy, incluyendo los descritos en esta tesis. Estudios in vitro indican que en la ELA la señalización a través de $P2X_7$ en astrocitos y microglía lleva a su activación proinflamatoria y a un aumento en la producción de ERONs que contribuyen a la muerte de las motoneuronas. Estudios in vivo en modelos animales y en pacientes de ELA muestran que la señalización purinérgica estaría disregulada en varios niveles, ya que se han encontrado alteraciones tanto en la expresión de los receptores como en las enzimas de degradación, a nivel central y periférico. La inactivación sistémica de $P2X_7$ en modelos animales ya sea por ablación genética o inhibición farmacológica ha mostrado resultados altamente reveladores. La ablación completa es perjudicial, mientras que la inhibición farmacológica iniciada luego del comienzo de síntomas sería protectora. Éstos resultados involucran al receptor $P2X_7$ en la modulación de la respuesta inflamatoria, posiblemente primero generando respuestas adaptativas y protectoras, y luego de que la enfermedad progresa contribuyendo a la expansión y profundización del daño (Ver en tabla 3).

Año	Hallazgo	Referencias
2006	La expresión de $P2X_7$ se encuentra aumentada en la microglía de pacientes de ELA	Yiangou et al. 2006
2007-8	Aumento en la inmunorreactividad para el receptor $P2X_7$ en motoneuronas en degeneración de animales $SOD1^{G93A}$	Casanovas et al. 2008
2009	Activación de $P2X_7$ en microglía induce la muerte de líneas celulares neuronales	D'Ambrosi et al. 2009
2010	Activación de $P2X_7$ en astrocitos espinales lleva a la muerte de las motoneuronas espinales.	Gandelman et al. 2010
2013	Delección de $P2X_7$ en ratones $SOD1^{G93A}$ aumenta la gliosis y muerte de motoneuronas.	Apolloni, Amadio, et al. 2013

2013	Activación de P2X$_7$ en microglía SOD1^{G93A} aumenta la expresión de miRNA proinflamatorios	Parisi et al. 2013
2013	Activación de P2X$_7$ en motoneuronas espinales lleva a la apoptosis a través de la vía de FAS.	Gandelman et al. 2013
2014	Administración de BBG a animales SOD1^{G93A} iniciada poco antes de los primeros síntomas redujo marcadores inflamatorios y retrasó la muerte de las motoneuronas, resultando en el inicio tardío de síntomas motores sin extender la sobrevida.	Apolloni et al. 2014
2015	En pacientes de ELA la expresión de CD39, enzima que hidroliza ATP, se encuentra disminuída.	Butovsky et al. 2015

Tabla 3. Estado actual del conocimiento del rol de la señalización purinérgica en la ELA.

HIPÓTESIS

Durante los procesos inflamatorios y degenerativos en el sistema nervioso el ATP se libera al medio extracelular por su fuga desde células necróticas y por su liberación altamente regulada a partir de células gliales y neuronas. En estos casos, la señalización por ATP extracelular cambia su típico rol homeostático y se convierte en amplificador de señales proinflamatorias y proapotóticas, principalmente a través del receptor $P2X_7$. De acuerdo con esto, la inhibición sistémica o focal de los receptores de ATP resulta en neuroprotección en varios modelos de enfermedades o injuria del sistema nervioso. En los últimos años se ha revelado la importancia de la señalización por ATP en el sistema nervioso durante la enfermedad, sin embargo los efectos específicos a nivel celular son poco conocidos. En el presente trabajo planteamos que la señalización por ATP a través del receptor $P2X_7$ extiende y amplifica la respuesta inflamatoria glial e induce estrés nitro-oxidativo, causando la pérdida de su típico soporte trófico que ofrecen a las motoneuronas circundantes. A su vez, planteamos que la activación del receptor $P2X_7$ en motoneuronas podría determinar su muerte directamente. Por último, proponemos que en el modelo animal de ELA $SOD1^{G93A}$ la inhibición de $P2X_7$ podría alterar el curso de la enfermedad, retrasando su comienzo o enlenteciendo su progresión. Los hallazgos incluídos en esta tesis constituirán un aporte al conocimiento del rol del ATP durante la enfermedad en el sistema nervioso, con especial importancia para las patologías caracterizadas por la activación de astrocitos y la muerte de motoneuronas como la ELA.

OBJETIVOS

1 – Investigar si la activación de la vía de ATP/P2X$_7$ en astrocitos aislados de médulas espinales causa estrés nitro-oxidativo y una alteración en su interacción con las motoneuronas circundantes que pueda llevar a su muerte.

2 - Estudiar el rol del receptor P2X$_7$ en astrocitos aislados del modelo animal de ELA SOD1^{G93A} en su comportamiento neurotóxico para motoneuronas.

3 – Determinar si la señalización a través de la vía de ATP/P2X7 es capaz de afectar a las motoneuronas directamente. Se estudiarán en forma detallada las vías activadas por P2X$_7$.

4 – Evaluar la capacidad del inhibidor de P2X$_7$ BBG administrado de manera sistémica de prevenir o enlentecer la enfermedad en el modelo animal de ELA SOD1^{G93A}.

Abordaje metodológico

Objetivo 1

Se utilizaron los protocolos descritos en Gandelman et al 2010 y Gandelman et al 2013. Para este objetivo se utilizaron cultivos primarios de astrocitos aislados de médulas espinales de ratas neonatas. Los astrocitos fueron incubados con ATP, agonistas y antagonistas de P2X$_7$. Los astrocitos tratados fueron lavados exhaustivamente y sobre ellos se sembraron motoneuronas aisladas de médulas espinales de embriones de rata. La supervivencia neuronal evaluada luego de 48 horas de cocultivo es indicativa del soporte trófico o de las acciones neurotóxicas de los astrocitos. Utilizando este modelo también se estudió mediante intervención farmacológica las vías y mecanismos implicados en la transformación del fenotipo

astrocitario de trófico a neurotóxico. En la figura 6 se observan los modelos celulares utilizados para estos experimentos. Los protocolos utilizados para la evaluación de las actividades astrocitarias que impactan la sobrevida de las motoneuronas se detallan en la figura 7.
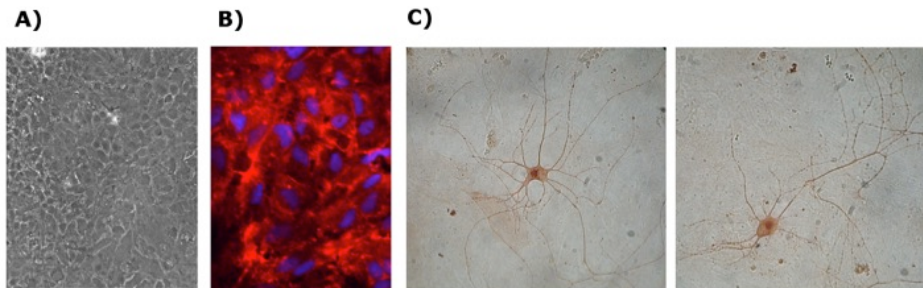
Fig. 6. Cultivos celulares utilizados para el desarrollo del objetivo 1. (A) monocapa confluente de astrocitos primarios de médulas espinales de ratas neonatas observados con microscopía de contraste de fases (1cm=40μm) y (B) inmunofluorescencia para P2X$_7$ (1cm=10μm) (C) Motoneuronas espinales embrionarias de ratas cultivadas sobre una monocapa de astrocitos espinales, visualizadas mediante inmunocitoquímica para el receptor p75 (1cm=40μm).
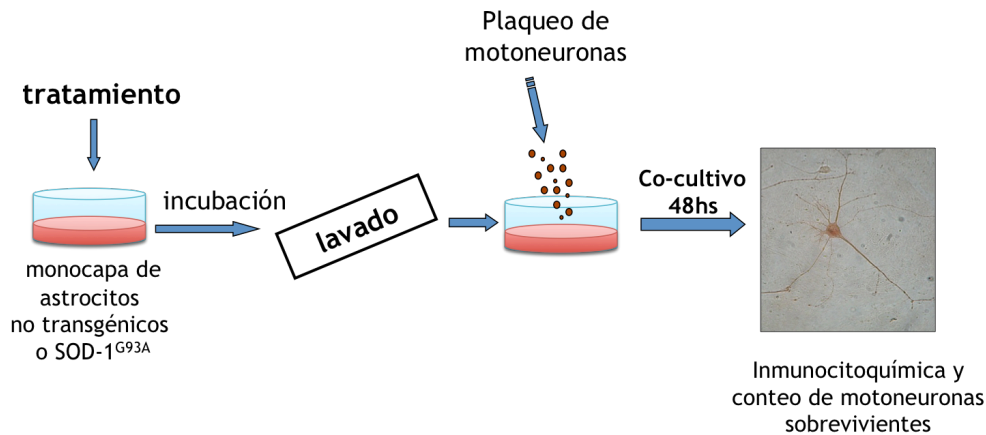
Fig. 7. Protocolo para la evaluación de las consecuencias de la actividad astrocitaria para motoneuronas. Los astrocitos fueron expuestos a diversos pre-tratamientos, éstos fueron eliminados completamente mediante el lavado y cambio de medio y motoneuronas fueron sembradas sobre los astrocitos, estableciendo cocultivos. Su sobrevida fue evaluada luego de 48 horas de cocultivo mediante inmunicitoquímica para el receptor p75, expresado en motoneuronas.

Objetivo 2

Se establecieron cultivos primarios de astrocitos a partir de médulas espinales de ratas neonatas que portan la mutación SOD1^{G93A} y que desarrollan una enfermedad similar a la ELA en humanos. Con un abordaje farmacológico se estudió si estos astrocitos presentan una desregulación basal de la señalización por ATP extracelular y cómo impacta su interacción con las motoneuronas.

Objetivo 3

Para el estudio del tercer objetivo se establecieron cultivos de motoneuronas aisladas de médulas espinales de embriones de rata y se evaluó su sobrevida luego de 48 horas. Se utilizaron los protocolos descritos en Gandelman et al 2010 y Gandelman et al 2013. La participación del receptor P2X$_7$ y los mecanismos por los

cuales las motoneuronas mueren luego de su activación se estudió mediante un abordaje farmacológico.

Objetivo 4

El inhibidor de P2X$_7$ BBG fue administrado en el agua de beber a ratas SOD1^{G93A} a partir de los 60 días de nacidas, cuando todavía no han desarrollado síntomas de la enfermedad. El inhibidor se administró hasta que las ratas se consideraron que se encontraban en las etapas terminales de la enfermedad y fueron sacrificadas, alrededor de los 133 días. Un grupo control de ratas al que no se le realizó ninguna adición a su agua de beber fue analizado en paralelo. La figura 8 muestran el aspecto típico de una rata SOD1^{G93A} sana (A) y en las etapas finales de la enfermedad (B), evidenciando la parálisis muscular de los miembros posteriores que no le permite incorporarse. Para determinar si el tratamiento es capaz de alterar la enfermedad las ratas fueron monitoreadas por 4 meses. Su peso fue registrado 3 veces por semana y su habilidad motora y resistencia fue evaluada con un test de Rotarod. Éste test evidencia pérdidas sutiles en la coordinación motora y balance típicas de las etapas iniciales de la enfermedad. Durante este test las ratas deben caminar sobre un cilindro que rota a una velocidad constante durante 3 minutos. Las ratas con deficiencias motoras no son capaces de completar este test y caen del cilindro antes de los 3 minutos. En la figura 8C se observan tres animales durante el test de rotarod.
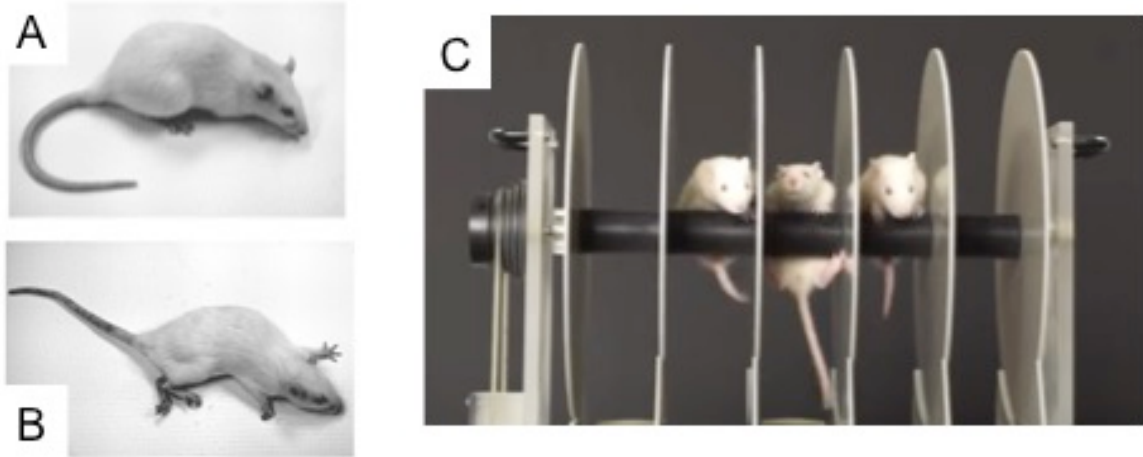
Fig. 8. Modelo animal y test utilizado para la determinación del potencial terapéutico del BBG. (A) Rata SOD1^{G93A} sana y (B) rata SOD1^{G93A} evidenciando los síntomas motores tardíos de la enfermedad. (C) Tres ratas durante el test de rotarod. La rata en el compartimento del medio exhibe dificultad de mantenerse sobre el cilindro. G93A

<u>RESULTADOS</u>

Los resultados obtenidos se presentarán en forma de comunicaciones científicas, la mayoría de las mismas fueron publicadas en revistas internacionales arbitradas. Cada sección de resultados está precedida por una breve sinopsis del trabajo donde se describen los principales hallazgos y se ubica al trabajo en el contexto de la tesis.

OBJETIVOS 1 y 2: El ATP y la activación de P2X$_7$ en astrocitos, implicancias para la ELA

Los resultados obtenidos durante el estudio de los objetivos 1 y 2 de esta tesis fueron comunicados en el artículo 1:

Gandelman M, Peluffo H, Beckman JS, Cassina P, Barbeito L. Extracellular ATP and the P2X$_7$ receptor in astrocyte-mediated motor neuron death: implications for Amyotrophic lateral sclerosis. J Neuroinflammation. 2010 Jun 9;7:33.

En este trabajo nos enfocamos en estudiar el rol de la señalización por la vía de ATP/P2X$_7$ en la inducción de un fenotipo neurotóxico en astrocitos. Partiendo de la hipótesis de que los niveles de ATP extracelular se encuentran aumentados de manera crónica durante la patología en el sistema nervioso, recreamos este escenario en astrocitos en cultivo mediante su exposición a ATP de manera repetida y sostenida. En respuesta, los astrocitos se activaron y presentaron actividad neurotóxica para motoneuronas, evidenciada por la muerte de motoneuronas en cocultivo y motoneuronas puras expuestas a medio condicionado por estos astrocitos. Estos resultados indican que los astrocitos liberaron un factor (o factores) neurotóxico(s) difusible(s) capaz de iniciar la muerte de motoneuronas.

El ATP liberado al medio extracelular y en el medio de cultivo es rápidamente degradado a ADP, AMP y adenosina, que es prontamente internalizada por las células. Debido a que los astrocitos poseen receptores para estos metabolitos y para confirmar que el efecto visto sobre los astrocitos luego del tratamiento con ATP no fue causado por ellos, expusimos astrocitos a estos productos de degradación y evaluamos su efecto. Encontramos que el ADP, el AMP y la adenosina producen un efecto opuesto al ATP. Éstos generaron un fenotipo trófico en los astrocitos, evidenciado por un mayor número de motoneuronas sobrevivientes en comparación con los controles no tratados.

Para estudiar la participación del receptor P2X$_7$ en específico utilizamos el agonista BzATP y el inhibidor BBG y encontramos que los efectos del ATP sobre astrocitos fueron causados por activación del receptor P2X$_7$. Debido a que el receptor P2X$_7$ es capaz de inducir la producción de ERONs en variados tipos celulares, investigamos si este podría ser el mecanismo por el cual la activación de P2X$_7$ en astrocitos inicia la producción de el factor o los factores neurotóxico(s) para motoneuronas. Tres agentes distintos capaces de reducir el estrés nitro-oxidativo previnieron la muerte de motoneuronas, indicando que las ERONs median el daño en astrocitos que deriva en su fenotipo neurotóxico.

En línea con el objetivo 2 de la presente tesis, realizamos cultivos de astrocitos derivados del modelo animal de ELA SOD1^{G93A} y estudiamos si presentan alteraciones en la señalización por ATP y P2X$_7$ y sus consecuencias para las motoneuronas. Trabajos previos de nuestro laboratorio revelaron que los astrocitos derivados de médulas espinales de ratas modelo de ELA SOD1^{G93A} presentan actividad neurotóxica para motoneuronas en cocultivo, induciendo su muerte. Para investigar si la señalización por ATP y P2X$_7$ podría ser responsable de su neurotoxicidad, astrocitos SOD1G93A en cultivo fueron tratados con el inhibidor de P2X$_7$ BBG y la enzima apirasa, que degrada el ATP en el medio de cultivo. Observamos que los astrocitos expuestos a estos fármacos no presentaron actividad neurotóxica para motoneuronas, siendo su sobrevida comparable con los controles no transgénicos. A su vez, la apirasa fue capaz de reducir la proliferación de los astrocitos SOD1^{G93A}, que se encuentra inherentemente aumentada. Este hallazgo indica que en los astrocitos SOD1^{G93A} la señalización por ATP extracelular se encuentra aumentada de manera basal, probablemente por su liberación incrementada al medio extracelular, derivando en una señalización autócrina.

Los resultados de el presente trabajo describen como la señalización por ATP extracelular a través del receptor P2X$_7$ en astrocitos podría contribuir a la muerte de motoneuronas en enfermedades neurodegenerativas como la ELA o el trauma

agudo a la médula espinal. La activación de $P2X_7$ en astrocitos produce ERONs, resultando en su activación y seguida de la liberación de un factor capaz de inducir muerte de motoneuronas. En astrocitos SOD1^{G93A} encontramos que los receptores $P2X_7$ se encuentran basalmente activados, contribuyendo a su actividad neurotóxica para motoneuronas. Durante la enfermedad, este incremento en la señalización basal por ATP extracelular podría no sólo impactar a los astrocitos, sino que también podría activar la microglía y causar daño a las motoneuronas de manera directa, señalizando a través de los receptores a ATP de esos tipos celulares. A raíz de los hallazgos del presente estudio, en los siguientes trabajos presentados en esta tesis investigaremos las consecuencias de la señalización por ATP extracelular en motoneuronas y exploraremos el potencial terapéutico de un inhibidor de $P2X_7$ in vivo en un modelo animal de ELA.

JOURNAL OF
NEUROINFLAMMATION

RESEARCH   **Open Access**

Extracellular ATP and the P2X$_7$ receptor in astrocyte-mediated motor neuron death: implications for amyotrophic lateral sclerosis

Mandi Gandelman[1,2], Hugo Peluffo[1,2], Joseph S Beckman[3], Patricia Cassina[2] and Luis Barbeito*[1,4]

Abstract

Background: During pathology of the nervous system, increased extracellular ATP acts both as a cytotoxic factor and pro-inflammatory mediator through P2X$_7$ receptors. In animal models of amyotrophic lateral sclerosis (ALS), astrocytes expressing superoxide dismutase 1 (SOD1^{G93A}) mutations display a neuroinflammatory phenotype and contribute to disease progression and motor neuron death. Here we studied the role of extracellular ATP acting through P2X$_7$ receptors as an initiator of a neurotoxic phenotype that leads to astrocyte-mediated motor neuron death in non-transgenic and SOD1^{G93A} astrocytes.

Methods: We evaluated motor neuron survival after co-culture with SOD1^{G93A} or non-transgenic astrocytes pretreated with agents known to modulate ATP release or P2X$_7$ receptor. We also characterized astrocyte proliferation and extracellular ATP degradation.

Results: Repeated stimulation by ATP or the P2X$_7$-selective agonist BzATP caused astrocytes to become neurotoxic, inducing death of motor neurons. Involvement of P2X$_7$ receptor was further confirmed by Brilliant blue G inhibition of ATP and BzATP effects. In SOD1^{G93A} astrocyte cultures, pharmacological inhibition of P2X$_7$ receptor or increased extracellular ATP degradation with the enzyme apyrase was sufficient to completely abolish their toxicity towards motor neurons. SOD1^{G93A} astrocytes also displayed increased ATP-dependent proliferation and a basal increase in extracellular ATP degradation.

Conclusions: Here we found that P2X$_7$ receptor activation in spinal cord astrocytes initiated a neurotoxic phenotype that leads to motor neuron death. Remarkably, the neurotoxic phenotype of SOD1^{G93A} astrocytes depended upon basal activation the P2X$_7$ receptor. Thus, pharmacological inhibition of P2X$_7$ receptor might reduce neuroinflammation in ALS through astrocytes.

Background

Amyotrophic lateral sclerosis (ALS) is characterized by the progressive degeneration of motor neurons in the spinal cord, brainstem and motor cortex, leading to respiratory failure and death of affected patients within a few years of diagnosis [1]. The discovery of mutations in the gene encoding the antioxidant enzyme Cu/Zn superoxide dismutase-1 (SOD1) in a subset of patients with familial ALS has led to the development of transgenic animal models expressing different SOD1 mutations [2]. These animal models recapitulate the human disease, exhibiting aberrant oxidative chemistry [3,4], neuroinflammation [5], endoplasmic reticulum stress [6], glutamate excitotoxicity [7], mitochondrial dysfunction [8] and protein misfolding and aggregation [9]. However, the mechanisms behind motor neuron death are unknown.

Accumulating evidence indicates that non-neuronal cells contribute to motor neuron dysfunction and death in ALS by the maintenance of a chronic inflammatory response [10-12]. Activated microglia accumulate in the spinal cord, producing inflammatory mediators and reactive oxygen and nitrogen species [11]. Astrocytes, the most abundant cells in the adult nervous system, also

* Correspondence: barbeito@pasteur.edu.uy
[1] Neurodegeneration Laboratory, Institut Pasteur, Montevideo, Uruguay
Full list of author information is available at the end of the article

become reactive and display inflammatory features [12,13]. Remarkably, astrocytes carrying SOD1 mutations release soluble factors that selectively induce the death of motor neurons [14-18]. Astrocytes carrying the SOD1^{G93A} mutation display mitochondrial dysfunction, increased nitric oxide and superoxide production and altered cytokine liberation profile [14,17,19-22]. Thus, SOD1 mutation causes astrocytes to display a neurotoxic phenotype dependent on autocrine/paracrine pro-inflammatory signaling and increased oxidative and nitrative stress [14,19,23].

In the central nervous system, extracellular adenosine-5'-triphosphate (ATP) has physiological roles in neurotransmission, glial communication, neurite outgrowth and proliferation [24]. Extracellular ATP levels markedly increase in the nervous system in response to ischemia, trauma and inflammatory insults [25-28]. In these cases, ATP is a potent immunomodulator regulating the activation, migration, phagocytosis and release of pro-inflammatory factors in immune and glial cells.

Extracellular ATP effects are mediated by metabotropic (P2Y) and ionotropic (P2X) receptors, both widely expressed in the nervous system [24]. The P2X$_7$ receptor (P2X$_7$r) is a ligand-gated cation channel that elicits a robust increase in intracellular calcium [29]. Of all P2 receptors, P2X$_7$r has the highest EC$_{50}$ (>100 μM) for ATP. The high extracellular concentrations of ATP needed to activate P2X$_7$r are most likely to arise under pathological conditions. In the normal rodent brain, P2X$_7$r expression in astrocytes is generally low, but quickly upregulated in response to brain injury or pro-inflammatory stimulation in cell culture conditions [30-32]. In astrocytes, P2X$_7$r activation can potentiate pro-inflammatory signaling, as it enhances IL-1β-induced activation of NF-κB and AP-1, leading to increased production of nitric oxide as well as increased production of the chemokines MCP-1 and IL-8 [33,34].

Inhibition of P2X$_7$r and other P2X receptors is neuroprotective in animal models of experimental autoimmune encephalomyelitis and Alzheimer's and Huntington's disease [35-37]. In addition, P2X$_7$r mediates motor neuron death after traumatic spinal cord injury, and systemic inhibition in vivo protects motor neurons and promotes functional recovery [25,38]. In ALS patients as well as SOD1^{G93A} animals, increased immunoreactivity for P2X$_7$r has been found in spinal cord microglia [39,40]. Furthermore, SOD1^{G93A} microglia in culture display an increased sensitivity to ATP, and P2X$_7$r activation drives a pro-inflammatory activation that leads to decreased survival of neuronal cell lines [41].

Despite the recognized detrimental role of extracellular ATP and P2X$_7$r signaling during nervous system pathol-

ogy, little is known about its effects on astrocytes or its possible role in ALS. We investigated whether ATP acting through P2X$_7$r could trigger a neurotoxic transformation of astrocytes leading to motor neuron death. We also explored whether ATP signaling in SOD1^{G93A} astrocytes is involved in the maintenance of their neurotoxic phenotype towards motor neurons.

Methods

Chemicals and reagents
Cell culture media and reagents, 5-bromo-2-deoxyuridine (BrdU), primary antibody against BrdU and secondary antibodies were purchased from Invitrogen (Life Technologies). The Malachite Green Phosphate Assay kit was purchased from Cayman Chemical. All other reagents were from Sigma.

Animals
Procedures using laboratory animals were in accordance with the international guidelines for the use of live animals and were approved by the Institutional Animal Care Organization of the School of Medicine, Universidad de la República (Uruguay) and by the Oregon State University IACUC.

Primary astrocyte cultures
Astrocytes were prepared from spinal cords of 1 day old rat pups as previously described [42]. Astrocytes were plated at a density of 2×10^4 cells/cm^2 and maintained in Dulbecco's modified Eagle's medium supplemented with 10% fetal bovine serum, HEPES (3.6 g/L), penicillin (100 IU/mL) and streptomycin (100 μg/mL). Monolayers were >98% pure as determined by GFAP immunoreactivity and devoid of OX$_{42}$-positive microglial cells. Transgenic SOD1^{G93A} and non-transgenic astrocytes were prepared in parallel using littermate pups previously genotyped by PCR.

Primary motor neuron cultures
Motor neurons were prepared from embryonic day 15 rat spinal cords as previously described [42,43]. Briefly, the dorsal horns of spinal cords were dissected and incubated in 0.05% trypsin for 15 minutes at 37°C, followed by mechanical dissociation. Motor neurons were then purified by centrifugation on an Optiprep cushion, followed by isolation of p75^{NTR} expressing motor neurons by immunoaffinity selection with the IgG 192 monoclonal antibody. For co-culture experiments, astrocyte monolayers were washed twice with phosphate buffered saline (PBS) after experimental treatments and then non-transgenic motor neurons were plated on top at a density of 350 cells/cm^2. Co-cultures were maintained for 48 hours in L15 medium supplemented with 0.63 mg/ml sodium bicarbonate, 5 μg/ml insulin, 0.1 mg/ml conalbumin, 0.1

mM putrescine, 30 nM sodium selenite, 20 nM progesterone, 20 mM glucose, 100 IU/ml penicillin, 100 μg/ml streptomycin, and 2% horse serum [42,43]. Pure motor neuron cultures were cultured for 48 hours on a polyornithine-laminin substrate in Neurobasal media supplemented with 2% horse serum, 25 μM L-glutamate, 25 μM 2-mercaptoethanol, 500 μM L-glutamine, and 2% B-27 supplement [42,43]. Survival was maintained by the addition of GDNF (1 ng/ml).

Astrocyte treatments

All astrocyte treatments were performed in DMEM 2% FBS for 48 hours unless otherwise stated. Stock solutions were prepared as 100× and added directly to the well after media change. Inhibitors were added 1 hour prior to subsequent treatment. As noted in Figure 1A, to determine the time-dependency of ATP exposure, media was replenished every 48 hours and 100 μM ATP was added. Thus, astrocytes treated for one day received a single ATP addition while astrocytes treated for three and five days correspondingly received 2 and 3 ATP additions.

Production of conditioned media and treatment of pure motor neuron cultures

To produce conditioned media, astrocytes were treated with ATP 3 times during the course of 5 days. Twenty-four hours after the last treatment, monolayers were washed 3 times with PBS and then incubated for 48 hours with Neurobasal media supplemented with 2% horse serum. Conditioned media was centrifuged to remove debris, aliquoted and stored at -80°C until use. Pure motor neuron cultures were exposed to astrocyte conditioned media 3 hours after plating by replacing 50% of their complete media with conditioned media. GDNF was then added to a final concentration of 1 ng/ml.

Motor neuron survival assessment

Motor neuron survival was assessed after 48 hours by counting all cells displaying intact neurites longer than 4 cells in diameter [42]. Counts were performed over an area of 0.9 cm^2 in 24-well plates. In pure cultures, motor neurons were counted under phase contrast. In co-cultures cells were fixed, immunostained for p75^{NTR} (Figure 1A) and counted [42]. In primary motor neuron cultures, the range of motor neuron death is generally limited to a subpopulation of 40 to 50% [44].

GFAP immunofluorescence

Astrocytes grown on coverslips were fixed with ice-cold 4% paraformaldehyde in PBS for 15 minutes. Cultures were permeabilized with 0.1% Triton X-100 in PBS for 15 min and blocked for 1 hour with 10% goat serum, 2% bovine serum albumin, and 0.1% Triton X-100 in PBS. Anti-GFAP monoclonal antibody diluted in blocking solution (1:400) was incubated overnight at 4°C. After

washing, cultures were incubated for 1 hour at room temperature with Alexa Fluor 488-conjugated goat anti-mouse antibody (1:500). Nuclei were stained with DAPI (1 μg/mL).

Assessment of astrocyte proliferation

Confluent astrocyte monolayers were treated with apyrase for 48 hours in DMEM 2% FBS. At the end of the first 24 hours, BrdU (10 μg/mL) was added. BrdU immunofluorescence was performed as described for GFAP with the addition of a DNA denaturalization step with 1 M hydrochloric acid (30 min at room temperature) after permeabilization. Percentage of BrdU nuclei was calculated as the number of coincident BrdU and DAPI stained nuclei over the total number of DAPI-stained nuclei.

Determination of ATP degradation by phosphate measurement

To determine extracellular ATP hydrolysis, extracellular phosphate production was measured with the Malachite Green Phosphate Assay kit. After the treatment, astrocyte cultures in 24 well plates were washed 3 times with a phosphate free buffer (2 mM CaCl$_2$, 120 mM NaCl, 5 mM KCl, 10 mM glucose, 20 mM Hepes, pH 7.4) and incubated in 500 μl with 3 mM ATP as described [45]. After 10 minutes, an aliquot of each well was removed and phosphate was immediately measured following the manufacturer's instructions.

Statistics

Each experiment was repeated at least three times and data are reported as mean ± SEM. Statistical analysis was performed by one-way analysis of variance, followed by a Student-Newman-Keuls test. Differences were declared statistically significant if $p < 0.05$. Statistics were performed using SigmaStat (Jandel Scientific, San Rafael, CA, USA).

Results

ATP caused non-transgenic astrocytes to induce motor neuron death

Exposure to extracellular ATP caused a neurotoxic activation of spinal cord astrocytes, which lead to death of co-cultured motor neurons in a time dependent-manner. Because ATP is quickly hydrolyzed in the extracellular media and to mimic pathological conditions with persistent ATP stimuli, we treated astrocytes repeatedly as shown in diagram in Figure 1B. Before plating motor neurons on top, astrocyte monolayers were thoroughly washed to remove any traces of the treatment. After 2 days of co-culture, motor neuron survival was assessed. Astrocytes exposed to a single addition of ATP 24 hours before co-culture showed no significant toxicity to motor neurons (Figure 1B). However, astrocytes exposed to two
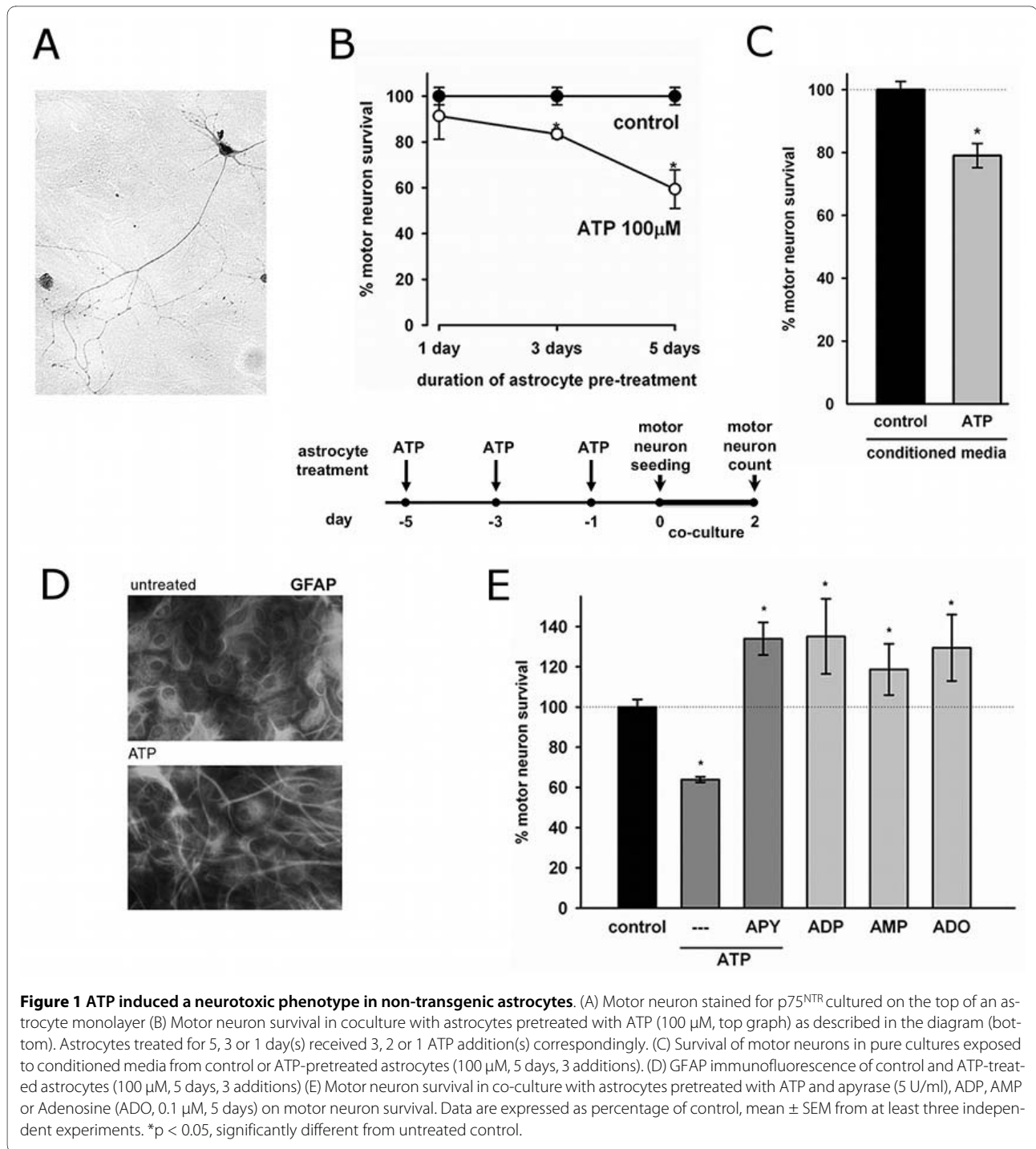
Figure 1 ATP induced a neurotoxic phenotype in non-transgenic astrocytes. (A) Motor neuron stained for p75[NTR] cultured on the top of an astrocyte monolayer (B) Motor neuron survival in coculture with astrocytes pretreated with ATP (100 μM, top graph) as described in the diagram (bottom). Astrocytes treated for 5, 3 or 1 day(s) received 3, 2 or 1 ATP addition(s) correspondingly. (C) Survival of motor neurons in pure cultures exposed to conditioned media from control or ATP-pretreated astrocytes (100 μM, 5 days, 3 additions). (D) GFAP immunofluorescence of control and ATP-treated astrocytes (100 μM, 5 days, 3 additions) (E) Motor neuron survival in co-culture with astrocytes pretreated with ATP and apyrase (5 U/ml), ADP, AMP or Adenosine (ADO, 0.1 μM, 5 days) on motor neuron survival. Data are expressed as percentage of control, mean ± SEM from at least three independent experiments. *$p < 0.05$, significantly different from untreated control.

additions of ATP (3 and 1 days before co-culture) decreased motor neuron survival by 27 ± 17%, and astrocytes treated with three ATP additions (5, 3 and 1 days before co-culture) decreased motor neuron survival by 36 ± 1.4% (Figure 1B). In addition, conditioned media from these astrocytes applied to purified motor neuron cultures plated on a laminin substrate induced a 20% decrease in survival (Figure 1C), suggesting ATP leads to

the release of a diffusible factor from astrocytes able to induce motor neuron death. Immunocytochemical analysis of these astrocytes evidenced morphological changes associated with activation, displaying long and thin processes with intense GFAP immunoreactivity as compared to the typical polygonal shape of resting astrocytes (Figure 1D).

To confirm that the effects seen on astrocytes were caused by ATP and not its degradation products ADP, AMP or adenosine (ADO), we treated astrocytes with ATP in combination with the enzyme apyrase (5 U/mL), which rapidly degrades ATP to AMP and phosphate. In this condition, the death of co-cultured motor neurons was completely prevented. Moreover, motor neuron survival increased above controls to $134 \pm 8\%$ (Figure 1E). Pretreatment of astrocytes directly with the products of ATP degradation ADP, AMP or adenosine (ADO) (0.1 μM added 3 times over five days as was done with ATP) caused an equivalent increase in astrocytic trophic support to motor neurons (Figure 1E).

P2X$_7$r activation causes astrocytes to promote motor neuron death

To investigate the role of P2X$_7$r as an initiator of astrocyte-mediated motor neuron death, we used the preferential P2X$_7$r agonist 2',3'-O-(4-benzoylbenzoyl)ATP (BzATP). Figure 2A shows that a 48-hour treatment of astrocytes with BzATP (10 μM) resulted in death of $30 \pm 3\%$ of co-cultured motor neurons. The effects of ATP and BzATP were prevented by the P2X$_7$r antagonist BBG (1 μM), suggesting that P2X$_7$r activation was required to induce the astrocyte neurotoxic phenotype (Figure 2A).

We then investigated whether the P2X$_7$r-induced phenotypic change in astrocytes could be prevented by agents known to modulate oxidative and nitrative stress. BzATP-treated astrocytes were no longer toxic to motor neurons when the astrocytes were treated with the nitric oxide synthase inhibitor L-NAME (nitro-L-arginine

methyl ester, 1 mM), the superoxide scavenger MnTBAP (Manganese (III) tetrakis (4-benzoic acid) porphyrin, 100 μM) and urate (200 μM) (Figure 2B). Urate efficiently scavenges peroxynitrite-derived free radicals and thereby inhibits tyrosine nitration of proteins [46,47].

Inhibition of ATP signaling in SOD1^{G93A} astrocytes prevents astrocyte-mediated motor neuron death and cell proliferation

Consistent with previous reports [14], spinal cord astrocytes from SOD1^{G93A} rats induced death of $37 \pm 8\%$ of co-cultured motor neurons. Remarkably, pre-incubation of SOD1^{G93A} astrocytes with apyrase to degrade endogenous extracellular ATP for 48 hours before co-culture completely prevented motor neuron death (Figure 3A). Pretreatment with the P2X$_7$r inhibitor BBG also restored motor neuron survival to non-transgenic levels (Figure 3A). This suggests that P2X$_7$r could be basally activated in SOD1^{G93A} astrocytes in an autocrine/paracrine manner, resulting in neurotoxicity to motor neurons.

Because purinergic signaling plays a key role in modulating astrocyte proliferation in pathological conditions [48,49], we assessed whether increased ATP signaling was involved in the proliferation of SOD1^{G93A} astrocytes. Cultured SOD1^{G93A} astrocytes showed a 4- to 5-fold increased proliferation rate as compared with non-transgenic astrocytes (Figure 3B). Proliferation in SOD1^{G93A} astrocytes was decreased in half by apyrase to the same level as apyrase-treated non-transgenic astrocytes (Figure 3B). The small increase in proliferation of non-transgenic astrocytes caused by apyrase could be caused by genera-
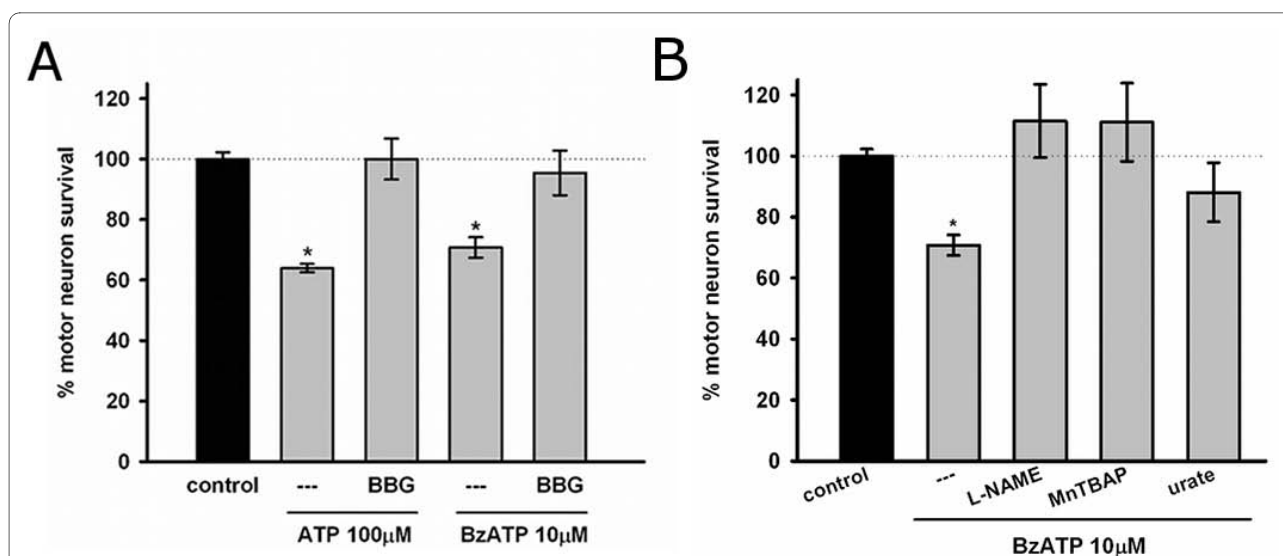
Figure 2 P2X$_7$r activation triggered astrocyte-mediated neurotoxicity by inducing oxidative stress. (A) Motor neuron survival in co-culture with astrocytes pre-treated with ATP (100 μM, 5 days) or BzATP (10 μM, 48 hours) and the P2X$_7$r inhibitor BBG (1 μM). (B) Motor neuron survival in co-culture with astrocytes pre-treated with NAME (1 mM), MnTBAP (0.1 mM) or urate (0.2 mM) and BzATP before co-culture. Data are expressed as the percentage of control, mean ± SEM from at least three independent experiments. *p < 0.05, significantly different from untreated control.
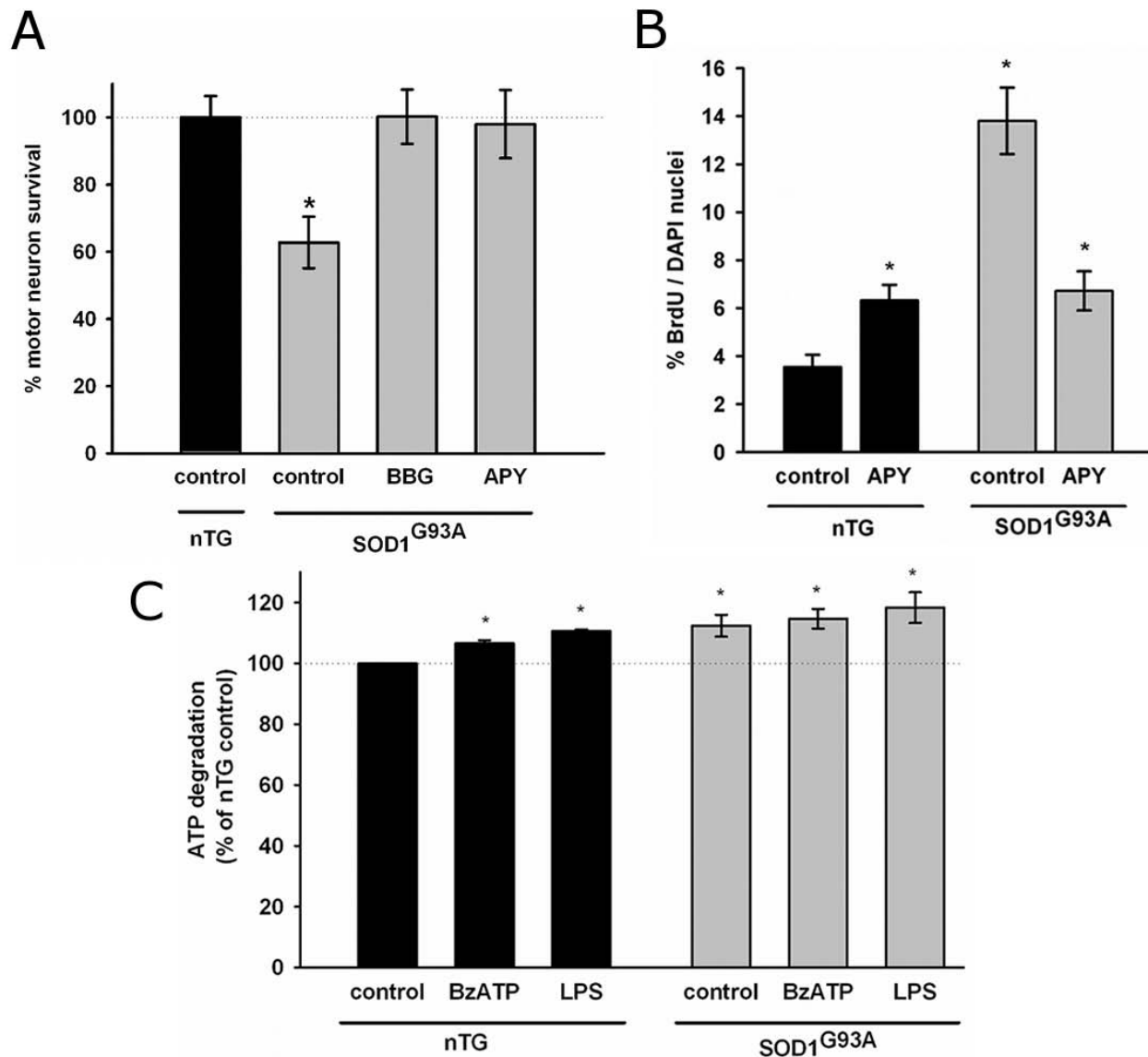
Figure 3 SOD1^{G93A} astrocytes exhibit ATP-dependent neurotoxicity, proliferation, and increased ATP degradation. (A) Motor neuron survival in co-culture with SOD1^{G93A} astrocytes pre-treated for 48 hours with the P2X$_7$r inhibitor BBG (1 μM) or the ATP-hydrolyzing enzyme apyrase (5 U/ml) (B) Effect of apyrase treatment on SOD1^{G93A} astrocyte proliferation in culture. (C) Degradation of exogenously added ATP by SOD1^{G93A} or non-transgenic astrocytes astrocytes. Data are expressed as percentage of non-transgenic control, mean ± SEM from at least three independent experiments. Data are expressed as percentage of non-transgenic control, mean ± SEM from at least three independent experiments. *$p < 0.05$, significantly different from non-transgenic control.

tion of adenosine, which has been shown to stimulate proliferation of astrocytes [49,50].

The increase in ATP signaling observed in SOD1^{G93A} astrocytes did not result from decreased extracellular degradation. On the contrary, ATP hydrolysis was 11% greater in SOD1^{G93A} astrocytes (Figure 3C). Similarly, stimulation with LPS or BzATP induced a comparable increase in ATP degradation in non-transgenic astrocytes. In SOD1^{G93A} astrocytes, these agents did not induce further ATP degradation.

Discussion

Extracellular ATP has become increasingly recognized to have a major role in neurodegenerative processes, but its role in astrocyte-mediated neuronal death has not been explored. Here, we found that spinal cord astrocytes assume a neurotoxic phenotype in response to extracellular ATP, leading to the induction of motor neuron death in co-cultures. Furthermore, evidence indicates that endogenous ATP stimulates SOD1^{G93A} astrocytes in basal conditions and contributes to the maintenance of their neurotoxic phenotype.

Non-transgenic astrocytes required multiple stimuli with ATP over several days to induce the neurotoxic phenotype, while a single stimulus with the P2X$_7$r-selective agonist BzATP was sufficient to activate astrocytes to induce the same extent of motor neuron death. BzATP is most potent as an agonist for P2X$_7$r, but it is also a weaker agonist of P2X$_1$r and P2X$_3$r [51-53]. The involvement of P2X$_7$r was further implicated in the activation of astrocyte neurotoxicity by the antagonist BBG, as it completely inhibited the action of ATP and BzATP. BBG is a selective antagonist for both P2X$_7$r and P2X$_5$r. [51-53]. Thus, P2X$_7$r appears to be the most likely receptor responsible for inducing the neurotoxic phenotype in astrocytes.

We have previously shown that oxidative stress induced by superoxide and nitric oxide forming peroxynitrite in non-transgenic astrocytes leads to a neurotoxic phenotype [19,42]. Here we found that oxidative stress induced by BzATP stimulation mediated the transition of non-transgenic astrocytes to a neurotoxic phenotype, as NOS inhibitors as well as superoxide and peroxynitrite scavengers prevented their neurotoxicity towards motor neurons. In a similar way, Skaper et al showed that P2X$_7$r activation in microglia stimulated peroxynitrite production and led to death of co-cultured neurons [54]. Thus, amplification of oxidative stress by P2X$_7$r signaling in microglia and astrocytes could lead to the generation of an adverse environment for vulnerable neurons during neurodegenerative processes.

Because SOD1^{G93A} astrocytes in culture display a neurotoxic phenotype that is maintained by chronic oxidative stress and autocrine pro-inflammatory signaling [14,17,19,20,22], we investigated whether they also presented alterations in extracellular ATP signaling. Indeed, our results indicate that SOD1^{G93A} astrocytes display basally augmented extracellular ATP signaling as evidenced by an ATP-dependent neurotoxic phenotype, increased ATP-dependent proliferation, and increased extracellular ATP metabolism. Thus, ATP emerges as an extracellular factor that could chronically maintain the SOD1^{G93A} astrocyte aberrant phenotype in an autocrine/paracrine manner.

We found that SOD1^{G93A} astrocytes degraded ATP faster than non-transgenic astrocytes, ruling out that their basal alteration in ATP signaling could be caused by a decrease in its extracellular degradation, thereby allowing ATP to accumulate near receptors. An increase in ATP degradation could also be induced in non-transgenic astrocytes exposed to BzATP or LPS. We have previously shown that LPS induces a neurotoxic phenotype in astrocytes, leading to motor neuron death [42]. Increased ATP degradation and/or ectonucleotidase upregulation has

been previously described in neural tissue after cortical stab wound and acute ischemia [55,56]. This phenomenon might reflect a cellular attempt to prevent over-activation of purinergic receptors during increases in extracellular ATP, thus promoting the return of extracellular ATP signaling to homeostasis.

Degradation of ATP by ectonucleotidases cannot only terminate deleterious ATP signaling, but also initiates ADP and adenosine signaling through P2Y and P1 receptors. To our surprise, in non-transgenic astrocytes, ATP degraded with apyrase, ADP, AMP, or adenosine led to ~35% more motor neuron attachment and survival compared to untreated controls. Because survival is determined 48 hours after plating of the motor neurons freshly isolated from spinal cords, any treatment that increases attachment of motor neurons will result in an increase of motor neuron survival above the untreated control. These results illustrate how the astrocyte phenotype can be modulated from toxic to highly trophic by changing the balance between ATP, ADP and adenosine signaling through P2X, P2Y or adenosine receptors.

In animal models of ALS, proliferative activated astrocytes interact with microglia to accelerate disease progression [57]. Remarkably, we found that modulating ATP signaling in SOD1^{G93A} astrocytes with apyrase or BBG blocked their neurotoxic phenotype, completely preventing astrocyte-mediated death of motor neurons. A role for ATP and P2X$_7$r in the SOD1^{G93A} model was recently proposed by D'Ambrosi et al [41], who showed that SOD1^{G93A} microglia are sensitized to BzATP activation. A combination of aberrant ATP signaling in astrocytes and microglia could generate a positive feedback loop driving a sustained inflammatory response in the spinal cord. The results presented here and the findings in SOD1^{G93A} microglia [41] suggest that P2X$_7$r inhibition in ALS could slow disease progression by decreasing astrocyte and microglial activation.

Taken together, the present work supports the idea that extracellular ATP acting through P2X$_7$r causes astrocytes to develop a neurotoxic phenotype. In SOD1^{G93A} astrocytes evidence suggests that P2X$_7$r is basally activated and contribute to their toxicity towards motor neurons. Thus, modulation of astrocyte P2X$_7$r during disease could lead to decreased oxidative stress and inflammatory signaling and in turn the switch to a more trophic phenotype towards neurons. A better understanding of ATP and P2X$_7$r signaling in astrocytes could contribute to the development of novel protective therapies in ALS and other neurodegenerative diseases where astrocytes are involved.

Author Details
[1]Neurodegeneration Laboratory, Institut Pasteur, Montevideo, Uruguay, [2]Departamento de Histología, Facultad de Medicina, Universidad de la República, Montevideo, Uruguay, [3]Linus Pauling Institute, Oregon State University, Corvallis, Oregon 97331, USA and [4]Instituto de Investigaciones Biológicas Clemente Estable, Montevideo, Uruguay

References
1. Rowland LP, Shneider NA: **Amyotrophic lateral sclerosis.** *N Engl J Med* 2001, **344**:1688-1700.
2. Rosen DR: **Mutations in Cu/Zn superoxide dismutase gene are associated with familial amyotrophic lateral sclerosis.** *Nature* 1993, **364**:362.
3. Beckman JS, Estevez AG, Crow JP, Barbeito L: **Superoxide dismutase and the death of motoneurons in ALS.** *Trends Neurosci* 2001, **24**:S15-20.
4. Harraz MM, Marden JJ, Zhou W, Zhang Y, Williams A, Sharov VS, Nelson K, Luo M, Paulson H, Schoneich C, Engelhardt JF: **SOD1 mutations disrupt redox-sensitive Rac regulation of NADPH oxidase in a familial ALS model.** *J Clin Invest* 2008, **118**:659-670.
5. Papadimitriou D, Le Verche V, Jacquier A, Ikiz B, Przedborski S, Re DB: **Inflammation in ALS and SMA: Sorting out the good from the evil.** *Neurobiol Dis* 2009.
6. Kikuchi H, Almer G, Yamashita S, Guegan C, Nagai M, Xu Z, Sosunov AA, McKhann GM, Przedborski S: **Spinal cord endoplasmic reticulum stress associated with a microsomal accumulation of mutant superoxide dismutase-1 in an ALS model.** *Proc Natl Acad Sci USA* 2006, **103**:6025-6030.
7. Rothstein JD, Tsai G, Kuncl RW, Clawson L, Cornblath DR, Drachman DB, Pestronk A, Stauch BL, Coyle JT: **Abnormal excitatory amino acid metabolism in amyotrophic lateral sclerosis.** *Ann Neurol* 1990, **28**:18-25.
8. Wong PC, Pardo CA, Borchelt DR, Lee MK, Copeland NG, Jenkins NA, Sisodia SS, Cleveland DW, Price DL: **An adverse property of a familial ALS-linked SOD1 mutation causes motor neuron disease characterized by vacuolar degeneration of mitochondria.** *Neuron* 1995, **14**:1105-1116.
9. Bruijn LI, Houseweart MK, Kato S, Anderson KL, Anderson SD, Ohama E, Reaume AG, Scott RW, Cleveland DW: **Aggregation and motor neuron toxicity of an ALS-linked SOD1 mutant independent from wild-type SOD1.** *Science* 1998, **281**:1851-1854.
10. Ilieva H, Polymenidou M, Cleveland DW: **Non-cell autonomous toxicity in neurodegenerative disorders: ALS and beyond.** *J Cell Biol* 2009, **187**:761-72.
11. McGeer PL, McGeer EG: **Inflammation and the degenerative diseases of aging.** *Ann N Y Acad Sci* 2004, **1035**:104-116.
12. Barbeito LH, Pehar M, Cassina P, Vargas MR, Peluffo H, Viera L, Estevez AG, Beckman JS: **A role for astrocytes in motor neuron loss in amyotrophic lateral sclerosis.** *Brain Res Brain Res Rev* 2004, **47**:263-274.
13. Bruijn LI, Miller TM, Cleveland DW: **Unraveling the mechanisms involved in motor neuron degeneration in ALS.** *Annu Rev Neurosci* 2004, **27**:723-749.
14. Vargas MR, Pehar M, Cassina P, Beckman JS, Barbeito L: **Increased glutathione biosynthesis by Nrf2 activation in astrocytes prevents**

15. p75NTR-dependent motor neuron apoptosis. *J Neurochem* 2006, **97**:687-696.
15. Di Giorgio FP, Boulting GL, Bobrowicz S, Eggan KC: **Human embryonic stem cell-derived motor neurons are sensitive to the toxic effect of glial cells carrying an ALS-causing mutation.** *Cell Stem Cell* 2008, **3**:637-648.
16. Di Giorgio FP, Carrasco MA, Siao MC, Maniatis T, Eggan K: **Non-cell autonomous effect of glia on motor neurons in an embryonic stem cell-based ALS model.** *Nat Neurosci* 2007, **10**:608-614.
17. Marchetto MC, Muotri AR, Mu Y, Smith AM, Cezar GG, Gage FH: **Non-cell-autonomous effect of human SOD1 G37R astrocytes on motor neurons derived from human embryonic stem cells.** *Cell Stem Cell* 2008, **3**:649-657.
18. Nagai M, Re DB, Nagata T, Chalazonitis A, Jessell TM, Wichterle H, Przedborski S: **Astrocytes expressing ALS-linked mutated SOD1 release factors selectively toxic to motor neurons.** *Nat Neurosci* 2007, **10**:615-622.
19. Cassina P, Cassina A, Pehar M, Castellanos R, Gandelman M, de Leon A, Robinson KM, Mason RP, Beckman JS, Barbeito L, Radi R: **Mitochondrial dysfunction in SOD1G93A-bearing astrocytes promotes motor neuron degeneration: prevention by mitochondrial-targeted antioxidants.** *J Neurosci* 2008, **28**:4115-4122.
20. Cassina P, Pehar M, Vargas MR, Castellanos R, Barbeito AG, Estevez AG, Thompson JA, Beckman JS, Barbeito L: **Astrocyte activation by fibroblast growth factor-1 and motor neuron apoptosis: implications for amyotrophic lateral sclerosis.** *J Neurochem* 2005, **93**:38-46.
21. Vargas MR, Pehar M, Cassina P, Martinez-Palma L, Thompson JA, Beckman JS, Barbeito L: **Fibroblast growth factor-1 induces heme oxygenase-1 via nuclear factor erythroid 2-related factor 2 (Nrf2) in spinal cord astrocytes: consequences for motor neuron survival.** *J Biol Chem* 2005, **280**:25571-25579.
22. Hensley K, Abdel-Moaty H, Hunter J, Mhatre M, Mou S, Nguyen K, Potapova T, Pye QN, Qi M, Rice H, Stewart C, Stroukoff K, West M: **Primary glia expressing the G93A-SOD1 mutation present a neuroinflammatory phenotype and provide a cellular system for studies of glial inflammation.** *J Neuroinflammation* 2006, **3**:2.
23. Pehar M, Vargas MR, Robinson KM, Cassina P, England P, Beckman JS, Alzari PM, Barbeito L: **Peroxynitrite transforms nerve growth factor into an apoptotic factor for motor neurons.** *Free Radic Biol Med* 2006, **41**:1632-1644.
24. Burnstock G: **Purinergic signalling and disorders of the central nervous system.** *Nat Rev Drug Discov* 2008, **7**:575-590.
25. Wang X, Arcuino G, Takano T, Lin J, Peng WG, Wan P, Li P, Xu Q, Liu QS, Goldman SA, Nedergaard M: **P2X7 receptor inhibition improves recovery after spinal cord injury.** *Nat Med* 2004, **10**:821-827.
26. Phillis JW, O'Regan MH, Perkins LM: **Adenosine 5'-triphosphate release from the normoxic and hypoxic in vivo rat cerebral cortex.** *Neurosci Lett* 1993, **151**:94-96.
27. Melani A, Turchi D, Vannucchi MG, Cipriani S, Gianfriddo M, Pedata F: **ATP extracellular concentrations are increased in the rat striatum during in vivo ischemia.** *Neurochem Int* 2005, **47**:442-448.
28. Piccini A, Carta S, Tassi S, Lasiglie D, Fossati G, Rubartelli A: **ATP is released by monocytes stimulated with pathogen-sensing receptor ligands and induces IL-1beta and IL-18 secretion in an autocrine way.** *Proc Natl Acad Sci USA* 2008, **105**:8067-8072.
29. North RA: **Molecular physiology of P2X receptors.** *Physiol Rev* 2002, **82**:1013-1067.
30. Franke H, Gunther A, Grosche J, Schmidt R, Rossner S, Reinhardt R, Faber-Zuschratter H, Schneider D, Illes P: **P2X7 receptor expression after ischemia in the cerebral cortex of rats.** *J Neuropathol Exp Neurol* 2004, **63**:686-699.
31. Lovatt D, Sonnewald U, Waagepetersen HS, Schousboe A, He W, Lin JH, Han X, Takano T, Wang S, Sim FJ, Goldman SA, Nedergaard M: **The transcriptome and metabolic gene signature of protoplasmic astrocytes in the adult murine cortex.** *J Neurosci* 2007, **27**:12255-12266.
32. Narcisse L, Scemes E, Zhao Y, Lee SC, Brosnan CF: **The cytokine IL-1beta transiently enhances P2X7 receptor expression and function in human astrocytes.** *Glia* 2005, **49**:245-258.
33. John GR, Simpson JE, Woodroofe MN, Lee SC, Brosnan CF: **Extracellular nucleotides differentially regulate interleukin-1beta signaling in primary human astrocytes: implications for inflammatory gene expression.** *J Neurosci* 2001, **21**:4134-4142.

34. Panenka W, Jijon H, Herx LM, Armstrong JN, Feighan D, Wei T, Yong VW, Ransohoff RM, MacVicar BA: **P2X7-like receptor activation in astrocytes increases chemokine monocyte chemoattractant protein-1 expression via mitogen-activated protein kinase.** *J Neurosci* 2001, **21:**7135-7142.

35. Ryu JK, McLarnon JG: **Block of purinergic P2X(7) receptor is neuroprotective in an animal model of Alzheimer's disease.** *Neuroreport* 2008, **19:**1715-1719.

36. Matute C, Torre I, Perez-Cerda F, Perez-Samartin A, Alberdi E, Etxebarria E, Arranz AM, Ravid R, Rodriguez-Antiguedad A, Sanchez-Gomez M, Domercq M: **P2X(7) receptor blockade prevents ATP excitotoxicity in oligodendrocytes and ameliorates experimental autoimmune encephalomyelitis.** *J Neurosci* 2007, **27:**9525-9533.

37. Diaz-Hernandez M, Diez-Zaera M, Sanchez-Nogueiro J, Gomez-Villafuertes R, Canals JM, Alberch J, Miras-Portugal MT, Lucas JJ: **Altered P2X7-receptor level and function in mouse models of Huntington's disease and therapeutic efficacy of antagonist administration.** *FASEB J* 2009, **23:**1893-1906.

38. Peng W, Cotrina ML, Han X, Yu H, Bekar L, Blum L, Takano T, Tian GF, Goldman SA, Nedergaard M: **Systemic administration of an antagonist of the ATP-sensitive receptor P2X7 improves recovery after spinal cord injury.** *Proc Natl Acad Sci USA* 2009, **106:**12489-12493.

39. Yiangou Y, Facer P, Durrenberger P, Chessell IP, Naylor A, Bountra C, Banati RR, Anand P: **COX-2, CB2 and P2X7-immunoreactivities are increased in activated microglial cells/macrophages of multiple sclerosis and amyotrophic lateral sclerosis spinal cord.** *BMC Neurol* 2006, **6:**12.

40. Casanovas A, Hernandez S, Tarabal O, Rossello J, Esquerda JE: **Strong P2X4 purinergic receptor-like immunoreactivity is selectively associated with degenerating neurons in transgenic rodent models of amyotrophic lateral sclerosis.** *J Comp Neurol* 2008, **506:**75-92.

41. D'Ambrosi N, Finocchi P, Apolloni S, Cozzolino M, Ferri A, Padovano V, Pietrini G, Carri MT, Volonte C: **The proinflammatory action of microglial P2 receptors is enhanced in SOD1 models for amyotrophic lateral sclerosis.** *J Immunol* 2009, **183:**4648-4656.

42. Cassina P, Peluffo H, Pehar M, Martinez-Palma L, Ressia A, Beckman JS, Estevez AG, Barbeito L: **Peroxynitrite triggers a phenotypic transformation in spinal cord astrocytes that induces motor neuron apoptosis.** *J Neurosci Res* 2002, **67:**21-29.

43. Henderson CE, Bloch-Gallego E, Camu W: *Purification and culture of embryonic motor neurons* Oxford: IRL Press; 1995.

44. Estevez AG, Sahawneh MA, Lange PS, Bae N, Egea M, Ratan RR: **Arginase 1 regulation of nitric oxide production is key to survival of trophic factor-deprived motor neurons.** *J Neurosci* 2006, **26:**8512-8516.

45. Wink MR, Braganhol E, Tamajusuku AS, Casali EA, Karl J, Barreto-Chaves ML, Sarkis JJ, Battastini AM: **Extracellular adenine nucleotides metabolism in astrocyte cultures from different brain regions.** *Neurochem Int* 2003, **43:**621-628.

46. Teng RJ, Ye YZ, Parks DA, Beckman JS: **Urate produced during hypoxia protects heart proteins from peroxynitrite-mediated protein nitration.** *Free Radic Biol Med* 2002, **33:**1243-1249.

47. Santos CX, Anjos EI, Augusto O: **Uric acid oxidation by peroxynitrite: multiple reactions, free radical formation, and amplification of lipid oxidation.** *Arch Biochem Biophys* 1999, **372:**285-294.

48. Neary JT, Kang Y: **Signaling from P2 nucleotide receptors to protein kinase cascades induced by CNS injury: implications for reactive gliosis and neurodegeneration.** *Mol Neurobiol* 2005, **31:**95-103.

49. Rathbone MP, Middlemiss PJ, Kim JK, Gysbers JW, DeForge SP, Smith RW, Hughes DW: **Adenosine and its nucleotides stimulate proliferation of chick astrocytes and human astrocytoma cells.** *Neurosci Res* 1992, **13:**1-17.

50. Ciccarelli R, Di Iorio P, D'Alimonte I, Giuliani P, Florio T, Caciagli F, Middlemiss PJ, Rathbone MP: **Cultured astrocyte proliferation induced by extracellular guanosine involves endogenous adenosine and is raised by the co-presence of microglia.** *Glia* 2000, **29:**202-211.

51. Cotrina ML, Nedergaard M: **Physiological and pathological functions of P2X7 receptor in the spinal cord.** *Purinergic Signal* 2009, **5:**223-232.

52. Surprenant A: **Functional properties of native and cloned P2X receptors.** *Ciba Found Symp* 1996, **198:**208-219. discussion 219-222

53. Bianchi BR, Lynch KJ, Touma E, Niforatos W, Burgard EC, Alexander KM, Park HS, Yu H, Metzger R, Kowaluk E, Jarvis MF, van Biesen T: **Pharmacological characterization of recombinant human and rat P2X receptor subtypes.** *Eur J Pharmacol* 1999, **376:**127-138.

54. Skaper SD, Facci L, Culbert AA, Evans NA, Chessell I, Davis JB, Richardson JC: **P2X(7) receptors on microglial cells mediate injury to cortical neurons in vitro.** *Glia* 2006, **54:**234-242.

55. Braun N, Zhu Y, Krieglstein J, Culmsee C, Zimmermann H: **Upregulation of the enzyme chain hydrolyzing extracellular ATP after transient forebrain ischemia in the rat.** *J Neurosci* 1998, **18:**4891-4900.

56. Nedeljkovic N, Bjelobaba I, Lavrnja I, Stojkov D, Pekovic S, Rakic L, Stojiljkovic M: **Early temporal changes in ecto-nucleotidase activity after cortical stab injury in rat.** *Neurochem Res* 2008, **33:**873-879.

57. Yamanaka K, Chun SJ, Boillee S, Fujimori-Tonou N, Yamashita H, Gutmann DH, Takahashi R, Misawa H, Cleveland DW: **Astrocytes as determinants of disease progression in inherited amyotrophic lateral sclerosis.** *Nat Neurosci* 2008, **11:**251-253.

OBJETIVO 3: La activación de P2X$_7$ en la muerte de motoneuronas

Los resultados obtenidos en el estudio del objetivo 3 se encuentran en la siguiente publicación:

Artículo 2

Gandelman M, Levy M, Cassina P, Barbeito L, Beckman JS. P2X$_7$ receptor-induced death of motor neurons by a peroxynitrite/FAS-dependent pathway. J Neurochem. 2013 Aug;126(3):382-8.

Este artículo fue seleccionado para ser resaltado en la siguiente editorial, adjuntada en el apéndice 2.

Browne SE. When too much ATP is a bad thing: a pivotal role for P2X$_7$ receptors in motor neuron degeneration. J Neurochem. 2013 Aug;126(3):301-4. doi: 10.1111/jnc.12321.

Durante el estudio del objetivo 1 mostramos que en los astrocitos SOD1^{G93A} el receptor P2X$_7$ se encuentra activado basalmente, indicando que su liberación de ATP podría encontrarse elevada de manera suficiente para activar este receptor. Este incremento en ATP extracelular podría no sólo impactar los receptores P2X$_7$ en astrocitos, sino que también podría señalizar en células adyacentes como las motoneuronas, que se encuentran en íntimo contacto. La inhibición sistémica de los receptores P2X$_7$ luego el trauma a la médula espinal es capaz de prevenir la muerte de un porcentaje considerable de motoneuronas (Wang *et al.* 2004; Peng *et al.* 2009). Similares resultados se han encontrado en otras condiciones neurológicas como la enfermedad de Alzheimer y Huntington. Sin embargo, las consecuencias específicas de la activación de P2X$_7$ en motoneuronas no es conocida. Utilizando un agonista de P2X$_7$ (BzATP), antagonistas y otros fármacos sobre motoneuronas en

cultivo logramos describir los efectos de la señalización por $P2X_7$ y las vías implicadas. Encontramos que la activación de $P2X_7$ resulta en apoptosis de motoneuronas a través de la vía de Fas/p38/NOS. Esta vía fue previamente descrita en motoneuronas deprivadas de factores tróficos y en motoneuronas que expresan $SOD1^{G93A}$. En esta vía apoptótica, encontramos que las motoneuronas liberan FAS-L, que señaliza autócrinamente activando los receptores Fas adyacentes e iniciando una cascada mediada por p38 que lleva a la producción de NO y radicales libres derivados, culminando en apopotósis dependiente de caspasas.

Para simular las condiciones en las que $P2X_7$ se podría activar in vivo, expusimos las motoneuronas a distintas concentraciones de ATP, el agonista endógeno de $P2X_7$. Encontramos que las dosis más bajas de ATP causaron la muerte de las motoneuronas, mientras que las dosis más altas no produjeron efecto. Interpretamos que esto se debió a que la degradación de las dosis más altas de ATP produjo una cantidad suficiente de adenosina capaz de contrarrestar los efectos de la activación de $P2X_7$. En motoneuronas se ha descrito previamente que la adenosina es capaz de transactivar a los receptores de neurotrofinas Trk, previniendo su muerte. Es posible que este fenómeno explique la protección observada en nuestros experimentos. Estos experimentos muestran que la degradación del ATP en el medio extracelular y su recaptación son capaz de regular sus efectos, en el rango desde perjudicial hasta protector.

En este trabajo vinculamos los hallazgos previos de otros laboratorios mostrando que los inhibidores de $P2X_7$ son capaces de proteger a las motoneuronas in vivo con un mecanismo específico por el cuál $P2X_7$ causa la muerte de motoneuronas. Describimos que la activación de $P2X_7$ causa la muerte de motoneuronas a través de la vía de Fas/p38/NOS. El silenciamiento de esta vía en motoneuronas de modelos animales de ELA mejora su función motora y extiende su sobreviviencia. En modelos de trauma de médula espinal su silenciamiento protege a las motoneuronas adyacentes al área dañada. La evidencia muestra que in vivo, tanto la inhibición de $P2X_7$ o de Fas mejora la supervivencia de las motoneuronas. En motoneuronas en

cultivo hallamos que estas dos vías se encuentra conectadas y es posible que este sea el caso también in vivo, abriendo las puertas para el desarrollo de nuevas terapias para las enfermedades en que $P2X_7$ y Fas se encuentran involucrados en la muerte de motoneuronas. De acuerdo con esto, en el siguiente capítulo investigaremos si un inhibidor de $P2X_7$ es capaz de alterar el curso de la enfermedad en un modelo animal de ELA.

ORIGINAL ARTICLE

P2X7 receptor-induced death of motor neurons by a peroxynitrite/FAS-dependent pathway

Mandi Gandelman,*,† Mark Levy,† Patricia Cassina,‡ Luis Barbeito*,§ and Joseph S. Beckman‡

*Neurodegeneration Laboratory, Institut Pasteur, Montevideo, Uruguay

†Linus Pauling Institute, Oregon State University, Corvallis, Qregon, USA

‡Departamento de Histología, Facultad de Medicina, Universidad de la República, Montevideo, Uruguay

§Instituto de Investigaciones Biológicas Clemente Estable, Montevideo, Uruguay

Abstract

The P2X7 receptor/channel responds to extracellular ATP and is associated with neuronal death and neuroinflammation in spinal cord injury and amyotrophic lateral sclerosis. Whether activation of P2X7 directly causes motor neuron death is unknown. We found that cultured motor neurons isolated from embryonic rat spinal cord express P2X7 and underwent caspase-dependent apoptosis when exposed to exceptionally low concentrations of the P2X7 agonist 2′(3′)-O-(4-Benzoylbenzoyl)-ATP. The P2X7 inhibitors BBG, oATP, and KN-62 prevented 2′(3′)-O-(4-Benzoylbenzoyl)-ATP-induced motor neuron death. The endogenous P2X7 agonist ATP induced motor neuron death at low concentrations (1-100 μM). High concentrations of ATP (1 mM) paradoxically became protective due to degradation in the culture media to produce adenosine and activate adenosine receptors. P2X7-induced motor neuron death was dependent on neuronal nitric oxide synthase-mediated production of peroxynitrite, p38 activation, and autocrine FAS signaling. Taken together, our results indicate that motor neurons are highly sensitive to P2X7 activation, which triggers apoptosis by activation of the well-established peroxynitrite/FAS death pathway in motor neurons.

Keywords: motor neuron disease, amyotrophic lateral sclerosis, purinergic, CD95, adenosine, nitric oxide.

J. Neurochem. (2013) **126**, 382–388.

*Read the **Editorial Highlight** for this article on page 301.*

Neurologic disorders like trauma, ischemia, and inflammation cause a marked increase in extracellular adenosine-5′-triphosphate (ATP) levels (Phillis *et al.* 1993; Wang *et al.* 2004; Melani *et al.* 2005; Piccini *et al.* 2008). The P2X7 receptor is a non-desensitizing ATP-gated cation channel that can induce pro-inflammatory responses in glia and immune cells that can indirectly initiate neuronal death (Burnstock 2008; Apolloni *et al.* 2009). P2X7 can also directly induce neuronal death (Burnstock 2008). Inhibition of P2X7 is neuroprotective in animal models of traumatic spinal cord injury, experimental autoimmune encephalomyelitis and Alzheimer's and Huntington's disease (Jun *et al.* 2007; Matute *et al.* 2007; Ryu and McLarnon 2008; Diaz-Hernandez *et al.* 2009).

Motor neurons are the most vulnerable neurons after traumatic spinal cord injury and in motor neuron diseases like amyotrophic lateral sclerosis (ALS) and spinal muscular atrophy. A role for P2X7 in inducing motor neuron death during traumatic spinal cord injury has been uncovered in a rat model, where ATP was dramatically increased in the peripheral regions of the injury (Wang *et al.* 2004). Activation of P2X7 in spinal cord motor neurons caused an irreversible increase in intracellular calcium (Wang *et al.* 2004), while systemic inhibition of P2X7 protected motor neurons, promoted functional recovery, decreased microglia and astrocyte activation, and limited neutrophil infiltration into the spinal cord (Peng *et al.* 2009).

In ALS patients as well as in the ALS animal models expressing mutant Cu,Zn superoxide dismutase (SOD1^{G93A}), growing evidence indicates that P2X7 could cause motor neuron death acting through astrocytes or microglia. Spinal cord microglia display increased immunoreactivity for P2X7 during the disease (Yiangou *et al.* 2006; Casanovas *et al.* 2008). Furthermore, cultured SOD1^{G93A} microglia display an increased sensitivity to ATP and P2X7 activation drives their pro-inflammatory activation (D'Ambrosi *et al.* 2009).

We have previously shown that P2X7 activation in astrocytes triggers a phenotype change and causes astrocytes to induce death of motor neurons in a co-culture model (Gandelman *et al.* 2010). In astrocytes cultured from SOD1^{G93A} rats, P2X7 is basally activated in an autocrine manner that maintains their neurotoxic phenotype toward motor neurons (Gandelman *et al.* 2010). These results indicate that part of the dysfunction of SOD^{G93A} astrocytes involves the release of enough ATP to activate P2X7 *in vivo*. Here, we investigated whether ATP might also activate P2X7 in motor neurons and result in motor neuron death.

Methods

Chemicals and reagents

Cell culture, PCR reagents, and secondary antibody were from Life Technologies (Eugene, OR, USA). FAS : FC and cleaved caspase 3 antibodies were from Cell Signaling Technologies (Danvers, MA, USA). An antibody directed against the intracellular C-terminal domain of P2X7 was from Alomone Labs (Jerusalem, Israel). All other reagents were purchased from Sigma-Aldrich (St. Louis, MO, USA).

Animals

Timed pregnant Sprague–Dawley rats were purchased from Harlan Laboratories (Livermore, CA, USA). Procedures using laboratory animals were in accordance with the international guidelines for the use of live animals and were approved by the Institutional Animal Care Organization of the School of Medicine, Universidad de la República (Montevideo, Uruguay) and by the Oregon State University IACUC.

Primary motor neuron cultures

Motor neurons were prepared from embryonic day 15 rat spinal cords as previously described (Henderson *et al.* 1995; Gandelman *et al.* 2010). Briefly, the ventral horns of spinal cords were dissected and incubated in 0.05% trypsin for 15 min at 37°C, followed by mechanical dissociation. Motor neurons were then purified by centrifugation on an Optiprep cushion, followed by isolation of p75^{NTR} expressing motor neurons by immunoaffinity selection with the IgG-192 monoclonal antibody. Approximately, 1500 motor neurons were plated in each well of a 24-well plate coated with poly-L-ornithine and laminin. Motor neurons were cultured in Neurobasal media supplemented with 2% horse serum, 2% B-27 supplement, 25 μM L-glutamate, 25 μM 2-mercaptoethanol and 500 μM L-glutamine (Henderson *et al.* 1995). Survival was maintained by the addition of glial cell-derived neurotrophic factor (1 ng/mL). Unless otherwise stated, motor neurons were treated 2 h after seeding, after they had attached and started differentiating. Motor neuron survival was assessed after culturing for 48 h by counting all cells displaying intact neurites longer than four cell diameters in two diameters of the well. Motor neurons were plated to yield 130 motor neurons per well under optimal growth conditions with each condition replicated in triplicate and then repeated with at least three separate motor neuron preparations. This method of measuring survival has been extensively used and validated for measuring motor neuron survival (Henderson *et al.* 1995; Estevez *et al.* 1998, 1999).

RT–PCR

Motor neurons were plated in 35 mm dishes and after 18 h RNA was extracted using Trizol according to the manufacturer's instructions. RT-PCR was performed using SuperScript® III One-Step RT-PCR System (Invitrogen, Eugene, OR, USA) by adding specific primers (P2X7 forward AAGGGAAAGAAGCCCCACGG, P2X7 reverse CCGCTTTTCCATGCCATTTT, Actin forward GAGCA ATGATCTTGATCTTCATGGTG, Actin reverse CCTTCCTTCC TGGGTATGGAATCC).

Immunofluorescence

Motor neurons were fixed with ice-cold 4% paraformaldehyde and 0.1% glutaraldehyde in phosphate buffered saline (PBS) for 15 min. Cultures were permeabilized with 0.1% Triton X-100 in PBS for 15 min and blocked for 1 h with 10% goat serum, 2% bovine serum albumin, and 0.1% Triton X-100 in PBS. Anti-cleaved caspase 3 or P2X7 monoclonal antibody diluted in blocking solution (1 : 100) was incubated overnight at 4°C. After washing, cultures were incubated for 1 h at 20°C with Alexa Fluor 488 or 568-conjugated goat anti-mouse antibody (1 : 500). Nuclei were stained with 4′,6-diamidino-2-phenylindole (DAPI; Life Technologies, Eugene, OR, USA) (1 μg/mL).

Statistics

Each experiment was repeated at least three times with separate motor neuron preparations and data are reported as mean ± SEM. Statistical analysis was performed by one-way analysis of variance, followed by a Student–Newman–Keuls test. Differences were declared statistically significant if $p < 0.05$. Statistics were performed using GraphPad Prism 4 (GraphPad Software, La Jolla, CA, USA).

Results

Activation of P2X7 in motor neurons leads to cell death

P2X7 was expressed in spinal motor neurons in culture (Fig. 1a). The presence of the mRNA for P2X7 receptor was evidenced by RT-PCR. In addition, the soma and neurites of all motor neurons showed intense immunoreactivity for the receptor (Fig. 1a and b). To investigate the effect of P2X7 activation on motor neurons, increasing concentrations of the P2X7 agonist 2′(3′)-*O*-(4-Benzoylbenzoyl)-ATP (BzATP) were added to the cultures 2 h after isolation and survival was assessed after 48 h. Concentrations of BzATP from 0.1 to 100 μM decreased motor neuron survival similarly, ranging from $74 \pm 3\%$ to $69 \pm 5\%$ (Fig. 2a). Only 0.01 μM BzATP had no observable effect on motor neuron survival. We saw no difference in death induced by BzATP whether motor neurons were exposed to BzATP immediately after plating or if treatment was delayed overnight to allow motor neurons to attach and extend neurites (Data not shown). Thus, BzATP decreased survival independently of motor neuron attachment and subsequent differentiation.

Inhibiting the P2X7 receptor with BBG, oATP, and KN-62 (1 μM) prevented motor neuron death caused by BzATP (at concentrations of 0.1, 10, and 100 μM), which strongly suggests the specific involvement of P2X7 in the induction of motor neuron death by BzATP (Fig. 2a). To investigate the effects of P2X7 activation in motor neurons in the rest of this study, we used treatments with 10 μM BzATP, which causes death of $32 \pm 2\%$ motor neurons and is generally recognized to activate P2X7 according to the typical pharmacological profile of this receptor (Donnelly-Roberts *et al.* 2009).

P2X7 activation triggers apoptosis by activation of the Fas/p38/NO pathway

An increase in Fas-L production followed by autocrine activation of the Fas death receptor results in caspase-dependent apoptosis in motor neurons deprived of trophic factors or expressing ALS-associated mutant Cu/Zn super-oxide dismutase-1 (SOD1). In this death pathway, Fas signals to p38, leading to NO production that causes motor neuron apoptosis (Raoul *et al.* 1999, 2002, 2006). To test whether this death pathway was activated following P2X7 stimulation, we blocked activation of Fas and found that motor neuron survival after BzATP exposure was restored ($92 \pm 7\%$ survival). In addition, the p38 inhibitor SB203580 (1 μM) was able to inhibit motor neuron death ($96 \pm 4\%$, Fig. 3a). Motor neuron death was also prevented by the general neuronal nitric oxide synthase (NOS) inhibitor L-NAME (100 μM) or the specific neuronal nitric oxide synthase (nNOS) inhibitor TRIM (10 μM, Handy *et al.* 1995). The effect of both inhibitors was reversed by the simultaneous addition of DETA-NONOate (10 μM, Fig. 3b). This concentration of DETA-NONOate will main-
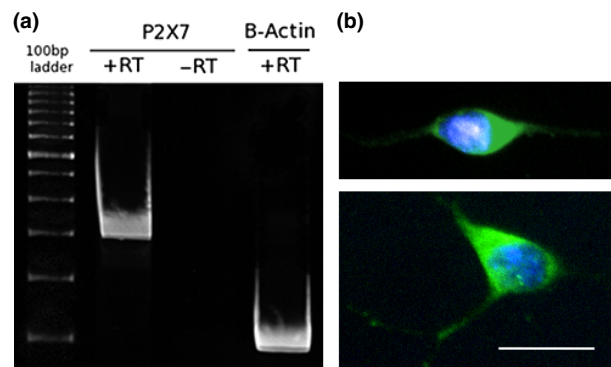
Fig. 1 Motor neurons in primary culture express P2X7. (a) Total RNA was extracted from cultured motor neurons 18 h after isolation and RT-PCR was performed to reveal the presence of P2X7 mRNA. (b) Motor neurons cultured for 18 h display immunoreactivity for P2X7 (green) in the soma and neurites. Nuclei were stained with DAPI (blue). The scale bar represents 20 μm.
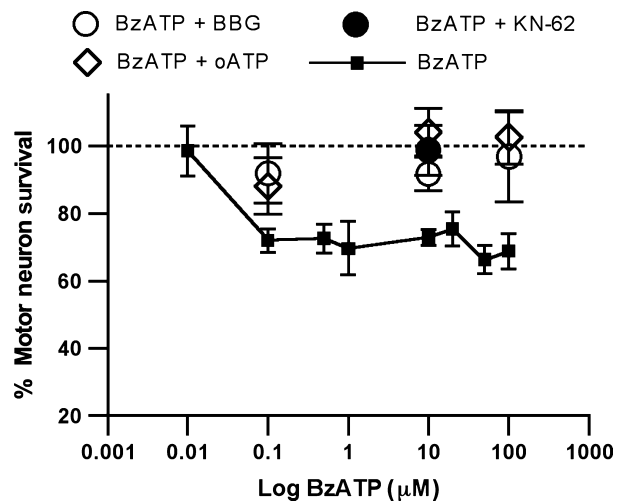
Fig. 2 Cultured motor neurons are highly sensitive to 2′(3′)-*O*-(4-Benzoylbenzoyl)-ATP (BzATP). Motor neuron survival in response to 0.1 to 100 μM BzATP (squares). The P2X7 inhibitors BBG (1 μM, triangles), oATP (1 μM, inverted triangles) and KN-62 (1 μM, diamonds) prevented motor neuron death induced by 0.1, 10, and 100 μM BzATP. Dotted line indicates survival in absence of BzATP (100%). All BzATP treatments at or above 0.1 μM resulted in significantly decreased survival compared to control cultures ($p < 0.05$). Survival after all of the antagonist treatments was not statistically different from the control cultures.

tain a flow of 40 nM nitric oxide over a 24 h period and does not induce motor neuron death by itself (Estevez *et al.* 1998).

Because P2X7 is known for elevating intracellular calcium levels and NO production by nNOS is activated by calcium, we investigated whether chelation could prevent motor neuron death. Pre-incubation of the cultures with BAPTA-AM (1 μM) prevented motor neuron death induced by
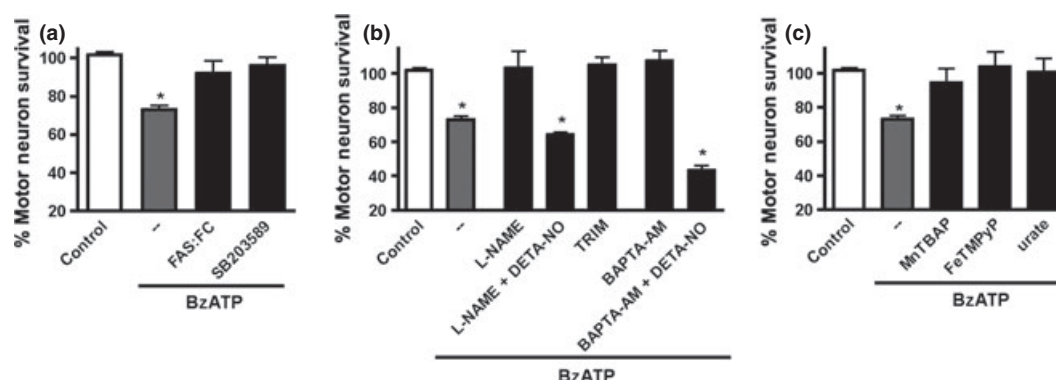
Fig. 3 2′(3′)-O-(4-Benzoylbenzoyl)-ATP (BzATP) triggered autocrine FAS/p38/neuronal nitric oxide synthase signaling. (a) Motor neuron death triggered by BzATP (10 μM) was prevented by SB203580 (10 μM) and FAS:FC. (b) L-NAME (100 μM), TRIM (1 μM), and BAPTA-AM (1 μM) prevented motor neuron death initiated by BzATP, while addition of DETA-NO (10 μM) reinstated death. (c) Motor neuron death caused by BzATP was prevented by addition of MnTBAP (10 μM), FeTMPyP (10 μM) or urate (200 μM). *$p < 0.05$, significantly different from control.

BzATP (Fig. 3b) and this protective effect was reversed by addition of DETA-NONOate (Fig. 3b). These results indicate a key role for calcium regulation of nNOS in motor neuron death initiated by BzATP. The regulation of intracellular calcium likely also involves additional modulation by endoplasmic reticulum and mitochondrial transporters in addition to P2X7.

NO itself is not toxic to motor neurons, but its diffusion-limited reaction with superoxide to form peroxynitrite is ultimately responsible for motor neuron death (Estevez *et al.* 1998). Because P2X7 activation is known to initiate production of superoxide in numerous immune and non-immune cell types (Hewinson and Mackenzie 2007), we tested whether superoxide and peroxynitrite played a role in BzATP-induced motor neuron death. The superoxide scavenger MnTBAP (10 μM) and the peroxynitrite scavenger FeTMPyP (10 μM) completely rescued motor neurons from death after P2X7 activation (Fig. 3c). In addition, urate (200 μM), which scavenges peroxynitrite-derived radicals and thereby inhibits tyrosine nitration of proteins (Santos *et al.* 1999; Robinson *et al.* 2004), was also able to prevent motor neuron death caused by P2X7 activation (Fig. 3c).

P2X7 activation triggered caspase-dependent death in motor neurons, as it was prevented by the general caspase inhibitor zVAD-fmk (10 μM) and the caspase 3 inhibitor DEVD-fmk (10 μM, Fig. 4a). In addition, extensive immunoreactivity for activated caspase 3 is evidenced in motor neurons 24 h after treatment with BzATP, in coincidence with fragmented nucleus, known hallmark of apoptosis (Fig. 4b). This agrees with previous reports providing evidence that Fas activates caspase-dependent apoptosis in motor neurons (Raoul *et al.* 1999).

ATP degradation to adenosine prevents P2X7–mediated motor neuron death

To more closely resemble conditions during injury or disease in the nervous system, we exposed motor neurons to ATP, the endogenous P2X7 agonist. Addition of 100 μM ATP-induced death of $27 \pm 7\%$ of motor neurons while 1 mM ATP did not cause any significant death ($8 \pm 4\%$, Fig. 5a).

Fig. 4 2′(3′)-O-(4-Benzoylbenzoyl)-ATP triggered caspase-dependent apoptosis. (a) Caspase inhibitors zVAD-fmk and devd-fmk (10 μM) prevented motor neuron death triggered by BzATP (10 μM). (b) Immunofluorescence of cultured motor neurons for cleaved caspase 3 (red), apparent only in motor neurons treated with BzATP. Nuclear morphology was evident with DAPI staining (blue). *$p < 0.05$, significantly different from control. The scale bar represents 20 μm.
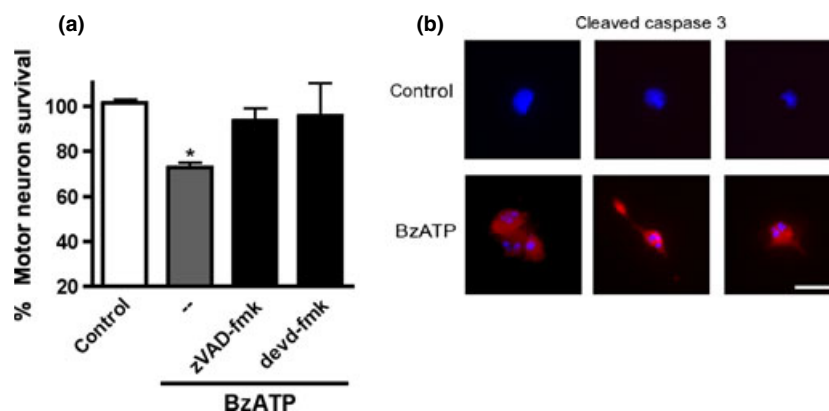
Because ATP quickly degrades to adenosine, which can increase motor neuron survival by trans-activating Trk receptors (Wiese *et al.* 2007), we hypothesized that degradation of 1 mM ATP could produce enough adenosine to prevent P2X7-mediated death. Indeed, we found that with caffeine (0.5 μM; an inhibitor of P1 receptors), addition of 1 mM ATP caused death of $26 \pm 7\%$ motor neurons. In addition, high concentrations of adenosine (200 μM) prevented motor neuron death initiated by BzATP (Fig. 5b), while lower doses (1 μM) had no effect, explaining why this antagonizing effect was not seen in motor neurons exposed to lower concentrations of ATP. In agreement with these results, exogenous addition of high doses of adenosine (100 and 200 μM) caused a small but significant increase in basal survival (115 ± 4 and $116 \pm 6\%$, respectively), while 1 μM adenosine had no effect (Fig. 5c).

Discussion

Accumulating evidence indicates that P2X7 mediates multiple detrimental effects in many nervous system diseases (Koles *et al.* 2005; Sperlagh *et al.* 2006). One of the earliest events after spinal cord trauma is ATP release in areas surrounding experimental spinal cord injury that is also associated with a P2X7 dependent irreversible increase in intracellular calcium (Wang *et al.* 2004). Surprisingly, the role of P2X7 has received limited investigation in ALS. Increased immunoreactivity for P2X7 in microglia has been observed in ALS tissues (Yiangou *et al.* 2006). We have recently shown that P2X7 activation caused astrocytes to become neurotoxic to motor neurons (Gandelman *et al.* 2010). Furthermore, P2X7 was basally activated in SOD1^{G93A} expressing astrocytes and was needed to maintain their neurotoxic phenotype. Here, we found motor neurons themselves can be a direct target of elevated extracellular ATP through activation of P2X7.

P2X7 activation in motor neurons triggered a peroxynitrite-fueled apoptotic cascade, previously described as a distinctive death pathway extensively characterized in the death of motor neurons from trophic factor deprivation, activation of the p75 receptor and expression of mutant SODs (Raoul *et al.* 1999, 2002, 2006; Pehar *et al.* 2005, 2006, 2007). The downstream signaling triggered by P2X7 involves activation of p38 MAPK that in turn activates an autocrine loop involving neuronal NOS activation and Fas signaling. It involves cycles of amplification of increasing nitric oxide synthesis by neuronal NOS, phosphorylation of p38 through death-associated protein 6/Apoptosis signal-regulating kinase 1, and further FAS-L release. Calcium entry because of P2X7 activation could increase nitric oxide synthesis by stimulating neuronal NOS activity. Supporting this concept, we found that the protection afforded by intracellular calcium chelation from P2X7 activation was reversed by a low steady state concentration of 40 nM nitric oxide.

We have previously shown that nitric oxide is not directly toxic to motor neurons via this pathway, but rather reacts with superoxide to form the oxidant peroxynitrite (Sahawneh *et al.* 2010). Here, motor neuron death triggered by P2X7 was prevented by two different peroxynitrite scavengers as well as by urate, a radical scavenger that strongly inhibits tyrosine nitration. Thus, the transformation of nitric oxide to peroxynitrite can serve as a switch controlling the survival versus death of stressed motor neurons. Peroxynitrite scavengers have also been shown to be protective in mutant SOD1 transgenic mouse models of ALS (Wu *et al.* 2003; Soon *et al.* 2011). In addition, nitration of a single tyrosine near the ATP binding pocket of HSP90 has recently been shown to be sufficient to activate motor neuron death through a mechanism that involves P2X7 and the release of FAS (Franco *et al.* 2013).

Fas is strongly implicated in controlling peroxynitrite-induced apoptosis of motor neurons in ALS (Sahawneh
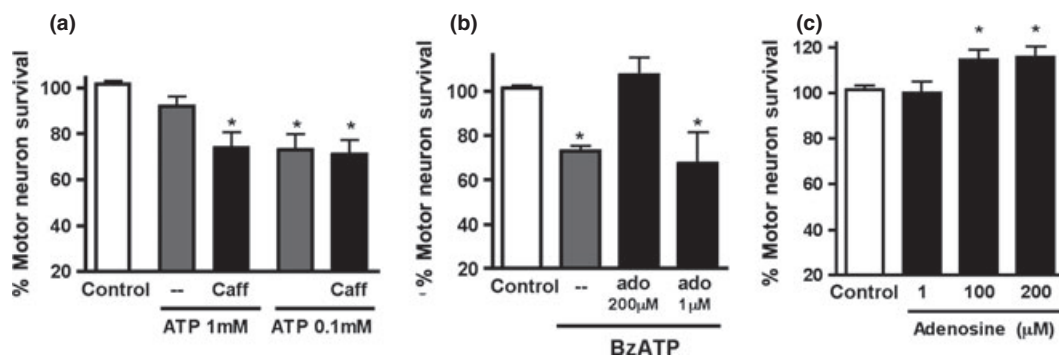
Fig. 5 High concentrations of adenosine produced by ATP degradation can prevent BzATP-induced motor neuron death. (a) Motor neuron survival in response to the indicated concentrations of ATP (1 mM and 100 μM) in presence or absence of caffeine (0.5 μM). (b) Adenosine at a concentration of 200 μM but not at 1 μM prevented motor neuron survival induced by BzATP (10 μM) (c) Basal motor neuron survival increased in response to 1, 100, and 200 μM adenosine. *$p < 0.05$, significantly different from control.

et al. 2010), and involved in spinal ischemia, axotomy of the facial nerve, sciatic nerve avulsion, and spinal cord injury (Matsushita *et al.* 2000, Sakurai *et al.* 1998, Ugolini *et al.* 2003, Martin *et al.* 2005, Casha *et al.* 2005, Demjen *et al.* 2004). Silencing Fas in the spinal cord of animal models of ALS models improves motor function and extends survival (Locatelli *et al.* 2007). In spinal cord injury, Fas inhibition specifically spares neurons and axons in the areas surrounding the injury (Casha *et al.* 2005, Demjen *et al.* 2004). Here, we found evidence that P2X7 activates Fas-induced death of cultured motor neurons via peroxynitrite, but whether P2X7 triggers this death pathway *in vivo* remains to be determined. Activation of P2X7 has recently been shown to be involved in FAS-induced death of Jurket cells (Aguirre *et al.* 2013).

The sensitivity of motor neurons to ATP in vitro was modulated by cleavage to adenosine, which can be catalyzed by extracellular nucleotidases such as CD39 as well as apyrase in culture serum. Adenosine has well established roles as anti-inflammatory and neuroprotective agent (Jacobson and Gao 2006). In our assays, direct addition of high doses of adenosine prevented motor neuron death triggered by BzATP, while lower doses had no protective effect. This likely explains how high concentrations of ATP (1 mM) paradoxically protected motor neurons while lower concentrations activated apoptosis via P2X7. Adenosine signaling through the A_{2A} receptor leads to transactivation of the neurotrophin TrkB receptor and prevents motor neuron death in vivo after facial nerve axotomy and in vitro caused by trophic factor deprivation (Wiese *et al.* 2007). In addition, A_{2A} activation reduces neuronal apoptosis and neurological deficit after spinal cord trauma (Genovese *et al.* 2010). Both P2X7 antagonists and A_{2A} agonists protect motor neurons from spinal cord trauma (Wang *et al.* 2004; Peng *et al.* 2009; Genovese *et al.* 2010). Thus, ATP-degrading enzymes in the microenvironment surrounding motor neurons might modulate disease progression by limiting the activation of P2X7 while stimulating adenosine receptors. Taken together our results reveal a new regulatory mechanism of motor neuron survival by being a target for elevated extracellular ATP released during the disease. Further knowledge of the interactions between these two pathways could help optimize the design of new highly targeted therapies to prevent motor neuron death in ALS and spinal cord injury.

Acknowledgements

References

Aguirre A., Shoji K. F., Saez J. C., Henriquez M. and Quest A. F. (2013) FasL-triggered death of Jurkat cells requires caspase 8-induced, ATP-dependent cross-talk between Fas and the purinergic receptor P2X(7). *J. Cell. Physiol.* **228**, 485–493.

Apolloni S., Montilli C., Finocchi P. and Amadio S. (2009) Membrane compartments and purinergic signalling: P2X receptors in neurodegenerative and neuroinflammatory events. *FEBS J.* **276**, 354–364.

Burnstock G. (2008) Purinergic signalling and disorders of the central nervous system. *Nat. Rev. Drug Discov.* **7**, 575–590.

Casanovas A., Hernandez S., Tarabal O., Rossello J. and Esquerda J. E. (2008) Strong P2X4 purinergic receptor-like immunoreactivity is selectively associated with degenerating neurons in transgenic rodent models of amyotrophic lateral sclerosis. *J. Comp. Neurol.* **506**, 75–92.

Casha S., Yu W. R. and Fehlings M. G. (2005) FAS deficiency reduces apoptosis, spares axons and improves function after spinal cord injury. *Exp. Neurol.* **196**, 390–400.

D'Ambrosi N., Finocchi P., Apolloni S., Cozzolino M., Ferri A., Padovano V., Pietrini G., Carri M. T. and Volonte C. (2009) The proinflammatory action of microglial P2 receptors is enhanced in SOD1 models for amyotrophic lateral sclerosis. *J. Immunol.* **183**, 4648–4656.

Demjen D., Klussmann S., Kleber S. *et al.* (2004) Neutralization of CD95 ligand promotes regeneration and functional recovery after spinal cord injury. *Nat. Med.* **10**, 389–395.

Diaz-Hernandez M., Diez-Zaera M., Sanchez-Nogueiro J., Gomez-Villafuertes R., Canals J. M., Alberch J., Miras-Portugal M. T. and Lucas J. J. (2009) Altered P2X7-receptor level and function in mouse models of Huntington's disease and therapeutic efficacy of antagonist administration. *FASEB J.* **23**, 1893–1906.

Donnelly-Roberts D. L., Namovic M. T., Han P. and Jarvis M. F. (2009) Mammalian P2X7 receptor pharmacology: comparison of recombinant mouse, rat and human P2X7 receptors. *Br. J. Pharmacol.* **157**, 1203–1214.

Estevez A. G., Spear N., Manuel S. M., Barbeito L., Radi R. and Beckman J. S. (1998) Role of endogenous nitric oxide and peroxynitrite formation in the survival and death of motor neurons in culture. *Prog. Brain Res.* **118**, 269–280.

Estevez A. G., Crow J. P., Sampson J. B., Reiter C., Zhuang Y., Richardson G. J., Tarpey M. M., Barbeito L. and Beckman J. S. (1999) Induction of nitric oxide-dependent apoptosis in motor neurons by zinc-deficient superoxide dismutase. *Science* **286**, 2498–2500.

Franco M. C., Ye Y., Refakis C. A. *et al.* (2013) Nitration of Hsp90 induces cell death. *Proc. Natl Acad. Sci. USA* **110**, E1102–E1111.

Gandelman M., Peluffo H., Beckman J. S., Cassina P. and Barbeito L. (2010) Extracellular ATP and the P2X7 receptor in astrocyte-mediated motor neuron death: implications for amyotrophic lateral sclerosis. *J. Neuroinflammation* **7**, 33.

Genovese T., Melani A., Esposito E. *et al.* (2010) Selective adenosine A (2a) receptor agonists reduce the apoptosis in an experimental model of spinal cord trauma. *J. Biol. Regul. Homeost. Agents* **24**, 73–86.

Handy R. L., Wallace P., Gaffen Z. A., Whitehead K. J. and Moore P.K. (1995) The antinociceptive effect of 1-(2-trifluoromethylphenyl) imidazole (TRIM), a potent inhibitor of neuronal nitric oxide synthase *in vitro*, in the mouse. *Br. J. Pharmacol.* **116**, 2349–2350.

Henderson C. E., Bloch-Gallego E. and Camu W. (1995) *Purification and culture of embryonic motor neurons:* Neural cell culture: a practical approach. IRL Press, Oxford.

Hewinson J. and Mackenzie A. B. (2007) P2X(7) receptor-mediated reactive oxygen and nitrogen species formation: from receptor to generators. *Biochem. Soc. Trans.* **35**, 1168–1170.

Jacobson K. A. and Gao Z. G. (2006) Adenosine receptors as therapeutic targets. *Nat. Rev. Drug Discov.* **5**, 247–264.

Jun D. J., Kim J., Jung S. Y. *et al.* (2007) Extracellular ATP mediates necrotic cell swelling in SN4741 dopaminergic neurons through P2X7 receptors. *J. Biol. Chem.* **282**, 37350–37358.

Koles L., Furst S. and Illes P. (2005) P2X and P2Y receptors as possible targets of therapeutic manipulations in CNS illnesses. *Drug News Perspect.* **18**, 85–101.

Locatelli F., Corti S., Papadimitriou D. *et al.* (2007) Fas small interfering RNA reduces motoneuron death in amyotrophic lateral sclerosis mice. *Ann. Neurol.* **62**, 81–92.

Martin L. J., Chen K. and Liu Z. (2005) Adult motor neuron apoptosis is mediated by nitric oxide and Fas death receptor linked by DNA damage and p53 activation. *J. Neurosci.* **25**, 6449–6459.

Matsushita K., Wu Y., Qiu J., Lang-Lazdunski L., Hirt L., Waeber C., Hyman B. T., Yuan J. and Moskowitz M. A. (2000) Fas receptor and neuronal cell death after spinal cord ischemia. *J. Neurosci.* **20**, 6879–6887.

Matute C., Torre I., Perez-Cerda F. *et al.* (2007) P2X(7) receptor blockade prevents ATP excitotoxicity in oligodendrocytes and ameliorates experimental autoimmune encephalomyelitis. *J. Neurosci.* **27**, 9525–9533.

Melani A., Turchi D., Vannucchi M. G., Cipriani S., Gianfriddo M. and Pedata F. (2005) ATP extracellular concentrations are increased in the rat striatum during in vivo ischemia. *Neurochem. Int.* **47**, 442–448.

Pehar M., Vargas M. R., Cassina P., Barbeito A. G., Beckman J. S. and Barbeito L. (2005) Complexity of astrocyte-motor neuron interactions in amyotrophic lateral sclerosis. *Neurodegener Dis.* **2**, 139–146.

Pehar M., Vargas M. R., Robinson K. M., Cassina P., England P., Beckman J. S., Alzari P. M. and Barbeito L. (2006) Peroxynitrite transforms nerve growth factor into an apoptotic factor for motor neurons. *Free Radic. Biol. Med.* **41**, 1632–1644.

Pehar M., Vargas M. R., Robinson K. M., Cassina P., Diaz-Amarilla P. J., Hagen T. M., Radi R., Barbeito L. and Beckman J. S. (2007) Mitochondrial superoxide production and nuclear factor erythroid 2-related factor 2 activation in p75 neurotrophin receptor-induced motor neuron apoptosis. *J. Neurosci.* **27**, 7777–7785.

Peng W., Cotrina M. L., Han X. *et al.* (2009) Systemic administration of an antagonist of the ATP-sensitive receptor P2X7 improves recovery after spinal cord injury. *Proc. Natl Acad. Sci. USA* **106**, 12489–12493.

Phillis J. W., O'Regan M. H. and Perkins L. M. (1993) Adenosine 5′-triphosphate release from the normoxic and hypoxic in vivo rat cerebral cortex. *Neurosci. Lett.* **151**, 94–96.

Piccini A., Carta S., Tassi S., Lasiglie D., Fossati G. and Rubartelli A. (2008) ATP is released by monocytes stimulated with pathogen-sensing receptor ligands and induces IL-1beta and IL-18 secretion in an autocrine way. *Proc. Natl Acad. Sci. USA* **105**, 8067–8072.

Raoul C., Henderson C. E. and Pettmann B. (1999) Programmed cell death of embryonic motoneurons triggered through the Fas death receptor. *J. Cell Biol.* **147**, 1049–1062.

Raoul C., Estevez A. G., Nishimune H., Cleveland D. W., deLapeyriere O., Henderson C. E., Haase G. and Pettmann B. (2002) Motoneuron death triggered by a specific pathway downstream of Fas. potentiation by ALS-linked SOD1 mutations. *Neuron* **35**, 1067–1083.

Raoul C., Buhler E., Sadeghi C., Jacquier A., Aebischer P., Pettmann B., Henderson C. E. and Haase G. (2006) Chronic activation in presymptomatic amyotrophic lateral sclerosis (ALS) mice of a feedback loop involving Fas, Daxx, and FasL. *Proc. Natl Acad. Sci. USA* **103**, 6007–6012.

Robinson K. M., Morre J. T. and Beckman J. S. (2004) Triuret: a novel product of peroxynitrite-mediated oxidation of urate. *Arch. Biochem. Biophys.* **423**, 213–217.

Ryu J. K. and McLarnon J. G. (2008) Block of purinergic P2X(7) receptor is neuroprotective in an animal model of Alzheimer's disease. *NeuroReport* **19**, 1715–1719.

Sahawneh M. A., Ricart K. C., Roberts B. R. *et al.* (2010) Cu, Zn-superoxide dismutase increases toxicity of mutant and zinc-deficient superoxide dismutase by enhancing protein stability. *J. Biol. Chem.* **285**, 33885–33897.

Sakurai M., Hayashi T., Abe K., Sadahiro M. and Tabayashi K. (1998) Delayed selective motor neuron death and fas antigen induction after spinal cord ischemia in rabbits. *Brain Res.* **797**, 23–28.

Santos C. X., Anjos E. I. and Augusto O. (1999) Uric acid oxidation by peroxynitrite: multiple reactions, free radical formation, and amplification of lipid oxidation. *Arch. Biochem. Biophys.* **372**, 285–294.

Soon C. P., Donnelly P. S., Turner B. J. *et al.* (2011) Diacetylbis(N(4)-methylthiosemicarbazonato) copper(II) (CuII(atsm)) protects against peroxynitrite-induced nitrosative damage and prolongs survival in amyotrophic lateral sclerosis mouse model. *J. Biol. Chem.* **286**, 44035–44044.

Sperlagh B., Vizi E. S., Wirkner K. and Illes P. (2006) P2X7 receptors in the nervous system. *Prog. Neurobiol.* **78**, 327–346.

Ugolini G., Raoul C., Ferri A., Haenggeli C., Yamamoto Y., Salaün D., Henderson C. E., Kato A. C., Pettmann B. and Hueber A. O. (2003) Fas/tumor necrosis factor receptor death signaling is required for axotomy-induced death of motoneurons in vivo. *J. Neurosci.* **23**, 8526–8531.

Wang X., Arcuino G., Takano T. *et al.* (2004) P2X7 receptor inhibition improves recovery after spinal cord injury. *Nat. Med.* **10**, 821–827.

Wiese S., Jablonka S., Holtmann B., Orel N., Rajagopal R., Chao M. V. and Sendtner M. (2007) Adenosine receptor A2A-R contributes to motoneuron survival by transactivating the tyrosine kinase receptor TrkB. *Proc. Natl Acad. Sci. USA* **104**, 17210–17215.

Wu A. S., Kiaei M., Aguirre N., Crow J. P., Calingasan N. Y., Browne S. E. and Beal M. F. (2003) Iron porphyrin treatment extends survival in a transgenic animal model of amyotrophic lateral sclerosis. *J. Neurochem.* **85**, 142–150.

Yiangou Y., Facer P., Durrenberger P., Chessell I. P., Naylor A., Bountra C., Banati R. R. and Anand P. (2006) COX-2, CB2 and P2X7-immunoreactivities are increased in activated microglial cells/macrophages of multiple sclerosis and amyotrophic lateral sclerosis spinal cord. *BMC Neurol.* **6**, 12.

OBJETIVO 4: Estudio del potencial terapéutico de un inhibidor de P2X$_7$ en un modelo animal de ELA

El objetivo 4 se encuentra comprendido en el artículo 3, que se encuentra pronto para su publicación:

Mandi Gandelman, Mark Levy, Luis Barbeito, Joseph Beckman. Systemic administration of the P2X$_7$ inhibitor Brilliant Blue G does not modify disease in SOD1G93A rats.

En los objetivos anteriores encontramos que la señalización a través de P2X$_7$ es capaz de inducir la muerte de motoneuronas de manera directa o mediante la promoción de actividad neurotóxica en los astrocitos. A su vez, los astrocitos SOD1G93A presentan activación basal de P2X$_7$, responsable de su neurotoxicidad innata hacia motoneuronas (Gandelman et al 2010; Gandelman et al, 2013). A raíz de estos hallazgos, nos planteamos que la inhibición de P2X7 en un modelo animal de ELA podría proteger a las motoneuronas y por lo tanto alterar el curso de la enfermedad de manera positiva.

La administración del inhibidor de P2X$_7$ BBG se inició a los 60 días de edad, antes de que las ratas comenzaran a mostrar síntomas de la enfermedad, ya que trabajos previos han mostrado que una proporción significativa de motoneuronas mueren antes de que los animales comiencen a mostrar síntomas. El inicio de la enfermedad es caracterizado por una disminución sutil en la coordinación motora, el balance y la resistencia, que se hacen evidentes mediante el test de rotarod, donde las ratas deben lograr caminar sobre un cilindro que gira sin caerse. No encontramos diferencias estadísticas en la edad en que las ratas en el grupo control y en el grupo tratado con BBG fallaron este test, indicando que la administración de BBG no es

capaz de retardar el inicio de la enfermedad. La duración de la enfermedad y la edad a la muerte tampoco fueron modificadas por el tratamiento con BBG.

El inhibidor de P2X$_7$ BBG ha mostrado resultados prometedores en varios estudios in vivo. A pesar de en el presente estudio la administración de BBG no logró modificar los parámetros estudiados, es posible que un cambios en el protocolo de administración y/o la concentración de BBG revelen su potencial protector en la ELA. Los estudios presentados en los capítulos anteriores de esta tesis establecen al receptor P2X$_7$ como un blanco para modular la inflamación en la médula espinal y proteger las motoneuronas, sin embargo su traducción a un tratamiento que logre una mejoría en la enfermedad in vivo deberá ser investigada de manera más extensa en el futuro.

Systemic administration of the P2X7 inhibitor Brilliant Blue G fails to extend survival in G93A SOD1 ALS rats

Mandi Gandelman[1,2], Mark Levy[1], Luis Barbeito[2], Joseph Beckman[1,3]

[1]Linus Pauling Institute, Department of Biochemistry and Biophysics, Oregon State University, Corvallis, Oregon 97331
[2]Neurodegeneration Laboratory, Institut Pasteur Montevideo, Uruguay
[3]Environmental Health Science Center, Oregon State University, Corvallis, Oregon 97331

ABSTRACT

Accumulating evidence suggests that activation of the P2X7 receptor by extracellular ATP could be involved in the pathogenesis of Amyotrophic Lateral Sclerosis, by directly causing motor neuron death and by aggravating the pro-inflammatory activation of astrocytes and microglia. We tested the hypothesis that sustained delivery of the P2X7 inhibitor Brilliant blue G starting before the onset of symptoms could modify the disease in SOD1G93A rats. We found that BBG did not modify the onset of the disease (119 ± 16 days in the control group vs. 116 ± 13 in the BBG group), progression (10.8 ± 3.1 days in the control group vs. 13.4 ± 4.3 in the BBG group) or survival (134 ± 13 days in the control group vs. 132 ± 15 days in the BBG group). In view of the asbsence of significant protection with BBG newer generation P2X7 inhibitors and alternative delivery protocols should be evaluated to determine whether inhibition of P2X7 has therapeutic potential for ALS patients.

INTRODUCTION

Extracellular ATP acting through the P2X7 receptor has numerous physiological roles in the nervous system, however during disease its activation can have a detrimental role and contribute to the progression of the pathology. Amyotrophic lateral sclerosis (ALS) is a devastating neurological disease, characterized by progressive degeneration of motor neurons accompanied by proinflammatory activation of surrounding microglia and astrocytes. Accumulating evidence suggests that P2X7 could play a role in ALS, activating microglia and astrocytes and also causing motor neuron death directly. In vitro studies have shown that activation of P2X7 receptor in microglia from ALS animal models amplifies their pro-inflammatory response and as a result they become increasingly toxic to neuronal cells (D'Ambrosi et al, 2009, Apolloni et al, 2013). In astrocytes, activation of P2X7 causes them to lose their

trophic properties and become neurotoxic to motor neurons. Astrocytes cultured from SOD1[G93A] animals display a basal activation of P2X7, required to maintain their innate neurotoxicity towards motor neurons. In addition, spinal motor neurons in culture are highly susceptible to P2X7 activation, leading to a signaling cascade fueled by oxidative stress that ends in their death (Gandelman et al 2010, 2013).

Mounting evidence showing the involvement of P2X7 in multiple motor neuron death pathways in ALS animal models prompted us to evaluate the effectiveness of early and sustained treatment with the P2X7 inhibitor BBG in altering the disease features in SOD1[G93A] rats.

MATERIALS AND METHODS

Rats. All animal protocols were conducted in accordance with guidelines established by the Public Health Service (PHS) *Policy on the Humane Care and Use of Laboratory Animals* and were approved by IACUC at Oregon State University. SOD1[G93A] rats (31) on a Sprague–Dawley background were obtained from Taconic (Germantown, NY) and were maintained by breeding SOD1[G93A] male rats with female wild-type animals on a Sprague–Dawley background. Expression of the SOD1[G93A] gene was determined by PCR analysis of tail DNA. Animals were housed 2 per cage in conventional polypropylene cage units under a 12:12hr light:dark cycle. Food and water were provided *ad libitum*. BBG was obtained from Sigma (St. Louis, MO).

At 60 days of age 33 rats were randomized into control (16 rats, 8 males and 8 females) and BBG (17 rats, 9 females and 8 males) treatment groups. The control group was provided with the standard water used by the animal facility and the BBG treatment group was offered water with BBG, adjusted to achieve a dos of 10mg/kg/day. The concentration of BBG was adjusted as needed to account for animal growth and water consumption. BBG has been administered previously through enteral or intraperitoneal route in several animal models, showing that a systemic delivery is a viable route to deliver this compound to the central nervous system (Gourine et al, 2005, Matute et al, 2007, Wang et al, 2004, Cervetto et al, 2013).

Body weight, survival and motor function. Body weight was logged three times weekly, starting at 60 days and continued throughout the lifespan of the animal. For SOD1[G93A] rats followed to end-stage, animals were sacrificed on, and time of death was defined as, the day when the rats had lost 25% of their maximum body weight. Previous observations from our laboratory have shown that at this point disease is very advanced and rats die 4-5 days after.

Disease onset was determined by evaluating the motor function of the animals using the rotarod performance test (TSE instruments, Chesterfield, MO). Rats were trained for a week by using a lower speed and shorter times than used for testing in order for them to become familiar with the test and the apparatus. Testing started at 60 days and was performed 3 times a week for 60 seconds at 20rpm. When rats failed to complete this test in two consecutive sessions disease onset was determined.

Statistics. Cumulative survival and disease onset statistics were calculated using Kaplan-Meier analysis (log rank test). All other analyses were performed using the Student unpaired t-test to compare data between groups of animals. All data are presented as mean ±S.E.M. We used Prism v.4 for statistical analysis.

RESULTS

Water consumption and growth in SOD1^{G93A} rats. BBG was administered starting at 60 days of age by dissolving it in the drinking water offered to rats. Figure 1 shows that addition of BBG did not modify the amount of water the animals ingested. Female rats treated with BBG showed typical weight gain, while male rats failed to achieve a normal growth rate and were in average 32 grams smaller than male rats that were offered water without BBG (table 1).
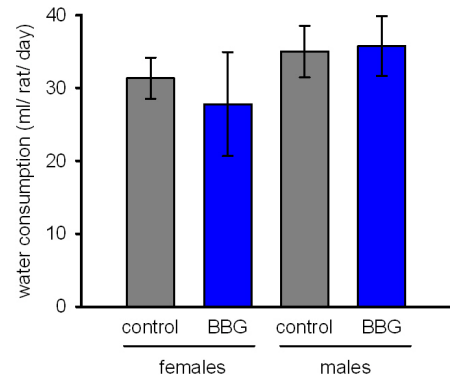
Figure 1. Water consumption in SOD1G93A rats. Average daily water consumption in rats that were offered water with BBG (blue bars) or regular water (gray bars). Means ± SEM are reported.

		peak weight (g)
MALES	control	410.14 ± 26.14
	BBG	378.11 ± 26.40*
FEMALES	control	236.25 ± 26.56
	bbg	229.29 ± 24.10

Table 1. Peak weight achieved by the SOD1^{G93A} rats before the onset of characteristic disease weight decline, categorized by gender and treatment. Peak weight was reduced by an average of 32.03g in males treated with BBG, as compared to the control group. There was no statistically significant difference in peak weight in the female groups. Means ± SEM are reported. * indicates $p < 0.05$.

Disease onset, duration and motor function in SOD1^{G93A} rats was not changed by BBG treatment. The onset of the disease is characterized by the start of a slow decline in weight and subtle motor uncoordination and loss of strength that is made evident by failure to perform the rotarod test. Rats in the control group failed at an average of 119±16 days of life

versus rats that were treated with BBG at 116±13 (Figure 1). The weight of the animals at onset was not significantly different across treatments for each gender (Table 2). Disease progressed equally for the control and treatment groups, and was 10.8±3.1 days long in the control group and 13.4±4.3 days in the BBG group. Table 2 shows there was no significant difference in disease length between males and females.
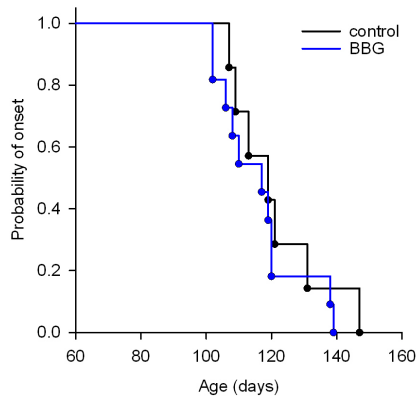
Figure 2. Disease onset in SOD1G93A rats was not modified by treatment with BBG. Control animals (black line) and animals treated with BBG (blue line) showed no statistical difference in their age at disease onset, defined as failure to perform the rotarod test.

		disease progression (days)	weight (g) at rotarod fail
M	control	11.7 ± 3.8	355±18
	BBG	14.0 ± 4.0	362±34
F	control	9.8 ± 2.4	228±71
	bbg	12.7 ± 4.6	204±20

Table 2. Length of disease progression and weight at day of rotarod fail discriminated by treatment group and gender (M – males, F- females). Disease progression was defined as the length of time between rotarod fail and death. Means ± SEM are reported. *$p < 0.05$

Lifespan of SOD1^{G93A} rats was not modified by treatment with BBG. Clinical death of animals in the control group was at 134±13 days and in the BBG group at 132±15 (Figure 3A). There was no significant difference across treatments or gender (Figure 3B and 3C).

DISCUSSION

Despite extensive research, the cause behind motor neuron degeneration in ALS has not been found, and only one drug that ameliorates disease is currently available to patients. Our group has previously shown that activation of P2X7 can cause motor neuron death directly and also by promoting the neurotoxic activities of astrocytes (Gandelman et al, 2010, 2013). We hypotesized that delivery of a P2X7 inhibitor to SOD1^{G93A} rats before the start of the disease could delay the onset and extend the survival by slowing down motor neuron death and decreasing inflammation in the spinal cord.

We found that the BBG administration protocol we tested did not alter the course of the disease in SOD1^{G93A} rats. All variables studied, namely disease onset, length of progression and survival remained unchanged. The P2X7 inhibitor BBG has shown promising results in
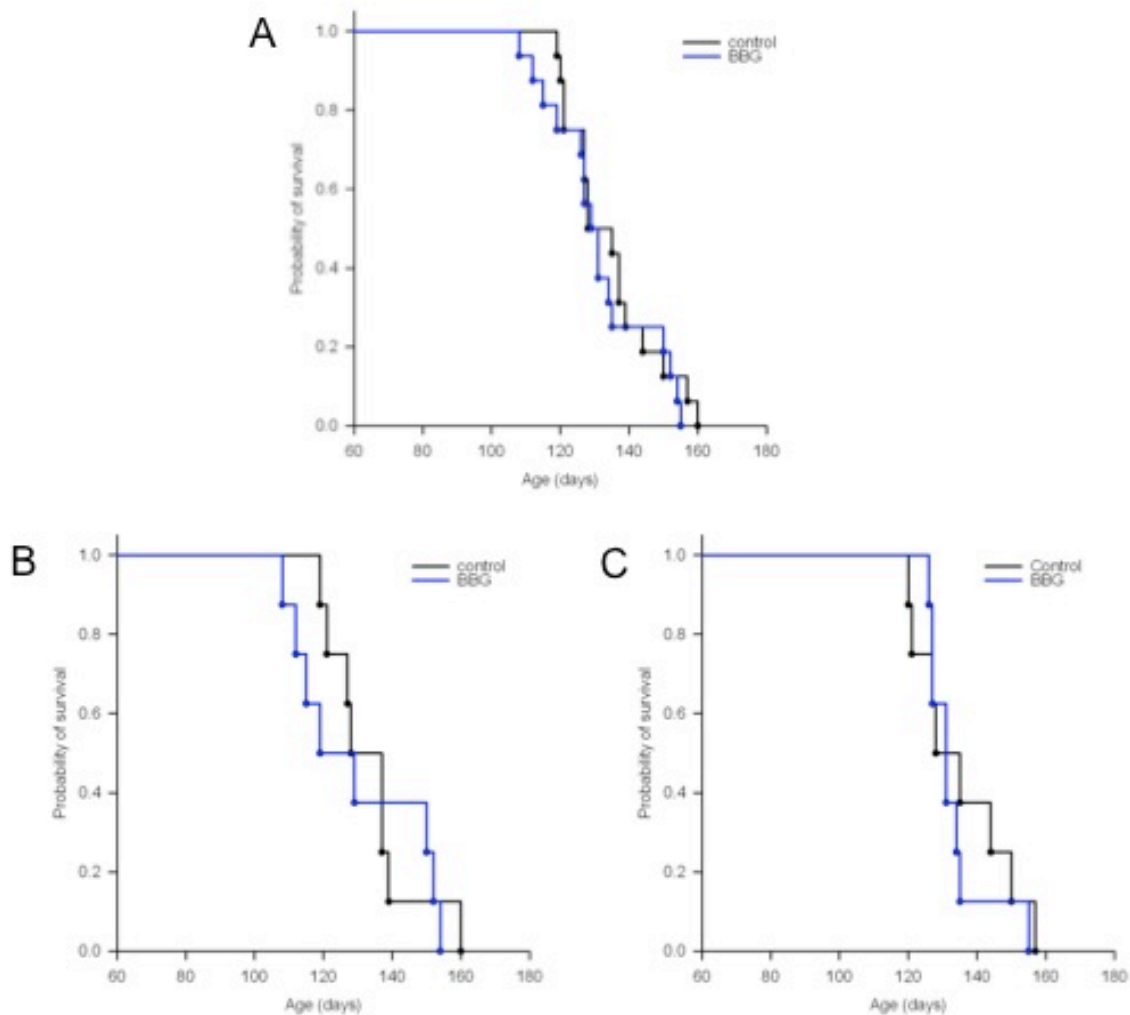
Figure 3 – Survival of BBG-treated or control SOD1G93A rats.
(a) Survival curves for all rats in the control group (black line) or BBG treatment group (blue line). Survival curves for only male (b) or female rats (c) for both treatment groups. Clinical death of animals was defined as the loss of 30% of their body weight.

neurological disease when administered enterally and for a prolonged period of time (Matute et al 2007), however our study was the first one to use such a protocol with SODG93A rats. Different P2X7 inhibitors and delivery routes could be potentially tested to find out if they could efficiently ameliorate the disease. Also, alternative time courses could be tested to find out if there is a critical window of treatment that was missed.

Inhibition of P2X7 is neuroprotective in animal models of traumatic spinal cord injury, experimental autoimmune encephalomyelitis, status epilepticus, and Alzheimer's and Huntington's disease (Matute et al. 2007; Ryu and McLarnon 2008; Diaz-Hernandez et al. 2009, Engel et al, 2012). Clinical trials with P2X7

antagonists are underway for the treatment of chronic inflammatory diseases, including Crohn's disease, rheumatoid arthritis and pain (Elsby et al 2011, Gever et al 2010). Despite the extensive in vitro evidence that points at a multidimensional involvement of P2X7 in death of motor neurons in ALS, in vivo studies have failed to show a clear picture. Genetic ablation of P2X7 in SOD1^{G93A} mice aggravated the ALS pathogenesis, however, life span in females was modestly extended (Apolloni et al, 2013). In a different study, administration of the P2X7 inhibitor BBG soon before disease symptoms start showed a mild amelioration of the disease progression, especially in males, however survival was not modified (Cervetto et al, 2013).

In vitro studies from our group and several others show that P2X7 is a potential target for therapeutic protection in ALS, however this has not been successfully translated to animal models. We did not achieve protection by administering BBG enterally before disease onset and continuing the treatment until the end stages of the disease. However, further research is warranted as new P2X7 antagonists with better pharmacological profiles are being rapidly developed.

REFERENCES

Matute C, Torre I, Pérez-Cerdá F, Pérez-Samartín A, Alberdi E, Etxebarria E, Arranz AM, Ravid R, Rodríguez-Antigüedad A, Sánchez-Gómez M, Domercq M. P2X(7) receptor blockade prevents ATP excitotoxicity in oligodendrocytes and ameliorates experimental autoimmune encephalomyelitis. J Neurosci. 2007 Aug 29;27(35):9525-33

Wang X, Arcuino G, Takano T, Lin J, Peng WG, Wan P, Li P, Xu Q, Liu QS, Goldman SA, Nedergaard M: P2X7 receptor inhibition improves recovery after spinal cord injury. Nat Med 2004, 10:821-827.

Cervetto C, Frattaroli D, Maura G, Marcoli M. Motor neuron dysfunction in a mouse model of ALS: Gender-dependent effect of P2X7 antagonism. Toxicology. 2013 Apr 11

Gourine AV, Poputnikov DM, Zhernosek N, Melenchuk EV, Gerstberger R, Spyer KM, Gourine VN. P2 receptor blockade attenuates fever and cytokine responses induced by lipopolysaccharide in rats. Br J Pharmacol. 2005 Sep;146(1):139-45.

D'Ambrosi, N., Finocchi, P., Apolloni, S., Cozzolino, M., Ferri, A., Padovano, V., Pietrini, G., Carri, M.T. and Volonte, C. (2009) The proinflammatory action of microglial P2 receptors is enhanced in SOD1 models for amyotrophic lateral sclerosis. J. Immunol., 183, 4648-4656.

Apolloni, S., Parisi, C., Pesaresi, M.G., Rossi, S., Carri, M.T., Cozzolino, M., Volonte, C. and D'Ambrosi, N. (2013) The NADPH Oxidase Pathway Is Dysregulated by the P2X7 Receptor in the SOD1-G93A Microglia Model of Amyotrophic Lateral Sclerosis. J. Immunol., 190, 5187-5195.

Elsby, R., Fox, L., Stresser, D., et al.(2011). In vitro risk assessment of AZD9056 perpetrating a transporter-mediated drug-drug interaction with methotrexate. Eur J Pharm

Sci, Vol. 43, No. 1, pp. 41-49, ISSN 1879-0720.

Gever, J. R., Soto, R., Henningsen, R. A., et al.(2010). AF-353, a novel, potent and orally bioavailable P2X3/P2X2/3 receptor antagonist. Br J Pharmacol, Vol. 160, No. 6, pp. 1387-1398, ISSN 1476-5381.

Engel T, Gomez-Villafuertes R, Tanaka K, Mesuret G, Sanz-Rodriguez A, Garcia-Huerta P, Miras-Portugal MT, Henshall DC, Diaz-Hernandez M. Seizure suppression and neuroprotection by targeting the purinergic P2X7 receptor during status epilepticus in mice. FASEB J. 2012 Apr;26(4):1616-28

Diaz-Hernandez, M., Diez-Zaera, M., Sanchez-Nogueiro, J., Gomez-Villafuertes, R., Canals, J. M., Alberch, J., Miras-Portugal, M. T. and Lucas, J. J. (2009) Altered P2X7-receptor level and function in mouse models of Huntington's disease and therapeutic efficacy of antagonist administration. FASEB J, 23, 1893-1906.

DISCUSIÓN

En la serie de trabajos presentados en esta tesis describimos como el incremento en el ATP extracelular puede conducir a la muerte de motoneuronas por activación de los receptores $P2X_7$ tanto en astrocitos como en motoneuronas. La inducción de estrés nitro-oxidativo luego de la activación de $P2X_7$ constituyó un mecanismo común tanto en astrocitos como motoneuronas. Sin embargo, en astrocitos no resultó en su muerte sino en un fenotipo neurotóxico mientras que en motoneuronas resultó en apoptosis. Dada la necesidad de traducir rápidamente nuestros hallazgos a nivel celular en terapias para los pacientes de ELA, estudiamos el potencial de un inhibidor de $P2X_7$ de modificar la enfermedad en un modelo animal de ELA, no obstante, el inhibidor elegido y el protocolo estudiado no resultó en una mejoría, por lo que nuevas estrategias de intervención deberán ser investigadas.

Efectos del ATP extracelular y de la activación de $P2X_7$ en astrocitos espinales

Los astrocitos responden a los insultos agudos y crónicos activándose y adoptando un fenotipo caracterizado por cambios morfológicos, proliferación, disfunción mitocondrial, secreción de factores y citoquinas pro y anti-inflamatorias y la inducción de estrés nitro-oxidativo entre otros (Barbeito *et al.* 2004). La activación de los astrocitos determina una alteración en su interacción con neuronas, glia y células inmunes, que puede ser trófica y pro-regenerativa o perjudicial dependiendo de la injuria y su contexto. En este trabajo mostramos que la exposición de astrocitos espinales en cultivo a ATP indujo su activación y el desarrollo progresivo de un fenotipo neurotóxico caracterizado por la liberación de un factor tóxico difusible para motoneuronas. La gran heterogeneidad de receptores a ATP determina que la respuesta celular se encuentre en gran manera condicionada por la intensidad, duración y distribución del estímulo, así como la presencia de otros eventos de señalización simultáneos. Los estudios in vivo sugieren que durante las

enfermedades neurodegenerativas donde existe un ambiente inflamatorio crónico las neuronas podrían encontrarse expuestas a estímulos por ATP de manera persistente y/o repetida (Wang *et al.* 2004; Matute *et al.* 2007; Burnstock et al, 2014). En el presente estudio mostramos que la estimulación repetida a lo largo del tiempo, incluso con bajas concentraciones de ATP, resulta en el desarrollo progresivo de un fenotipo neurotóxico glial, evidenciado por la muerte de motoneuronas co-cultivadas con estos astrocitos. En contraste, una exposición única al agonista de $P2X_7$ BzATP fue suficiente para generar estos cambios en los astrocitos, indicando que la activación específica de este receptor genera una potente y rápida respuesta de los astrocitos. En pacientes y modelos animales de ELA y Enfermedad de Alzheimer la expresión de este receptor se encuentra aumentada y se ha encontrado que su activación determina respuestas pro-inflamatorias a nivel del sistema inmune y nervioso (Parvathenani *et al.* 2003; Yiangou *et al.* 2006; Burnstock 2014) El influjo de calcio que sigue a su activación podría llevar a la activación de enzimas como la NOS, cicloxigenasa y NADPH oxidasa, resultando en un aumento de ERONs y la inducción de estrés nitro-oxidativo en células vulnerables. Por lo tanto, evidenciamos que el receptor P2X7 en astrocitos constituye un blanco terapéutico para modular las actividades de los astrocitos que llevan a la muerte de motoneuronas espinales en enfermedades como el trauma espinal o la ELA.

La producción de ERONs en respuesta a la activación del receptor $P2X_7$ se encuentra ampliamente documentada en células inmunes y microglía (Suh *et al.* 2001; Hewinson and Mackenzie 2007; Hewinson *et al.* 2008; Kim *et al.* 2007). Nuestro laboratorio ha mostrado previamente que la combinación de superóxido y óxido nítrico formando peroxinitrito determina la activación de los astrocitos y su transición a un fenotipo neurotóxico para motoneuronas adyacentes (Cassina *et al.* 2002; Cassina *et al.* 2005; Vargas *et al.* 2006). En este trabajo mostramos que la activación de P2X7 llevó a la producción de peroxinitrito, derivando en el desarrollo de un fenotipo neurotóxico y la muerte de motoneuronas.

Existen múltiples blancos por los cuáles el estrés nitro-oxidativo es capaz de dañar las células. En Cassina et al. (2008) mostramos que las mitocondrias aisladas de médulas espinales de animales SOD1^{G93A} muestran elevados niveles de proteínas nitradas, evidenciando el daño nitro-oxidativo en estas células (ver apéndice 1). En astrocitos SOD1^{G93A}, la producción de superóxido y peroxinitrito determinó su neurotoxicidad hacia motoneuronas; la modulación de su producción fue capaz de revertir la muerte de motoneuronas causada por los astrocitos SOD1^{G93A}. La administración de un antioxidante dirigido específicamente hacia las mitocondrias de astrocitos SOD1^{G93A} no sólo fue capaz de revertir el daño nitro-oxidativo, sino que además previno la muerte de motoneuronas mediadas por estos astrocitos y restableció la función mitocondrial (Cassina *et al.* 2008, ver apéndice 1). Adicionalmente, el restablecimiento de la función mitocondrial con DCA in vivo fue capaz de extender la sobrevida de animales SOD1^{G93A} y mejorar su desempeño motor (Miquel *et al.* 2012, ver apéndice 1). Es de sumo interés estudiar si la activación de P2X$_7$ y subsiguiente producción de ERONs son responsables de la disfunción mitocondrial observada en animales SOD1^{G93A}. P2X$_7$ podría construir un blanco por el cuál se podría prevenir el daño mitocondrial y por lo tanto proteger a las motoneuronas.

Los astrocitos se encuentran en íntima relación espacial y funcional con las neuronas. Además de interactuar con las neuronas contiguas, los astrocitos activados son capaces de secretar factores pro-inflamatorios, que llevan a la propagación del daño a zonas adyacentes. Incubando a las motoneuronas en cultivo con medios condicionados de astrocitos pre-tratados con ATP mostramos que el insulto con ATP causó la liberación de uno o varios factores al medio extracelular capaces de inducir muerte de motoneuronas. El porcentaje de motoneuronas apoptóticas fue menor cuando fueron expuestas a medio condicionado de astrocitos en comparación con las motoneuronas que fueron directamente co-cultivadas sobre éstos. Esta diferencia podría deberse a la posible degradación de los factores tóxicos en la manipulación y almacenamiento del medio condicionado o podría manifestar la necesidad de contacto íntimo entre los dos tipos celulares para la inducción de la

muerte. Sería de suma importancia identificar el factor difusible capaz de inducir muerte de motoneuronas, ya que constituiría un nuevo blanco para el diseño de terapias que logren prevenir los efectos del ATP extracelular descritos en el presente trabajo.

Rol del ATP en astrocitos SOD1^{G93A}

Estudios previos de nuestro laboratorio y otros muestran que los astrocitos derivados del modelo animal de ELA SOD1^{G93A} presentan un fenotipo neurotóxico que lleva a la muerte de motoneuronas en co-cultivo (Vargas et al. 2006; Nagai et al. 2007; Haidet-Phillips et al. 2011). Debido a que este fenotipo se encuentra perpetuado por el estrés nitro-oxidativo y la señalización pro-inflamatoria autócrina, investigamos si la señalización por P2X$_7$ también podría encontrarse alterada. Notablemente, encontramos que en los astrocitos SOD1^{G93A} el receptor P2X$_7$ se encuentra activado basalmente, determinando su neurotoxicidad para motoneuronas y un incremento en su proliferación. Los mecanismos que determinan esta activación basal no fueron objeto de nuestro estudio, sin embargo podemos hipotetizar que la concentración de ATP extracelular debe encontrarse aumentada a nivel suficiente para activar P2X$_7$. Dado que los canales de panexina son activados en respuesta a la activación del receptor P2X$_7$, y son capaces de liberar ATP al medio extracelular (Dahl 2015; Suadicani *et al.* 2012) es posible que en nuestro modelo éstos podrían ser responsables del aumento observado, liberando ATP en respuesta al aumento de calcio intracelular multifactorial típico de las enfermedades neurodegenerativas de desarrollo prolongado. La densidad y ubicación de los receptores P2X$_7$ en la membrana celular también podría contribuir a las alteraciones vistas.

Encontramos dos evidencias principales de que en los astrocitos SOD1^{G93A} P2X$_7$ se encuentra activado basalmente. Primero, la supresión de la señalización por ATP mediante la inhibición del receptor P2X$_7$ o la hidrólisis del ATP durante los 2 días previos al establecimiento de co-cultivos fue suficiente para prevenir la

neurotoxicidad de los astrocitos SOD1^{G93A}. Éstas intervenciones restablecieron la supervivencia de las motoneuronas, retornando al mismo nivel que en las cultivadas sobre astrocitos no transgénicos. De la misma manera que los astrocitos activados mediante el tratamiento con ATP experimental, encontramos que los astrocitos SOD1^{G93A} son capaces de liberar un factor (o factores) neurotóxico(s) para motoneuronas (Vargas et al., 2006; Nagai et al., 2007). Sería de suma importancia la identificación de éste factor (o factores) para poder bloquear su acción. Asimismo, sería de interés investigar si es posible prevenir su liberación mediante la inhibición de P2X$_7$ o la prevención del aumento del ATP extracelular, posiblemente utilizando inhibidores que tengan a los canales de panexina como blanco.

La segunda evidencia que apoya la activación basal de P2X$_7$ en astrocitos SOD1G93A fue una significativa reducción de su proliferación, normalmente aumentada, mediante la hidrólisis del ATP extracelular por la enzima apirasa. Encontramos que los astrocitos no transgénicos respondieron a la apirasa con un leve aumento de su proliferación, y que a su vez la proliferación no fue completamente revertida en los astrocitos SOD1^{G93A}. Esto podría deberse a las propiedades mitogénicas de la adenosina que fue producida a partir de la hidrólisis del ATP extracelular (Neary *et al.* 1998; Neary *et al.* 2005). La proliferación de los astrocitos SOD1^{G93A} se encuentra aumentada posiblemente en respuesta al ambiente inflamatorio y estrés nitro-oxidativo al que se encuentran sometidos. Sin embargo las vías específicas que determinan este aumento no han sido descritas. Debido a que el ATP es capaz de inducir tanto la respuesta inflamatoria, el estrés nitro-oxidativo y un incremento en la proliferación de astrocitos hipotetizamos que el ATP extracelular podría ser uno de los factores responsables de la elevada proliferación en astrocitos SOD1^{G93A} y nuestros experimentos confirmaron el rol de la señalización purinérgica en esta alteración del metabolismo celular.

Encontramos que los astrocitos SOD1^{G93A} fueron capaces de degradar ATP extracelular más rápidamente que los astrocitos no transgénicos, a niveles comparables con astrocitos activados con LPS o BzATP. Éstos resultados indican

que las alteraciones basales en la señalización por ATP en los astrocitos SOD1^{G93A} no fueron causadas por una disminución en su degradación que permitiría su acumulación extracelular, sino que probablemente se deba a un aumento en su liberación. Existen reportes previos del incremento en la degradación de ATP extracelular asociado al aumento de la actividad de ectonucleotidasas en tejidos nerviosos luego de isquemia aguda y herida punzante cortical (Braun *et al.* 1998; Kegel *et al.* 1997; Zimmermann *et al.* 1998). Este fenómeno reflejaría el intento celular de prevenir la activación de los receptores a ATP que podrían magnificar y expandir el daño tisular, promoviendo el retorno a la homeostasis.

La degradación del ATP extracelular determina el fin de la señalización por ATP y el comienzo de la señalización por sus productos de degradación ADP y adenosina, capaces de activar receptores P2Y y P1. Encontramos que la exposición de astrocitos no transgénicos a ADP, AMP y adenosina resultó en un aumento de su soporte trófico hacia motoneuronas, observándose un aumento en su sobrevida de ≈35% en comparación con controles no tratados. Estos resultados ilustran como el comportamiento de los astrocitos puede ser modulado del rango tóxico al altamente trófico mediante los cambios en el balance de la señalización por ATP y sus productos de degradación ADP y adenosina. De estos hallazgos emerge la importancia de la fina modulación de la liberación del ATP, su degradación y la expresión de variados receptores en la función e integridad del sistema nervioso durante la salud y la enfermedad. A su vez se evidencian una variedad de blancos a distintos niveles para intervenciones terapéuticas que tendrían el mismo fin común, prevenir la activación del receptor P2X$_7$.

En microglía derivada del modelo animal de ELA SOD1^{G93A} se ha observado un aumento en la expresión de P2X$_7$ y una disminución en su habilidad de degradar el ATP extracelular. Esto deriva en una mayor sensibilidad a la estimulación con BzATP, mostrando respuestas pro-inflamatorias mayores que la microglía no transgénica (D'Ambrosi *et al.* 2009; Apolloni *et al.* 2013b; Parisi *et al.* 2013). La

combinación de la señalización aberrante por P2X$_7$ en astrocitos y microglía podría generar un ambiente pro-inflamatorio sostenido y auto-propagado mediante la señalización redundante entre estos dos tipos celulares.

La evidencia acumulada por nuestro grupo y otros indica que la degeneración de motoneuronas en modelos animales de ELA sería iniciada por una disfunción intrínseca de motoneuronas, sin embargo, los astrocitos y la microglía son capaces de modular la intensidad y expansión del daño, por lo que tienen un rol determinante en la progresión y severidad de la enfermedad (Yamanaka *et al.* 2008b; Nagai *et al.* 2007; Vargas *et al.* 2006; Haidet-Phillips *et al.* 2011). La liberación incrementada de ATP por parte de astrocitos SOD1^{G93A} podría no sólo impactar a los astrocitos y las motoneuronas, sino que también podría activar a la microglía y a las células inmunes infiltrantes y perjudicar a oligondendrocitos, alterando completamente el entorno de las motoneuronas.

En nuestro trabajo describimos una disfunción específica en la señalización extracelular de los astrocitos SOD1^{G93A} que determina la muerte de las motoneuronas. La identificación de los mecanismos por los cuáles los astrocitos modulan la sobrevida de las motoneuronas es crucial no sólo para encontrar nuevos fármacos para tratar la ELA sino que también para la terapias de células madre. El reemplazo de las motoneuronas afectadas no sería suficiente, ya que las nuevas células se estarían arraigando en el ambiente neurotóxico dictado por los astrocitos. La modulación de sus actividades neurotóxicas por lo tanto sería crucial para lograr la remisión de la enfermedad mediante la terapia de células madre. El reemplazo de motoneuronas es también considerado dificultoso por sus largos axones y sinápsis neuromusculares establecidas, por lo que el reemplazo de los astrocitos neurotóxicos por astrocitos tróficos derivados de células madre se postula como una alternativa más simple y con beneficios a corto plazo. De hecho, el transplante de precursores gliales en ratones SOD1^{G93A} resulta en su diferenciación en astrocitos, reduciendo la microgliosis y extendiendo la sobrevida de los animales, asociado con mejoras en el desempeño motor (Lepore *et al.* 2011; Lepore and Maragakis 2007).

Efectos del ATP extracelular y la activación de P2X$_7$ en motoneuronas

Teniendo en cuenta que los astrocitos SOD1^{G93A} son capaces de liberar ATP en cantidad suficiente para activar P2X$_7$ autócrinamente, nos planteamos la posibilidad de que el ATP sea capaz de alcanzar a las motoneuronas adyacentes, activando a sus receptores P2X$_7$. A pesar del avance rápido en el conocimiento y de la importancia de la señalización extracelular por ATP y P2X$_7$ en las enfermedades neurológicas, los esfuerzos han sido principalmente enfocados hacia su rol en las células inmunes y gliales, mediadoras de la inflamación, y sus efectos sobre las neuronas no son conocidos (Burnstock 2014). Nuestros principales hallazgos en éste ámbito son resumidos en la figura 9. Encontramos que las motoneuronas espinales son un blanco directo para el ATP extracelular, ya que la activación de P2X$_7$ fue capaz de causar la muerte de un porcentaje significativo de la población de motoneuronas cultivadas. Este efecto fue observado a concentraciones muy bajas de BzATP y fue independiente de la concentración, posiblemente porque las motoneuronas son cultivadas a extremadamente baja densidad, incrementando considerablemente la disponibilidad del BzATP y enlenteciendo su degradación.

Encontramos que la activación de P2X$_7$ en motoneuronas inició una cascada apoptótica dependiente de la producción de peroxinitrito. Ésta vía ha sido previamente descrita como el mecanismo responsable de la muerte de motoneuronas deprivadas de factores tróficos, luego de la activación de p75 y en consecuencia de la expresión de SOD mutante (Pehar *et al.* 2006; Pehar *et al.* 2007; Raoul *et al.* 1999; Raoul *et al.* 2006). La señalización a través de P2X$_7$ fue seguida de un influjo de calcio y activación de p38 MAPK y NOS, derivando en la activación autócrina del receptor Fas en la membrana celular. La activación de Fas es un conocido estímulo que lleva al aumento del nivel de NO celular, generándose así un ciclo que se auto-amplifica y culminó en la muerte de las motoneuronas.

Nuestro grupo y otros han mostrado previamente que el óxido nítrico no causa la muerte de motoneuronas directamente, sino que requiere la producción simultánea de superóxido y su combinación a peroxinitrito, siendo éste el efector del daño nitro-oxidativo, activando la señalización que lleva a la apoptosis (Estévez *et al.* 1998; Sahawneh *et al.* 2010). De hecho, aquí mostramos que las porfirinas consumidoras de superóxido y peroxinitrito y el urato, que previene el daño por nitración, fueron capaces de revertir la apoptosis iniciada por la activación de P2X$_7$. De acuerdo con esto se ha descrito previamente in vivo que los compuestos capaces de consumir peroxinitrito eficazmente protegen a las motoneuronas en modelos animales de ELA, indicando que este mecanismo podría contribuir a la muerte de las motoneuronas in vivo.

In vivo, el rol de Fas en la estimulación de la producción de peroxinitrito se ha estudiado en la ELA, isquemia espinal, axotomía del nervio facial, avulsión de nervio sacro y trauma de médula espinal (Matsushita et al. 2000; Sakurai et al. 1998; Ugolini et al. 2003; Demjen et al. 2004; Casha et al. 2005). El silenciamiento de Fas en el médula espinal de modelos animales de ELA mejora su desempeño motor y extiende su sobrevida (Locatelli et al. 2007). Luego de trauma de médula espinal, la inhibición de Fas protege a las neuronas y axones adyacentes a la zona del trauma (Casha et al. 2005; Demjen et al. 2004). En el presente trabajo mostramos que el receptor P2X$_7$ es capaz de activar la vía de muerte de Fas a través de la producción de peroxinitrito. Es posible que la activación de P2X$_7$-Fas se encuentre implicada in vivo en las patologías mencionadas, donde existe activación de Fas y muerte neuronal. La investigación de su participación en la cascada de muerte in vivo es de sumo interés y podría significar el hallazgo de un nuevo blanco terapéutico para múltiples patologías.

Desde la publicación de los resultados donde describimos la vía de P2X$_7$-Fas en la muerte de motoneuronas, esta vía ha sido implicada en la muerte de motoneuronas causada por HSP90 nitrada por un laboratorio asociado (Franco *et al.* 2013; Franco *et al.* 2015). HSP90 nitrada se forma en consecuencia de la exposición de HSP90 a

peroxinitrito. Ésta modificación determina un cambio de su típica función reparadora a pro-apoptótica. La forma nitrada de HSP90 es capaz de estimular el receptor $P2X_7$, generando un influjo de calcio que moviliza vesículas intracelulares conteniendo FasL hacia la membrana extracelular, activando el receptor Fas y causando la muerte de las motoneuronas. La forma nitrada de HSP90 se ha encontrado in vivo en modelos de ALS y trauma de médula espinal, por lo que estos hallazgos constituyen un avance en la identificación de los efectores específicos de la muerte celular en condiciones de estrés nitro-oxidativo y las vías implicadas.

Luego de caracterizados los efectos de la activación específica de $P2X_7$ en motoneuronas, nos preguntamos cómo se traducen estos hallazgos frente a su estimulación con su agonista endógeno, ATP. Concentraciones altas de ATP no fueron capaces de inducir la muerte de motoneuronas, mientras que concentraciones más bajas causaron la muerte a niveles comparables con el BzATP. Encontramos que la degradación de concentraciones altas de ATP adicionadas al medio de cultivo fueron capaces de generar suficiente adenosina para activar los receptores a adenosina (receptores P1 o A) y prevenir la muerte por activación de $P2X_7$. La adenosina posee un conocido rol anti-inflamatorio y neuroprotector. En motoneuronas en específico, la adenosina activando el receptor A_{2A} lleva a la transactivación del receptor TrkB, capaz de prevenir la muerte en modelos de deprivación de factores tróficos y axotomía de nervio facial (Wiese *et al.* 2007). Adicionalmente, la activación de A_{2A} reduce la apoptosis neuronal y el déficit neurológico luego del trauma a la médula espinal (Genovese *et al.* 2010). Tanto los antagonistas de $P2X_7$ como los agonistas de A_{2A} son capaces de proteger a las motoneuronas luego del trauma espinal, sin embargo la conexión entre estos dos eventos de señalización no había sido descrita previa a nuestro trabajo (Wang *et al.* 2004; Peng *et al.* 2009; Genovese *et al.* 2010). Nuestros resultados muestran que las enzimas responsables de la degradación del ATP extracelular poseen un importante rol en la modulación de la señalización por ATP y sus metabolitos, pudiendo tanto detener la muerte de motoneuronas mediante la prevención de la señalización por $P2X_7$ como estimular su sobrevida a través de la producción de adenosina.
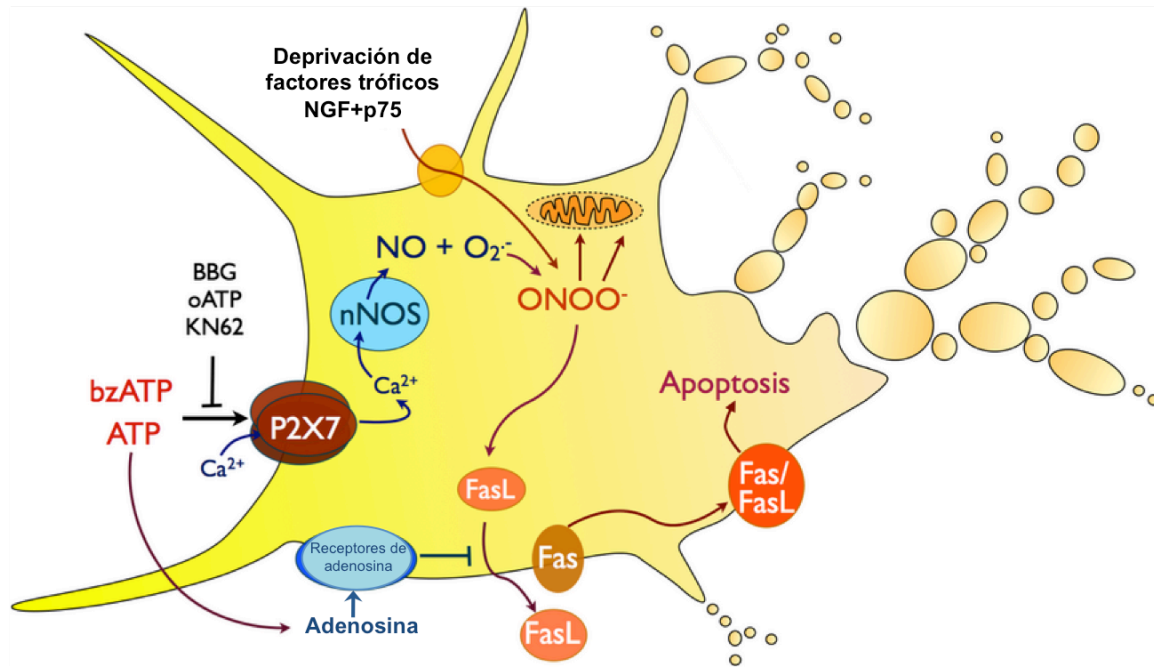
Figura 9 – **Mecanismos de muerte de motoneuronas por activación de P2X$_7$.** El ATP y BzATP son capaces de activar el receptor P2X$_7$ en la superficie de las motoneuronas, provocando un aumento en el calcio intracelular que activa la enzima nNOS y lleva a la producción de peroxinitrito. La mitocondria es blanco del peroxinitrito, iniciando una cascada de daño intracelular que deriva en la liberación de FasL y la activación autócrina de Fas, resultando en apoptosis. La señalización a través de los receptores de adenosina es capaz de interferir con la señalización proapoptótica e impedir la muerte de las motoneuronas. Modificado de Gandelman et al, 2013.

Inhibición sistémica de P2X$_7$ en un modelo animal de ELA

Nuestros extensos hallazgos que muestran el rol del ATP y el receptor P2X$_7$ en la activación de los astrocitos y la muerte de motoneuronas nos impulsaron a estudiar los efectos de la inhibición de P2X$_7$ in vivo en un modelo animal de ELA, las ratas SOD1^{G93A}. Debido a que la activación de P2X$_7$ cumple principalmente un rol pro-inflamatorio en células inmunes y gliales, y ésta se presenta tempranamente en los animales SOD1^{G93A}, administramos el inhibidor de P2X$_7$ desde el destete de las ratas a los 60 días de vida. A esta edad se observan las primeras alteraciones a nivel

celular y tisular, y los síntomas motores se detectan clínicamente alrededor de 2 meses después.

Encontramos que la administración de BBG no fue capaz de alterar el curso de la enfermedad en las ratas SOD1^{G93A}. Tanto la edad al inicio de la enfermedad, su progresión y la edad a la muerte clínica no difirieron del grupo control. El inhibidor BBG ha mostrado resultados alentadores en variados modelos animales de condiciones neurológicas, incluyendo trauma de médula espinal, enfermedad de Alzheimer y Parkinson, migrañas y la encefalitis autoinmune experimental (Wang *et al.* 2004; Chen *et al.* 2014; Carmo *et al.* 2014; Göröncsér and Sperlágh 2014; Matute *et al.* 2007). En Matute et al (2007), un protocolo de administración similar al utilizado en el presente estudio (con vía de administración enteral y a largo plazo) mostró la ausencia de efectos tóxicos y una alta eficacia en la prevención del daño neurológico en un modelo de EAE. En un modelo de trauma espinal, la administración de BBG resultó altamente protectora para las motoneuronas adyacentes al área dañada (Wang *et al.* 2004).

El BBG atraviesa la barrera hematoencefálica y no ha mostrado efectos tóxicos, incluso luego de su administración sistémica y prolongada, por lo que es un excelente candidato farmacológico (Matute *et al.* 2007; Apolloni *et al.* 2014; Cervetto *et al.* 2013). Sin embargo, existen numerosos inhibidores de P2X$_7$ en desarrollo y etapa de prueba por parte de múltiples corporaciones farmacéuticas, y se propone que tendrían el potencial de ser los anti-inflamatorios y analgésicos de cuarta generación.

En modelos de ELA los estudios de la inhibición de P2X$_7$ son escasos e inconcluyentes. La ablación genética de P2X$_7$ en ratones SOD1^{G93A} agravó la enfermedad, sin embargo las hembras vieron su sobrevida modestamente extendida (Apolloni *et al.* 2013b; Apolloni *et al.* 2013a; Cervetto *et al.* 2013). La administración de BBG iniciada poco antes de los primeros síntomas fue capaz de reducir la inflamación y retrasar la muerte de las motoneuronas, resultando en el inicio tardío

de síntomas motores, sin embargo esta intervención no logró extender la sobrevida de los animales (Apolloni *et al.* 2014). Nuestras investigaciones en animales SOD1G93A y las de otros grupos indican que dadas las variadas funciones y extensa distribución de P2X7 existe un amplio rango de resultados posibles frente a su inhibición. La evidencia actual indica que el receptor P2X7 cumpliría un rol en la modulación de la inflamación adaptativa y protectora observada en etapas pre-clínicas y en la inflamación perjudicial observada en las etapas más avanzadas de la enfermedad.

Sería necesaria la investigación de múltiples inhibidores y la diversificación de protocolos de administración para ganar un conocimiento más profundo que permita iniciar estudios clínicos en pacientes de ELA. La naturaleza multisistémica y multifactorial tanto de la ELA como de la señalización purinérgica determinan que su modulación pueda generar respuestas complejas, que deben ser estudiadas en profundidad para ganar el conocimiento necesario para combatir la ELA.

CONCLUSIONES

La alta diversidad y especialización de la señalización extracelular purinérgica determina sus múltiples roles durante la función celular y tisular normal. Estos mismos atributos determinan que su contribución durante la enfermedad sea compleja y de alta importancia. Como señal extracelular proinflamatoria y proapotótica, contribuye a la propagación y amplificación del daño o disfunción original, constituyendo un blanco terapéutico por el cuál detener la expansión y profundización de enfermedades cuya causa primordial no es conocida.

En los trabajos presentados en esta tesis contribuimos específicamente al conocimiento de las consecuencias de la señalización purinérgica en astrocitos y motoneuronas espinales. En la figura 10 se esquematizan y resumen los principales hallazgos presentados en esta tesis y se describe nuestra hipótesis global sobre los efectos del ATP en el diálogo bidireccional de las células estudiadas. Encontramos que el receptor $P2X_7$ cumple una función central, determinado la activación neurotóxica de astrocitos e iniciando una cascada apoptótica en motoneuronas. La inducción de estrés nitro-oxidativo a través de la producción de peroxinitrito constituyó un mecanismo común en los dos tipos celulares estudiados.

En astrocitos derivados del modelo animal $SOD1^{G93A}$, encontramos una desregulación basal de la señalización autócrina por ATP, que determinó su neurotoxicidad hacia motoneuronas y alta tasa de proliferación. En la ELA las células que rodean a las motoneuronas son capaces de determinar su muerte o sobrevida, indicando que el estado astrocitario y la comunicación extracelular cumplen un rol vital. Nuestros hallazgos aportan al conocimiento de los mecanismos específicos por los cuáles los astrocitos son capaces de modular la sobrevida de las motoneuronas..

En motoneuronas, describimos la cascada de señalización que sigue a la activación de $P2X_7$, encontrando que la activación del receptor de membrana Fas y la amplificación de la producción de peroxinitrito determinó su muerte por apoptosis. La vía de Fas se encuentra implicada en la muerte de motoneuronas in vivo en modelos animales de ELA y su inhibición es capaz de proteger a las motoneuronas. Nuestros resultados en astrocitos SOD1^{G93A} revelan el potencial rol de los astrocitos en la activación de esta vía, mostrando un mecanismo específico por el cual los astrocitos influencian la sobrevida de las motoneuronas adyacentes. El conocimiento en profundidad de las señales purinérgicas que determinan la degeneración de las motoneuronas ofrecería nuevos blancos para desarrollar fármacos capaces de interceptar y detener estas señales antes de que encuentren sus efectores.
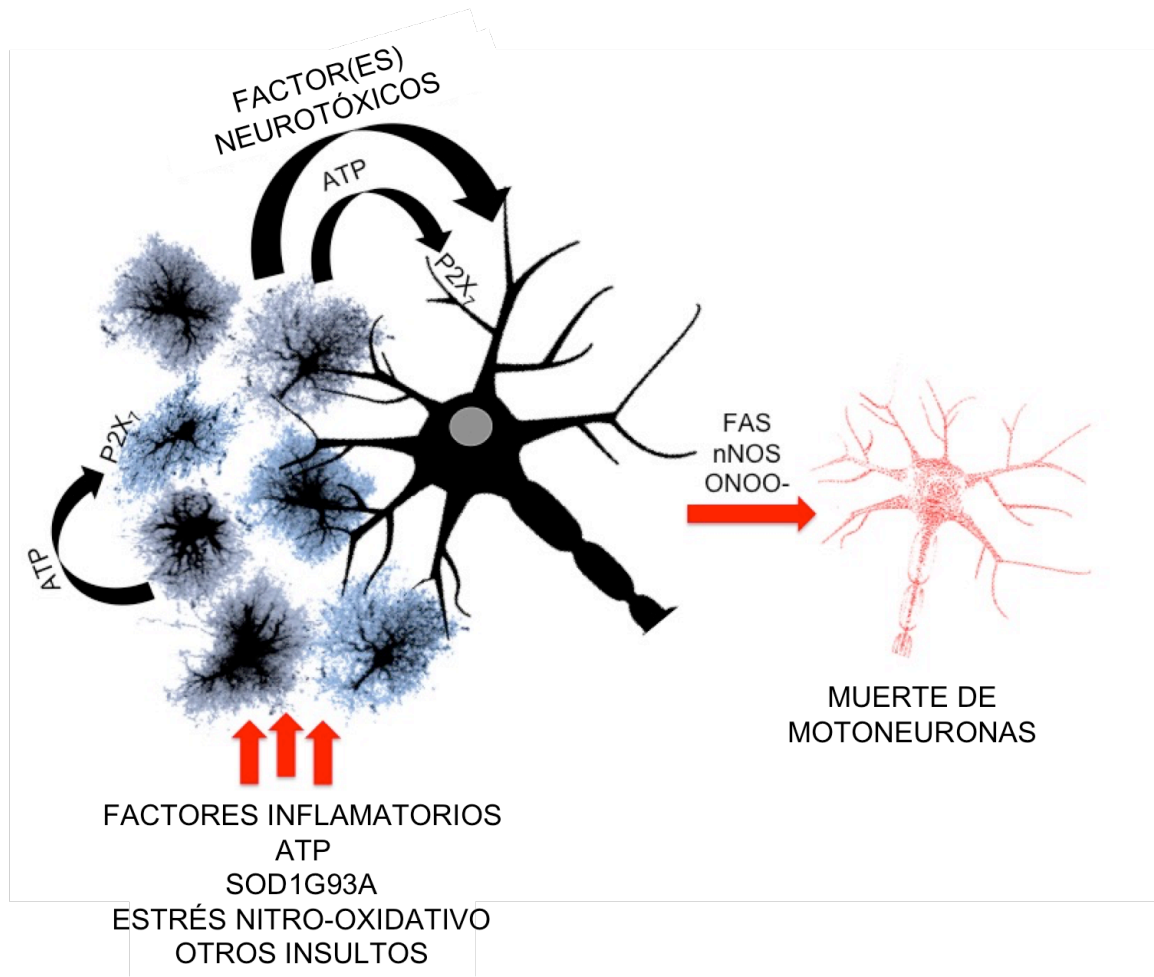
Fig 10. Esquema representativo de los efectos de la activación de P2X₇ para astrocitos y motoneuronas. Múltiples insultos son capaces de activar a los astrocitos, estimulando la liberación de ATP y su señalización a través de P2X₇ en los mismos astrocitos. Ésto provoca la liberación de un factor neurotóxico que induce la muerte de motoneuronas. El ATP liberado por los astrocitos también sería capaz de activar el receptor P2X₇ en motoneuronas, determinando la activación de la vía autoamplificante de FAS/NOS que causa la muerte de motoneuronas.

Bibliografía

Abe K., Pan L. H., Watanabe M., Kato T., Itoyama Y. (1995) Induction of nitrotyrosine-like immunoreactivity in the lower motor neuron of amyotrophic lateral sclerosis. *Neurosci. Lett.* **199**, 152–4.

Abramov A. Y., Jacobson J., Wientjes F., Hothersall J., Canevari L., Duchen M. R. (2005) Expression and modulation of an NADPH oxidase in mammalian astrocytes. *J. Neurosci.* **25**, 9176–84.

Anderson C. M., Bergher J. P., Swanson R. A. (2004) ATP-induced ATP release from astrocytes. *J. Neurochem.* **88**, 246–56.

Apolloni S., Amadio S., Montilli C., Volonté C., D'Ambrosi N. (2013a) Ablation of P2X7 receptor exacerbates gliosis and motoneuron death in the SOD1-G93A mouse model of amyotrophic lateral sclerosis. *Hum. Mol. Genet.* **22**, 4102–16.

Apolloni S., Amadio S., Parisi C., Matteucci A., Potenza R. L., Armida M., Popoli P., D'Ambrosi N., Volonté C. (2014) Spinal cord pathology is ameliorated by P2X7 antagonism in a SOD1-mutant mouse model of amyotrophic lateral sclerosis. *Dis. Model. Mech.* **7**, 1101–9.

Apolloni S., Montilli C., Finocchi P., Amadio S. (2009) Membrane compartments and purinergic signalling: P2X receptors in neurodegenerative and neuroinflammatory events. *FEBS J.* **276**, 354–64.

Apolloni S., Parisi C., Pesaresi M. G., Rossi S., Carrì M. T., Cozzolino M., Volonté C., D'Ambrosi N. (2013b) The NADPH oxidase pathway is dysregulated by the P2X7 receptor in the SOD1-G93A microglia model of amyotrophic lateral sclerosis. *J. Immunol.* **190**, 5187–95.

Arbeloa J., Pérez-Samartín A., Gottlieb M., Matute C. (2012) P2X7 receptor blockade prevents ATP excitotoxicity in neurons and reduces brain damage after ischemia. *Neurobiol. Dis.* **45**, 954–61.

Avignone E., Ulmann L., Levavasseur F., Rassendren F., Audinat E. (2008) Status epilepticus induces a particular microglial activation state characterized by enhanced purinergic signaling. *J. Neurosci.* **28**, 9133–44.

Bal-Price A., Moneer Z., Brown G. C. (2002) Nitric oxide induces rapid, calcium-dependent release of vesicular glutamate and ATP from cultured rat astrocytes. *Glia* **40**, 312–23.

Barbeito L. H., Pehar M., Cassina P., Vargas M. R., Peluffo H., Viera L., Estévez A. G., Beckman J. S. (2004) A role for astrocytes in motor neuron loss in amyotrophic lateral sclerosis. *Brain Res. Rev.* **47**, 263–274.

Barrera N. P., Ormond S. J., Henderson R. M., Murrell-Lagnado R. D., Edwardson J. M. (2005) Atomic force microscopy imaging demonstrates that P2X2 receptors are trimers but that P2X6 receptor subunits do not oligomerize. *J. Biol. Chem.* **280**, 10759–65.

Beal M. F., Ferrante R. J., Browne S. E., Matthews R. T., Kowall N. W., Brown R. H. (1997) Increased 3-nitrotyrosine in both sporadic and familial amyotrophic lateral sclerosis. *Ann. Neurol.* **42**, 644–54.

Beckman J. S. (2002) Protein tyrosine nitration and peroxynitrite. *FASEB J.* **16**, 1144–1144.

Beckman J. S., Beckman T. W., Chen J., Marshall P. A., Freeman B. A. (1990) Apparent hydroxyl radical production by peroxynitrite: implications for endothelial injury from nitric oxide and superoxide. *Proc. Natl. Acad. Sci. U. S. A.* **87**, 1620–4.

Beckman J. S., Carson M., Smith C. D., Koppenol W. H. (1993) ALS, SOD and peroxynitrite. *Nature* **364**, 584–584.

Beckman J. S., Chen J., Ischiropoulos H., Crow J. P. (1994) Oxidative chemistry of peroxynitrite. *Methods Enzymol.* **233**, 229–240.

Beers D. R., Zhao W., Liao B., Kano O., Wang J., Huang A., Appel S. H., Henkel J. S. (2011) Neuroinflammation modulates distinct regional and temporal clinical responses in ALS mice. *Brain. Behav. Immun.* **25**, 1025–35.

Bennett M. V. L., Garré J. M., Orellana J. A., Bukauskas F. F., Nedergaard M., Sáez J. C. (2012) Connexin and pannexin hemichannels in inflammatory responses of glia and neurons. *Brain Res.* **1487**, 3–15.

Bjelobaba I., Parabucki A., Lavrnja I., Stojkov D., Dacic S., Pekovic S., Rakic L., Stojiljkovic M., Nedeljkovic N. (2011) Dynamic changes in the expression pattern of ecto-5'-nucleotidase in the rat model of cortical stab injury. *J. Neurosci. Res.* **89**, 862–73.

Braganhol E., Wink M. R., Lenz G., Battastini A. M. O. (2013) Purinergic signaling in glioma progression. *Adv. Exp. Med. Biol.* **986**, 81–102.

Braun N., Lenz C., Gillardon F., Zimmermann M., Zimmermann H. (1997) Focal cerebral ischemia enhances glial expression of ecto-5'-nucleotidase. *Brain Res.* **766**, 213–26.

Braun N., Zhu Y., Krieglstein J., Culmsee C., Zimmermann H. (1998) Upregulation of the enzyme chain hydrolyzing extracellular ATP after transient forebrain ischemia in the rat. *J. Neurosci.* **18**, 4891–900.

Browne S. E. (2013) When too much ATP is a bad thing: A pivotal role for P2X7 receptors in motor neuron degeneration. *J. Neurochem.* **126**, 301–304.

Bruzzone S., Guida L., Zocchi E., Franco L., Flora A De (2001) Connexin 43 hemi channels mediate Ca2+-regulated transmembrane NAD+ fluxes in intact cells. *FASEB J.* **15**, 10–12.

Burnstock G. (1972) Purinergic nerves. *Pharmacol. Rev.* **24**, 509–81.

Burnstock G. (2006) Purinergic signalling. *Br. J. Pharmacol.* **147 Suppl**, S172–81.

Burnstock G. (2014) Purinergic signalling: from discovery to current developments. *Exp. Physiol.* **99**, 16–34.

Burnstock G. (2015) An introduction to the roles of purinergic signalling in neurodegeneration, neuroprotection and neuroregeneration. *Neuropharmacology.*

Butovsky O., Jedrychowski M. P., Cialic R., Krasemann S., Murugaiyan G., Fanek Z., Greco D. J., et al. (2015) Targeting miR-155 restores abnormal microglia and attenuates disease in SOD1 mice. *Ann. Neurol.* **77**, 75–99.

Carmo M. R. S., Menezes A. P. F., Nunes A. C. L., Pliássova A., Rolo A. P., Palmeira C. M., Cunha R. A., Canas P. M., Andrade G. M. (2014) The P2X7 receptor antagonist Brilliant Blue G attenuates contralateral rotations in a rat model of Parkinsonism through a combined control of synaptotoxicity, neurotoxicity and gliosis. *Neuropharmacology* **81**, 142–152.

Casanovas A., Hernández S., Tarabal O., Rosselló J., Esquerda J. E. (2008) Strong P2X4 purinergic receptor-like immunoreactivity is selectively associated with degenerating neurons in transgenic rodent models of amyotrophic lateral sclerosis. *J. Comp. Neurol.* **506**, 75–92.

Casha S., Yu W. R., Fehlings M. G. (2005) FAS deficiency reduces apoptosis, spares axons and improves function after spinal cord injury. *Exp. Neurol.* **196**, 390–400.

Cassina P., Cassina A., Pehar M., Castellanos R., Gandelman M., León A. de, Robinson K. M., et al. (2008) Mitochondrial dysfunction in SOD1G93A-bearing astrocytes promotes motor neuron degeneration: prevention by mitochondrial-targeted antioxidants. *J. Neurosci.* **28**, 4115–4122.

Cassina P., Pehar M., Vargas M. R., Castellanos R., Barbeito A. G., Estevez A. G., Thompson J. A., Beckman J. S., Barbeito L. (2005) Astrocyte activation by fibroblast growth factor-1 and motor neuron apoptosis: implications for amyotrophic lateral sclerosis. *J. Neurochem.* **93**, 38–46.

Cassina P., Peluffo H., Pehar M., Martinez-Palma L., Ressia A., Beckman J. S., Estévez A. G., Barbeito L. (2002) Peroxynitrite triggers a phenotypic transformation in spinal cord astrocytes that induces motor neuron apoptosis. *J. Neurosci. Res.* **67**, 21–9.

Cavaliere F., Amadio S., Sancesario G., Bernardi G., Volonté C. (2004) Synaptic P2X7 and oxygen/glucose deprivation in organotypic hippocampal cultures. *J. Cereb. Blood Flow Metab.* **24**, 392–8.

Cavaliere F., Dinkel K., Reymann K. (2005) Microglia response and P2 receptor participation in oxygen/glucose deprivation-induced cortical damage. *Neuroscience* **136**, 615–23.

Cervetto C., Frattaroli D., Maura G., Marcoli M. (2013) Motor neuron dysfunction in a mouse model of ALS: gender-dependent effect of P2X7 antagonism. *Toxicology* **311**, 69–77.

Chen L., Brosnan C. F. (2006) Exacerbation of experimental autoimmune encephalomyelitis in P2X7R-/- mice: evidence for loss of apoptotic activity in lymphocytes. *J. Immunol.* **176**, 3115–26.

Chen X., Hu J., Jiang L., Xu S., Zheng B., Wang C., Zhang J., Wei X., Chang L., Wang Q. (2014) Brilliant Blue G improves cognition in an animal model of Alzheimer's disease and inhibits amyloid-β-induced loss of filopodia and dendrite spines in hippocampal neurons. *Neuroscience* **279**, 94–101.

Cherian P. P., Siller-Jackson A. J., Gu S., Wang X., Bonewald L. F., Sprague E., Jiang J. X. (2005) Mechanical strain opens connexin 43 hemichannels in osteocytes: a novel mechanism for the release of prostaglandin. *Mol. Biol. Cell* **16**, 3100–6.

Chever O., Lee C.-Y., Rouach N. (2014) Astroglial connexin43 hemichannels tune basal excitatory synaptic transmission. *J. Neurosci.* **34**, 11228–32.

Cruz C. M., Rinna A., Forman H. J., Ventura A. L. M., Persechini P. M., Ojcius D. M. (2006) ATP Activates a Reactive Oxygen Species-dependent Oxidative Stress Response and Secretion of Proinflammatory Cytokines in Macrophages. *J. Biol. Chem.* **282**, 2871–2879.

D'Ambrosi N., Finocchi P., Apolloni S., Cozzolino M., Ferri A., Padovano V., Pietrini G., Carrì M. T., Volonté C. (2009) The proinflammatory action of microglial P2 receptors is enhanced in SOD1 models for amyotrophic lateral sclerosis. *J. Immunol.* **183**, 4648–56.

Dahl G. (2015) ATP release through pannexon channels. *Philos. Trans. R. Soc. Lond. B. Biol. Sci.* **370**.

Daré E., Schulte G., Karovic O., Hammarberg C., Fredholm B. B. (2007) Modulation of glial cell functions by adenosine receptors. *Physiol. Behav.* **92**, 15–20.

Davalos D., Grutzendler J., Yang G., Kim J. V, Zuo Y., Jung S., Littman D. R., Dustin M. L., Gan W.-B. (2005) ATP mediates rapid microglial response to local brain injury in vivo. *Nat. Neurosci.* **8**, 752–8.

Delarasse C., Auger R., Gonnord P., Fontaine B., Kanellopoulos J. M. (2011) The purinergic receptor P2X7 triggers alpha-secretase-dependent processing of the amyloid precursor protein. *J. Biol. Chem.* **286**, 2596–606.

Demjen D., Klussmann S., Kleber S., Zuliani C., Stieltjes B., Metzger C., Hirt U. A., et al. (2004) Neutralization of CD95 ligand promotes regeneration and functional recovery after spinal cord injury. *Nat. Med.* **10**, 389–395.

Díaz-Hernández M., Díez-Zaera M., Sánchez-Nogueiro J., Gómez-Villafuertes R., Canals J. M., Alberch J., Miras-Portugal M. T., Lucas J. J. (2009) Altered P2X7-receptor level and function in mouse models of Huntington's disease and therapeutic efficacy of antagonist administration. *FASEB J.* **23**, 1893–906.

Domercq M., Perez-Samartin A., Aparicio D., Alberdi E., Pampliega O., Matute C. (2010) P2X7 receptors mediate ischemic damage to oligodendrocytes. *Glia* **58**, 730–40.

Engel T., Jimenez-Pacheco A., Miras-Portugal M. T., Diaz-Hernandez M., Henshall D. C. (2012) P2X7 receptor in epilepsy; role in pathophysiology and potential targeting for seizure control. *Int. J. Physiol. Pathophysiol. Pharmacol.* **4**, 174–87.

Estévez A. G., Spear N., Manuel S. M., Radi R., Henderson C. E., Barbeito L., Beckman J. S. (1998) Nitric oxide and superoxide contribute to motor neuron apoptosis induced by trophic factor deprivation. *J. Neurosci.* **18**, 923–31.

Färber K., Markworth S., Pannasch U., Nolte C., Prinz V., Kronenberg G., Gertz K., et al. (2008) The ectonucleotidase cd39/ENTPDase1 modulates purinergic-mediated microglial migration. *Glia* **56**, 331–41.

Ferrante R. J., Browne S. E., Shinobu L. A., Bowling A. C., Baik M. J., MacGarvey U., Kowall N. W., Brown R. H., Beal M. F. (1997) Evidence of increased oxidative damage in both sporadic and familial amyotrophic lateral sclerosis. *J. Neurochem.* **69**, 2064–74.

Feuvre R. A. Le, Brough D., Touzani O., Rothwell N. J. (2003) Role of P2X7 receptors in ischemic and excitotoxic brain injury in vivo. *J. Cereb. Blood Flow Metab.* **23**, 381–4.

Franco M. C., Ricart K. C., Gonzalez A. S., Dennys C. N., Nelson P. A., Janes M. S., Mehl R. A., Landar A., Estévez A. G. (2015) Nitration of Hsp90 on Tyrosine 33 Regulates Mitochondrial Metabolism. *J. Biol. Chem.* **290**, 19055–66.

Franco M. C., Ye Y., Refakis C. A., Feldman J. L., Stokes A. L., Basso M., Melero
    Fernandez de Mera R. M., et al. (2013) Nitration of Hsp90 induces cell death.
    Proc. Natl. Acad. Sci. **110**, E1102–E1111.

Franke H., Günther A., Grosche J., Schmidt R., Rossner S., Reinhardt R., Faber-
    Zuschratter H., Schneider D., Illes P. (2004) P2X7 receptor expression after
    ischemia in the cerebral cortex of rats. *J. Neuropathol. Exp. Neurol.* **63**, 686–99.

Gandelman M., Levy M., Cassina P., Barbeito L., Beckman J. S. (2013) P2X7 receptor-
    induced death of motor neurons by a peroxynitrite/FAS- dependent pathway. *J.
    Neurochem.* **126**, 382–388.

Gandelman M., Peluffo H., Beckman J. S., Cassina P., Barbeito L. (2010) Extracellular
    ATP and the P2X7 receptor in astrocyte-mediated motor neuron death:
    implications for amyotrophic lateral sclerosis. *J Neuroinflammation* **7**, 33.

Gao X.-F., Wang W., Yu Q., Burnstock G., Xiang Z.-H., He C. (2011) Astroglial P2X7
    receptor current density increased following long-term exposure to rotenone.
    Purinergic Signal. **7**, 65–72.

Genovese T., Melani A., Esposito E., Paterniti I., Mazzon E., Paola R. Di, Bramanti P.,
    Linden J., Pedata F., Cuzzocrea S. (2010) Selective adenosine A(2a) receptor
    agonists reduce the apoptosis in an experimental model of spinal cord trauma.
    J. Biol. Regul. Homeost. Agents **24**, 73–86.

Giaume C., Leybaert L., Naus C. C., Sáez J. C. (2013) Connexin and pannexin
    hemichannels in brain glial cells: properties, pharmacology, and roles. *Front.
    Pharmacol.* **4**, 88.

Gölöncsér F., Sperlágh B. (2014) Effect of genetic deletion and pharmacological
    antagonism of P2X7 receptors in a mouse animal model of migraine. *J.
    Headache Pain* **15**, 24.

Gong Y. H., Parsadanian A. S., Andreeva A., Snider W. D., Elliott J. L. (2000) Restricted
    expression of G86R Cu/Zn superoxide dismutase in astrocytes results in
    astrocytosis but does not cause motoneuron degeneration. *J. Neurosci.* **20**, 660–
    5.

Gourine A. V, Dale N., Llaudet E., Poputnikov D. M., Spyer K. M., Gourine V. N. (2007)
    Release of ATP in the central nervous system during systemic inflammation:
    real-time measurement in the hypothalamus of conscious rabbits. *J. Physiol.*
    585, 305–16.

Gurney M. E., Pu H., Chiu A. Y., Dal Canto M. C., Polchow C. Y., Alexander D. D.,
    Caliendo J., Hentati A., Kwon Y. W., Deng H. X. (1994) Motor neuron
    degeneration in mice that express a human Cu,Zn superoxide dismutase
    mutation. *Science* **264**, 1772–5.

Guthrie P. B., Knappenberger J., Segal M., Bennett M. V, Charles A. C., Kater S. B.
    (1999) ATP released from astrocytes mediates glial calcium waves. *J. Neurosci.*
    19, 520–8.

Haidet-Phillips A. M., Hester M. E., Miranda C. J., Meyer K., Braun L., Frakes A., Song
    S., et al. (2011) Astrocytes from familial and sporadic ALS patients are toxic to
    motor neurons. *Nat. Biotechnol.* **29**, 824–8.

Haynes S. E., Hollopeter G., Yang G., Kurpius D., Dailey M. E., Gan W.-B., Julius D. (2006) The P2Y12 receptor regulates microglial activation by extracellular nucleotides. *Nat. Neurosci.* **9**, 1512–9.

Hedlund E., Isacson O. (2008) ALS model glia can mediate toxicity to motor neurons derived from human embryonic stem cells. *Cell Stem Cell* **3**, 575–6.

Henkel J. S., Beers D. R., Zhao W., Appel S. H. (2009) Microglia in ALS: the good, the bad, and the resting. *J. Neuroimmune Pharmacol.* **4**, 389–98.

Hewinson J., Mackenzie A. B. (2007) P2X(7) receptor-mediated reactive oxygen and nitrogen species formation: from receptor to generators. *Biochem. Soc. Trans.* **35**, 1168–70.

Hewinson J., Moore S. F., Glover C., Watts A. G., MacKenzie A. B. (2008) A key role for redox signaling in rapid P2X7 receptor-induced IL-1 beta processing in human monocytes. *J. Immunol.* **180**, 8410–20.

Honda S., Sasaki Y., Ohsawa K., Imai Y., Nakamura Y., Inoue K., Kohsaka S. (2001) Extracellular ATP or ADP induce chemotaxis of cultured microglia through Gi/o-coupled P2Y receptors. *J. Neurosci.* **21**, 1975–82.

Howland D. S., Liu J., She Y., Goad B., Maragakis N. J., Kim B., Erickson J., et al. (2002) Focal loss of the glutamate transporter EAAT2 in a transgenic rat model of SOD1 mutant-mediated amyotrophic lateral sclerosis (ALS). *Proc. Natl. Acad. Sci. U. S. A.* **99**, 1604–9.

Ignarro L. J., Buga G. M., Wood K. S., Byrns R. E., Chaudhuri G. (1987a) Endothelium-derived relaxing factor produced and released from artery and vein is nitric oxide. *Proc. Natl. Acad. Sci. U. S. A.* **84**, 9265–9.

Ignarro L. J., Byrns R. E., Buga G. M., Wood K. S. (1987b) Endothelium-derived relaxing factor from pulmonary artery and vein possesses pharmacologic and chemical properties identical to those of nitric oxide radical. *Circ. Res.* **61**, 866–79.

Ischiropoulos H., Zhu L., Chen J., Tsai M., Martin J. C., Smith C. D., Beckman J. S. (1992) Peroxynitrite-mediated tyrosine nitration catalyzed by superoxide dismutase. *Arch. Biochem. Biophys.* **298**, 431–437.

Jun D.-J., Kim J., Jung S.-Y., Song R., Noh J.-H., Park Y.-S., Ryu S.-H., et al. (2007) Extracellular ATP mediates necrotic cell swelling in SN4741 dopaminergic neurons through P2X7 receptors. *J. Biol. Chem.* **282**, 37350–8.

Kang J., Kang N., Lovatt D., Torres A., Zhao Z., Lin J., Nedergaard M. (2008) Connexin 43 hemichannels are permeable to ATP. *J. Neurosci.* **28**, 4702–11.

Kegel B., Braun N., Heine P., Maliszewski C. R., Zimmermann H. (1997) An ecto-ATPase and an ecto-ATP diphosphohydrolase are expressed in rat brain. *Neuropharmacology* **36**, 1189–200.

Kim J.-E., Kang T.-C. (2011) The P2X7 receptor–pannexin-1 complex decreases muscarinic acetylcholine receptor–mediated seizure susceptibility in mice. *J. Clin. Invest.* **121**, 2037–2047.

Kim J.-E., Kwak S.-E., Jo S.-M., Kang T.-C. (2009) Blockade of P2X receptor prevents astroglial death in the dentate gyrus following pilocarpine-induced status epilepticus. *Neurol. Res.* **31**, 982–8.

Kim S. Y., Moon J. H., Lee H. G., Kim S. U., Lee Y. B. (2007) ATP released from beta-amyloid-stimulated microglia induces reactive oxygen species production in an autocrine fashion. *Exp. Mol. Med.* **39**, 820–7.

Labasi J. M., Petrushova N., Donovan C., McCurdy S., Lira P., Payette M. M., Brissette W., Wicks J. R., Audoly L., Gabel C. A. (2002) Absence of the P2X7 receptor alters leukocyte function and attenuates an inflammatory response. *J. Immunol.* **168**, 6436–45.

Lazarowski E. R., Boucher R. C., Harden T. K. (2000) Constitutive release of ATP and evidence for major contribution of ecto-nucleotide pyrophosphatase and nucleoside diphosphokinase to extracellular nucleotide concentrations. *J. Biol. Chem.* **275**, 31061–8.

Lee H. G., Won S. M., Gwag B. J., Lee Y. B. (2011) Microglial P2X$_7$ receptor expression is accompanied by neuronal damage in the cerebral cortex of the APPswe/PS1dE9 mouse model of Alzheimer's disease. *Exp. Mol. Med.* **43**, 7–14.

León-Otegui M., Gómez-Villafuertes R., Díaz-Hernández J. I., Díaz-Hernández M., Miras-Portugal M. T., Gualix J. (2011) Opposite effects of P2X7 and P2Y2 nucleotide receptors on α-secretase-dependent APP processing in Neuro-2a cells. *FEBS Lett.* **585**, 2255–2262.

Lepore A. C., Maragakis N. J. (2007) Targeted stem cell transplantation strategies in ALS. *Neurochem. Int.* **50**, 966–75.

Lepore A. C., O'Donnell J., Kim A. S., Williams T., Tuteja A., Rao M. S., Kelley L. L., Campanelli J. T., Maragakis N. J. (2011) Human Glial-Restricted Progenitor Transplantation into Cervical Spinal Cord of the SOD1G93A Mouse Model of ALS. *PLoS One* **6**, e25968.

Lino M. M., Schneider C., Caroni P. (2002) Accumulation of SOD1 Mutants in Postnatal Motoneurons Does Not Cause Motoneuron Pathology or Motoneuron Disease. *J. Neurosci.* **22**, 4825–4832.

Locatelli F., Corti S., Papadimitriou D., Fortunato F., Bo R. Del, Donadoni C., Nizzardo M., et al. (2007) Fas small interfering RNA reduces motoneuron death in amyotrophic lateral sclerosis mice. *Ann. Neurol.* **62**, 81–92.

Mancuso R., Navarro X. (2015) Amyotrophic lateral sclerosis: Current perspectives from basic research to the clinic. *Prog. Neurobiol.*

Matsushita K., Wu Y., Qiu J., Lang-Lazdunski L., Hirt L., Waeber C., Hyman B. T., Yuan J., Moskowitz M. A. (2000) Fas receptor and neuronal cell death after spinal cord ischemia. *J. Neurosci.* **20**, 6879–87.

Matute C., Torre I., Perez-Cerda F., Perez-Samartin A., Alberdi E., Etxebarria E., Arranz A. M., et al. (2007) P2X7 Receptor Blockade Prevents ATP Excitotoxicity in Oligodendrocytes and Ameliorates Experimental Autoimmune Encephalomyelitis. *J. Neurosci.* **27**, 9525–9533.

Meissner F., Molawi K., Zychlinsky A. (2010) Mutant superoxide dismutase 1-induced IL-1 accelerates ALS pathogenesis. *Proc. Natl. Acad. Sci.* **107**, 13046–13050.

Melani A., Turchi D., Vannucchi M. G., Cipriani S., Gianfriddo M., Pedata F. (2005) ATP extracellular concentrations are increased in the rat striatum during in vivo ischemia. *Neurochem. Int.* **47**, 442–8.

Miller T. M., Kaspar B. K., Kops G. J., Yamanaka K., Christian L. J., Gage F. H., Cleveland D. W. (2005) Virus-delivered small RNA silencing sustains strength in amyotrophic lateral sclerosis. *Ann. Neurol.* **57**, 773–6.

Miquel E., Cassina A., Martínez-Palma L., Bolatto C., Trías E., Gandelman M., Radi R., Barbeito L., Cassina P. (2012) Modulation of astrocytic mitochondrial function by dichloroacetate improves survival and motor performance in inherited amyotrophic lateral sclerosis. *PLoS One* **7**, 1–9.

Morandini A. C., Savio L. E. B., Coutinho-Silva R. (2014) The role of P2X7 receptor in infectious inflammatory diseases and the influence of ectonucleotidases. *Biomed. J.* **37**, 169–77.

Morrone F. B., Oliveira D. L., Gamermann P., Stella J., Wofchuk S., Wink M. R., Meurer L., Edelweiss M. I. A., Lenz G., Battastini A. M. O. (2006) In vivo glioblastoma growth is reduced by apyrase activity in a rat glioma model. *BMC Cancer* **6**, 226.

Nagai M., Re D. B., Nagata T., Chalazonitis A., Jessell T. M., Wichterle H., Przedborski S. (2007) Astrocytes expressing ALS-linked mutated SOD1 release factors selectively toxic to motor neurons. *Nat. Neurosci.* **10**, 615–22.

Neary J. T., Kang Y., Shi Y.-F. (2005) Cell cycle regulation of astrocytes by extracellular nucleotides and fibroblast growth factor-2. *Purinergic Signal.* **1**, 329–36.

Neary J. T., McCarthy M., Kang Y., Zuniga S. (1998) Mitogenic signaling from P1 and P2 purinergic receptors to mitogen-activated protein kinase in human fetal astrocyte cultures. *Neurosci. Lett.* **242**, 159–62.

Nedeljkovic N., Bjelobaba I., Subasic S., Lavrnja I., Pekovic S., Stojkov D., Vjestica A., Rakic L., Stojiljkovic M. (2006) Up-regulation of ectonucleotidase activity after cortical stab injury in rats. *Cell Biol. Int.* **30**, 541–6.

Nedergaard M. (2013) Neuroscience. Garbage truck of the brain. *Science* **340**, 1529–30.

Nicke A., Bäumert H. G., Rettinger J., Eichele A., Lambrecht G., Mutschler E., Schmalzing G. (1998) P2X1 and P2X3 receptors form stable trimers: a novel structural motif of ligand-gated ion channels. *EMBO J.* **17**, 3016–28.

Oyanguren-Desez O., Rodríguez-Antigüedad A., Villoslada P., Domercq M., Alberdi E., Matute C. (2011) Gain-of-function of P2X7 receptor gene variants in multiple sclerosis. *Cell Calcium* **50**, 468–72.

Pacher P., Beckman J. S., Liaudet L. (2007) Nitric oxide and peroxynitrite in health and disease. *Physiol. Rev.* **87**, 315–424.

Parisi C., Arisi I., D'Ambrosi N., Storti A. E., Brandi R., D'Onofrio M., Volonté C. (2013) Dysregulated microRNAs in amyotrophic lateral sclerosis microglia modulate genes linked to neuroinflammation. *Cell Death Dis.* **4**, e959.

Parvathenani L. K., Tertyshnikova S., Greco C. R., Roberts S. B., Robertson B., Posmantur R. (2003) P2X7 mediates superoxide production in primary microglia and is up-regulated in a transgenic mouse model of Alzheimer's disease. *J. Biol. Chem.* **278**, 13309–17.

Pehar M., Cassina P., Vargas M. R., Castellanos R., Viera L., Beckman J. S., Estévez A. G., Barbeito L. (2004) Astrocytic production of nerve growth factor in motor

neuron apoptosis: implications for amyotrophic lateral sclerosis. *J. Neurochem.* **89**, 464–73.

Pehar M., Vargas M. R., Robinson K. M., Cassina P., Diaz-Amarilla P. J., Hagen T. M., Radi R., Barbeito L., Beckman J. S. (2007) Mitochondrial Superoxide Production and Nuclear Factor Erythroid 2-Related Factor 2 Activation in p75 Neurotrophin Receptor-Induced Motor Neuron Apoptosis. *J. Neurosci.* **27**, 7777–7785.

Pehar M., Vargas M. R., Robinson K. M., Cassina P., England P., Beckman J. S., Alzari P. M., Barbeito L. (2006) Peroxynitrite transforms nerve growth factor into an apoptotic factor for motor neurons. *Free Radic. Biol. Med.* **41**, 1632–44.

Peng W., Cotrina M. L., Han X., Yu H., Bekar L., Blum L., Takano T., Tian G.-F., Goldman S. A., Nedergaard M. (2009) Systemic administration of an antagonist of the ATP-sensitive receptor P2X7 improves recovery after spinal cord injury. *Proc. Natl. Acad. Sci. U. S. A.* **106**, 12489–93.

Peters O. M., Ghasemi M., Brown R. H. (2015) Emerging mechanisms of molecular pathology in ALS. *J. Clin. Invest.* **125**, 1767–79.

Phatnani H., Maniatis T. (2015) Astrocytes in Neurodegenerative Disease. *Cold Spring Harb. Perspect. Biol.* **7**.

Philips T., Robberecht W. (2011) Neuroinflammation in amyotrophic lateral sclerosis: role of glial activation in motor neuron disease. *Lancet. Neurol.* **10**, 253–63.

Phillis J. W., O'Regan M. H., Perkins L. M. (1993) Adenosine 5'-triphosphate release from the normoxic and hypoxic in vivo rat cerebral cortex. *Neurosci. Lett.* **151**, 94–6.

Pramatarova A., Laganière J., Roussel J., Brisebois K., Rouleau G. A. (2001) Neuron-specific expression of mutant superoxide dismutase 1 in transgenic mice does not lead to motor impairment. *J. Neurosci.* **21**, 3369–74.

Queiroz G., Gebicke-Haerter P. J., Schobert A., Starke K., Kügelgen I. von (1997) Release of ATP from cultured rat astrocytes elicited by glutamate receptor activation. *Neuroscience* **78**, 1203–8.

Ralph G. S., Radcliffe P. A., Day D. M., Carthy J. M., Leroux M. A., Lee D. C. P., Wong L.-F., et al. (2005) Silencing mutant SOD1 using RNAi protects against neurodegeneration and extends survival in an ALS model. *Nat. Med.* **11**, 429–33.

Rana S., Dringen R. (2007) Gap junction hemichannel-mediated release of glutathione from cultured rat astrocytes. *Neurosci. Lett.* **415**, 45–8.

Raoul C., Buhler E., Sadeghi C., Jacquier A., Aebischer P., Pettmann B., Henderson C. E., Haase G. (2006) Chronic activation in presymptomatic amyotrophic lateral sclerosis (ALS) mice of a feedback loop involving Fas, Daxx, and FasL. *Proc. Natl. Acad. Sci.* **103**, 6007–6012.

Raoul C., Henderson C. E., Pettmann B. (1999) Programmed cell death of embryonic motoneurons triggered through the Fas death receptor. *J. Cell Biol.* **147**, 1049–62.

Re D. B., Verche V. Le, Yu C., Amoroso M. W., Politi K. A., Phani S., Ikiz B., et al. (2014) Necroptosis drives motor neuron death in models of both sporadic and familial ALS. *Neuron* **81**, 1001–8.

Reaume A. G., Elliott J. L., Hoffman E. K., Kowall N. W., Ferrante R. J., Siwek D. F., Wilcox H. M., et al. (1996) Motor neurons in Cu/Zn superoxide dismutase-deficient mice develop normally but exhibit enhanced cell death after axonal injury. *Nat. Genet.* **13**, 43–7.

Retamal M. A., Reyes E. P., García I. E., Pinto B., Martínez A. D., González C. (2015) Diseases associated with leaky hemichannels. *Front. Cell. Neurosci.* **9**, 267.

Rizzo F., Riboldi G., Salani S., Nizzardo M., Simone C., Corti S., Hedlund E. (2014) Cellular therapy to target neuroinflammation in amyotrophic lateral sclerosis. *Cell. Mol. Life Sci.* **71**, 999–1015.

Rosen D. R., Siddique T., Patterson D., Figlewicz D. A., Sapp P., Hentati A., Donaldson D., Goto J., O'Regan J. P., Deng H. X. (1993) Mutations in Cu/Zn superoxide dismutase gene are associated with familial amyotrophic lateral sclerosis. *Nature* **362**, 59–62.

Rowland L. P., Shneider N. A. (2001) Amyotrophic lateral sclerosis. *N. Engl. J. Med.* **344**, 1688–700.

Ryu J. K., McLarnon J. G. (2008) Block of purinergic P2X(7) receptor is neuroprotective in an animal model of Alzheimer's disease. *Neuroreport* **19**, 1715–9.

Sahawneh M. A., Ricart K. C., Roberts B. R., Bomben V. C., Basso M., Ye Y., Sahawneh J., Franco M. C., Beckman J. S., Estévez A. G. (2010) Cu,Zn-superoxide dismutase increases toxicity of mutant and zinc-deficient superoxide dismutase by enhancing protein stability. *J. Biol. Chem.* **285**, 33885–97.

Sakurai M., Hayashi T., Abe K., Sadahiro M., Tabayashi K. (1998) Delayed selective motor neuron death and fas antigen induction after spinal cord ischemia in rabbits. *Brain Res.* **797**, 23–8.

Santiago M. F., Veliskova J., Patel N. K., Lutz S. E., Caille D., Charollais A., Meda P., Scemes E. (2011) Targeting pannexin1 improves seizure outcome. *PLoS One* **6**, e25178.

Scemes E., Giaume C. (2006) Astrocyte calcium waves: what they are and what they do. *Glia* **54**, 716–25.

Solle M., Labasi J., Perregaux D. G., Stam E., Petrushova N., Koller B. H., Griffiths R. J., Gabel C. A. (2001) Altered cytokine production in mice lacking P2X(7) receptors. *J. Biol. Chem.* **276**, 125–32.

Stout C. E., Costantin J. L., Naus C. C. G., Charles A. C. (2002) Intercellular calcium signaling in astrocytes via ATP release through connexin hemichannels. *J. Biol. Chem.* **277**, 10482–8.

Suadicani S. O., Brosnan C. F., Scemes E. (2006) P2X7 receptors mediate ATP release and amplification of astrocytic intercellular Ca2+ signaling. *J. Neurosci.* **26**, 1378–85.

Suadicani S. O., Iglesias R., Wang J., Dahl G., Spray D. C., Scemes E. (2012) ATP signaling is deficient in cultured Pannexin1-null mouse astrocytes. *Glia* **60**, 1106–16.

Suh B. C., Kim J. S., Namgung U., Ha H., Kim K. T. (2001) P2X7 nucleotide receptor mediation of membrane pore formation and superoxide generation in human promyelocytes and neutrophils. *J. Immunol.* **166**, 6754–63.

Trumbull K. A., McAllister D., Gandelman M. M., Fung W. Y., Lew T., Brennan L., Lopez N., Morré J., Kalyanaraman B., Beckman J. S. (2012) Diapocynin and apocynin administration fails to significantly extend survival in G93A SOD1 ALS mice. *Neurobiol. Dis.* **45**, 137–144.

Ugolini G., Raoul C., Ferri A., Haenggeli C., Yamamoto Y., Salaün D., Henderson C. E., Kato A. C., Pettmann B., Hueber A.-O. (2003) Fas/tumor necrosis factor receptor death signaling is required for axotomy-induced death of motoneurons in vivo. *J. Neurosci.* **23**, 8526–31.

Vargas M. R., Johnson J. A. (2010) Astrogliosis in amyotrophic lateral sclerosis: role and therapeutic potential of astrocytes. *Neurotherapeutics* **7**, 471–81.

Vargas M. R., Pehar M., Cassina P., Beckman J. S., Barbeito L. (2006) Increased glutathione biosynthesis by Nrf2 activation in astrocytes prevents p75NTR-dependent motor neuron apoptosis. *J. Neurochem.* **97**, 687–696.

Verderio C., Matteoli M. (2001) ATP mediates calcium signaling between astrocytes and microglial cells: modulation by IFN-gamma. *J. Immunol.* **166**, 6383–91.

Volonté C., Apolloni S., Skaper S. D., Burnstock G. (2012) P2X7 receptors: channels, pores and more. *CNS Neurol. Disord. Drug Targets* **11**, 705–21.

Wang X., Arcuino G., Takano T., Lin J., Peng W. G., Wan P., Li P., et al. (2004) P2X7 receptor inhibition improves recovery after spinal cord injury. *Nat. Med.* **10**, 821–7.

Wiese S., Jablonka S., Holtmann B., Orel N., Rajagopal R., Chao M. V, Sendtner M. (2007) Adenosine receptor A2A-R contributes to motoneuron survival by transactivating the tyrosine kinase receptor TrkB. *Proc. Natl. Acad. Sci. U. S. A.* **104**, 17210–5.

Wink M. R., Braganhol E., Tamajusuku A. S. K., Casali E. A., Karl J., Barreto-Chaves M. L., Sarkis J. J. F., Battastini A. M. O. (2003) Extracellular adenine nucleotides metabolism in astrocyte cultures from different brain regions. *Neurochem. Int.* **43**, 621–8.

Wink M. R., Braganhol E., Tamajusuku A. S. K., Lenz G., Zerbini L. F., Libermann T. A., Sévigny J., Battastini A. M. O., Robson S. C. (2006) Nucleoside triphosphate diphosphohydrolase-2 (NTPDase2/CD39L1) is the dominant ectonucleotidase expressed by rat astrocytes. *Neuroscience* **138**, 421–32.

Witting A., Chen L., Cudaback E., Straiker A., Walter L., Rickman B., Möller T., Brosnan C., Stella N. (2006) Experimental autoimmune encephalomyelitis disrupts endocannabinoid-mediated neuroprotection. *Proc. Natl. Acad. Sci. U. S. A.* **103**, 6362–7.

Xie L., Kang H., Xu Q., Chen M. J., Liao Y., Thiyagarajan M., O'Donnell J., et al. (2013) Sleep drives metabolite clearance from the adult brain. *Science* **342**, 373–7.

Yamanaka K., Boillee S., Roberts E. A., Garcia M. L., McAlonis-Downes M., Mikse O. R., Cleveland D. W., Goldstein L. S. B. (2008a) Mutant SOD1 in cell types other than motor neurons and oligodendrocytes accelerates onset of disease in ALS mice. *Proc. Natl. Acad. Sci. U. S. A.* **105**, 7594–9.

Yamanaka K., Chun S. J., Boillee S., Fujimori-Tonou N., Yamashita H., Gutmann D. H., Takahashi R., Misawa H., Cleveland D. W. (2008b) Astrocytes as determinants of disease progression in inherited amyotrophic lateral sclerosis. *Nat. Neurosci.* **11**, 251–3.

Yegutkin G. G. (2014) Enzymes involved in metabolism of extracellular nucleotides and nucleosides: functional implications and measurement of activities. *Crit. Rev. Biochem. Mol. Biol.* **49**, 473–97.

Yegutkin G. G., Samburski S. S., Jalkanen S. (2003) Soluble purine-converting enzymes circulate in human blood and regulate extracellular ATP level via counteracting pyrophosphatase and phosphotransfer reactions. *FASEB J.* **17**, 1328–30.

Yiangou Y., Facer P., Durrenberger P., Chessell I. P., Naylor A., Bountra C., Banati R. R., Anand P. (2006) COX-2, CB2 and P2X7-immunoreactivities are increased in activated microglial cells/macrophages of multiple sclerosis and amyotrophic lateral sclerosis spinal cord. *BMC Neurol.* **6**, 12.

Zimmermann H., Braun N., Kegel B., Heine P. (1998) New insights into molecular structure and function of ectonucleotidases in the nervous system. *Neurochem. Int.* **32**, 421–5.

Otros mecanismos que participan en la supervivencia de motoneuronas y la función astrocitaria.

Durante la realización de esta tesis tuve el privilegio de colaborar con variados proyectos desarrollándose paralelamente en el laboratorio. Estos proyectos no se relacionaron directamente con la función de $P2X_7$, sin embargo abordaron otros mecanismos que controlan a la supervivencia de motoneuronas y el comportamiento de los astrocitos durante la enfermedad. Mi participación en estos proyectos aportó una gran experiencia y perspectiva que solidificaron mi formación como estudiante de postgrado. A continuación se adjuntan las publicaciones resultantes de estos proyectos, antecedidas de una breve discusión.

Estudio 1: El potencial terapéutico de la apocinina y diapocinina en un modelo animal de ELA.

El texto suplementario se adjunta en el apéndice 3.

A pesar de que se han invertido años de investigación en las causas que llevan a la muerte de motoneuronas en la ELA y a investigar fármacos con potencial terapéutico, actualmente un único medicamento se encuentra disponible para los pacientes que padecen esta enfermedad, con una eficacia altamente limitada. En la búsqueda de nuevas estrategias para tratar a los pacientes de ELA un estudio altamente prometedor propuso que la inhibición de la enzima NADPH oxidasa (Nox) podría ser altamente efectiva en retardar la progresión de la ELA. En modelos animales de ELA, la administración de apocinina, un inhibidor de esta enzima, produjo una extensión de la sobevivencia de animales SOD1G93A de casi 4 meses (Engelhart et al 2008). Esta extensión fue dramáticamente mayor que todos los otros fármacos estudiados anteriormente, que sólo logran extender su sobrevida por un máximo de 2-3 semanas. El mecanismo por el cual la apocinina inhibe Nox no es conocido, pero se ha mostrado que su estado activado require su dimerización a diapocinina. Si la diapocinina es de hecho el metabolito activo de la apocinina in vivo, su administración directa tendría varias ventajas. Se eliminaría la dependencia de peroxidasas que median su dimerización y son limitantes para esta reacción. A su vez, la diapocinina es un inhibidor más potente que la apocinina, por lo que se podría administrar en concentraciones más bajas. Su estructura también determina una mayor hidrofobicidad, por lo que podría cruzar la barrera hematoencefálica

más fácilmente. En este estudio comparamos la eficacia de la apocinina y la diapocinina para extender la sobrevida de ratones SOD1^{G93A} y para promover la sobreviviencia de motoneuronas derivadas de animales SOD1^{G93A} en cultivo.

Las motoneuronas SOD1^{G93A} en cultivo presentan una particular sensibilidad al óxido nítrico, 40% mueren luego de su exposición, mientras que en las motoneuronas no transgénicas no se evidencia ningún efecto perjudicial (Estevez et al, 2008; Sahwaneh et al, 2010). Tanto la apocinina como la diapocinina efectivamente protegieron las motoneuronas SOD1^{G93A}, sin embargo la diapocinina fue protectora a concentraciones menores que la apocinina, que requirió concentraciones extremadamente altas para ejercer su actividad. Estos resultados indican que la diapocinina es capaz de proteger las motoneuronas SOD1^{G93A} y que su perfil farmacológico podría ser más favorable que el de la apocinina.

A pesar de los dramáticos efectos de la apocinina en la sobrevida de animales SOD1^{G93A} reportados anteriormente y nuestros hallazgos en motoneuronas aisladas, nuestros experimentos in vivo no mostraron ningún efecto de la apocinina y la diapocinina en la sobrevida de estos animales. Se utilizó el protocolo de tratamiento utilizado por Engelhart et al 2008, sin embargo sus resultados no pudieron ser reproducidos. Variaciones de este protocolo tampoco mostraron una extensión significativa en la sobrevida de los ratones SOD1^{G93A}. Tanto la apocinina como la diapocinina fueron detectadas en tejido cerebral y de médula espinal de los ratones tratados, mostrando que la apocinina de hecho penetró la barrera hematoencefálica y fue convertida a diapocinina. Las razones por las cuáles los resultados reportados en Engelhart et al 2008 no pudieron ser reproducidos no se encuentran claras y garantizan investigación futura.
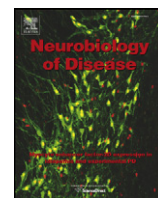
Diapocynin and apocynin administration fails to significantly extend survival in G93A SOD1 ALS mice

Kari A. Trumbull [a], Donna McAllister [b], Mandi M. Gandelman [a,c], Whitney Y. Fung [a], Thomas Lew [a], Lucy Brennan [a], Nathan Lopez [a], Jeff Morré [d,e], Balaraman Kalyanaraman [b], Joseph S. Beckman [a,e,*]

[a] Linus Pauling Institute, Department of Biochemistry and Biophysics, Oregon State University, Corvallis, OR 97331, USA
[b] Department of Biophysics and Free Radical Research Center, Medical College of Wisconsin, Milwaukee, WI, USA
[c] Neurodegeneration Laboratory, Institut Pasteur Montevideo, Uruguay
[d] Department of Chemistry, Oregon State University, Corvallis, OR 97331, USA
[e] Environmental Health Science Center, Oregon State University, Corvallis, OR 97331, USA

ARTICLE INFO

ABSTRACT

NADPH oxidase has recently been identified as a promising new therapeutic target in ALS. Genetic deletion of NADPH oxidase (Nox2) in the transgenic SOD1^{G93A} mutant mouse model of ALS was reported to increase survival remarkably by 97 days. Furthermore, apocynin, a widely used inhibitor of NADPH oxidase, was observed to dramatically extend the survival of the SOD1^{G93A} ALS mice even longer to 113 days (Harraz et al. J Clin Invest 118: 474, 2008). Diapocynin, the covalent dimer of apocynin, has been reported to be a more potent inhibitor of NADPH oxidase. We compared the protection of diapocynin to apocynin in primary cultures of SOD1^{G93A}-expressing motor neurons against nitric oxide-mediated death. Diapocynin, 10 μM, provided significantly greater protection compared to apocynin, 200 μM, at the lowest statistically significant concentrations. However, administration of diapocynin starting at 21 days of age in the SOD1^{G93A}-ALS mouse model did not extend lifespan. Repeated parallel experiments with apocynin failed to yield protection greater than a 5-day life extension in multiple trials conducted at two separate institutions. The maximum protection observed was an 8-day extension in survival when diapocynin was administered at 100 days of age at disease onset. HPLC with selective ion monitoring by mass spectrometry revealed that both apocynin and diapocynin accumulated in the brain and spinal cord tissue to low micromolar concentrations. Diapocynin was also detected in the CNS of apocynin-treated mice. The failure to achieve significant protection with either apocynin or diapocynin raises questions about the utility for treating ALS patients.

© 2011 Elsevier Inc. All rights reserved.

Introduction

Recently, a dramatic extension has been reported on the lifespan in the high expressing SOD1^{G93A} mouse model of amyotrophic lateral sclerosis (ALS). Disruption of NADPH oxidase (Nox), either as genetic knockouts or through pharmacological inhibition, extended the survival of the ALS mice by about 100 days—the greatest protection ever observed in this animal model (Marden et al., 2007; Harraz et al., 2008). The evidence implicating a role for Nox in the SOD1^{G93A} mouse model is particularly intriguing because Nox catalyzes the formation of superoxide from NADPH and oxygen while SOD1 is the primary cytosolic scavenger of superoxide. The Nox family, which includes seven different known isoforms expressed in various tissue, consists of membrane-associated enzymes that require several cytosolic subunits to bind in order to activate superoxide formation (Bedard and Krause, 2007; Lambeth, 2004). Nox2 (gp91^{phox}) is primarily found in phagocytes and involved in host defense. In the central nervous system (CNS), Nox2 is the predominant isoform found in microglia, astrocytes and neuron cells. Although most highly expressed in the colon, Nox1 is also expressed in the CNS (Sorce and Krause, 2009).

Marden et al. (2007) reported homozygous knockouts of both Nox1 and Nox2 substantially increased the survival of the hybrid B6SJL transgenic SOD1^{G93A} mouse model of ALS with the greatest effect in the Nox2 knockout. Nox2 extended life by 97 days, whereas the Nox1 knockout increased survival by 33 days. The heterozygous Nox2 and Nox1 knockout ALS mice also showed an increased survival of 54 days and 11 days, respectively. Furthermore, a redox-dependent activation of rac1 modulated by SOD1 was identified for Nox activation (Harraz et al., 2008). This interaction was disrupted by

ALS-associated mutations in SOD1, which were found to activate Nox to produce superoxide.

However, an earlier investigation into the role of Nox in ALS by Wu et al. (2006) observed *Nox2* deletion in an ALS mouse model to be less protective on lifespan. Deletion of *Nox2* (gp91[phox]) in the congenic C57BL/6J transgenic SOD1[G93A] mouse model of ALS only increased survival by 15 days. The difference in strain background, hybrid B6SJL versus congenic C57BL/6J, of the transgenic SOD1[G93A]-ALS mice was suggested to partially account for the discrepancy in survival (Marden et al., 2007). Engelhardt's group also observed the occurrence of lethal eye infections only in the Nox2 knockout transgenic SOD1[G93A]-ALS mice, which might contribute to the discrepancy in survival as well with Przedborski's study (Marden et al., 2007). The eye infections manifested by accumulated secretion that occurred 2–3 weeks before the onset of disease symptoms and resulted in death within 1 week. Cultures of eye secretions tested positive for *Staphylococcus aureus* and histopathology analysis identified abnormalities in two ocular glands. About 75% of these affected mice were successfully treated with antibiotics, ceftazidime and gentamycin. These two antibiotics were reported to have no effect on the progression or survival of SOD1[G93A]-ALS mice expressing Nox1 and Nox2 (Marden et al., 2007).

No therapeutic treatment has been found to delay the progression of motor neuron degeneration by more than 2–3 weeks in the high expressing SOD1[G93A]-ALS mouse model. However, a subsequent study by the Engelhardt group reported a similar significant protection in survival of the hybrid B6SJL SOD1[G93A]-ALS mice with apocynin (Harraz et al., 2008), a widely used putative inhibitor of Nox (van den Worm, 2001; Stefanska and Pawliczak, 2008). A high dose of 300 mg/kg/day apocynin administered beginning at 14 days increased survival by a remarkable 113 days over controls and delayed disease onset and progression. Lower dosages of apocynin started at 14 days old, 150 mg/kg/day and 30 mg/kg/day, showed impressive extension of lifespan as well, 81 days and 56 days respectively. Administration of 300 mg/kg/day apocynin at a later age, beginning at 60 and 80 days old, extended lifespan to a lesser extent, 38 and 13 days, respectively. Eye infections were also observed in the apocynin-treated ALS mice prior to the development of disease symptoms.

Apocynin, also known as acetovanillone, is a plant-derived *ortho*-methoxy substituted catechol, which has shown to exhibit anti-inflammatory properties attributed to Nox inhibition (van den Worm, 2001; Stefanska and Pawliczak, 2008). In activated human neutrophils, apocynin is reported to have a 10 μM inhibitory concentration at 50% (IC_{50}) on Nox (Simons et al., 1990). Apocynin is proposed to inhibit the assembly of the activated Nox complex (Stolk, et al., 1994; Ximenes et al., 2007). The mechanism is still unclear but diapocynin, a covalent dimer of apocynin, appears to be the activated metabolite of apocynin produced during neutrophil activation by myeloperoxidase-mediated oxidation (Fig. 1) (Stolk, et al., 1994; Johnson et al., 2002; Steffen et al., 2008).
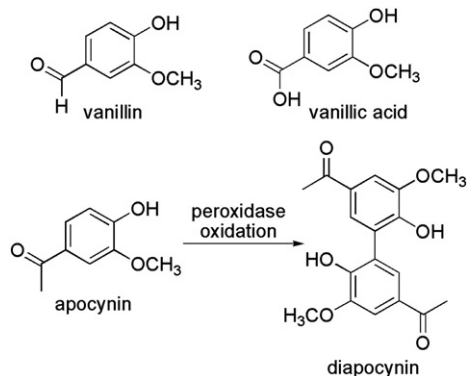
Fig. 1. Structures of vanillin, vanillic acid, apocynin, and diapocynin – the covalent dimer of apocynin.

We sought to compare the efficacy of diapocynin to apocynin at extending the survival in the hybrid B6SJL SOD1[G93A]-ALS mouse model. Administration of diapocynin could potentially offer greater protection than apocynin if it is the active metabolite of apocynin in vivo. Administration of diapocynin would remove the necessity for peroxidase involvement that might limit diapocynin formation in vivo. As a potential therapeutic agent, diapocynin should be more likely to cross the blood-brain barrier due to its greater hydrophobicity and potentially could be efficacious at lower dosages.

Materials and methods

Chemicals and reagents

Acetovanillone (Apocynin), ferrous sulfate heptahydrate, sodium persulfate, vanillic acid and other reagents were purchased from Sigma-Aldrich in the highest purity available. Reagents and primers for PCR were purchased from Invitrogen. Cell culture media and supplements were from GIBCO (Life Technologies). Glial Cell Line-Derived Neurotrophic Factor (GDNF) was purchased from R&D Systems and NOC-18 from Alexis (Enzo Life Sciences).

Synthesis of diapocynin

Diapocynin was synthesized by oxidative coupling of apocynin and adapted from a literature protocol (Wang et al., 2008). Apocynin, 4 g, was added to deionized water, 400 ml, in an Erlenmeyer flask and heated while stirring until solution was gently boiling. Addition of ferrous sulfate heptahydrate (0.30 g), followed by sodium persulfate (3.2 g) to generate sulfate radical *in situ* as the oxidizing agent, resulted in the formation of a brown precipitate. The solution was allowed to cool for 10 min and then filtered. The precipitate was dissolved in 3 M NH_4OH and then reprecipitated with 6 M HCl. The diapocynin precipitate was filtered, washed with boiling water, 3×150 ml, followed by boiling methanol, 3×150 ml. Diapocynin (3.1 g, 77% yield) was dried in vacuo. ^{1}H NMR (Bruker AC 300 MHz, DMSO-d_6): 2.49 (CH_3), 3.90 (OCH_3), 7.45 and 7.46 (aromatic CH), 9.47 (OH) ppm. MS (ESI): [M–H]−$m/z = 329.1$.

Animal models

Animal procedures and experiments were performed in accordance with the NIH Guidelines for the Care and Use of Laboratory Animals and approved by the Oregon State University and the Medical College of Wisconsin Animal Care and Use Committees. Hemizygous transgenic male rats overexpressing human mutant SOD1[G93A], NTac:SD-Tg(SOD1G93A)L26H purchased from Taconic (Germantown, NY), were bred with wild-type Sprague–Dawley females, NTac:SD to obtain rat embryos for motor neuron cultures. Male transgenic mice overexpressing human mutant SOD1[G93A], B6SJL-Tg(SOD1-G93A) 1Gur/J, and the nontransgenic wildtype B6SJLF1/J females were purchased from the Jackson Laboratory (Bar Harbor, ME). The mouse line was maintained by breeding hemizygous SOD1[G93A] males with wildtype B6SJLF1/J females. When indicated, specific generations of transgenic SOD1[G93A] male breeder, F2, F6 and F7, were mated with F1 nontransgenic female breeders as well as littermate matched F7 nontransgenic females bred with F7 transgenic SOD1[G93A] male breeders. Transgenic offspring were identified by PCR with tail DNA using primers specific for human SOD1. This high expressing transgenic ALS mouse line develops disease onset at about 100 days of age and reach clinical death by about 125 days of age (Gurney et al., 1994). Mice were housed in a control environment with free access to food and water. Starting at 60 days of age until the age of clinical death, mice were weighted and motor performance evaluated by paw grip endurance twice a week (Weydt et al., 2003). During end-stage illness, advanced symptomatic mice were individually housed and

provided gruel with water soaked chow fines twice a day. Clinical death was determined as the age when the mice could no longer right themselves within 15 s of being place on their side and were euthanized.

Primary motor neuron cultures and treatments

Motor neurons were prepared as previously described (Cassina et al., 2002; Henderson et al., 1995). Rat embryos on embryonic day 15 were genotyped by PCR and cultures of SOD1^{G93A} motor neurons and non-transgenic were carried out in parallel. Briefly, the dorsal horns of spinal cords were dissected and incubated in 0.05% trypsin for 15 min at 37 °C, followed by mechanical dissociation. Motor neurons were then purified by centrifugation on an Optiprep cushion, followed by isolation of p75^{NTR} expressing motor neurons by immunoaffinity selection with the IgG 192 monoclonal antibody. Motor neuron cultures were plated at a density of 300 cells/cm^2 in 24 well plates precoated with polyornithine and laminin and maintained in Neurobasal media supplemented with 2% horse serum, 25 μM L-glutamate, 25 μM 2-mercaptoethanol, 500 μM L-glutamine, and 2% B-27 supplement at 37 °C in a 5% CO$_2$ humidified atmosphere (Cassina et al., 2002; Henderson et al., 1995). Survival was maintained by the addition of GDNF (1 ng/ml). Two hours after plating apocynin or diapocynin were added from 200× stock solutions prepared in DMSO and half an hour later DETANONOate (20 μM) was added to generate a low steady state concentration of nitric oxide (~100 nM). DETA-NONOate was resupplied after 24 h.

Motor neuron survival was assessed after 48 h of treatment by counting all phase-bright cells with intact neurites longer than 4 body diameters in 2 diameters of the well. Values were expressed as percentage of the number of motor neurons present in control wells maintained with GDNF.

Treatment of ALS mice

Apocynin-treated water was prepared following Engelhardt's protocol, method A (Harraz et al., 2008). Apocynin was added to warm sterile water, about 60 °C, at a concentration of 1 mg/ml, 2 mg/ml or 5 mg/ml and stirred. Treatment water was allowed to cool to room temperature before administered to mice. When indicated, apocynin was alternately prepared, method B, by its addition to sterile water and heated to 60 °C while stirred, then cooled to room temperature. A concentration of 1 mg/ml translates to a dose of about 150 mg/kg/day, 2 mg/ml about 300 mg/kg/day and 5 mg/ml about 750 mg/kg/day based on an average ALS mouse, weighing between 25 and 30 g, consumes on average 4 ml water/day (Bachmanov et al., 2002). Treatment was administered at 21 or 100 days of age to littermate matched control ALS mice.

Apocynin-antibiotic treatment was prepared by adding 0.1 mg/ml gentamycin and 0.1 mg/ml ceftazidime to the cooled apocynin treatment water. For this treatment group of mice, animals were switched from regular apocynin water to apocynin-antibiotic water at 100 days of age. The same concentration of antibiotics were added to sterile water and administered at 100 days of age to the littermate matched control mice for this group.

Diapocynin requires dilute buffering to dissolve in water therefore at a concentration of 1 mg/ml diapocynin was added to sterile water and dissolved by increasing to pH ~10 with 1 M NaOH. Once fully dissolved, 1 M HCl was added to the solution until pH 7.6–7.8, for a concentration of 10 mM saline in the diapocynin treatment. Control treatment for littermate matched mice was prepared by making a 10 mM saline solution with the same pH as diapocynin treatment. Diapocynin treatment, which translates to a dosage of 150 mg/kg/day, or saline treatment was administered at 21 days or 100 days of age to littermate matched control mice.

Vanillic acid treatment was prepared by adding 0.5 mg/ml or 1 mg/ml to sterile water and heated to 60 °C. Once dissolved, it was allowed to cool to room temperature before administered to littermate matched control mice. A concentration of 0.5 mg/ml translates to a dosage of 75 mg/kg/day and 1 mg/ml to 150 mg/kg/day.

Treatment water was replaced weekly. Mice were provided gruel with chow fines soaked in treatment or control water during advanced clinical symptoms.

Tissue preparation and treatment extraction

Mice at the age of clinical death were euthanized by isofluorane intoxication then transcardially perfused with 20 ml of heparinized-saline solution. Brain and spinal cord tissues were removed, flash frozen and stored at −80 °C until analysis.

Extraction of treatment compounds was adapted from literature protocol (Wang et al., 2008). Tissue was homogenized in 10 volumes of 17 mM NH$_4$OH, pH 8.0. Ammonium acetate buffer, 1.0 M at pH 5.0, at 0.3 volume, was added to aliquots of tissue homogenates. In trial experiments to hydrolyze potential glycosyl linkages to apocynin or diapocynin, samples were incubated overnight at 37 °C with 10 units/ml β-glucuronidase (Sigma) or without. Samples were centrifuged at 13,000 rpm for 20 min and the supernatant removed. Organic extraction of the supernatant with 3 volumes chloroform–methanol (3:1) followed by centrifugation at 3000 rpm for 20 min. An aliquot of the upper aqueous layer was removed for HPLC-MS analysis.

HPLC-MS tissue analysis

The HPLC-MS data for apocynin and diapocynin was acquired on a Perkin-Elmer Sciex API 365 triple quadrupole mass spectrometer (Applied Biosystems, Foster City, CA) in negative ion mode using turbo ion spray. Chromatographic separations were performed with a Shimadzu Prominence CBM-20 HPLC (Shimadzu Scientific Instruments, Columbia, MD) with auto sampler and equipped with a XTerra MS C8 (2.5 μm, 2.1 × 50 mm) column. Analyses were run in isocratic mode with methanol-acetonitrile (35:65) with 0.1% formic acid at 0.2 ml/min flow rate for 3 min. Multiple reaction monitoring analysis of two transitions was conducted for apocynin, 165.1-150.0 *m/z*, and diapocynin, 329.1–313.1 *m/z*. The corresponding peaks were identified using Q1 full scan comparing retention times and mass spectra of apocynin and diapocynin with those obtained for the standards. Standards were prepared by spiking non-treated control tissue to account for observed matrix suppression at varying concentrations. Minor background noise in non-spiked non-treated control tissue was adjusted for in reported values of treated tissue.

Statistics

Reported values for the motor neuron culture studies are the mean ± SEM of at least 3 independent experiments carried out in triplicates. Statistical analysis was performed by one-way ANOVA, followed by a Fisher's LSD test using KaleidaGraph (Synergy Software). Kaplan–Meier survival curves were generated using SigmaPlot 11 and compared using the log-rank test. Body weight analysis and paw grip endurance test analysis are reported as the mean ± SD using KaleidaGraph and statistical analysis was performed by Student's *t*-test. A *P*-value less than 0.05 was considered statistically significant.

Results

Motor neuron culture experiments

Motor neurons isolated from transgenic SOD1^{G93A} rat models of ALS in primary culture display increased sensitivity to nitric oxide

(Sahawneh et al., 2010). About 40% of SOD1^{G93A} motor neurons underwent apoptosis after 48 h, as previously reported (Sahawneh et al., 2010), when exposed to a steady state concentration of 80 nM nitric oxide (Fig. 2). Both diapocynin and apocynin were effective at preventing motor neuron death after nitric oxide treatment. Diapocynin was protective at lower concentrations, between 10 to 50 µM, but appeared to be toxic to motor neurons at a higher concentration of 200 µM (Fig. 2A). Apocynin was protective at higher concentrations between 200 µM to 1 mM and did not appear to be toxic over the range tested (Fig. 2B).

Diapocynin administered at weaning

No significant protective effect was observed at extending survival in either the hybrid B6SJL SOD1^{G93A} male or female ALS mice when 150 mg/kg/day of diapocynin was administered beginning at 21 days of age, Table 1. Weight loss was mildly diminished and paw grip endurance mildly increased in the saline control groups compared to the diapocynin treated male and female groups (Supplementary Figure S1).

Diapocynin administered at disease onset

A statistically significant protective effect in mean survival of 8 days was observed in the SOD1^{G93A} total male and female mice
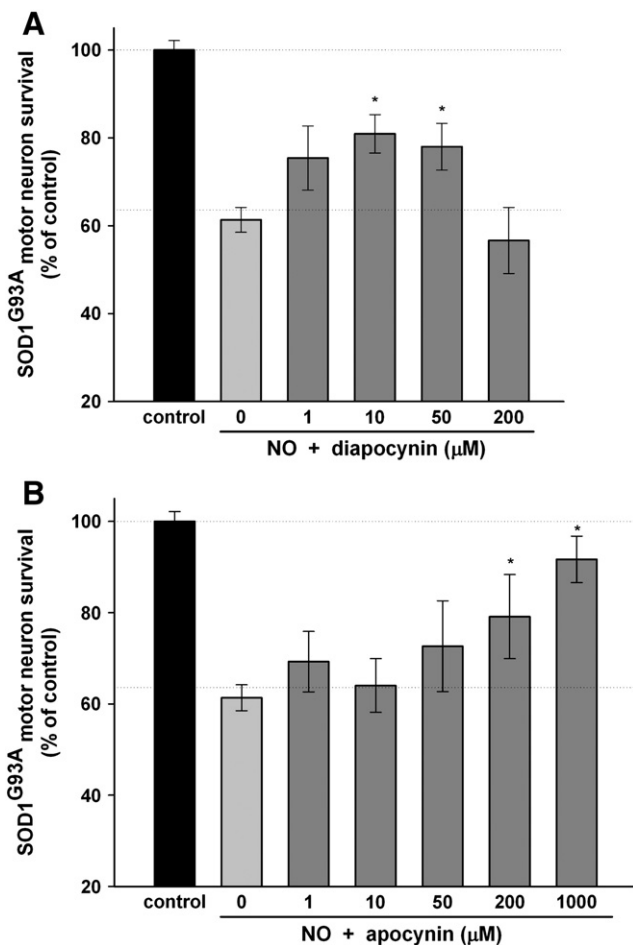
Fig. 2. Diapocynin and apocynin protect SOD1G93A primary motor neurons against nitric oxide mediated death in cell culture. In transgenic SOD1G93A motor neurons, nitric oxide treatment causes death of about 40% of motor neurons after 48 h. (A) Survival of motor neurons pretreated with 1, 10, 50 or 200 µM diapocynin before exposure to nitric oxide. (B) Survival of motor neurons pretreated with 1, 10, 50, 200 or 1000 µM apocynin before exposure to nitric oxide. Data are expressed as percentage of control, mean ± SEM from at least 3 independent experiments. *p<0.05, significantly different from motor neurons treated with nitric oxide only.

Table 1
Survival analysis, dosage and start age of treatment versus control administered to the SOD1^{G93A} mice.

Treatment	Dosage (mg/kg/day)	Mean survival ± SEM (sample number)		ΔSurvival	Trial
		Treated	Control		
Diapocynin 21 day start	150				a[1]
Male		126 ± 2 (12)	127 ± 2 (12)	−1	
Female		130 ± 3 (12)	133 ± 3 (12)	−3	
Total		128 ± 2 (24)	130 ± 2 (24)	−2	
Diapocynin 100 day start	150				a[1]
Male		130 ± 2 (12)	123 ± 2 (12)	+7 (P=<0.007)	
Female		139 ± 2 (12)	129 ± 2 (12)	+10 (P=<0.003)	
Total		134 ± 2 (24)	126 ± 2 (24)	+8 (P=<0.001)	
Apocynin − antibiotics 21 day start	300				a
Male		129 ± 2 (12)	127 ± 3 (12)	+2	
Female		130 ± 2 (12)	131 ± 2 (12)	−1	
Total		130 ± 2 (24)	129 ± 2 (24)	+1	
Apocynin + antibiotics 21 day start +100 day start	300 15				a[2]
Male		131 ± 3 (12)	126 ± 2 (12)	+5	
Female		131 ± 2 (12)	132 ± 2 (12)	−1	
Total		131 ± 2 (24)	129 ± 2 (24)	+2	
Apocynin dose response 21 day start	150	126 ± 2 (12)	128 ± 2 (13)	−2	b[3]
	300	133 ± 3 (14)		+5	
	750	135 ± 2 (11)	135 ± 3 (11)	0	b
Apocynin 100 day start	300				a
Male		130 ± 2 (12)	127 ± 2 (12)	+3	
Female		134 ± 2 (12)	131 ± 2 (12)	+3	
Total		132 ± 2 (24)	129 ± 2 (24)	+3	
Vanillic acid 21 day start					b[3]
	75	127 ± 5 (6)	128 ± 2 (6)	−1	
	150	133 ± 4 (4)		+5	

[a] Performed at Oregon State University.
[b] Performed at Medical College of Wisconsin.
[1] Control group was administered saline at the specified age.
[2] Antibiotics started at 100 days of age for apocynin group and control group.
[3] Randomized trial of 2 treatment dosages with 1 control group.

combined when 150 mg/kg/day of diapocynin was administered at 100 days of age at disease onset (Fig. 3 and Table 1). The protection was greater in female mice compared to male mice. Weight loss was mildly diminished and paw grip endurance mildly increased after 100 days of age for diapocynin treated male and female mice (Supplementary Figure S2).

Apocynin plus antibiotics administration

In the diapocynin trial starting at 21 days, a parallel trial was conducted using apocynin with and without antibiotics to replicate the Harraz et al. (2008) experiments. Administration of 300 mg/kg/day apocynin started at 21 days of age had no protective effect on survival (Table 1). Weight loss was mildly diminished in apocynin treated males between 70 to 100 days. No other protection was observed in weight loss or paw grip endurance (Supplementary Figure S3).

No signs of lethal eye infections were observed in the mice prior to disease onset. However, accumulated eye discharge was observed in about 50% of treated and non-treated control ALS mice at the end-stage of disease, about 2–6 days prior to diagnosis of clinical death. In consultation with the veterinary care staff, the cause was attributed to
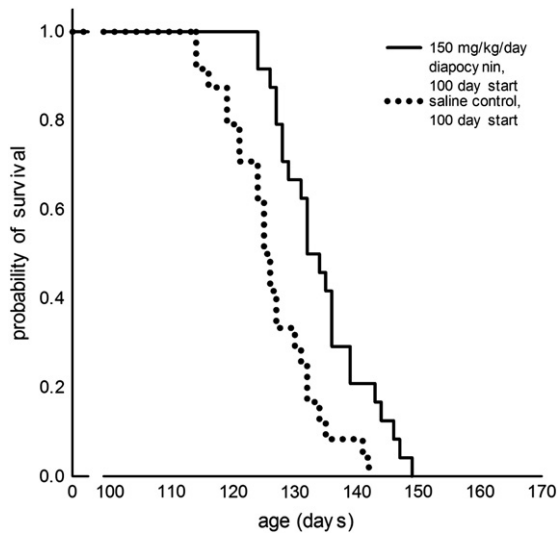
Fig. 3. Survival analysis of transgenic SOD1G93A mice treated with 150 mg/kg/day diapocynin starting at 100 days of age. Kaplan-Meier probability of survival analysis shows total male and female mice combined per cohort administered diapocynin (134 ± 2 days, n = 24) compared to saline control (126 ± 2, n = 24), p < 0.001.

decreased grooming due to compromised forelimb mobility and no evidence was found for eye infections. However, 17 eye culture tests and 3 necropsies were performed on advanced symptomatic male and female mice displaying eye discharge in various treatment or control groups. Necropsy results on two 21 day start apocynin treatment mice and one 100 day start apocynin treatment showed no significant findings and the ocular glands were normal. Eye swab culture tests identified several species from 9 eye swabs: unidentified yeast spp. (*Candida albicans* or *Cryptococcus spp.* were excluded), *Enterococcus spp.*, *Staphylococcus spp.* (coagulase negative), *Streptococcus spp.* (alpha-hemolytic), *Pasteurella spp.*, and *Corynebacterium spp.* The other eight eye cultures reported mixed Gram-positive bacteria with no significant bacteria isolated. There were no predominate species in any specific treatment or control group: *Enterococcus spp.* were isolated from a non-treated control mouse and a 21 day start apocynin treated mouse; *Streptococcus spp.* from control and 21 day start diapocynin mice; *Staphylococcus spp.* from control and 21 day start diapocynin mice; *Pasteurella spp.* from control and 100 day start apocynin mice.

Several β-lactam antibiotics have been shown to be neuroprotective in ALS mouse models in vitro (Rothstein et al., 2005). One of the antibiotics used in Engelhardt's study, ceftazidime, is a β-lactam antibiotic (Harraz et al., 2008). Although not every apocynin-treated mouse in Engelhardt's study was treated with antibiotics, only about 50% of the mice showed signs of eye infections, perhaps the ceftazidime as part of the antibiotic treatment was contributing some synergistic protective effect with apocynin treatment, since the antibiotic control group did not show any protection. Therefore, we proceeded to administer a group of apocynin-treated and non-treated control ALS mice with the same antibiotic mixture used in the Engelhardt study despite no signs of lethal eye infections.

At 100 days of age, the average age of disease onset, 0.1 mg/ml gentamycin and 0.1 mg/ml ceftazidime antibiotics were administered in the drinking water of both the apocynin-treated mice, 300 mg/kg/day started at 21 days of age, and the littermate control mice on non-treated water. Antibiotics were administered at the average age of onset due to minimal observed hind-limb impairment since Engelhardt's study reported eye infections occurred, therefore antibiotic treatment started, prior to disease development. A 5-day statistically non-significant extension in survival was observed for the male apocynin-antibiotic treatment group whereas no difference was observed in the female group (Table 1). Overall, antibiotic treatment had no significant effect on survival with or without apocynin. Weight

loss was mildly diminished in apocynin-antibiotic treated males after 100 days of age until clinical death, while no difference was observed in the female group (Supplementary Figure S4). The male apocynin-antibiotic group exhibited a mild loss in paw grip endurance while the female apocynin-antibiotic group was mildly increased compared to the antibiotic control groups (Supplementary Figure S4).

Apocynin administered at disease onset

A statistically non-significant 3-day extension in life was observed in male and female ALS mice when 300 mg/kg/day apocynin was administered in the drinking water starting at 100 days of age (Table 1). No difference was observed between treatment and control groups in body weight loss and the paw grip endurance test (Supplementary Figure S5).

Apocynin dose response

In the second independent study, apocynin was similarly not protective on the lifespan of the hybrid B6SJL SOD1^{G93A} ALS mice when administered three different dosages. Apocynin treatment, 150 mg/kg/day and 300 mg/kg/day started at 21 days, showed no significant protection (Fig. 4 and Table 1). An even higher dose of 750 mg/kg/day apocynin did not affect survival in the ALS mice (Table 1).

Apocynin treatment in the previous experiments was prepared by the alternate method B (see Materials and methods). To account for any difference that might be due to the way apocynin treatment was prepared compared to Engelhardt's method (method A)—even though HPLC-MS analysis of apocynin treatment by either method A or B was found to be identical—mice were treated with 300 mg/kg/day apocynin prepared by either method A or B at 21 days of age. No significant difference in survival was observed between the apocynin preparation groups (Table 2).

Varying genetic background on apocynin treatment

The genetic background in the hybrid B6SJL SOD1^{G93A} mouse model can potentially drift through breeding, which can affect lifespan from transgene copy number drops and littermate clustering
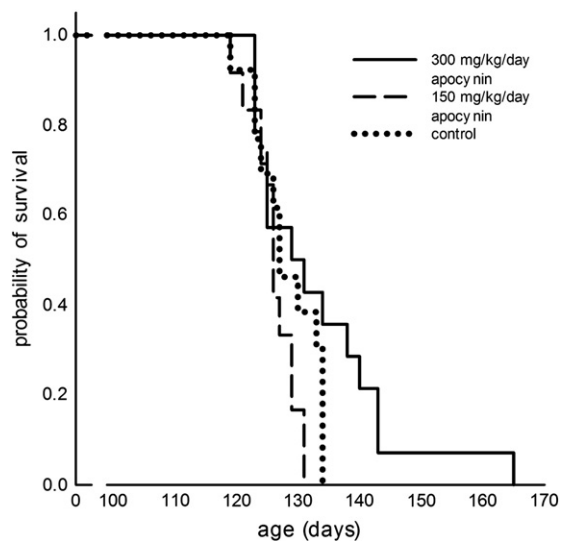
Fig. 4. Survival analysis of apocynin treated SOD1G93A mice started at 21 days of age. Kaplan-Meier probability of survival analysis shows total male and female mice combined per cohort given dosage of 150 mg/kg/day apocynin (126 ± 2 days, n = 12) or 300 mg/kg/day apocynin (133 ± 3 days, n = 14) compared to control (128 ± 2 days, n = 13). Mean survival of apocynin treated mice on 300 mg/kg/day appears augmented by one mouse that lived to 165 days, which may be due to a spontaneous drop in copy number of the G93A SOD1 transgene (Alexander et al., 2004).

Table 2
Survival analysis of apocynin treated SOD1^{G93A} mice comparing preparation methods of apocynin and parent generations.

Apocynin treatment	Dosage (mg/kg/day)	Mean survival ± SEM (sample number)	Trial
Preparation	300		b[1]
Method A		130 ± 2 (30)	
Method B		133 ± 3 (14)	
Father generation	300		b[2]
F2 males		133 ± 2 (28)	
F6 males		138 ± 3 (8)	
Mother generation	300		b[3]
F1 females		132 ± 2 (21)	
Littermate females		129 ± 3 (12)	

b. Performed at Medical College of Wisconsin.

[1] See Materials and methods for preparation methods.

[2] F generations of hemizygous SOD1^{G93A} male mice mated with F1 wildtype B6SJLF1/J females.

[3] F generation of wildtype B6SJLF1/J females mated with F7 hemizygous SOD1^{G93A} male mice, littermate females were F7 generation.

(Alexander et al., 2004; Heiman-Patterson et al., 2005; Scott et al., 2008). The hybrid B6SJL SOD1^{G93A} mouse line is generally maintained by breeding a hemizygous transgenic male back to a wild-type B6SJL F1 female. To examine if protection by apocynin may be influenced by variability in genetic background in this mouse model and affect the extent of survival, two trials were conducted varying the generation of the parent male and parent female breeders. Apocynin treated offspring, 300 mg/kg/day at 21 days, of two generations of the transgenic SOD1^{G93A} male breeder either in the F2 generation or F6 generation both mated with F1 wild-type female breeders, were compared. A 5-day statistically non-significant difference in survival was observed between apocynin-treated offspring (Table 2). Furthermore, apocynin treated offspring, 300 mg/kg/day at 21 days, of either wild-type F1 generation females or wild-type F7 generation littermate-matched female breeders were mated with F7 generation transgenic SOD1^{G93A} male breeders. A 3-day statistically non-significant difference in the mean survival was observed between these apocynin treated offspring (Table 2).

Vanillic acid therapeutic study

Vanillic acid is structurally related to apocynin (Fig. 1) and, although reported to be a weaker inhibitor of Nox in neutrophils (van den Worm

et al., 2001), has been found to be a more potent inhibitor of Nox in human umbilical vein endothelial cell lysates (Steffen et al., 2008). Therefore, vanillic acid administration to SOD1^{G93A} mice was investigated in a pilot study. No significant protective effect on survival was observed with vanillic acid treatment at two different dosages, 75 mg/kg/day and 150 mg/kg/day, starting at 21 days of age. A statistically non-significant 5 day difference was observed between the control group and 150 mg/kg/day vanillic acid treatment group (Table 1).

HPLC-MS tissue analysis of SOD1^{G93A}-ALS treated mice

Diapocynin and apocynin were extracted from brain and spinal cord tissue from treated ALS mice and quantified by HPLC-MS analysis (Fig. 5). In treated mice started at 21 days, diapocynin was detected at levels about one-third to one-fifth of apocynin. In the treated mice started at 100 days, diapocynin and apocynin were only detected in brain tissue whereas treatment levels in the spinal cord fell within the margin of error and are not reported (Fig. 5). Diapocynin measured in the 100 day treated brain tissue was about 10 times lower than the 21 day treated brain tissue. Apocynin was about 14 times lower in the 100 day brain tissue compared to the 21 day brain tissue.
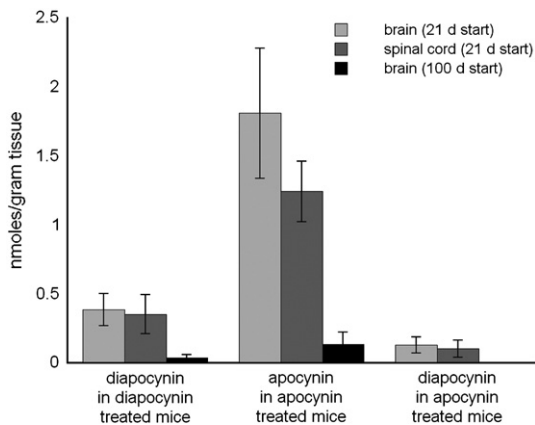
Diapocynin was detected in brain and spinal cord tissue from apocynin treated mice started at 21 days old, showing apocynin was converted into diapocynin in vivo and accumulated in the CNS (Fig. 5). The diapocynin concentration measured was about 7–8% of the apocynin concentration in the corresponding tissue. To confirm diapocynin was converted in vivo and not during sample processing, control tissue samples were spiked with apocynin and processed similarly. The detected levels of diapocynin in apocynin spiked tissue fell within the margin of error. Therefore, the detected diapocynin in apocynin treatment was not an artifact formed during the processing of the samples.

Apocynin has been previously reported to form glycoconjugates as the major metabolite in vivo after i.p. administration (Wang et al., 2008). Samples of brain and spinal cord tissue from apocynin and diapocynin treated mice started at 21 days of age were incubated with β-glucuronidase, to hydrolyze the glycosyl linkage if present, and without. No significant difference was observed between the samples therefore this step was not continued in further processing of samples (data not shown).

Discussion

Apocynin has been experimentally used to inhibit superoxide production by Nox in Alzheimer's, Parkinson's, multiple sclerosis, amyotrophic lateral sclerosis, and stroke (Bedard and Krause, 2007; Sorce and Krause, 2009). It was originally isolated from the roots of *Apocynum cannabinum* in 1883 and found in a Himalayan plant, *Picrorhiza kurroa,* which has been a thousand year history of human use as part of traditional Indian Ayurvedic medicine. Because of the low toxicity and general lack of side effects, apocynin is an attractive therapeutic candidate for human patients suffering from ALS (van den Worm, 2001; Stefanska and Pawliczak, 2008).

In several different cell-based models, apocynin has been shown to protect motor neurons from mutant SOD1 toxicity. Apparent superoxide production by Nox was reduced along with increased cell viability when apocynin was present in glial cells expressing mutant SOD1 (Harraz et al., 2008). Motor neurons derived from human embryonic stem cells co-cultured with human primary astrocytes expressing mutant SOD1 displayed an increased survival in the presence of apocynin (Marchetto et al., 2008). In SOD1^{G93A} primary motor neurons, we found apocynin to be protective against nitric oxide-mediated death, albeit at concentrations that are far higher than can be achieved in vivo. Diapocynin was protective at lower concentrations that are closer to being achievable in the CNS.

Fig. 5. CNS tissue analysis by HPLC-MS using selective ion monitoring of mice administered 150 mg/kg/day diapocynin and 300 mg/kg/day apocynin started at 21 and 100 days of age. Diapocynin and apocynin were measured in brain and spinal cord tissues of treated mice. Diapocynin was detected in tissue of apocynin treated mice started at 21 days of age. Treatment was not detected in spinal cord tissue when administered at 100 days of age. Measurements represent mean ± SD from at least 6 samples and reported in nmoles of treatment per gram of tissue.

These results supported the investigation of diapocynin as a more potent therapeutic agent to treat ALS.

However, we were unable to show any significant extension in survival with diapocynin or apocynin treatment in the SOD1^{G93A} mouse model. The only statistically significant protection was an 8-day increase in lifespan observed when 150 mg/kg/day of diapocynin was administered at disease onset at 100 days of age. The CNS concentrations of diapocynin were barely detectable in this group and less than the treatment groups that showed no extension in lifespan by administering either diapocynin or apocynin at 21 days of age. Possibly, later administration of diapocynin may have another action in muscle or some other alternative target. It is also possible that the slight protection obtained was a statistical fluke arising from the multiple trials conducted.

We were unable to find a basis for our failure to replicate the impressive protective effect by apocynin observed by Engelhardt's group at extending the survival in the ALS mouse model by 113 days (Harraz et al., 2008). Both studies used the same genetic background, the hybrid B6SJL line most commonly used with SOD1^{G93A} mice. The earliest age apocynin treatment was started in our study was at 21 days of age, which was the minimum age for weaning in our experience. The Engelhardt study was started at 14 days old, though it is unclear whether the mice were weaned early. The 7-day difference in administration of apocynin might contribute to the lack in protective we observed. However, Harraz et al. (2008) report protection of 38 days even when the apocynin treatment was begun at 60 days of age.

Antibiotic treatments used to treat lethal eye infections could not account for the absence of protection. Although other groups have found that several β-lactam antibiotics can be neuroprotective in ALS-SOD1 mice, Harraz et al. (2008) found no therapeutic effect of the antibiotic treatment on ALS disease progression. We also found no therapeutic benefit. The β-lactam ceftriaxone delayed the loss of muscle strength and body weight and extended survival by 10 days in the hybrid B6SJL SOD1^{G93A}-ALS mouse model (Rothstein et al., 2005). The related β-lactam, ceftazidime, was used in our trial at a dosage of 15 mg/kg/day, which was about 10 times lower than the dose of ceftriaxone, and started 2 weeks later than the studies showing protection from β-lactam treatment. However, we observed no evidence of eye infections in any of the treated ALS mice in studies conducted at two different institutions. Nevertheless, the same mixture and dosage of antibiotics in Engelhardt's study was not protective when administered to the apocynin-treated and littermate-matched controls.

Similar results for a lack of protection at extending survival with apocynin treatment in the SOD1^{G93A}-ALS mouse model have been reported by the ALS Therapy Development Institute (ALS TDI, http://www.als.net). They used a dosage of 150 mg/kg/day apocynin started at two different ages, 30 and 50 days old. No statistically significant protection was observed in the treated mice. Even at 150 mg/kg/day apocynin (starting at age 14 days), Engelhardt's group reported substantial protection by apocynin by 81 days. A mild protection in the loss of body weight in apocynin treated mice was observed by the ALS TDI.

Only a few studies have examined the metabolites of apocynin in vivo (Daly et al., 1960; Gjertsen et al., 1988; Wang et al., 2008). Daly et al. (1960) and Gjertsen et al. (1988) reported comparable results with the majority of apocynin, about 80%, recovered in the urine as its glucuronide conjugate after i.p. administration of apocynin in rats. Small quantities of other metabolic conversion products of apocynin were also detected, the highest detected in 0.5% as the para-isomer, but diapocynin was not reported as an identified metabolite. These earlier studies were conducted before a conversion mechanism for apocynin to diapocynin in vivo was proposed. The more recent study by Wang et al. (2008) specifically focused on examining the potential formation of diapocynin in vivo after i.p. administration of 5 mg/kg apocynin in rats. Diapocynin was not detected by HPLC-MS in plasma

or tissue as a metabolite of apocynin within 30 min to 2 h after administration. The glycoconjugate was found as reported in previous studies (Wang et al., 2008).

We were able to detect diapocynin and apocynin accumulation in low micromolar concentrations in the CNS by HPLC-MS-MS using selective ion monitoring. Diapocynin was also present in apocynin-treated mice at about 7–8% of the apocynin concentration. Thus, diapocynin may be a significant metabolite of apocynin even in diseases without significant neutrophil activation. To the best of our knowledge, this is the first report to measure diapocynin in the CNS in apocynin-treated mice. Diapocynin was only detected in the long term apocynin treated mice which ingested apocynin for about 100 days and may explain the contrasting data from previous studies which analyzed tissue shortly after i.p. injections of apocynin.

In summary, we have not been able to reproduce the previously reported dramatic neuroprotection by apocynin in the ALS mouse model in two separate laboratories. Reasons for this discrepancy are not clear, despite investigating dosage, antibiotics, gender, or the drift in the genetic background from breeding for multiple generations of both female and male breeders. Tissue analysis of brain and spinal cord confirmed both apocynin and diapocynin accumulated in the CNS to micromolar levels in the experimental animals.

Despite the difference in efficacy, apocynin may still be found to be protective in human ALS patients. Results from our study along with supporting evidence from other in vitro studies, stress the importance of testing diapocynin when examining the potential therapeutic properties of apocynin. Although therapeutic protection in ALS animal models has not yet been effectively translated into successful therapeutics in human ALS patients, meta-analysis suggests drugs with anti-inflammatory and antioxidant actions appear to be promising (Benatar, 2007; Barber and Shaw, 2010). Therapeutic drugs that exert these properties have been more effective when administered at disease onset, which is when diapocynin was modestly effective in our study. More studies are clearly needed before embarking on human clinical trials using apocynin supplementation. Our results do not rule out a role of Nox isozymes in the pathogenesis of ALS because apocynin and diapocynin are at best only modest Nox inhibitors. Knockout of NOX has been shown to modestly increase the survival of ALS-mutant SOD transgenic mice (Wu et al., 2006). Hence, the development of more potent Nox inhibitors is worthy of further investigation in ALS.

Acknowledgments

Appendix A. Supplementary data

Supplementary data to this article can be found online at doi:10.1016/j.nbd.2011.07.015.

References

Alexander, G.M., Erwin, K.L., Byers, N., Deitch, J.S., Augelli, B.J., Blankenhorn, E.P., Heiman-Patterson, T.D., 2004. Effects of transgene copy number on survival in the G93A SOD1 transgenic mouse model of ALS. Brain Res. Mol. Brain Res. 130, 7–15.
Bachmanov, A.A., Reed, D.R., Beauchamp, G.K., Tordoff, M.G., 2002. Food intake, water intake, and drinking spout side preference of 28 mouse strains. Behav. Genet. 32, 435–443.

Barber, S.C., Shaw, P.J., 2010. Oxidative stress in ALS: key role in motor neuron injury and therapeutic target. Free Radic. Biol. Med. 48, 629–641.

Bedard, K., Krause, K., 2007. The NOX family of ROS-generating NADPH oxidases: physiology and pathophysiology. Physiol. Rev. 87, 245–313.

Benatar, M., 2007. Lost in translation: treatment trials in the SOD1 mouse and in human ALS. Neurobiol. Dis. 26, 1–13.

Cassina, P., Peluffo, H., Pehar, M., Martinez-Palma, L., Ressia, A., Beckman, J.S., Estevez, A.G., Barbeito, L., 2002. Peroxynitrite triggers a phenotypic transformation in spinal cord astrocytes that induces motor neuron apoptosis. J. Neurosci. Res. 67, 21–29.

Daly, J.W., Axelrod, J., Witkop, B., 1960. Dynamic aspects of enzymatic O-methylation and -demethylation of catechols in vitro and in vivo. J. Biol. Chem. 235, 1155–1159.

Gjertsen, F.B., Solheim, E., Scheline, R.R., 1988. Metabolism of aromatic plant ketones in rats: acetovanillone and paeonol. Xenobiotica 18, 225–234.

Gurney, M.E., Pu, H., Chiu, A.Y., Dal Canto, M.C., Polchow, C.Y., Alexander, D.D., Caliendo, J., Hentati, A., Kwon, Y.W., Deng, H.X., et al., 1994. Motor neuron degeneration in mice that express a human Cu, Zn superoxide dismutase mutation. Science 264, 1772–1775.

Harraz, M.M., Marden, J.J., Zhou, W., Zhang, Y., Williams, A., Sharov, V.S., Nelson, K., Luo, M., Paulson, H., Schöneich, C., Engelhardt, J.F., 2008. SOD1 mutations disrupt redox-sensitive Rac regulation of NADPH oxidase in a familial ALS model. J. Clin. Invest. 118, 474–478.

Heiman-Patterson, T.D., Deitch, J.S., Blankenhorn, E.P., Erwin, K.L., Perreault, M.J., Alexander, B.K., Byers, N., Toman, I., Alexander, G.M., 2005. Background and gender effects on survival in the TgN(SOD1-G93A)1Gur mouse model of ALS. J. Neurol. Sci. 236, 1–7.

Henderson, C.E., Bloch-Gallego, E., Camu, W., 1995. Purification and Culture of Embryonic Motor Neurons. IRL Press, Oxford.

Johnson, D.K., Schillinger, K.J., Kwait, D.M., Hughes, C.V., McNamara, E.J., Ishmael, F., O'Donnell, R.W., Chang, M.M., Hogg, M.G., Dordick, J.S., Santhanam, L, Ziegler, L.M., Holland, J.A., 2002. Inhibition of NADPH oxidase activation in endothelial cells by ortho-methoxy-substituted catechols. Endothelium 9, 191–203.

Lambeth, J.D., 2004. NOX enzymes and the biology of reactive oxygen. Nat. Rev. Immunol. 4, 181–189.

Marchetto, M.C.N., Muotri, A.R., Mu, Y., Smith, A.M., Cezar, G.G., Gage, F.H., 2008. Non-cell-autonomous effect of human SOD1^{G37R} astrocytes on motor neurons derived from human embryonic stem cells. Cell Stem Cell 3, 649–657.

Marden, J.J., Harraz, M.M., Williams, A.J., Nelson, K., Luo, M., Paulson, H., Engelhardt, J.F., 2007. Redox modifier genes in amyotrophic lateral sclerosis in mice. J. Clin. Invest. 117, 2913–2919.

Rothstein, J.D., Patel, S., Regan, M.R., Haenggeli, C., Huang, Y.H., Bergles, D.E., Jin, L., Hoberg, M.D., Vidensky, S., Chung, D.S., Toan, S.V., Bruijn, L.I., Su, Z., Gupta, P., Fisher, P.B., 2005. B-lactam antibiotics offer neuroprotection by increasing glutamate transporter expression. Nature 433, 73–77.

Sahawneh, M.A., Ricart, K.C., Roberts, B.R., Bomben, V.C., Basso, M., Sahawneh, J., Franco, M.C., Beckman, J.S., Estévez, A.G., 2010. Cu, Zn-superoxide dismutase increases toxicity of mutant and zinc-deficient superoxide dismutase by enhancing protein stability. J. Biol. Chem. 285, 33885–33897.

Scott, S., Kranz, J.E., Cole, J., Lincecum, J.M., Thompson, K., Kelly, N., Bostrom, A., Theodoss, J., Al-Nakhala, B.M., Vieira, F.G., Ramasubbu, J., Heywood, J.A., 2008. Design, power, and interpretation of studies in the standard murine model of ALS. Amyotroph Lateral Scler 9, 4–15.

Simons, J.M., 't Hart, B.A., Ip Vai Ching, T.R., Dijk, H.V., Labadie, R.P., 1990. Metabolic activation of natural phenols into selective oxidative burst agonists by activated human neutrophils. Free Radic. Biol. Med. 8, 251–258.

Sorce, S., Krause, K., 2009. NOX enzymes in the central nervous system: from signaling to disease. Antioxid Redox Signal 11, 2481–2504.

Stefanska, J., Pawliczak, R., 2008. Apocynin: molecular aptitudes. Mediators Inflamm 106507.

Steffen, Y., Gruber, C., Schewe, T., Sies, H., 2008. Mono-O-methylated flavanols and other flavonoids as inhibitors of endothelial NADPH oxidase. Arch. Biochem. Biophys. 469, 209–219.

Stolk, J., Hiltermann, T.J., Dijkman, J.H., Verhoeven, A.J., 1994. Characteristics of the inhibition of NADPH oxidase activation in neutrophils by apocynin, a methoxy-substituted catechol. Am. J. Respir. Cell Mol. Biol. 11, 95–102.

van den Worm, Edwin. Investigation of apocynin, a potent NADPH oxidase inhibitor. PhD dissertation, Utrecht University, 2001.

van den Worm, E., Beukelman, C.J., Van den Berg, A.J.J., Kroes, B.H., Labadie, R.P., Van Dijk, H., 2001. Effects of methoxylation of apocynin and analogs on the inhibition of reactive oxygen species production by stimulated human neutrophils. Eur. J. Pharmacol. 433, 225–230.

Wang, Q., Smith, R.E., Luchtefeld, R., Sun, A.Y., Simonyi, A., Luo, R., Sun, G.Y., 2008. Bioavailability of apocynin through its conversion to glycoconjugate but not to diapocynin. Phytomedicine 15, 496–503.

Weydt, P., Hong, S.Y., Kliot, M., Möller, T., 2003. Assessing disease onset and progression in the SOD1 mouse model of ALS. Neuroreport 14, 1051–1054.

Wu, D.C., Ré, D.B., Nagai, M., Ischiropoulos, H., Przedborski, S., 2006. The inflammatory NADPH oxidase enzyme modulates motor neuron degeneration in amyotrophic lateral sclerosis mice. Proc. Natl. Acad Sci. USA 103, 12132–12137.

Ximenes, V.F., Kanegae, M.P., Rissato, S.R., Galhiane, M.S., 2007. The oxidation of apocynin catalyzed by myeloperoxidse: proposal for NADPH oxidase inhibition. Arch. Biochem. Biophys. 457, 134–141.

Estudio 2: Rol de la mitocondria en la neurotoxicidad de los astrocitos SOD1[G93A].

Artículo 5

Cassina P, Cassina A, Pehar M, Castellanos R, Gandelman M, de León A, Robinson KM, Mason RP, Beckman JS, Barbeito L, Radi R. Mitochondrial dysfunction in SOD1G93A-bearing astrocytes promotes motor neuron degeneration: prevention by mitochondrial-targeted antioxidants. J Neurosci. 2008 Apr 16;28(16):4115-22. doi: 10.1523

Artículo 6

Miquel E, Cassina A, Martínez-Palma L, Bolatto C, Trías E, Gandelman M, Radi R, Barbeito L, Cassina P. Modulation of astrocytic mitochondrial function by dichloroacetate improves survival and motor performance in inherited Amyotrophic Lateral Sclerosis. PLoS One. 2012;7(4):e34776. doi: 10.1371

La disfunción mitocondrial es uno de los mecanismos patogénicos que promueven la neurodegeneración en la ELA. Se han descrito alteraciones en la función mitocondrial en la médula espinal y músculo de pacientes y modelos animales de ELA (Manfredi y Xu, 2005), sin embargo, se desconoce si las mitocondrias de los astrocitos se encuentran afectadas y si esto podría ser uno de los factores que determinan su neurotoxicidad hacia motoneuronas. En los siguientes dos trabajos se estudiaron las alteraciones mitocondriales de astrocitos SOD1[G93A] y como éstas influencian la sobrevida de motoneuronas. Encontramos que los astrocitos SOD1[G93A] presentaron una disminución en su consumición de oxígeno y coeficiente de respiración mitocondrial. Estas alteraciones se encontraron asociadas con un incremento en la producción de superóxido y nitración de proteínas mitocondriales. La administración del antioxidante Mito-Q, que se dirige y acumula selectivamente

en las mitocondrias, redujo el daño nitro-oxidativo y restauró el coeficiente de respiración. Notablemente, este antioxidante fue capaz de revertir la actividad neurotóxica de los astrocitos SOD1^{G93A}, previniendo la muerte de motoneuronas en cocultivo. Los resultados de este trabajo indican que la mitocondria de los astrocitos constituye un nuevo blanco terapéutico, beneficiándose de fármacos que incrementen la actividad mitocondrial y disminuyan el estrés nitro-oxidativo.

En el segundo trabajo se evaluó la capacidad del compuesto dicloroacetato (DCA) de restaurar la función mitocondrial y extender la sobrevida de los animales SOD1^{G93A}. El DCA inhibe a la proteína quinasa de la enzima piruvato deshidrogenasa, (PDH) manteniéndola desfosforilada, su forma activa. La enzima PDH se localiza en la matriz mitocondrial y media la producción de acetil coenzima-A a partir del piruvato, alimentado la cadena respiratoria. Por lo tanto, la activación de la enzima PDH encausa la glucosa hacia su oxidación en la cadena respiratoria, desfavoreciendo la glicólisis. Como consecuencia los niveles de lactato descienden y la consumición de oxígeno y síntesis de ATP aumentan, restaurando la actividad mitocondrial.

En una primera aproximación, astrocitos aislados de animales SOD1^{G93A} fueron expuestos a DCA. Encontramos que el DCA fue capaz de restaurar su coeficiente de respiración a niveles comparables con los astrocitos no transgénicos. Notablemente, el DCA también previno su actividad neurotóxica hacia motoneuronas, restaurando su sobrevida. Para evaluar si el DCA podría también proteger a las motoneuronas in vivo, se administró a ratones SOD1^{G93A} en el agua de beber a partir de los 70 días de vida. El tratamiento con DCA fue capaz de normalizar el coeficiente de respiración mitocondrial y extender la sobrevida de los ratones enfermos por dos semanas. Analizando las médulas espinales de estos ratones, se encontró que el DCA disminuyó la reactividad astrocitaria y previno la muerte de motoneuronas. Periferalmente, fue capaz de proteger las uniones neuromusculares, hallazgo que se reflejó en la conservación de la fuerza muscular de los ratones tratados hasta etapas avanzadas de la enfermedad. Estos resultados demuestran que la restauración de la

actividad mitocondrial en astrocitos por DCA es capaz de modificar el curso de la enfermedad en animales transgénicos, y podría ser potencialmente beneficiosa para pacientes con ELA.

Neurobiology of Disease

Mitochondrial Dysfunction in SOD1^{G93A}-Bearing Astrocytes Promotes Motor Neuron Degeneration: Prevention by Mitochondrial-Targeted Antioxidants

Patricia Cassina,[1,3]* **Adriana Cassina,**[2,3]* **Mariana Pehar,**[4] **Raquel Castellanos,**[1] **Mandi Gandelman,**[1,5] **Andrés de León,**[1,5] **Kristine M. Robinson,**[7] **Ronald P. Mason,**[6] **Joseph S. Beckman,**[7] **Luis Barbeito,**[3,4,5] **and Rafael Radi**[2,3]

[1]Departamento de Histología, [2]Departamento de Bioquímica, and [3]Center for Free Radical and Biomedical Research, Facultad de Medicina, Universidad de la República, 11800 Montevideo, Uruguay, [4]Instituto de Investigaciones Biológicas Clemente Estable, 11600 Montevideo, Uruguay, [5]Neurodegeneration Laboratory, Institut Pasteur, 11400 Montevideo, Uruguay, [6]Laboratory of Pharmacology and Chemistry, National Institute of Environmental Health Science, National Institutes of Health, Research Triangle Park, North Carolina 27709, and [7]Department of Biochemistry and Biophysics, Linus Pauling Institute, Oregon State University, Corvallis, Oregon 97331

Mitochondrial dysfunction and oxidative stress contribute to motor neuron degeneration in amyotrophic lateral sclerosis (ALS). Recent reports indicate that astrocytes expressing the mutations of superoxide dismutase-1 (SOD1) may contribute to motor neuron injury in ALS. Here, we provide evidence that mitochondrial dysfunction in SOD1^{G93A} rat astrocytes causes astrocytes to induce apoptosis of motor neurons. Mitochondria from SOD1^{G93A} rat astrocytes displayed a defective respiratory function, including decreased oxygen consumption, lack of ADP-dependent respiratory control, and decreased membrane potential. Protein 3-nitrotyrosine was detected immunochemically in mitochondrial proteins from SOD1^{G93A} astrocytes, suggesting that mitochondrial defects were associated with nitroxidative damage. Furthermore, superoxide radical formation in mitochondria was increased in SOD1^{G93A} astrocytes. Similar defects were found in mitochondria isolated from the spinal cord of SOD1^{G93A} rats, and pretreatment of animals with the spin trap 5,5-dimethyl-1-pyrroline N-oxide restored mitochondrial function, forming adducts with mitochondrial proteins *in vivo*. As shown previously, SOD1^{G93A} astrocytes induced death of motor neurons in cocultures, compared with nontransgenic ones. This behavior was recapitulated when nontransgenic astrocytes were treated with mitochondrial inhibitors. Remarkably, motor neuron loss was prevented by preincubation of SOD1^{G93A} astrocytes with antioxidants and nitric oxide synthase inhibitors. In particular, low concentrations ($\sim$10 nM) of two mitochondrial-targeted antioxidants, ubiquinone and carboxy-proxyl nitroxide, each covalently coupled to a triphenylphosphonium cation (Mito-Q and Mito-CP, respectively), prevented mitochondrial dysfunction, reduced superoxide production in SOD1^{G93A} astrocytes, and restored motor neuron survival. Together, our results indicate that mitochondrial dysfunction in astrocytes critically influences motor neuron survival and support the potential pharmacological utility of mitochondrial-targeted antioxidants in ALS treatment.

Key words: mitochondria; ALS; astrocytes; SOD1; free radicals; antioxidants

Introduction

Mitochondrial dysfunction and oxidative stress have been involved in amyotrophic lateral sclerosis (ALS) pathogenesis [for review, see Dupuis et al. (2004), Bruijn et al. (2004), and Manfredi and Xu (2005)]. Previous reports described decreased mitochondrial respi-

ratory activity in spinal cords from transgenic (Tg) superoxide dismutase-1 (SOD1)^{G93A} mice (Jung et al., 2002; Mattiazzi et al., 2002) and in cellular models of the disease (Menzies et al., 2002). However, it is unknown whether mitochondrial dysfunction in ALS affects non-neuronal cells in addition to motor neurons. In mutant SOD1 chimeric mice, toxicity to motor neurons requires damage from mutant SOD1 acting within non-neuronal cells (Clement et al., 2003). Most importantly, non-neuronal cells that do not express mutant SOD1 extend survival of mutant-expressing motor neurons, supporting a role for glia in ALS pathology and raising the concept of the so-called nonautonomous nature of motor neuron death in ALS (Clement et al., 2003).

Astrocytic activation occurs in both human and animal models of ALS (Barbeito et al., 2004; Bruijn et al., 2004). We have shown that astrocytes may contribute to motor neuron loss. Reactive astrocytes upregulate nitric oxide (·NO) production and NGF (nerve growth factor) expression, which induces motor

neuron death through p75 receptor signaling (Cassina et al., 2002, 2005; Pehar et al., 2004). These effects can be prevented by increasing antioxidant defenses in astrocytes either by activation of Nrf2 transcription factor or antioxidant treatment (Vargas et al., 2005). Remarkably, astrocytes expressing SOD1 mutations become neurotoxic for motor neurons (Vargas et al., 2006; Nagai et al., 2007), suggesting a common link between SOD1 mutations, oxidative stress, and astrocyte-induced neuronal death.

Herein, we provide experimental evidence that mitochondria in SOD1^{G93A}-expressing astrocytes display severe impairment of oxygen consumption and ADP-dependent respiratory control, which is associated with enhanced mitochondrial superoxide formation and local oxidative and nitrative damage [referred to herein as nitroxidative stress; for review, see Peluffo and Radi (2007)]. In addition, mitochondrial dysfunction results in decreased ability to sustain motor neuron survival and can be prevented by mitochondrial-targeted antioxidants. Together, our results suggest that mitochondrial activity in astrocytes greatly influences their subsequent ability to regulate motor neuron survival.

Materials and Methods

Materials. JC-1, 3,8-phenanthridine diamine-hexyl triphenylphosphonium iodide (MitoSOX Red), and MitoTracker Deep Red were provided by Invitrogen (Carlsbad, CA). Culture media and serum were from Invitrogen. 5,5-Dimethyl-1-pyrroline *N*-oxide (DMPO) was from Alexis Biochemicals (San Diego, CA) and further purified by double distillation. Antibodies to DMPO–protein adducts and protein 3-nitrotyrosine were raised as previously described (Cassina et al., 2000; Mason, 2004). The manganese porphyrin manganese(III) *meso*-tetrakis[(*N*-ethyl)pyridinium-2-yl]porphyrin (MnTE-2-PyP), mito-ubiquinone (Mito-Q; a mixture of mitoquinol [10-(3,6-dihydroxy-4,5-dimethoxy-2-methylphenyl) decyl] triphenylphosphonium bromide and mitoquinone [10-(4,5-dimethoxy-2-methyl-3,6-dioxo-1,4-cyclohexadien-1-yl)decyl] triphenylphosphonium bromide) and mito-carboxy-proxyl nitroxide (Mito-CP) were kindly provided by Dr. Ines Batinic-Haberle (Duke University Medical Center, Durham, NC) (Batinic-Haberle et al., 1998), Dr. Michael Murphy (Medical Research Council, Dunn Human Nutrition Unit, Cambridge, UK) (Kelso et al., 2001), and Dr. Balaranan Kalyanaraman (Medical College of Wisconsin, Milwaukee, WI) (Jauslin et al., 2003), respectively. All other reagents were from Sigma (St. Louis, MO).

Animals. Procedures using laboratory animals were in accordance with the international guidelines for the use of live animals and were approved by the Institutional Animal Committee. In this study, Sprague Dawley SOD1^{WT} transgenic rats, which overexpressed the wild-type form of SOD1, were obtained from Dr. Pak Chan (Stanford University, Palo Alto, CA) and remain healthy for at least 2 years (Chan et al., 1998). Sprague Dawley SOD1^{G93A} L26H rats, which develop motor neuron disease between 104 and 121 d of age, were kindly provided by Dr. David S. Howland (Wyeth Research, Princeton, NJ) (Howland et al., 2002). Onset typically appeared as hindlimb abnormal gait affecting one limb first (considered as early symptomatic) and progress very quickly (1–2 d) to overt hindlimb paralysis. Within 1–2 d, the second hindlimb is involved, although animals could still ambulate through the use of forepaws. Affected rats typically reached end-stage disease very quickly, in an average of 11 d after onset of symptoms.

Cell culture. Primary transgenic SOD1^{G93A}, SOD1^{WT}, and nontransgenic astrocytes cultures were prepared either from spinal cords or brain of 1- to 2-d-old rat pups according to the procedures of Saneto and De Vellis (1987) with minor modifications (Cassina et al., 2002). The neonates were previously genotyped by PCR, and neonates bearing the SOD1 mutation were used for preparing SOD1^{G93A}-bearing astrocyte cultures and the nontransgenic littermates as control cultures. Astrocytes were plated at a density of 2×10^4 cells/cm^2 and maintained in DMEM supplemented with 10% fetal bovine serum, HEPES (3.6 g/L), penicillin (100 IU/ml), and streptomycin (100 μg/ml). Astrocyte monolayers were

>98% pure as determined by GFAP immunoreactivity and devoid of OX$_{42}$-positive microglial cells. Motor neurons were obtained from embryonic day 15 (E15) rat spinal cord by a combination of metrizamide-gradient centrifugation and immunopanning with the monoclonal antibody IgG192 against p75^{NTR} (Henderson et al., 1993). For coculture experiments, only wild-type motor neurons were plated on rat astrocyte monolayers at a density of 300 cells/cm^2 and maintained for 48 h in L15 medium supplemented with 0.63 mg/ml bicarbonate, 5 μg/ml insulin, 0.1 mg/ml conalbumin, 0.1 mM putrescine, 30 nM sodium selenite, 20 nM progesterone, 20 mM glucose, 100 IU/ml penicillin, 100 μg/ml streptomycin, and 2% horse serum, fixed with paraformaldehyde at 4% plus 0.1% glutaraldehyde in PBS at 4°C for 15 min, and then processed for immunocytochemistry as described previously (Cassina et al., 2002).

Cell treatment. Confluent astrocyte monolayers were transferred to supplemented L15 media prior to treatment. Astrocyte monolayers were incubated with rotenone (2 μM), antimycin A (5 μM), sodium azide (5 μM), fluorocitrate (250–100 μM), DMPO (75 mM), MnTE-2-PyP (10 μM), Mito-Q (10–100 nM), or Mito-CP (10–100 nM) for 24 h before mitochondrial purification or motor neuron plating after washing twice with PBS supplemented with (in mM) 0.8 MgCl$_2$, 1 CaCl$_2$, and 5 glucose.

Mitochondrial preparation. Intact spinal cord or astrocyte culture mitochondria were prepared by differential centrifugation as described previously (Cassina and Radi, 1996). Briefly, rats were anesthetized, and the spinal cord or cerebral cortex was removed and washed extensively, minced, and homogenized with a small tissue grinder. Tissue fragments were disrupted using a Potter-Elvehjem homogenizer in homogenization buffer containing 0.3 M sucrose, 5 mM morpholinepropanesulfonic acid, 5 mM potassium phosphate, 1 mM EGTA, and 0.1% bovine serum albumin (BSA). Confluent astrocyte monolayers were cell scraped in respiration buffer, homogenized, and centrifuged at 1500 × *g*, and mitochondria were isolated from the supernatant by centrifugation at 13,000 × *g*. Mitochondrial pellets were resuspended in minimal volume of homogenization buffer.

Oxygen consumption studies. Mitochondrial respiration was measured polarographically using a Cole-Parmer (Vernon Hills, IL) oximeter fitted with a water-jacketed Clark-type electrode (model 5300; YSI, Yellow Springs, OH) in an incubation chamber of 1.6 ml capacity as described previously (Cassina and Radi, 1996). Briefly, oxygen consumption studies were performed in homogenization buffer at 37°C, pH 7.4, at 0.2–0.5 mg/ml mitochondria. Glutamate–malate (2.5 mM each) and succinate (5 mM) were used to quantify complex I- and II-dependent respiration, respectively. Rotenone (2 μM) and antimycin A (AA; 2 μM) were used as complex I and III inhibitors, respectively. For each complex respiration, we also tested the addition of the ATPase inhibitor oligomycin (5 μM) and the mitochondrial uncoupler carbonyl cyanide 4-(trifluoromethoxy) phenylhydrazone (FCCP) (supplemental Fig. S1, available at www. jneurosci.org as supplemental material). ADP was used to evaluate mitochondrial coupling. The respiratory control ratio (RCR) was calculated as the ratio of oxygen consumption rates after (state 3) and before (state 4) ADP addition. The purity of the mitochondrial fraction was confirmed by measuring cytochrome *c* oxidase and lactate dehydrogenase activities as markers of mitochondria and cytosol, respectively (Radi et al., 1991).

Motor neuron counting. Motor neurons on the astrocyte monolayer were identified by p75 immunocytochemistry as previously described (Cassina et al., 2002). Motor neuron survival was assessed by counting all p75-positive cells displaying neurites longer than four cell diameters in an area of 0.90 cm^2 along a diagonal in 24-well plates. The mean density of motor neurons in control cocultures was 88 ± 5 cells/cm^2.

Determination of superoxide generation by microscopy. Astrocyte monolayers were switched from 10% FBS to low serum (2% horse serum) for 48 h before analysis. Cultured cells were transferred to the heated stage (37°C) of a Zeiss (Thornwood, NY) LSM510 confocal microscope with constant 5% CO$_2$ and imaged with a 63× oil-immersion objective using 405 nm excitation (Robinson et al., 2006). Untreated, live astrocytes were imaged to set instrument parameters and minimize autofluorescence from 400 nm excitation. Astrocytes were then incubated with 0.3 μM MitoSOX Red for 15 min and washed, and the media were replaced. After MitoSOX Red images were obtained, astrocytes were

incubated with 4′,6′-diamidino-2-phenylindole (DAPI) and 3.5 nM MitoTracker Deep Red.

Flow cytometric analysis of superoxide production and mitochondrial membrane potential. The probe JC-1 was used to measure mitochondrial membrane potential (Almeida et al, 2001) and MitoSOX Red to measure mitochondrial superoxide (Mukhopadhyay et al., 2007). Cells were mildly trypsinized and resuspended at a density of 4×10^5 cells/ml in prewarmed (37°C) PBS solution supplemented with 20 mM glucose and 2% FBS, pH 7.4, containing JC1 (2 μM) or MitoSOX Red (2.5 μM). After a 15 min incubation period at 37°C in the dark, cell suspensions were centrifuged and resuspended in probe-free solution. Data acquisition was performed in a CyAn ADP cytometer (Dako, High Wycombe, UK). Astrocytes were gated to exclude subcellular debris as differentiated by forward and side scatter. Probes were excited with a 488 nm laser. JC-1 monomer fluorescence signal was detected on FL1 (green fluorescence, centered around 530 nm), and JC-1 aggregates on the FL2 detector (red fluorescence, centered around 575 nm). Mean fluorescence intensity values for FL1 and FL2 were obtained for all experiments. The relative aggregate/monomer (red/green) fluorescence intensity values were used for data presentation. These values were expressed in a percentage scale, with the red/green fluorescence ratio values of nontransgenic astrocytes (3.7 ± 0.30) considered as 100% and the red/green fluorescence ratio values of FCCP-treated transgenic astrocytes considered as 0%. MitoSOX Red fluorescence was detected in FL2 (red fluorescence, centered around 575 nm) and expressed as a percentage of nontransgenic cells.

Determination of mitochondrial membrane potential. Astrocyte monolayers were rinsed twice with prewarmed Hank's solution and incubated with 30 μM JC-1 in Hank's solution for 30 min at 37°C. Cells were rinsed, mounted, and kept at 37°C. Epifluorescence was examined using a Nikon (Tokyo, Japan) Eclipse TE 200 microscope with the appropriate filters. Fluorescence was monitored in a multifunctional microplate reader Fluostar Galaxy from BMG Labtech (Winooski, VT) using 490 nm excitation/535 nm emission for the monomeric form and 570 nm excitation/595 nm emission for the aggregate of JC-1. Mitochondrial membrane potential is shown as a ratio of the fluorescence of aggregate (aqueous phase) and monomer (membrane-bound) forms of JC-1 and was pooled with data obtained by cytometry.

Immunohistochemistry. Early symptomatic SOD1G93A rats (105–120 d) were injected 48 and 24 h before perfusion with 200 mg/kg DMPO intraperitoneally. Under deep anesthesia (35 mg/kg pentobarbital), rats were transcardially perfused with 0.9% saline followed by 4% paraformaldehyde fixative. The spinal cords were removed and embedded in Paraplast. Five micrometer tissue sections were preincubated with 0.3% hydrogen peroxide in methanol, washed, and permeabilized with 0.1% Triton X-100 in PBS for 15 min and blocked for 2 h with 10% goat serum, 2% BSA, and 0.1% Triton X-100 in PBS. The primary polyclonal anti-DMPO 1:400 was diluted in blocking solution and incubated overnight at 4°C. After washing with PBS, cultures were incubated with secondary anti-rabbit biotinylated antibody 1:250 in blocking solution for 1 h and then with streptavidin–horseradish peroxidase 1 μg/ml in Tris-HCl, pH 7.4 (both from Jackson ImmunoResearch, West Grove, PA), for 1 h at room temperature. Development was performed with 0.5 mg/ml DAB solution and 0.01% (v/v) hydrogen peroxide in 0.05 M Tris-HCl. The slides were counterstained with hematoxylin. Images were captured by a Nikon digital camera coupled to a Nikon Eclipse TE 200 epifluorescence microscope.

Western blot analysis. Protein samples were separated on a 10% SDS-polyacrylamide gel and transferred to nitrocellulose membrane (GE Healthcare, Piscataway, NJ) overnight at 100 mA at 4°C. For DMPO Western blotting, membranes were blocked for 1 h in Tris-buffered saline (TBS), 2.5% BSA, and 2.5% casein and then 1 h incubation with primary anti-DMPO antibody at 1:5000 dilution in the same buffer plus 0.2% Tween 20 (washing buffer). After washing, the membrane was incubated with peroxidase-conjugated secondary antibody (Bio-Rad, Hercules, CA) diluted in 0.3% Tween 20 plus 0.1% bovine serum albumin for 1 h. For nitrotyrosine Western blotting, membranes were blocked for 1 h in TBS, 0.6% Tween 20, and 5% bovine serum albumin, followed by 1 h incubation with primary anti-nitrotyrosine antibody at 1:2000 dilution in the same buffer (Brito et al., 1999). After washing with

0.6% Tween 20 in TBS, the membrane was incubated with peroxidase-conjugated secondary antibody (Bio-Rad) diluted in 0.3% Tween 20 plus 0.1% bovine serum albumin for 1 h. Then both membranes were washed and developed using the ECL chemiluminescent detection system (GE Healthcare). Densitometric analysis was performed using the NIH ImageJ program.

Statistics. Each experiment was repeated at least three times, and data are reported as the mean $\pm$ SEM. Comparison of the means was performed by one-way ANOVA. Pairwise tests between any two means used the Student–Newman–Keuls test, and differences were declared statistically significant if $p < 0.05$. When normality test failed, comparison of the means was performed by one-way ANOVA on ranks followed by the Kruskal–Wallis test. All statistics were performed using the SigmaStat Software (SPSS, Chicago, IL).

Results

Decreased mitochondrial respiration associated with oxidative stress in the SOD1G93A rat spinal cord

To assess whether the electron transport chain (ETC) function was altered in mitochondria from SOD1G93A rats, we measured oxygen consumption in mitochondria preparations from the spinal cord. We selected early symptomatic animals (120 d of age) to perform the study. We stimulated mitochondrial respiration by either glutamate–malate or succinate, which supply reducing equivalents through complex I and II, respectively (Fig. 1A,B; supplemental Fig. S1, available at www.jneurosci.org as supplemental material). In this assay, addition of ADP increases oxygen consumption only in well coupled mitochondria preparations. Here, glutamate–malate or succinate induced oxygen consumption in mitochondria from both transgenic and nontransgenic rats. However, the addition of ADP increased oxygen consumption only in mitochondria from nontransgenic spinal cords, indicating that coupling, and therefore the ability to synthesize ATP, was significantly impaired in spinal cord mitochondria from symptomatic SOD1G93A rats (Fig. 1A,B). Remarkably, such defect could be prevented by the systemic administration of the spin trap DMPO (50 mg/kg) to symptomatic animals 48 and 24 h before mitochondrial isolation (Fig. 1A,B). DMPO is a nitroxide that reacts with a variety of radicals, including protein radicals, to form DMPO–protein radical adducts. We then explored whether DMPO was able to trap mitochondrial protein radicals *in vivo* using a specific antibody that recognizes DMPO nitrone–protein adducts (Detweiler et al., 2002). Indeed, in biological systems the unstable protein–DMPO nitroxide radical adduct can be oxidized by one electron to a stable and electron paramagnetic resonance-silent protein–DMPO nitrone adduct, which can be recognized immunochemically (Detweiler et al., 2005). Western blot analysis showed an increase in DMPO–protein adducts in mitochondrial protein extracts from DMPO-treated SOD1G93A rat spinal cords compared with DMPO-treated nontransgenic animals (Fig. 1C). In agreement, immunohistochemistry of spinal cord sections revealed an increase in DMPO–protein adducts staining in both neuropil and motor neurons from transgenic animals, whereas a low background was observed in nontransgenic ones (Fig. 1D).
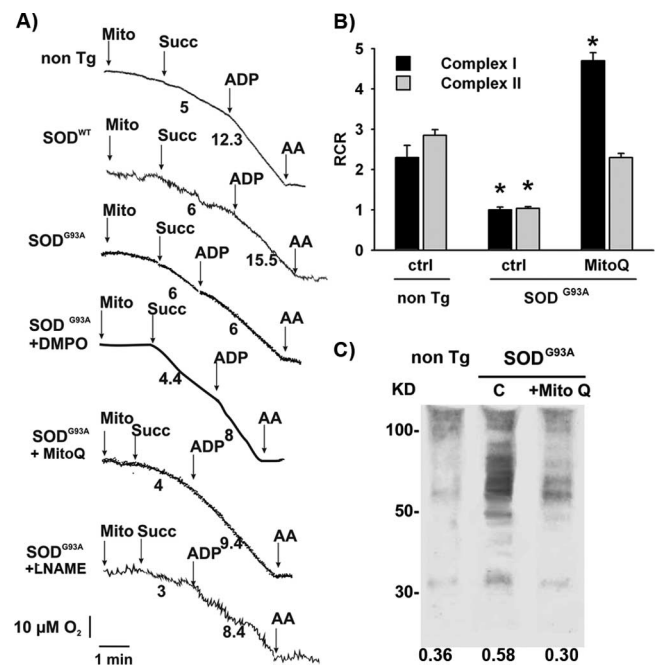
Antioxidants and NOS inhibition restored the uncoupled mitochondrial activity in cultured SOD1G93A-expressing astrocytes

To determine whether mitochondrial respiration was affected in SOD1G93A astrocytes, we isolated mitochondria from pure astrocyte cultures obtained from nontransgenic, SOD1WT, or SOD1G93A transgenic neonate rats, which overexpressed either wild-type or G93A mutation of SOD1, respectively. We used the
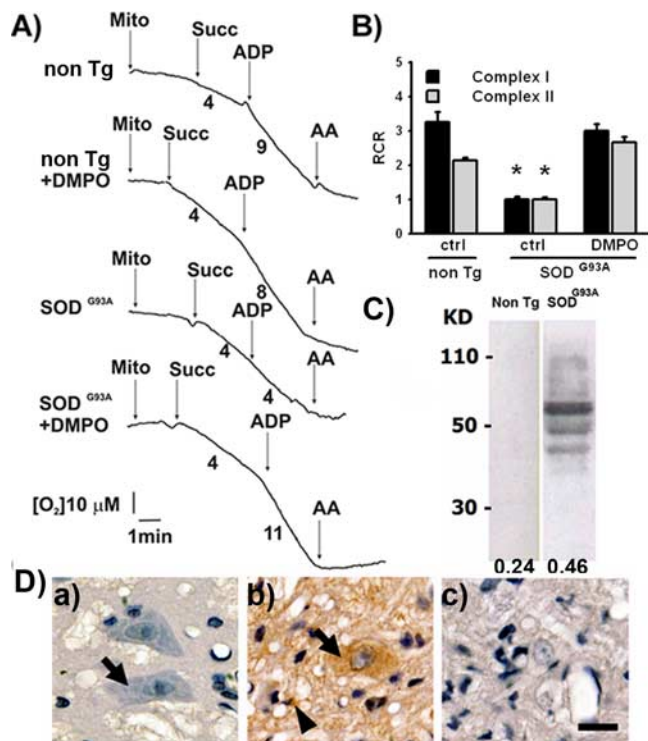
Figure 1. Respiratory complex II-dependent oxygen consumption in spinal cord mitochondria. **A**, Representative state-4 and state-3 oxygen consumption curves in the presence of succinate (Succ; 5 mM) in intact rat spinal cord mitochondria (0.5 mg/ml). Numbers under the traces represent micromolar O_2 per minute. **B**, Calculated respiratory control ratio for spinal cord mitochondria from the indicated treatments. Data are mean ± SEM from three independent experiments. *$p < 0.05$, significantly different from non-Tg control. **C**, Immunoblotting of mitochondrial protein from the lumbar spinal cord of DMPO-injected rats. Ten micrograms of mitochondrial protein were seeded per lane in 13% acrylamide gel. Anti-DMPO antibody was used at 1:5000. Numbers on the left indicate molecular weights, and numbers on the bottom indicate the mean optical density for each lane. This is a representative blot from three independent experiments. **D**, Immunohistochemistry in sections of the anterior horn of DMPO-injected nontransgenic rats (**a**), DMPO-injected early symptomatic SOD1^{G93A} rats (120 d of age; **b**), and vehicle-injected SOD1^{G93A} rats (**c**). Note the intense punctuate immunolabeling in both motor neurons (arrows) and surrounding glial cells (arrowheads) in **b** compared with lack of labeling in **a**. DMPO was injected intraperitoneally (50 mg/kg) 48 and 24 h before mitochondrial isolation, and anti-DMPO was used at 1:400. Scale bar, 20 μm. Images are representative from three independent experiments.

Figure 2. Antioxidants and NOS inhibition reestablished mitochondrial respiration and decreased protein 3-nitrotyrosine levels in mitochondrial proteins from SOD1^{G93A} astrocytes. **A**, Representative oxygen consumption curves by mitochondria isolated from cultured cerebral cortex astrocytes prepared from non-Tg or transgenic SOD1^{WT} or SOD1^{G93A} rat neonates treated as indicated. Mitochondrial respiration was evaluated as indicated in Figure 1. DMPO (75 mM, 48 h), Mito-Q (10 nM, 24 h), or L-NAME (5 mM, 24 h) were added to the culture medium of SOD1^{G93A} before mitochondrial isolation. Numbers under the traces indicate the absolute values of state-3 and -4 respiration in micromolar O_2 per minute. **B**, Calculated respiratory control ratio for complex I and II of astrocyte mitochondria from the indicated groups. Data are mean ± SEM from four independent experiments. *$p < 0.05$, significantly different from non-Tg control. **C**, Protein 3-nitrotyrosine immunoblotting of mitochondrial proteins from the same samples used to measure oxygen consumption in **A**. Thirty micrograms of mitochondrial protein were seeded per lane in 13% acrylamide gel. Numbers on the left indicate molecular weights, and numbers on the bottom indicate the mean optical density for each lane. This is a representative blot from three independent experiments.

cerebral cortex instead of the spinal cord as a source to provide sufficient yield of mitochondria for respiratory experiments. Mitochondria from SOD1^{G93A}-bearing astrocytes showed a decrease in both complex I- and II-dependent respiration rate and no increase in oxygen consumption in response to ADP compared with mitochondria from nontransgenic or SOD1^{WT} (Fig. 2A,B; supplemental Fig. S1, available at www.jneurosci.org as supplemental material). The defect was comparable with that observed in whole spinal cord mitochondrial preparations (Fig. 1A,B). When SOD1^{G93A} astrocytes were preincubated with DMPO (75 mM) for 48 h before mitochondria isolation, the respiratory control rate was partially reestablished. The detection of oxidative damage in mitochondria associated with organelle dysfunction described in Figure 1 prompted us to test the recently designed mitochondrial-targeted antioxidants Mito-Q and Mito-CP. These compounds have been developed by covalently coupling to triphenylphosphonium cation, thereby allowing these compounds be preferentially taken up by mitochondria (Kelso et al., 2001). They have been shown to be effective in preventing oxidative damage at substantially lower concentra-

tions than other antioxidants (Jauslin et al., 2003; Dhanasekaran et al., 2005). Transgenic astrocytes preincubated with Mito-Q (20 nM) for 24 h recovered the ability to increase oxygen consumption after addition of ADP and restored the RCR (and therefore coupling) to control values more effectively than DMPO (Fig. 2A,B). The preincubation of non-Tg astrocytes with Mito-Q did not affect mitochondrial respiration (data not shown). We have previously described that SOD1^{G93A} transgenic astrocytes produce more nitric oxide than nontransgenic ones (Vargas et al., 2006). Because nitric oxide may be contributing to oxidative damage, we then pretreated transgenic astrocytes with the nitric oxide synthase (NOS) inhibitor L-N-nitroarginine methyl ester (L-NAME; 5 mM) and also found that this restores the RCR (Fig. 2A). Western blot analysis of mitochondrial protein extracts from the same mitochondrial samples used for the oxygen consumption studies revealed changes in protein 3-nitrotyrosine immunodetection, a well established biomarker of nitric oxide-derived oxidants (Radi, 2004). The samples from SOD1^{G93A}-bearing astrocytes exhibited an increase in 3-nitrotyrosine-immunoreactive bands compared with nontransgenic ones. Furthermore, Mito-Q-treated SOD1^{G93A} astrocytes showed a decrease in 3-nitrotyrosine immunoreactivity (Fig. 2C), indicating that Mito-Q treatment diminished nitroxidative damage to mitochondrial proteins.

Superoxide generation and membrane potential determination in SOD1^{G93A} astrocyte mitochondria

To evaluate mitochondrial oxidant formation in SOD1^{G93A} astrocytes, cultures were incubated with MitoSOX Red, a specific and mitochondrial-targeted detection probe for superoxide radical (O$_2^{\bullet-}$) (Robinson et al., 2006). SOD1^{G93A} transgenic astrocytes showed an approximate twofold increase in fluorescence emission from the superoxide product of MitoSOX Red as detected using the selective excitation wavelength at 405 nm (Fig. 3A). Mitochondrial superoxide generation was measured simultaneously in a large population of astrocytes by flow cytometry as has been recently published (Mukhopadhyay et al., 2007), using 5 μM antimycin A, a complex III inhibitor that increases mitochondrial superoxide production, as a positive control (Fig. 3B). The mean fluorescence intensity showed increase in SOD1^{G93A} astrocytes compared with SOD1^{WT} or non-Tg astrocytes. The increment was reduced to the nontransgenic levels when SOD1^{G93A} astrocytes were treated with Mito-Q (Fig. 3B). However, basal levels of fluorescence are likely to reflect direct redox interactions of MitoSOX with ETC components in addition to the O$_2^{\bullet-}$-dependent reactions. To further characterize the mitochondrial dysfunction, we used the JC1 fluorescent probe to measure mitochondrial membrane potential by flow cytometry as previously published (Almeida et al., 2001). The ratio of the fluorescence of aggregate and monomer forms of JC-1 also reflected a decrease in mitochondrial membrane potential in SOD1^{G93A} transgenic astrocytes (Fig. 3C). The ability to concentrate the JC-1 probe in mitochondria was equally decreased in both cortical and spinal cord astrocytes (supplemental Fig. S2, available at www.jneurosci.org as supplemental material).

Astrocytes fail to support motor neuron survival after mitochondrial dysfunction: protective action of mitochondrial-targeted antioxidants

We then analyzed whether SOD1^{G93A} astrocytic mitochondrial dysfunction could affect motor neuron survival in a coculture model of ALS previously described by our group (Cassina et al., 2002). A feeder layer of SOD1^{G93A} astrocytes decreased the survival of nontransgenic motor neurons by 50% compared with a feeder layer of nontransgenic astrocytes (Fig. 4) or with SOD1^{WT} astrocytes (supplemental Fig. S3, available at www.jneurosci.org as supplemental material). Pretreatment of SOD1^{G93A} astrocytes with the NOS inhibitor L-NAME (5 mM), the spin trap DMPO (75 mM), or the metalloporphyrin catalytic antioxidant MnTE-2-PyP (10 μM) before motor neuron plating enhanced motor neuron survival to the level of that obtained on a feeder layer of nontransgenic astrocytes (Fig. 4). On the other hand, induction of mitochondrial dysfunction by pretreatment of nontransgenic astrocytes with different ETC inhibitors decreased motor neuron survival in coculture conditions (Fig. 4), which was reversed by L-NAME and MnTE treatment (data not shown). We used rotenone (2 μM), antimycin A (5 μM), and sodium azide (5 μM), complex I, complex III, and complex IV inhibitors, respectively. Furthermore, we used fluorocitrate (100–250 μM), which blocks the activity of Krebs cycle enzyme aconitase and has been recently shown to induce inhibition of astrocyte mitochondria and increase vulnerability of cocultured neurons to glutamate toxicity (Voloboueva et al., 2007). The ETC inhibitors did not affect astrocyte viability at the concentration used (data not shown). Preincubation of SOD1^{G93A}-bearing astrocytes with Mito-CP or Mito-Q for 24 h, at much lower concentrations than used for compounds in Figure 4, resulted in increased motor neuron survival in cocultures to a degree similar to that achieved over a
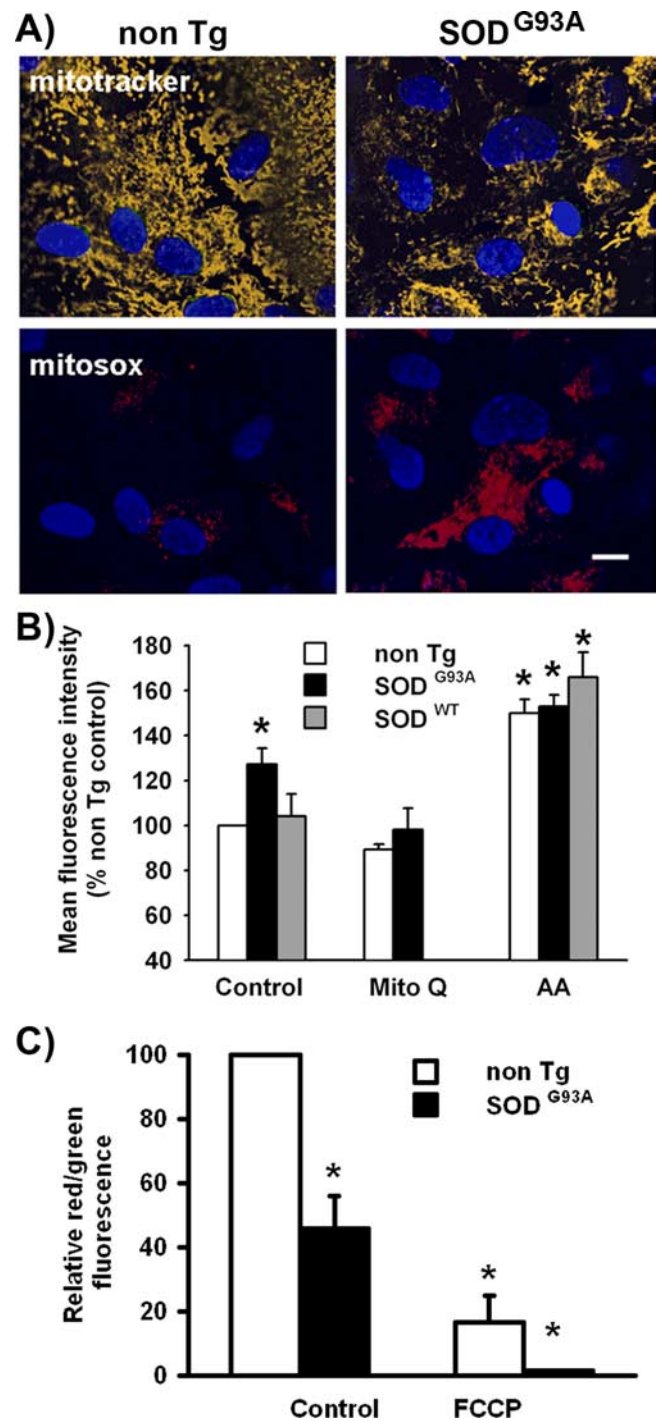
Figure 3. Increased superoxide generation and decreased mitochondrial membrane potential ($\Delta\Psi$) in SOD1^{G93A} astrocytes. *A*, Fluorescence micrographs of cultured astrocytes with MitoTracker Deep Red (top row, yellow) and MitoSOX Red (bottom row, red). Astrocyte monolayers were treated as indicated in Materials and Methods. Nuclei are stained with DAPI (blue). Scale bar, 100 μm. *B*, Data are mean fluorescence intensity of MitoSOX Red emission measured by flow cytometry in nontransgenic (white bars), SOD1^{G93A} (black bars), or SOD1^{WT} (gray bars) astrocyte cultures treated for 24 h with Mito-Q or antimycin A as positive control. Data are mean $\pm$ SEM from three independent determinations. *$p < 0.05$, significantly different from non-Tg control. *C*, Mitochondrial membrane potential as a ratio of the fluorescence of aggregate and monomer forms of JC-1 in SOD1^{G93A} (black bars) and nontransgenic (white bars) astrocytes in control and after addition of the uncoupler FCCP. These values were expressed in a percentage scale, with the red/green fluorescence ratio values of nontransgenic astrocytes (3.7 $\pm$ 0.30) considered as 100% and the red/green fluorescence ratio values of FCCP-treated transgenic astrocytes considered as 0%. Data are mean $\pm$ SEM from three independent experiments. *$p < 0.05$, significantly different from non-Tg control.
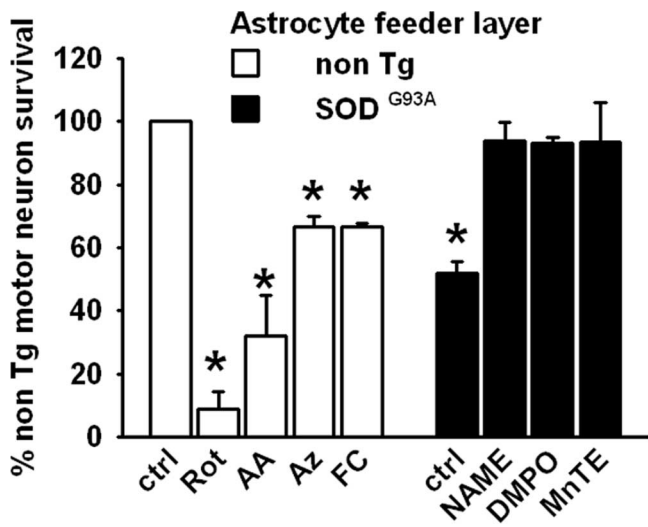
Figure 4. Motor neuron survival in the presence of astrocytes. Motor neuron survival 48 h after plating either on nontransgenic or SOD1^{G93A} astrocyte monolayers as indicated. The non-Tg astrocyte monolayers were previously treated with rotenone (Rot; 2 μM), antimycin A (AA; 5 μM), sodium azide (Az; 5 μM) or fluorocitrate (FC; 100 μM) and the SOD1^{G93A} astrocyte monolayers with L-NAME (5 mM), DMPO (75 mM), or MnTE (10 μM) for 24 h as indicated and washed, and then a nontransgenic motor neuron suspension was added. Motor neuron counting was performed as described in Materials and Methods. Data are presented as a percentage of the non-Tg control group. Data are mean ± SEM from three independent experiments. *$p <$ 0.05, significantly different from non-Tg control.
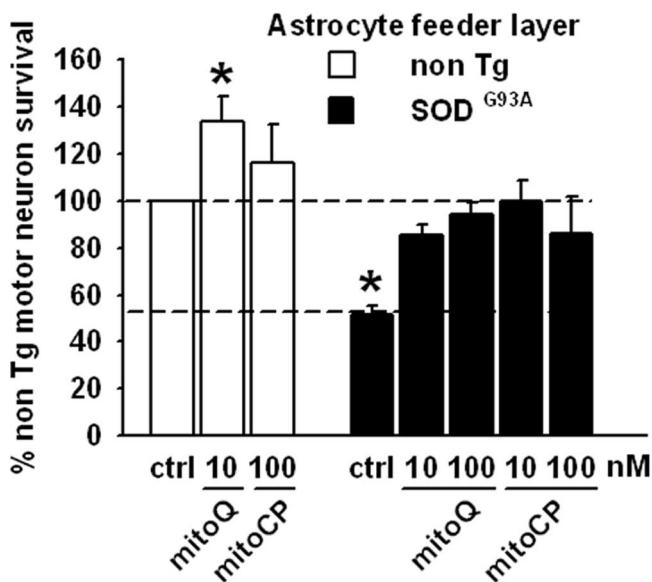
Figure 5. Restoration of motor neuron survival by mitochondrial-targeted antioxidants. Motor neuron survival 48 h after plating either on nontransgenic or SOD1^{G93A} astrocyte monolayers as indicated. The non-Tg or the SOD1^{G93A}-bearing monolayers were previously treated with Mito-Q (10–100 nM) or Mito-CP (10–100 nM) for 24 h as indicated and washed, and then a nontransgenic motor neuron suspension was added. Dotted lines indicate the 100 and 55% motor neuron survival obtained in control conditions over a nontransgenic or SOD1^{G93A} astrocyte feeder layer, respectively. Data are presented as described in Figure 4. Data are mean ± SEM from three independent experiments. *$p <$ 0.05, significantly different from non-Tg control.

nontransgenic astrocyte monolayer (Fig. 5). Indeed, the pretreatment of nontransgenic astrocytes with both compounds improved the motor neuron survival obtained in the control condition (Fig. 5).

Discussion

Herein, we provide evidence that mitochondrial dysfunction linked to nitroxidative stress in SOD1^{G93A} astrocytes promotes the death of neighboring motor neurons. Previous studies have shown decreased mitochondrial function in SOD1^{G93A} ALS mice (Jung et al., 2002; Mattiazzi et al., 2002) and motor neuron cell lines transfected with ALS mutated forms of SOD1 (Menzies et al., 2002; Fukada et al., 2004). Our findings indicate for the first time that mitochondrial defects and enhanced generation of oxidants including $O_2^{\cdot-}$ are occurring in cultured SOD1^{G93A} astrocytes but not in SOD1^{WT} astrocytes, which cause SOD1^{G93A} astrocytes to become neurotoxic for motor neurons. Furthermore, this can be prevented by mitochondrial-targeted antioxidants and NOS inhibitors. Together, these results support the idea that nitroxidative stress-induced mitochondrial defects in astrocytes may contribute to disease pathogenesis.

Defective mitochondrial respiration in SOD1^{G93A} astrocytes seems to be associated with nitroxidative stress as shown by: (1) the extensive formation of DMPO–protein adducts and protein 3-nitrotyrosine in isolated mitochondria from both spinal cord and astrocyte cultures and (2) the fact the spin trap DMPO, a NOS inhibitor, and, in particular, low concentrations of mitochondrial-targeted antioxidants (Mito-Q and Mito-CP) completely reversed mitochondrial dysfunction *in vitro* and/or *in vivo*. Use of DMPO allowed us to combine the specificity of spin trapping and the sensitivity of antigen-antibody interactions to detect the *in vivo* formation of protein radicals. The immunodetection of protein–DMPO radical adducts has been used before for Western blotting of isolated proteins (Detweiler et al., 2005), but here we show for the first time that it is also suitable for Western blotting and immunohistochemistry *in vivo*, after systemic DMPO administration to animals. In fact, this approach provides a new tool to detect free radical damage *in vivo*, extending the utility of other markers, including 3-nitrotyrosine (Abe et al., 1997; Bruijn et al., 1997) and hydroxynonenal–protein adducts (Pedersen et al., 1998). It is not fully clear how trapping protein radicals with DMPO was beneficial to the cells; most likely, the formation of protein radical–DMPO adducts will block free radical-propagating reactions (Nauser et al., 2005). Accordingly, DMPO treatment has been shown to increase the lifespan in SOD1^{G93A} transgenic mice (Liu et al., 2002). Overall, the results with DMPO further support the impact of oxidative stress in ALS pathology and prompted us to evaluate the efficacy of more specific redox-based therapies.

Previously, it has been shown that SOD1^{G93A} astrocytes are toxic for motor neurons in coculture via diffusible factors (Vargas et al., 2006; Nagai et al., 2007). A mechanism involving oxidative stress, increased ·NO production, and decreased glutathione levels has been proposed (Vargas et al., 2006). Here, we show evidence that defective mitochondrial respiration leads to the establishment of a neurotoxic astrocyte phenotype. Decrease of mitochondrial respiration in nontransgenic astrocyte cultures by ETC inhibitors, particularly azide-dependent inhibition of cytochrome *c* oxidase and fluorocitrate-dependent inhibition of aconitase, resulted in decreased motor neuron survival, suggesting that mitochondrial function in astrocytes is necessary to support motor neuron survival. Furthermore, restoration of astrocytic mitochondrial respiration with antioxidants Mito-Q and Mito-CP prevented the neurotoxic phenotype. In addition, we have recently shown that these mitochondrial-targeted antioxidants are effective in preventing cell death in pure motor neuron cultures challenged with proapoptotic stimuli that trigger ROS

formation (Pehar et al., 2007). As a first step toward mitochondria-specific therapies, the Murphy and Kalyanaraman laboratories have developed bioactive molecules delivered to mitochondria by covalent attachment to the triphenylphosphonium cation through an alkyl chain (Kelso et al., 2001; Dhanasekaran et al., 2005). The delocalized positive charge of these lipophilic cations enables them to permeate lipid bilayers easily and to possibly accumulate several hundredfold within mitochondria. This selective uptake greatly increases the efficacy and specificity of molecules designed to interact with mitochondria while also decreasing harmful side reactions. In this work, we show that Mito-Q is effective in restoring mitochondrial respiration and preventing neurotoxicity in SOD1^{G93A}-bearing astrocytes at much smaller doses than those used for other antioxidants. The effects of Mito-Q are likely to be combined effects, resulting in decreased steady-state levels of superoxide (decrease of MitoSOX oxidation) and peroxynitrite (decrease of mitochondrial protein nitration). Additional studies are required to further define the specific protective mechanism at the cellular level, but the mitochondrial-targeted antioxidants provide a new potential therapy to be tested in ALS models.

One potential functional consequence of mitochondrial dysfunction in ALS is the impairment of energy metabolism and increased generation of oxidants. Overexpression of SOD1^{G93A} in a cell line reproduces mitochondrial abnormal morphology and decreased respiration rate (Menzies et al., 2002) and makes the cells highly dependent on glycolysis, suggesting that SOD1^{G93A} expression may induce a switch to anaerobic metabolism to maintain ATP levels. Such observations in a cell line might be relevant to understand the impact of SOD1^{G93A} in astrocytes that are known to switch from aerobic to glycolytic metabolism in response to ETC inhibition by ·NO (Almeida et al., 2001). Recently, we showed overproduction of ·NO in SOD1^{G93A} astrocytes (Vargas et al., 2006). In addition, here we demonstrate that there is an increase in mitochondrial $O_2^{•-}$ formation in SOD1^{G93A} astrocytes using a novel and specific mitochondrial-targeted fluorescent probe. Because mutant SOD1 has been shown to mediate aberrant oxidative chemistry in neuronal cells (Estevez et al., 1999; Zimmerman et al., 2007), increased ·NO and $O_2^{•-}$ would facilitate the formation of peroxynitrite, which can damage key mitochondrial enzymes (Radi et al., 2002; Quijano et al., 2005). The mutated forms of SOD1 can be found inside mitochondria (Jaarsma et al., 2001; Higgins et al., 2002; Liu et al., 2004; Vijayvergiya et al., 2005) and may shift the redox state of respiratory complexes (Ferri et al., 2006) or disrupt the association of cytochrome *c* with the inner membrane (Kirkinezos et al., 2005). Furthermore, aggregates of wild-type and mutant SOD1 in the mitochondria from transgenic mouse spinal cord correlate with exacerbation of the disease (Deng et al., 2006). All the previous mechanisms may contribute to increase nitroxidative damage inside mitochondria. Accordingly, DMPO, L-NAME, Mito-Q, and MnTE-2-PyP restored mitochondrial respiration and also prevented astrocyte-derived neurotoxicity. It has been recently shown that MnTE-2-PyP in the Mn^{3+} oxidation state is reduced by complex I and complex II of the mitochondrial ETC, and the reduced (Mn^{2+}) complex reacts and decomposes peroxynitrite, suggesting that Mn-porphyrins may act as peroxynitrite reduction catalysts *in vivo* and protect mitochondria from oxidative damage (Ferrer-Sueta et al., 2006; Spasojević et al., 2007). These results emphasize the key role of nitroxidative stress in astrocytes in the pathogenesis of neurodegenerative diseases.

It needs to be established whether compounds that ameliorate mitochondrial dysfunction might be beneficial in ALS. Compounds that can improve the bioenergetics of mitochondria such as Mn-porphyrins have been shown to increase the lifespan in SOD1^{G93A} transgenic mice (Wu et al., 2003). Our results support that astrocytes might be a target for redox-based therapies in ALS. In summary, we have shown that astrocytes from SOD1^{G93A} transgenic animals exhibiting an altered mitochondrial activity are neurotoxic for motor neurons. The restoration of mitochondrial function after mitochondrial-targeted antioxidant treatment opens hope for more specific tools to treat a wide range of neurodegenerative disorders.

References

Abe K, Pan LH, Watanabe M, Konno H, Kato T, Itoyama Y (1997) Upregulation of protein-tyrosine nitration in the anterior horn cells of amyotrophic lateral sclerosis. Neurol Res 19:124–128.

Almeida A, Almeida J, Bolanos JP, Moncada S (2001) Different responses of astrocytes and neurons to nitric oxide: the role of glycolytically generated ATP in astrocyte protection. Proc Natl Acad Sci USA 98:15294–15299.

Barbeito LH, Pehar M, Cassina P, Vargas MR, Peluffo H, Viera L, Estevez AG, Beckman JS (2004) A role for astrocytes in motor neuron loss in amyotrophic lateral sclerosis. Brain Res Brain Res Rev 47:263–274.

Batinic-Haberle I, Benov L, Spasojevic I, Fridovich I (1998) The ortho effect makes manganese(III) meso-tetrakis(N-methylpyridinium-2-yl)porphyrin a powerful and potentially useful superoxide dismutase mimic. J Biol Chem 273:24521–24528.

Brito C, Naviliat M, Tiscornia AC, Vuillier F, Gualco G, Dighiero G, Radi R, Cayota AM (1999) Peroxynitrite inhibits T lymphocyte activation and proliferation by promoting impairment of tyrosine phosphorylation and peroxynitrite-driven apoptotic death. J Immunol 162:3356–3366.

Bruijn LI, Beal MF, Becher MW, Schulz JB, Wong PC, Price DL, Cleveland DW (1997) Elevated free nitrotyrosine levels, but not protein-bound nitrotyrosine or hydroxyl radicals, throughout amyotrophic lateral sclerosis (ALS)-like disease implicate tyrosine nitration as an aberrant in vivo property of one familial ALS-linked superoxide dismutase 1 mutant. Proc Natl Acad Sci USA 94:7606–7611.

Bruijn LI, Miller TM, Cleveland DW (2004) Unraveling the mechanisms involved in motor neuron degeneration in ALS. Annu Rev Neurosci 27:723–749.

Cassina A, Radi R (1996) Differential inhibitory action of nitric oxide and peroxynitrite on mitochondrial electron transport. Arch Biochem Biophys 328:309–316.

Cassina AM, Hodara R, Souza JM, Thomson L, Castro L, Ischiropoulos H, Freeman BA, Radi R (2000) Cytochrome c nitration by peroxynitrite. J Biol Chem 275:21409–21415.

Cassina P, Peluffo H, Pehar M, Martinez-Palma L, Ressia A, Beckman JS, Estevez AG, Barbeito L (2002) Peroxynitrite triggers a phenotypic transformation in spinal cord astrocytes that induces motor neuron apoptosis. J Neurosci Res 67:21–29.

Cassina P, Pehar M, Vargas MR, Castellanos R, Barbeito AG, Estevez AG, Thompson JA, Beckman JS, Barbeito L (2005) Astrocyte activation by fibroblast growth factor-1 and motor neuron apoptosis: implications for amyotrophic lateral sclerosis. J Neurochem 93:38–46.

Chan PH, Kawase M, Murakami K, Chen SF, Li Y, Calagui B, Reola L, Carlson E, Epstein CJ (1998) Overexpression of SOD1 in transgenic rats protects vulnerable neurons against ischemic damage after global cerebral ischemia and reperfusion. J Neurosci 18:8292–8299.

Clement AM, Nguyen MD, Roberts EA, Garcia M, Boillee S, Rule M, McMahon AP, Doucette W, Siwek D, Ferrante RJ, Brown RH, Julien JP, Goldstein LS, Cleveland DW (2003) Wild-type nonneuronal cells extend survival of SOD1 mutant motor neurons in ALS mice. Science 302:113–117.

Deng HX, Shi Y, Furukawa Y, Zhai H, Fu R, Liu E, Gorrie GH, Khan MS, Hung WY, Bigio EH, Lukas T, Dal Canto MC, O'Halloran TV, Siddique T (2006) Conversion to the amyotrophic lateral sclerosis phenotype is associated with intermolecular linked insoluble aggregates of SOD1 in mitochondria. Proc Natl Acad Sci USA 103:7142–7147.

Detweiler CD, Deterding LJ, Tomer KB, Chignell CF, Germolec D, Mason RP (2002) Immunological identification of the heart myoglobin radical formed by hydrogen peroxide. Free Radic Biol Med 33:364–369.

Detweiler CD, Lardinois OM, Deterding LJ, de Montellano PR, Tomer KB, Mason RP (2005) Identification of the myoglobin tyrosyl radical by

immuno-spin trapping and its dimerization. Free Radic Biol Med 38:969–976.

Dhanasekaran A, Kotamraju S, Karunakaran C, Kalivendi SV, Thomas S, Joseph J, Kalyanaraman B (2005) Mitochondria superoxide dismutase mimetic inhibits peroxide-induced oxidative damage and apoptosis: role of mitochondrial superoxide. Free Radic Biol Med 39:567–583.

Dupuis L, Gonzalez de Aguilar JL, Oudart H, de Tapia M, Barbeito L, Loeffler JP (2004) Mitochondria in amyotrophic lateral sclerosis: a trigger and a target. Neurodegener Dis 1:245–254.

Estevez AG, Crow JP, Sampson JB, Reiter C, Zhuang Y, Richardson GJ, Tarpey MM, Barbeito L, Beckman JS (1999) Induction of nitric oxide-dependent apoptosis in motor neurons by zinc-deficient superoxide dismutase. Science 286:2498–2500.

Ferrer-Sueta G, Hannibal L, Batinic-Haberle I, Radi R (2006) Reduction of manganese porphyrins by flavoenzymes and submitochondrial particles: a catalytic cycle for the reduction of peroxynitrite. Free Rad Biol Med 41:503–512.

Ferri A, Cozzolino M, Crosio C, Nencini M, Casciati A, Butler Gralla E, Rotilio G, Selverstone VJ, Carri MT (2006) Familial ALS-superoxide dismutases associate with mitochondria and shift their redox potentials. Proc Natl Acad Sci USA 103:13860–13865.

Fukada K, Zhang F, Vien A, Cashman NR, Zhu H (2004) Mitochondrial proteomic analysis of a cell line model of familial amyotrophic lateral sclerosis. Mol Cell Proteomics 12:1211–1223.

Henderson CE, Camu W, Mettling C, Gouin A, Poulsen K, Karihaloo M, Rullamas J, Evans T, McMahon SB, Armanini MP, Berkemeier L, Phillips HS, Rosenthal A (1993) Neurotrophins promote motor neuron survival and are present in embryonic limb bud. Nature 363:266–270.

Higgins CM, Jung C, Ding H, Xu Z (2002) Mutant Cu, Zn superoxide dismutase that causes motoneuron degeneration is present in mitochondria in the CNS. J Neurosci 22:RC215(1–6).

Howland DS, Liu J, She Y, Goad B, Maragakis NJ, Kim B, Erickson J, Kulik J, DeVito L, Psaltis G, DeGennaro LJ, Cleveland DW, Rothstein JD (2002) Focal loss of the glutamate transporter EAAT2 in a transgenic rat model of SOD1 mutant-mediated amyotrophic lateral sclerosis (ALS). Proc Natl Acad Sci USA 99:1604–1609.

Jaarsma D, Rognoni F, van Duijn W, Verspaget HW, Haasdijk ED, Holstege JC (2001) CuZn superoxide dismutase (SOD1) accumulates in vacuolated mitochondria in transgenic mice expressing amyotrophic lateral sclerosis-linked SOD1 mutations. Acta Neuropathol (Berl) 102:293–305.

Jauslin ML, Meier T, Smith RA, Murphy MP (2003) Mitochondria-targeted antioxidants protect Friedreich Ataxia fibroblasts from endogenous oxidative stress more effectively than untargeted antioxidants. FASEB J 17:1972–1974.

Jung C, Higgins CM, Xu Z (2002) Mitochondrial electron transport chain complex dysfunction in a transgenic mouse model for amyotrophic lateral sclerosis. J Neurochem 83:535–545.

Kelso GF, Porteous CM, Coulter CV, Hughes G, Porteous WK, Ledgerwood EC, Smith RA, Murphy MP (2001) Selective targeting of a redox-active ubiquinone to mitochondria within cells: antioxidant and antiapoptotic properties. J Biol Chem 276:4588–4596.

Kirkinezos IG, Bacman SR, Hernandez D, Oca-Cossio J, Arias LJ, Perez-Pinzon MA, Bradley WG, Moraes CT (2005) Cytochrome c association with the inner mitochondrial membrane is impaired in the CNS of G93A-SOD1 mice. J Neurosci 25:164–172.

Liu J, Lillo C, Jonsson PA, Vande Velde C, Ward CM, Miller TM, Subramaniam JR, Rothstein JD, Marklund S, Andersen PM, Brannstrom T, Gredal O, Wong PC, Williams DS, Cleveland DW (2004) Toxicity of familial ALS-linked SOD1 mutants from selective recruitment to spinal mitochondria. Neuron 43:5–17.

Liu R, Li B, Flanagan SW, Oberley LW, Gozal D, Qiu M (2002) Increased mitochondrial antioxidative activity or decreased oxygen free radical propagation prevent mutant SOD1-mediated motor neuron cell death and increase amyotrophic lateral sclerosis-like transgenic mouse survival. J Neurochem 80:488–500.

Manfredi G, Xu Z (2005) Mitochondrial dysfunction and its role in motor neuron degeneration in ALS. Mitochondrion 2:77–87.

Mason RP (2004) Using anti-5,5-dimethyl-1-pyrroline N-oxide (anti-DMPO) to detect protein radicals in time and space with immuno-spin trapping. Free Radic Biol Med 36:1214–1223.

Mattiazzi M, D'Aurelio M, Gajewski CD, Martushova K, Kiaei M, Beal MF, Manfredi G (2002) Mutated human SOD1 causes dysfunction of oxidative phosphorylation in mitochondria of transgenic mice. J Biol Chem 277:29626–29633.

Menzies FM, Cookson MR, Taylor RW, Turnbull DM, Chrzanowska-Lightowlers ZM, Dong L, Figlewicz DA, Shaw PJ (2002) Mitochondrial dysfunction in a cell culture model of familial amyotrophic lateral sclerosis. Brain 125:1522–1533.

Mukhopadhyay P, Rajesh M, Yoshihiro K, Hasko G, Pacher P (2007) Simple quantitative detection of mitochondrial superoxide production in live cells. Biochem Biophys Res Commun 358:203–208.

Nagai M, Re DB, Nagata T, Chalazonitis A, Jessell TM, Wichterle H, Przedborski S (2007) Astrocytes expressing ALS-linked mutated SOD1 release factors selectively toxic to motor neurons. Nat Neurosci 5:615–622.

Nauser T, Koppenol WH, Gebicki JM (2005) The kinetics of oxidation of GSH by protein radicals. Biochem J 392:693–701.

Pedersen WA, Fu W, Keller JN, Markesbery WR, Appel S, Smith RG, Kasarskis E, Mattson MP (1998) Protein modification by the lipid peroxidation product 4 hydroxynonenal in the spinal cords of amyotrophic lateral sclerosis patients. Ann Neurol 44:819–824.

Pehar M, Cassina P, Vargas MR, Castellanos R, Viera L, Beckman JS, Estevez AG, Barbeito L (2004) Astrocytic production of nerve growth factor in motor neuron apoptosis: implications for amyotrophic lateral sclerosis. J Neurochem 89:464–473.

Pehar M, Vargas MR, Robinson KM, Cassina P, Díaz-Amarilla PJ, Hagen TM, Radi R, Barbeito L, Beckman JS (2007) Mitochondrial superoxide production and nuclear factor erythroid 2-related factor 2 activation in p75 neurotrophin receptor-induced motor neuron apoptosis. J Neurosci 27:7777–7785.

Peluffo G, Radi R (2007) Biochemistry of protein tyrosine nitration in cardiovascular pathology. Cardiovasc Res 75:291–302.

Quijano C, Cassina A, Castro L, Rodríguez M, Radi R. (2005) Peroxynitrite: a mediator of nitric-oxide dependent mitochondrial dysfunction in pathology. In: Nitric oxide, cell signaling, and gene expression (Cadenas E, Lamas S, eds), pp 99–143. New York: Marcel Dekker.

Radi R (2004) Nitric oxide, oxidants, and protein tyrosine nitration. Proc Natl Acad Sci USA 101:4003–4008.

Radi R, Turrens JF, Chang LY, Bush KM, Crapo JD, Freeman BA (1991) Detection of catalase in rat heart mitochondria. J Biol Chem 266:22028–22034.

Radi R, Cassina A, Hodara R, Quijano C, Castro L (2002) Peroxynitrite reactions and formation in mitochondria. Free Radic Biol Med 33:1451–1464.

Robinson KM, Janes MS, Pehar M, Monette JS, Ross MF, Hagen TM, Murphy MP, Beckman JS (2006) Selective fluorescent imaging of superoxide in vivo using ethidium-based probes. Proc Natl Acad Sci USA 103:15038–15043.

Saneto RP, De Vellis J (1987) Neuronal and glial cells: cell culture of the central nervous system. In: Neurochemistry: a practical approach (Turner AJ, Brachelard HS, eds), pp 27–63. Washington, DC: IRL.

Spasojević I, Chen Y, Noel TJ, Yu Y, Cole MP, Zhang L, Zhao Y, St Clair DK, Batinić-Haberle I (2007) Mn porphyrin-based superoxide dismutase (SOD) mimic, MnIIITE-2-PyP5+, targets mouse heart mitochondria. Free Radic Biol Med 42:1193–1200.

Vargas MR, Pehar M, Cassina P, Martinez-Palma L, Thompson JA, Beckman JS, Barbeito L (2005) Fibroblast growth factor-1 induces heme oxygenase-1 via nuclear factor erythroid 2-related factor 2 (Nrf2) in spinal cord astrocytes: consequences for motor neuron survival. J Biol Chem 280:25571–25579.

Vargas MR, Pehar M, Cassina P, Beckman JS, Barbeito L (2006) Increased glutathione biosynthesis by Nrf2 activation in astrocytes prevents p75NTR-dependent motor neuron apoptosis. J Neurochem 97:687–696.

Vijayvergiya C, Beal MF, Buck J, Manfredi G (2005) Mutant superoxide dismutase 1 forms aggregates in the brain mitochondrial matrix of amyotrophic lateral sclerosis mice. J Neurosci 25:2463–2470.

Voloboueva LA, Suh SW, Swanson RA, Giffard RG (2007) Inhibition of mitochondrial function in astrocytes: implications for neuroprotection. J Neurochem 102:1383–1394.

Wu AS, Kiaei M, Aguirre N, Crow JP, Calingasan NY, Browne SE, Beal MF (2003) Iron porphyrin treatment extends survival in a transgenic animal model of amyotrophic lateral sclerosis. J Neurochem 85:142–150.

Zimmerman MC, Oberley LW, Flanagan SW (2007) Mutant SOD1-induced neuronal toxicity is mediated by increased mitochondrial superoxide levels. J Neurochem 102:609–618.

PLoS one

Modulation of Astrocytic Mitochondrial Function by Dichloroacetate Improves Survival and Motor Performance in Inherited Amyotrophic Lateral Sclerosis

Ernesto Miquel[1][9], Adriana Cassina[2,3][9], Laura Martínez-Palma[1], Carmen Bolatto[1], Emiliano Trías[4], Mandi Gandelman[1], Rafael Radi[2,3], Luis Barbeito[5,3], Patricia Cassina[1,3]*

1 Departamento de Histología y Embriología, Facultad de Medicina, Universidad de la República, Montevideo, Uruguay, 2 Departamento de Bioquímica, Facultad de Medicina, Universidad de la República, Montevideo, Uruguay, 3 CEINBIO, Facultad de Medicina, Universidad de la República, Montevideo, Uruguay, 4 Instituto de Investigaciones Biológicas Clemente Estable, Montevideo, Uruguay, 5 Institut Pasteur de Montevideo, Montevideo, Uruguay

Abstract

Mitochondrial dysfunction is one of the pathogenic mechanisms that lead to neurodegeneration in Amyotrophic Lateral Sclerosis (ALS). Astrocytes expressing the ALS-linked $SOD1^{G93A}$ mutation display a decreased mitochondrial respiratory capacity associated to phenotypic changes that cause them to induce motor neuron death. Astrocyte-mediated toxicity can be prevented by mitochondria-targeted antioxidants, indicating a critical role of mitochondria in the neurotoxic phenotype. However, it is presently unknown whether drugs currently used to stimulate mitochondrial metabolism can also modulate ALS progression. Here, we tested the disease-modifying effect of dichloroacetate (DCA), an orphan drug that improves the functional status of mitochondria through the stimulation of the pyruvate dehydrogenase complex activity (PDH). Applied to astrocyte cultures isolated from rats expressing the $SOD1^{G93A}$ mutation, DCA reduced phosphorylation of PDH and improved mitochondrial coupling as expressed by the respiratory control ratio (RCR). Notably, DCA completely prevented the toxicity of $SOD1^{G93A}$ astrocytes to motor neurons in coculture conditions. Chronic administration of DCA (500 mg/L) in the drinking water of mice expressing the $SOD1^{G93A}$ mutation increased survival by 2 weeks compared to untreated mice. Systemic DCA also normalized the reduced RCR value measured in lumbar spinal cord tissue of diseased $SOD1^{G93A}$ mice. A remarkable effect of DCA was the improvement of grip strength performance at the end stage of the disease, which correlated with a recovery of the neuromuscular junction area in extensor digitorum longus muscles. Systemic DCA also decreased astrocyte reactivity and prevented motor neuron loss in $SOD1^{G93A}$ mice. Taken together, our results indicate that improvement of the mitochondrial redox status by DCA leads to a disease-modifying effect, further supporting the therapeutic potential of mitochondria-targeted drugs in ALS.

Introduction

ALS is a fatal paralytic neurodegenerative disease characterized by motor neuron loss, which leads to death within 3–5 years of diagnosis. No therapy is available other than riluzole, which extends the lifespan of patients by only 3–6 months [1]. Mitochondrial dysfunction can contribute to motor neuron degeneration in ALS and description of mitochondrial alterations have been fully documented in the spinal cord and the muscle from patients and animal models linked to SOD mutations (for review see [2,3]). Astrocytes from rats expressing $SOD1^{G93A}$ display reduced mitochondrial ability to synthesize ATP and produce increased levels of nitric oxide [4], superoxide and peroxynitrite [5] and accordingly, these effects can be reverted with mitochondria-targeted antioxidants [5]. Interestingly, mitochondrial dysfunction in astrocytes is associated to neurotoxic phenotypic changes that reduce motor neuron survival [5].

Astrocytes surrounding motor neurons are known to modulate ALS progression. Indeed, analyses of chimeric mice composed of mixtures of normal and mutated SOD1–expressing cells have offered evidence that motor neuron death is non–cell-autonomous [6]. Restricted mutated SOD1 expression in astrocytes is not sufficient for disease development [7]. However, selective reduction of mutated SOD1 in astrocytes increases disease duration after onset as determined by mating mice expressing mutated SOD1 transgenes flanked by lox sites to mice carrying a Cre-encoding sequence under control of the promoter from GFAP [8]. This is accompanied by delayed microglial activation, in accordance with studies using the same technology for microglia [9]. Damage induced by mutated SOD1 in astrocytes determines a phenotype that is neurotoxic for motor neurons in culture and may account for the role of astrocytes in disease progression [4,10,11]. Indeed, the recent isolation of astrocytes with aberrant

phenotype (referred to as "AbA cells") from primary spinal cord cultures of symptomatic SOD1[G93A] rats with unprecedented proliferative and neurotoxic capacity [12] further supports a role for astrocytes in ALS progression. It remains to be determined whether the neurotoxic phenotype of SOD1[G93A]-expressing astrocytes may be reverted by the improvement of mitochondrial metabolism and in turn slow disease progression.

The organohalide dichloroacetate (DCA) is a well-characterized inhibitor of the protein kinase of the pyruvate dehydrogenase (PDH) [13]. PDH, located in the mitochondrial matrix, in its active unphosphorylated state mediates acetyl coenzyme-A formation from pyruvate, which feeds the electron transport chain responsible for ATP synthesis and oxygen consumption. Phosphorylation of PDH by PDH kinase (PDK) generates its inactive phosphorylated state. DCA-mediated inhibition of PDK renders most of PDH in the active form and then pyruvate metabolism switches towards glucose oxidation to CO_2 in the mitochondria (Fig. 1). Another mechanism by which DCA may favor PDH activity is to decrease degradation of the E1 alpha subunit of the complex. It has been claimed that changes in E1 alpha subunit phosphorylation could affect susceptibility to proteases that may lead to an increase in the amount of the total enzyme [14].

In the central nervous system, DCA enhances glucose and lactate oxidation to CO_2 and reduces lactate release mainly in astrocytes compared to having almost no effects on neurons, which supports the compartmentalization of glucose metabolism between astroglia and neurons [15]. The fraction of total PDH in the inactive phosphorylated form is normally greater in astroglia than in neurons, a situation that favors lactate export from astroglia to neurons but it can be modulated by DCA [15]. DCA administration in vivo activates brain PDH activity [16], indicating that it crosses the blood-brain barrier, and DCA is currently used clinically to lower elevated lactate levels in cerebrospinal fluid of patients with mitochondrial disorders [17,18]. However, it is unknown whether DCA may offer benefits in neurological disorders associated to mitochondrial dysfunction. Specifically, it is not known whether DCA may prevent the in vivo and in vitro neurotoxic influence of SOD1[G93A] astrocytes in ALS models by regulating their mitochondrial respiration.

Here we provide evidence that DCA reduced astrocyte neurotoxicity to motor neurons in culture and furthermore, applied to
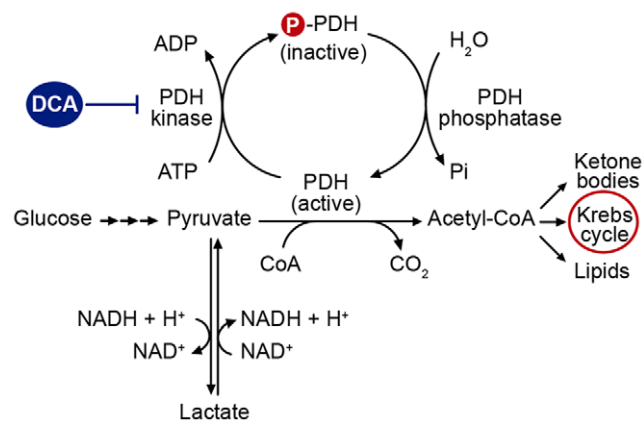
Figure 1. Site of action of dichloroacetate. DCA inhibits the mitochondrial enzyme PDH kinase, thereby maintaining the PDH complex in its unphosphorylated catalytically active state and facilitating the aerobic oxidation of glucose.
doi:10.1371/journal.pone.0034776.g001

ALS mice, slowed disease progression and enhanced motor strength.

Results

Effect of DCA on SOD1[G93A] astrocytes

To evaluate the effects of DCA on PDH we exposed cultures of SOD1[G93A] astrocytes to DCA (5 mM, 24 h) and total and phosphorylated forms of PDH were quantified by western blotting assay using specific antibodies (anti PDH-E1α subunit and anti PDH-E1α-pSer[293] respectively). As expected, exposure of both non-transgenic (non Tg) and SOD1[G93A] astrocytes to DCA reduced phosphorylated PDH relative levels (Fig. 2A–B). However, this effect was greater in SOD1[G93A] astrocytes than in non Tg ones. DCA also increased total levels of PDH in non Tg astrocytes according to previous reports [14]. Total PDH levels were basally increased in SOD1[G93A] untreated astrocytes.

DCA treatment improved mitochondrial coupling in SOD1[G93A] astrocytes as determined by high-resolution respirometry expressed by the respiratory control ratio (RCR). The RCR value calculated for untreated SOD1[G93A] astrocytes was significantly reduced (by 45%) compared to non Tg astrocytes as described previously [5]. DCA-treated SOD1[G93A] astrocytes showed a significant increase in the RCR to the level of that shown by non Tg astrocytes (Fig. 2C). We observed that DCA also reduced the proliferation rate in SOD1[G93A] astrocytes that was otherwise increased by 100% with respect to non Tg ones (Fig. 2D).

### DCA prevented the toxicity of SOD1[G93A] astrocytes to motor neurons

SOD1[G93A] astrocytes display neurotoxic influence for motor neurons in culture, which can be reverted by mitochondria-targeted antioxidants [5]. In order to elucidate whether improving mitochondrial function with DCA in SOD1[G93A] astrocytes was also beneficial for motor neuron survival we plated purified motor neurons on top of DCA-pretreated (0.5–5 mM, 24 h) SOD1[G93A] astrocyte monolayers. This treatment significantly increased motor neuron survival grown on top of SOD1[G93A] astrocytes to the level of that shown by non Tg astrocytes (Fig. 3).

DCA increased survival of SOD1[G93A] mice

To assess whether DCA could also exert protective effects on the progressive paralysis in SOD1[G93A] mice, the compound was administered from 70 days of age until death in the drinking water (500 mg/L) as previously described in an animal model of Huntington's disease [19]. DCA was well tolerated and did not show apparent signs of intoxication, such as weight loss, disease or premature death, when compared to non-treated SOD1[G93A] and non Tg control mice. Treatment with DCA significantly increased survival both in males and females as compared with control mice treated with water only (males ctrl n = 9: 126.9±2.6 days, DCA n = 9: 138.0±2.8 days; females ctrl n = 10: 130.0±1.87 days DCA n = 9: 138.4±2.42 days; Fig. 4A, B). Disease onset was not significantly affected by DCA (males ctrl n = 7: 99.4±3.0 days; DCA n = 6: 106.2±2.3 days; females ctrl n = 5: 104.2 days±5.1; DCA n = 8: 111.3±6.7 days).

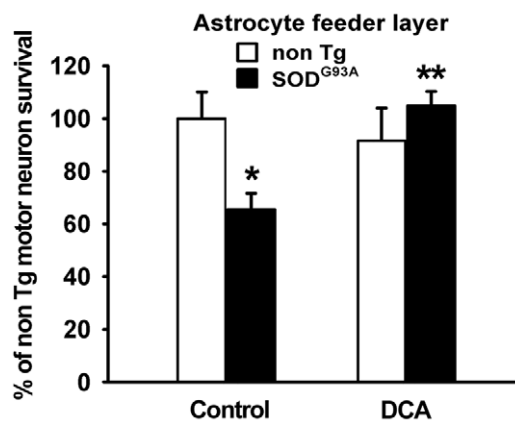### DCA improved motor performance and maintained motor unit integrity in SOD1[G93A] mice

ALS is characterized by progressive muscle weakness and paralysis. Therefore, we sought to determine the effect of DCA on motor performance of SOD1[G93A] mice. Notably, DCA signifi-
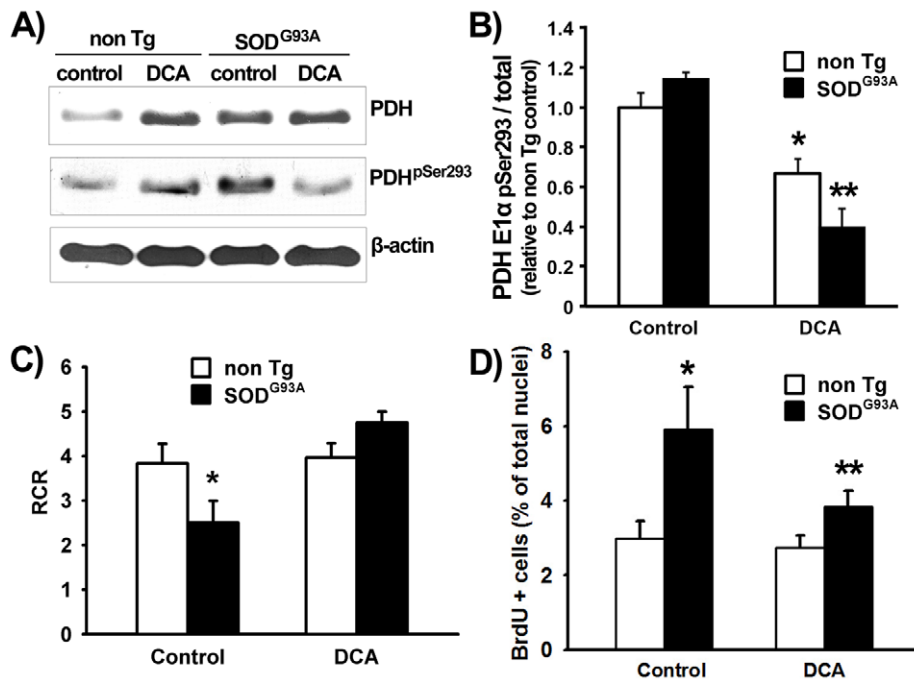
Figure 2. DCA recovers mitochondrial respiration rate and controls proliferation in SOD1[G93A] astrocytes. A) Representative immunoblot for PDH-E1α(pSer[293]), total PDH-E1α, and β-actin of lysates from non Tg and SOD1[G93A] astrocytes after 24 h treatment with DCA or vehicle as described in Methods. B) Quantification of the PDH-E1α(pSer[293]) to total PDH-E1α ratio between relative densitometric levels normalized against vehicle-treated non Tg astrocytes. C) Calculated respiratory control ratio (RCR) for mitochondria from non Tg or SOD1[G93A]-bearing astrocytes treated with DCA or vehicle as indicated. D) Percentage of BrdU immunoreactive nuclei of non Tg and SOD1[G93A] astrocytes after 24 h treatment with DCA. Data for panels B, C, and D are expressed as mean ± SEM from three independent experiments performed in duplicate. *p<0.05, significantly different from non Tg control. **p<0.05, significantly different from SOD1[G93A] control.
doi:10.1371/journal.pone.0034776.g002

cantly improved grip strength performance at the end stage of the disease (from 100 days of age onward) in male mice compared to control transgenic ones (Fig. 5A). Grip strength did not improve in females (data not shown). Because there is a correlation between the number of active motor units and the force produced by a muscle, we decided to observe the neuromuscular junction (NMJ)

Figure 3. DCA prevents SOD1[G93A] astrocyte neurotoxicity to motor neurons. Motor neuron survival 72 h after plating either on non Tg or SOD1[G93A]-bearing astrocytes pretreated with DCA or vehicle as indicated. Data are expressed as percentage of non Tg control, mean ± SEM from four independent experiments. *p<0.05, significantly different from non Tg control. **p<0.05, significantly different from SOD1[G93A] control.
doi:10.1371/journal.pone.0034776.g003

morphology of two muscles with different fiber composition, extensor digitorum longus (EDL) and soleus. The NMJs of EDL muscle in DCA-treated mice displayed normal size (measured as total area) and shape, which is in agreement with the improvement of grip strength (Fig. 5B). In control SOD1[G93A] mice, the receptor area decreased in size, as did the spaces between synaptic regions, leading to an overall compaction of the junction. A 20-day DCA treatment from 70 days of age onward showed a significant increase in junction area in EDL muscles compared with untreated mice. Neuromuscular junctions in soleus muscles did not show significant improvements with DCA treatment (data not shown).

DCA treatment improved mitochondrial function in the spinal cord of SOD1[G93A] mice

To assess whether DCA improved mitochondrial function *in vivo*, high-resolution respirometry was monitored in mechanically dissociated spinal cords obtained from mice after 20 days of DCA administration (from 70 days of age). The RCR value calculated for untreated SOD1[G93A] mice spinal cords was significantly reduced compared to non Tg littermates according to previous reports [20]. In contrast, DCA-treated SOD1[G93A] mice showed a significant increase in the RCR compared to the untreated group (Fig. 6).

DCA reduced motor neuron loss and astrocyte reactivity in the spinal cord of SOD1[G93A] mice

We sought to determine the effect of DCA administration in the loss of motor neurons in the spinal cord. We noted the already described reduced motor neuron somas at lumbar spinal segments
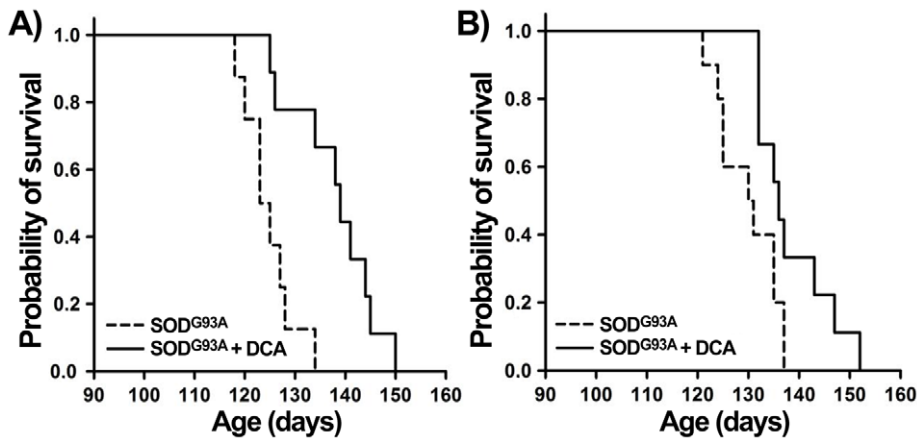
Figure 4. DCA increases mean survival of SOD1^G93A transgenic mice. Kaplan-Meyer survival curves from DCA-treated and control SOD1^G93A male (A) and female (B) mice. DCA was administered in drinking water from 70 days of age until death as detailed in materials and methods. 9 animals per group, p<0.05, Kaplan-Meyer log-rank test.
doi:10.1371/journal.pone.0034776.g004
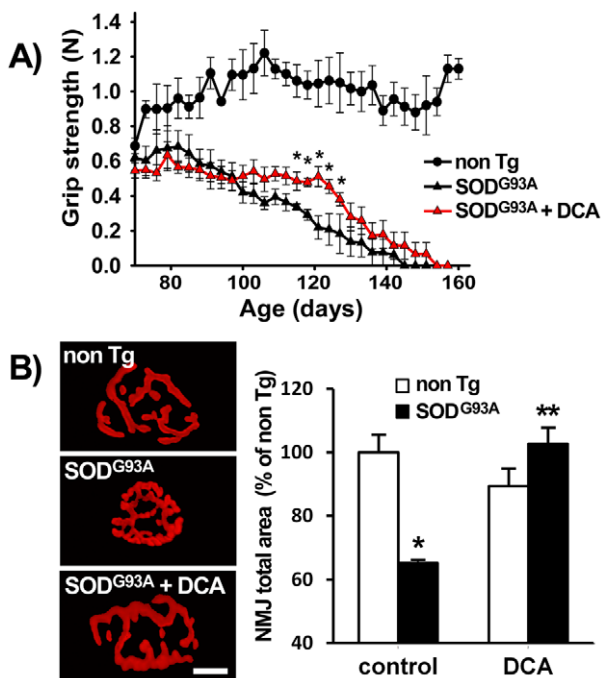
Figure 5. DCA delays loss of grip strength and neuromuscular junction shrinkage in SOD1^G93A mice. A) Hind-limb grip strength records from non Tg or SOD1^G93A male mice treated with DCA or vehicle as indicated. DCA-treated non Tg animals did not show differences with control ones and data are not shown in order to simplify the graph. Data are mean ± SEM from 9 animals per group. *p<0.05, significantly different from SOD1^G93A control. B) ACh receptors labeled with TMR-BgTx in representative EDL neuromuscular junctions from non Tg (top), SOD1^G93A control (middle) or DCA-treated SOD1^G93A (bottom). Quantification of total TMR-BgTx-stained neuromuscular area in the different groups of animals. Data are expressed as percentage of non Tg control, mean ± SEM from 15–35 neuromuscular junctions from 2–4 animals per group. *p<0.05, significantly different from non Tg control. **p<0.05, significantly different from SOD1^G93A control. Scale bar: 30 μm.
doi:10.1371/journal.pone.0034776.g005

for the SOD1^G93A mice when compared to non Tg littermates (Fig. 7 left column). DCA treatment rescued 25% of motor neurons at the lumbar level (Rexed lamina IX). In addition, we assayed astrocytic GFAP immunoreactivity in the spinal cord as a cellular element contributing to disease progression [8]. Astrocyte reactivity as determined by GFAP immunofluorescence was increased in the SOD1^G93A mice in contrast to non Tg littermates as previously described [21,22]. DCA treatment induced a marked reduction (70%) in GFAP immunoreactivity in the spinal cord, when compared to the vehicle-treated group (Fig. 7 right column).

Discussion

It is intriguing that rat [4], mouse [10,11] and also human [23] astrocytes expressing mutated SOD1 exert toxic effects on motor neurons. Here, we report that DCA was sufficient to reverse mitochondrial dysfunction in astrocytes from SOD1^G93A rats and, at the same time, the phenotypic features that make astrocytes toxic for motor neurons. Significantly, we provide convincing
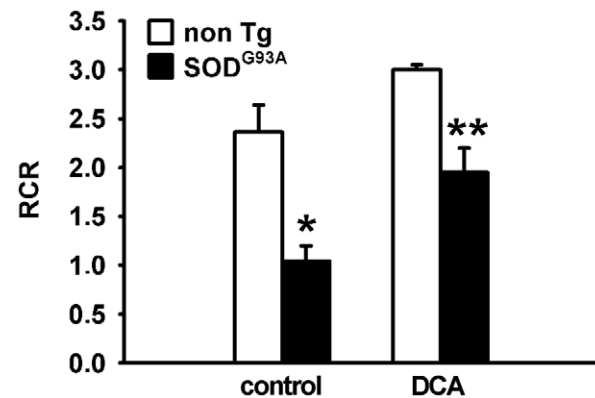
Figure 6. DCA improves mitochondrial function in the spinal cord of SOD1^G93A mice. Calculated respiratory control ratio (RCR) for spinal cord mitochondria from non Tg or SOD1^G93A mice treated with DCA or vehicle as indicated. Data are mean ± SEM from three independent experiments. *p<0.05, significantly different from non Tg control. **p<0.05, significantly different from SOD1^G93A control.
doi:10.1371/journal.pone.0034776.g006
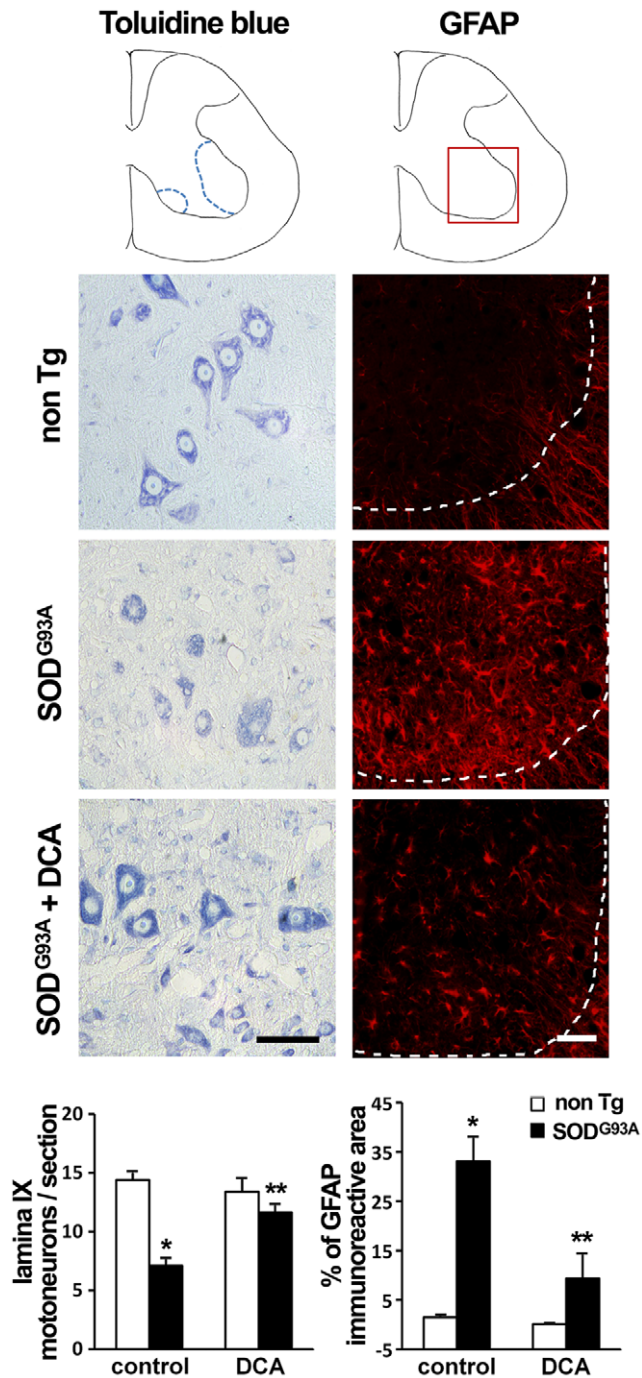
Figure 7. DCA reduces motor neuron loss and astrocyte reactivity in the spinal cord of SOD1^{G93A} mice. Representative Toluidine blue stain (left column) and GFAP immunofluorescence (red, right column) in anterior horn spinal cord sections from non Tg (top), SOD1^{G93A} control (middle) or DCA-treated SOD1^{G93A} (bottom) mice. Dotted lines in right column panels indicate the limit between grey and white matter. The graphs indicate the number of neuronal somas located in Rexed lamina IX (left) and the percentage of GFAP immunoreactive area in the ventral horn (right) in the indicated groups of animals. The corresponding measurement areas are drawn in the top. Data are mean ± SEM from at least three animals per group as indicated in Methods. *p<0.05, significantly different from non Tg control, **p<0.05, significantly different from SOD1^{G93A} control. Scale bars: 50 µm.
doi:10.1371/journal.pone.0034776.g007

preclinical data that systemic DCA administration decreases astrocytosis, motor neuron death and prolongs motor performance and survival of SOD1^{G93A} ALS mice. Since DCA has been used in humans for decades in the treatment of lactic acidosis and inherited mitochondrial diseases [18], these results suggest that DCA may be employed in clinical trials for ALS.

How DCA attenuates the damage induced by the expression of mutated SOD1 in astrocytes still needs to be clarified. Mitochondria represent a specific site of mutated SOD1 accumulation. In particular, it accumulates in the outer membrane and the intermembrane space, where it induces mitochondrial damage and metabolic dysfunction [3,5]. Oxidative stress to astrocyte mitochondria may underlie the transformation to a neurotoxic phenotype [5,24]. Reactive oxygen species (ROS) produced in mitochondria may affect signal transduction pathways through oxidation/reduction of cysteine residues in kinases, phosphatases, and other regulatory factors [25] leading to different, even opposite cellular responses. By stimulating pyruvate consumption, DCA improves the redox balance of mitochondria, which may result in normalization of altered mitochondria-regulated signaling [26]. Furthermore, DCA applied to mice at doses similar to the ones we have used but for a longer period of time significantly induced antioxidant enzyme activities, including superoxide dismutase, catalase and glutathione peroxidase [27], suggesting an indirect antioxidant effect of DCA.

Interestingly, DCA beneficial effects on survival and motor performance were more pronounced in males than in females. Similar results have been described in previous studies where different approaches resulted in beneficial effects only in males [28]. Men have higher risk of suffering ALS than women [29], and sex differences have also been reported in SOD1^{G93A} mutant rats [30] and mice [31–34] particularly when large numbers of animals are compared [35]. These observations suggest that gender differences may be partially a result of sex hormone action and in fact estrogen modulates disease progression in SOD1^{G93A} mice [36,37]. Among the various neuroprotective mechanisms proposed for estrogen actions, the ability to modulate mitochondrial function [38] and oxidative stress is particularly interesting in this context. Furthermore, the fact that increased ROS levels were observed in SOD1^{G93A} males but not in females [28] suggests that in the latter the redox balance between pro- and anti-oxidant mechanisms is already shifted toward neuroprotection, masking DCA beneficial effects.

Previous works have suggested an alteration of mitochondrial redox metabolism in ALS. Indeed, recent metabolomic analysis of cerebrospinal fluid [39] or serum [40] by (1)H NMR spectroscopy in ALS patients, revealed abnormal metabolite patterns that may indicate perturbation of glucose metabolism. Among the approaches that aim to restore mitochondrial function and energy production, pyruvate administration to ALS mice has been assessed [41,42]. However, results were contradictory probably due to differences in doses and animal strains. Nonetheless, pharmacological administration of DCA did improve mitochondrial function underscoring the potential of metabolic modulation to neutralize the progression of the disease.

In addition to mitochondrial dysfunction, SOD1^{G93A} astrocytes also exhibited an increased proliferation rate. Although these two events might seem unconnected, evidence obtained in cancer cells indicates that in fact they are mutually related. Otto Warburg in the 1920s described that increased proliferation rate in cancer cells is associated to glycolytic metabolism rather than to mitochondrial oxidation of pyruvate [43]. In accordance, DCA reverses the glycolytic metabolism in several cancer cell lines along with reduced proliferation [44]. Our data showing that DCA treatment of SOD1^{G93A} astrocytes improved mitochondrial function and

also decreased their proliferation rate suggest common activation of transduction pathways between cancer cells and SOD1^{G93A} astrocytes. Moreover, we have found evidence of unregulated proliferation and lack of replicative senescence in a population of phenotypically aberrant astrocytes isolated from SOD1^{G93A} rats [12]. Thus, the possibility exists that chronic mitochondrial dysfunction in neonatal astrocytes promotes long term changes in astrocyte phenotype and their neurotoxic potential. Although not analyzed in our study, several cellular pathways might mediate the increased proliferation rate of SOD1^{G93A} astrocytes. Among them we can include up-regulation of the isoform A of the lactate dehydrogenase (LDH-A) [45], activation of E3 ubiquitin ligase APC/C-Cdh1 [46], or modulation of transduction pathways by depolarized mitochondria [47].

Systemic DCA likely improves mitochondrial status in several other cell types relevant to ALS, including neurons and skeletal muscle. In the central nervous system, astrocytes seem to preferentially respond to DCA due to having a greater fraction of total PDH in the inactive phosphorylated form than neurons [15]. DCA might also exert a direct effect on skeletal muscle. It is interesting to note that DCA-treated animals remained with increased grip strength until death compared to untreated animals. Noticeably, the EDL muscle fibers of DCA-treated mice displayed neuromuscular junctions with normal size and shape, suggesting DCA could delay the progressive neuromuscular junction destruction characteristic of animals with ALS [48]. Furthermore, DCA has been effective in recovering the function of ischemic muscle [49], suggesting an effect stimulating muscle trophism or decreasing deleterious inflammation.

The present study supports the potential use of DCA in multi-drug approaches to treat ALS. DCA has been also shown to be protective in models of Huntington's disease, which also involves non-cell-autonomous mechanisms [19], suggesting a more general effect in neurodegenerative diseases. Taken together these data raise the possibility that DCA might have therapeutic benefits in ALS patients.

Materials and Methods

Materials

Culture media and serum were obtained from Invitrogen (Carlsbad, CA). All other reagents were from Sigma Chemical Co (Saint Louis, MO) unless otherwise specified.

Ethics Statement

Procedures using laboratory animals were in accordance with international guidelines and were approved by the Institutional Animal Committee (Comisión honoraria de experimentación animal de la Universidad de la República http://www.chea.csic.edu.uy; CHEA).

Animals

Transgenic ALS mice carrying the G93A mutation for human SOD1, strain B6SJL-TgN(SOD1-G93A)1Gur [50], were obtained from Jackson Laboratories (Bar Harbor, ME, USA) and genotyped as previously described [51]. Mice were housed under controlled conditions with free access to food and water. Sprague-Dawley NTac:SD-TgN(SOD1G93A)L26H rats were obtained from Taconic (Hudson, NY; [52]) and were bred locally by crossing with wild-type Sprague-Dawley female rats.

Dichloroacetate treatment trial

Male and female transgenic mice and non-transgenic littermates were divided randomly into the following groups (n = 9 per group):

A) transgenic control and B) non-transgenic control groups which received regular drinking water; C) transgenic DCA treatment and D) non-transgenic DCA treatment groups, administered with dichloroacetate (DCA; Sigma, St. Louis, MO). DCA was added to tap water in a 500 mg/L concentration and placed into water bottles. A daily dose of 100 mg/kg was used based on a daily water intake of 5 ml. The DCA solution was made fresh twice a week, with the total consumed volume measured in order to ensure a constant dose.

The treatment was performed from presymptomatic stage (70 days old) to death. Animals were observed weekly for onset of disease symptoms, as well as progression to death. Onset of disease was scored as the first observation of abnormal gait or overt hind limb weakness. End-stage of the disease was scored as complete paralysis of both hind limbs and the inability of the animals to right themselves after being placed on their side.

Cell cultures

Astrocyte cultures: Primary rat spinal cord astrocyte cultures were prepared from transgenic SOD1^{G93A} and non-transgenic 1-day-old pups, genotyped by PCR, as previously described [4,53]. Briefly, cells were plated at a density of 2×10^4 cells/cm^2 in 35 mm Petri dishes or 24-well plates (Nunc, Naperville, IL, USA) and maintained in Dulbecco's modified Eagle's medium (DMEM) supplemented with 10% fetal bovine serum (FBS), HEPES (3.6 g/L), penicillin (100 IU/mL) and streptomycin (100 μg/mL). Astrocyte monolayers were >98% pure as determined by GFAP immunoreactivity.

Astrocyte-motor neuron cocultures: motor neuron preparations were obtained from embryonic day 15 (E15) rat spinal cord by a combination of optiprep (1:10 in L15 medium, SIGMA St. Louis, MO) gradient centrifugation and immunopanning with the monoclonal antibody IgG192 against p75 neurotrophin receptor as previously described [53], then plated on rat astrocyte monolayers at a density of 300 cells/cm^2 and maintained for 48 h in L15 supplemented medium as described [53].

Treatment of cultures and motor neuron counting

Confluent astrocyte monolayers were changed to L15 supplemented media prior treatment. Stock solution of DCA (SIGMA St. Louis, MO) was prepared in distilled water and directly applied to astrocyte monolayers at the indicated concentrations. For co-culture experiments, astrocyte monolayers were treated with DCA for 24 h and motor neurons were plated in fresh L15 supplemented media, after washing twice with Dulbecco's phosphate buffered saline (DPBS). Motor neuron survival was assessed after 48 h by directly counting all p75 immunoreactive cells displaying neurites longer than 4 cell bodies in diameter [53].

Proliferation assessment

Confluent astrocyte cultures were incubated with 10 μg/ml bromo deoxyuridine (BrdU) and 5 mM DCA or vehicle in DMEM 2% FBS for 24 h. Cells were fixed in 4% paraformaldehyde, incubated in 1 N HCl for 1 h and immunofluorescence to detect BrdU using 1:300 diluted mouse monoclonal antibody (Dako) was performed. Alexa Fluor^{488} conjugated goat anti-mouse (Invitrogen) was used as secondary antibody, and propidium iodide to counterstain total nuclei. At least 600 nuclei were counted for each point. Proliferation is expressed as the percentage of BrdU immunoreactive nuclei with respect to total propidium iodide stained nuclei.

Immunoblot analysis

Cells were treated with DCA as described above. After 24 h of treatment, proteins were extracted from cells in 1% SDS supplemented with 2 mM sodium orthovanadate and Cømplete protease inhibitor cocktail (Roche). Lysates were resolved by electrophoresis on 12% SDS-polyacrylamide gels and transferred to a polyvinylidene fluoride membrane (PVDF; Thermo). The membrane was blocked for 1 h at room temperature in 5% skimmed milk in TBS-T (Tris-buffered saline with 0.1% Tween). The membrane was then probed overnight with primary antibodies in 1% skimmed milk in TBS-T at 4°C, washed in TBS-T, and then probed with the appropriate horseradish peroxidase (HRP)-conjugated secondary antibody for 60 min at room temperature. Primary antibodies were rabbit polyclonal phosphodetect anti-PDH-E1α(pSer^{293}) 1:500 (AP1062; Calbiochem) and mouse monoclonal anti-PDHE1α 1:750 (#456600, Invitrogen). Secondary antibodies were anti-rabbit (1:2500) and anti-mouse (1:5000) HRP conjugates (Thermo). Proteins were visualized with ECL western blotting substrate (Pierce Biotechnology). β-actin was used as a loading control. Densitometric analysis was performed using ImageJ software. The relative levels of pSer^{293} E1α and total E1α were quantified. The pSer^{293} to total E1α ratio was calculated and normalized against vehicle-treated non Tg mice.

Histological analysis and immunofluorescence

Transgenic and non-transgenic mice groups (n = 3 per group) were treated as described above, from 70 days of age. After 20 days, mice were transcardially perfused with 4% paraformaldehyde fixative in DPBS under deep anesthesia (pentobarbital, 50 mg/kg i.p.). The lumbar spinal cords were postfixed and embedded in paraplast. 5 µm-thick, serial sections were stained with toluidine blue or processed for immunofluorescence. For GFAP immunodetection, sections were permeabilized (0.2% Triton X-100 in PBS) and unspecific binding blocked (10% goat serum, 2% BSA, 0.2% Triton X-100 in DPBS), incubated with primary antibody (mouse monoclonal Cy-3 conjugated anti-GFAP; 1:600, Sigma) overnight, and mounted with glycerol. Images were obtained using an Olympus IX81 epifluorescence microscope.

Assessment of motor neuron number and astrogliosis in the lumbar spinal cord

The number of motor neurons was assessed by counting every cell on lamina IX of Rexed displaying motor neuron morphology with nucleus and nucleolus on every fifth toluidine blue stained 5 µm section (at least 25 sections per animal) through the lumbar spinal cord.

Quantification of astrogliosis was performed on images obtained from every fifth GFAP immunostained section (20 sections from each group) using ImageJ software (NIH). Ventral horn area occupied by GFAP immunofluorescence was measured and expressed as a percentage of total ventral horn area in each section.

Oxygen consumption

Oxygen consumption studies were performed either on spinal cord tissue or in astrocyte monolayers. Tissue or cell respiration was evaluated using Oxygraph 2 K (Oroboros Instruments Corp). Oxygen consumption was recorded at 37°C in intact cells or spinal cord tissue. The rate of oxygen consumption was calculated by means of the equipment software (DataLab) and was expressed as pmol of $O_2 \cdot s^{-1} \cdot ml^{-1}$.

For cell respiration, astrocyte monolayers were treated with DCA (0.5 and 5 mM) or vehicle for 24 h. Then, astrocytes were scraped and resuspended at 2×10^6 cells/ml in culture medium.

Mitochondrial oxygen consumption and RCR (respiratory control ratio) was calculated as: RCR = maximum uncoupled flux (FCCP)−(antimycin A-inhibited flux)/(oligomycin-inhibited flux)−(antimycin A-inhibited flux) of intact cells respiring, oxygen consumption after addition of 2 µg/ml oligomycin, 0.5 µM steps of FCCP (carbonyl cyanide p-trifluoromethoxyphenylhydrazone and followed by 2.5 µM antimycin A respectively as described [54].

For spinal cord studies 70 day-old mice were treated with DCA or vehicle for 20 days (n = 3 per group). Then, immediately following sacrifice, lumbar spinal cords were dissected. Spinal cord samples were immediately rinsed in respiration medium (Sucrose 110 mM, Mops 60 mM, EGTA 0.5 mM, BSA 1 g/l, MgCL2 3 mM, KH$_2$PO$_4$ 10 mM, HEPES 20 mM, pH 7,1) and set in the Oroboros oxygraph for high resolution respirometry. Mitochondrial oxygen consumption was measured as indicated in cell studies.

Grip strength measurements

Motor function was tested with a Grip Strength Meter (San Diego Instruments, San Diego CA). Tests were performed by allowing the animals to grasp the platform with both hind limbs, followed by pulling the animals until they released the platform. The force measurement was recorded twice a week from week 6 (baseline) until death in four separate trials.

Neuromuscular junction measurements

The extensor digitorum longus (EDL) and the soleus muscles from the same animals used for oxygen consumption studies were dissected immediately after sacrifice. Muscles were immersed for 60 minutes in 0.5% paraformaldehyde in DPBS, rinsed with DPBS (three times, 15 minutes each) and mechanically dissociated into small bundles of fibers using fine forceps under a stereomicroscope. The teased fibers were incubated with a blocking buffer containing 50 mM glycine, 1% BSA and 0.5% Triton X-100 for at least 3 hours and then in tetramethylrhodamine-conjugated α-bungarotoxin (TMR-BgTx) (T0195 Sigma; 1:1500 in blocking buffer) overnight (ON) at 4°C. After washing (three times, 20 minutes each) under agitation with PBS, fibers were left ON at 4°C in glycerol-Tris pH 8.8 (4:1) which was used as mounting medium for all the preparations.

Image acquisition and quantitative image processing: the teased fiber preparations were observed by epifluorescence using an Olympus IX81 microscope. For each EDL muscle the images of 15–35 neuromuscular junctions were taken and stored for later analysis using Adobe Photoshop software. The total area, defined as the area delimited by the external outline of the TMR-BgTx - stained endplate marked with the Lasso tool, including both stained and non-stained areas was measured. The resulting numbers of selected pixels were counted with the Histogram tool. Data were expressed as percentage of neuromuscular junction total area from non transgenic control animals.

Statistics

Survival curves were compared by Kaplan-Meier analysis with the Log-rank test using Sigmaplot 12 (Systat software). All culture assays were performed in duplicate and each experiment was repeated at least three times. Quantitative data were expressed as mean ± SEM and ANOVA and Student's t test were used for statistical analysis, with p<0.05 considered significant. When the normality test failed, comparison of the means was performed by one-way ANOVA on ranks followed by the Kruskal–Wallis test. Data from GFAP were analyzed using a one-way ANOVA and compared by all pairwise multiple comparison procedures (Holm-Sidak method). All statistics computations were performed using

the Sigma Stat System (1994, Jandel Scientific, San Rafael, CA, USA), or GraphPad InStat software, version 3.06.

Acknowledgments

Author Contributions

Conceived and designed the experiments: EM AC LB PC. Performed the experiments: EM AC LMP CB MG ET PC. Analyzed the data: EM AC LMP PC. Contributed reagents/materials/analysis tools: RR LB PC. Wrote the paper: EM AC RR LB PC.

References

1. Miller RG, Mitchell JD, Lyon M, Moore DH (2007) Riluzole for amyotrophic lateral sclerosis (ALS)/motor neuron disease (MND). Cochrane Database Syst Rev. CD001447 p.
2. Dupuis L, Gonzalez de Aguilar JL, Oudart H, de Tapia M, Barbeito L, et al. (2004) Mitochondria in amyotrophic lateral sclerosis: a trigger and a target. Neurodegener Dis 1: 245–254.
3. Kawamata H, Manfredi G (2010) Mitochondrial dysfunction and intracellular calcium dysregulation in ALS. Mech Ageing Dev 131: 517–526.
4. Vargas MR, Pehar M, Cassina P, Beckman JS, Barbeito L (2006) Increased glutathione biosynthesis by Nrf2 activation in astrocytes prevents p75NTR-dependent motor neuron apoptosis. J Neurochem 97: 687–696.
5. Cassina P, Cassina A, Pehar M, Castellanos R, Gandelman M, et al. (2008) Mitochondrial Dysfunction in SOD1G93A-Bearing Astrocytes Promotes Motor Neuron Degeneration: Prevention by Mitochondrial-Targeted Antioxidants. Journal of Neuroscience 28: 4115–4122.
6. Clement AM, Nguyen MD, Roberts EA, Garcia ML, Boillee S, et al. (2003) Wild-type nonneuronal cells extend survival of SOD1 mutant motor neurons in ALS mice. Science 302: 113–117.
7. Gong YH, Parsadanian AS, Andreeva A, Snider WD, Elliott JL (2000) Restricted expression of G86R Cu/Zn superoxide dismutase in astrocytes results in astrocytosis but does not cause motoneuron degeneration. J Neurosci 20: 660–665.
8. Yamanaka K, Chun SJ, Boillee S, Fujimori-Tonou N, Yamashita H, et al. (2008) Astrocytes as determinants of disease progression in inherited amyotrophic lateral sclerosis. Nat Neurosci 11: 251–253.
9. Boillee S, Vandevelde C, Cleveland D (2006) ALS: A Disease of Motor Neurons and Their Nonneuronal Neighbors. Neuron 52: 39–59.
10. Nagai M, Re DB, Nagata T, Chalazonitis A, Jessell TM, et al. (2007) Astrocytes expressing ALS-linked mutated SOD1 release factors selectively toxic to motor neurons. Nature Neuroscience 10: 615–622.
11. Di Giorgio FP, Carrasco MA, Siao MC, Maniatis T, Eggan K (2007) Non-cell autonomous effect of glia on motor neurons in an embryonic stem cell-based ALS model. Nat Neurosci 10: 608–614.
12. Diaz-Amarilla P, Olivera-Bravo S, Trias E, Cragnolini A, Martinez-Palma L, et al. (2011) Phenotypically aberrant astrocytes that promote motoneuron damage in a model of inherited amyotrophic lateral sclerosis. Proc Natl Acad Sci U S A 108: 18126–18131.
13. Knoechel TR, Tucker AD, Robinson CM, Phillips C, Taylor W, et al. (2006) Regulatory roles of the N-terminal domain based on crystal structures of human pyruvate dehydrogenase kinase 2 containing physiological and synthetic ligands. Biochemistry 45: 402–415.
14. Morten KJ, Caky M, Matthews PM (1998) Stabilization of the pyruvate dehydrogenase E1alpha subunit by dichloroacetate. Neurology 51: 1331–1335.
15. Itoh Y (2003) Dichloroacetate effects on glucose and lactate oxidation by neurons and astroglia in vitro and on glucose utilization by brain in vivo. Proceedings of the National Academy of Sciences 100: 4879–4884.
16. Abemayor E, Kovachich GB, Haugaard N (1984) Effects of dichloroacetate on brain pyruvate dehydrogenase. J Neurochem 42: 38–42.
17. Stacpoole PW (1989) The pharmacology of dichloroacetate. Metabolism 38: 1124–1144.
18. Stacpoole PW, Kerr DS, Barnes C, Bunch ST, Carney PR, et al. (2006) Controlled clinical trial of dichloroacetate for treatment of congenital lactic acidosis in children. Pediatrics 117: 1519–1531.
19. Andreassen OA, Ferrante RJ, Huang HM, Dedeoglu A, Park L, et al. (2001) Dichloroacetate exerts therapeutic effects in transgenic mouse models of Huntington's disease. Ann Neurol 50: 112–117.
20. Mattiazzi M, D'Aurelio M, Gajewski CD, Martushova K, Kiaei M, et al. (2002) Mutated human SOD1 causes dysfunction of oxidative phosphorylation in mitochondria of transgenic mice. J Biol Chem 277: 29626–29633.
21. Levine JB, Kong J, Nadler M, Xu Z (1999) Astrocytes interact intimately with degenerating motor neurons in mouse amyotrophic lateral sclerosis (ALS). Glia 28: 215–224.
22. Barbeito AG, Martinez-Palma L, Vargas MR, Pehar M, Manay N, et al. (2010) Lead exposure stimulates VEGF expression in the spinal cord and extends survival in a mouse model of ALS. Neurobiol Dis 37: 574–580.
23. Marchetto MC, Muotri AR, Mu Y, Smith AM, Cezar GG, et al. (2008) Non-cell-autonomous effect of human SOD1 G37R astrocytes on motor neurons derived from human embryonic stem cells. Cell Stem Cell 3: 649–657.
24. Vargas MR, Johnson DA, Sirkis DW, Messing A, Johnson JA (2008) Nrf2 Activation in Astrocytes Protects against Neurodegeneration in Mouse Models of Familial Amyotrophic Lateral Sclerosis. Journal of Neuroscience 28: 13574–13581.
25. Burhans WC, Heintz NH (2009) The cell cycle is a redox cycle: linking phase-specific targets to cell fate. Free Radic Biol Med 47: 1282–1293.
26. Antico Arciuch VG, Alippe Y, Carreras MC, Poderoso JJ (2009) Mitochondrial kinases in cell signaling: Facts and perspectives. Adv Drug Deliv Rev 61: 1234–1249.
27. Hassoun EA, Cearfoss J (2011) Dichloroacetate- and Trichloroacetate-Induced Modulation of Superoxide Dismutase, Catalase, and Glutathione Peroxidase Activities and Glutathione Level in the livers of Mice after Subacute and Subchronic exposure. Toxicol Environ Chem 93: 332–344.
28. Naumenko N, Pollari E, Kurronen A, Giniatullina R, Shakirzyanova A, et al. (2011) Gender-Specific Mechanism of Synaptic Impairment and Its Prevention by GCSF in a Mouse Model of ALS. Front Cell Neurosci 5: 26.
29. Haverkamp LJ, Appel V, Appel SH (1995) Natural history of amyotrophic lateral sclerosis in a database population. Validation of a scoring system and a model for survival prediction. Brain 118(Pt 3): 707–719.
30. Suzuki M, Tork C, Shelley B, McHugh J, Wallace K, et al. (2007) Sexual dimorphism in disease onset and progression of a rat model of ALS. Amyotroph Lateral Scler 8: 20–25.
31. Kirkinezos IG, Hernandez D, Bradley WG, Moraes CT (2003) Regular exercise is beneficial to a mouse model of amyotrophic lateral sclerosis. Ann Neurol 53: 804–807.
32. Cudkowicz ME, Pastusza KA, Sapp PC, Mathews RK, Leahy J, et al. (2002) Survival in transgenic ALS mice does not vary with CNS glutathione peroxidase activity. Neurology 59: 729–734.
33. Mahoney DJ, Rodriguez C, Devries M, Yasuda N, Tarnopolsky MA (2004) Effects of high-intensity endurance exercise training in the G93A mouse model of amyotrophic lateral sclerosis. Muscle Nerve 29: 656–662.
34. Alves CJ, de Santana LP, dos Santos AJ, de Oliveira GP, Duobles T, et al. (2011) Early motor and electrophysiological changes in transgenic mouse model of amyotrophic lateral sclerosis and gender differences on clinical outcome. Brain Res 1394: 90–104.
35. Heiman-Patterson TD, Sher RB, Blankenhorn EA, Alexander G, Deitch JS, et al. (2011) Effect of genetic background on phenotype variability in transgenic mouse models of amyotrophic lateral sclerosis: a window of opportunity in the search for genetic modifiers. Amyotroph Lateral Scler 12: 79–86.
36. Groeneveld GJ, Van Muiswinkel FL, Sturkenboom JM, Wokke JH, Bar PR, et al. (2004) Ovariectomy and 17beta-estradiol modulate disease progression of a mouse model of ALS. Brain Res 1021: 128–131.
37. Trieu VN, Uckun FM (1999) Genistein is neuroprotective in murine models of familial amyotrophic lateral sclerosis and stroke. Biochem Biophys Res Commun 258: 685–688.
38. Arnold S, Victor MB, Beyer C (2012) Estrogen and the regulation of mitochondrial structure and function in the brain. J Steroid Biochem Mol Biol.
39. Blasco H, Corcia P, Moreau C, Veau S, Fournier C, et al. (2010) 1H-NMR-based metabolomic profiling of CSF in early amyotrophic lateral sclerosis. PLoS ONE 5: e13223.
40. Kumar A, Bala L, Kalita J, Misra UK, Singh RL, et al. (2010) Metabolomic analysis of serum by (1) H NMR spectroscopy in amyotrophic lateral sclerosis. Clin Chim Acta 411: 563–567.
41. Park JH, Hong YH, Kim HJ, Kim SM, Kim MJ, et al. (2007) Pyruvate slows disease progression in a G93A SOD1 mutant transgenic mouse model. Neurosci Lett 413: 265–269.
42. Esposito E, Capasso M, di Tomasso N, Corona C, Pellegrini F, et al. (2007) Antioxidant strategies based on tomato-enriched food or pyruvate do not affect disease onset and survival in an animal model of amyotrophic lateral sclerosis. Brain Res 1168: 90–96.
43. Warburg O, Wind F, Negelein E (1927) The Metabolism of Tumors in the Body. J Gen Physiol 8: 519–530.
44. Bonnet S, Archer SL, Allalunis-Turner J, Haromy A, Beaulieu C, et al. (2007) A mitochondria-K+ channel axis is suppressed in cancer and its normalization promotes apoptosis and inhibits cancer growth. Cancer Cell 11: 37–51.
45. Seth P, Grant A, Tang J, Vinogradov E, Wang X, et al. (2011) On-target inhibition of tumor fermentative glycolysis as visualized by hyperpolarized pyruvate. Neoplasia 13: 60–71.
46. Almeida A, Bolanos JP, Moncada S (2010) E3 ubiquitin ligase APC/C-Cdh1 accounts for the Warburg effect by linking glycolysis to cell proliferation. Proc Natl Acad Sci U S A 107: 738–741.
47. Antico Arciuch VG, Galli S, Franco MC, Lam PY, Cadenas E, et al. (2009) Akt1 intramitochondrial cycling is a crucial step in the redox modulation of cell cycle progression. PLoS ONE 4: e7523.

48. Dupuis L, Loeffler JP (2009) Neuromuscular junction destruction during amyotrophic lateral sclerosis: insights from transgenic models. Curr Opin Pharmacol 9: 341–346.

49. Wilson JS, Rushing G, Johnson BL, Kline JA, Back MR, et al. (2003) Dichloroacetate increases skeletal muscle pyruvate dehydrogenase activity during acute limb ischemia. Vasc Endovascular Surg 37: 191–195.

50. Gurney ME, Pu H, Chiu AY, Dal Canto MC, Polchow CY, et al. (1994) Motor neuron degeneration in mice that express a human Cu,Zn superoxide dismutase mutation. Science 264: 1772–1775.

51. Vargas MR (2005) Fibroblast Growth Factor-1 Induces Heme Oxygenase-1 via Nuclear Factor Erythroid 2-related Factor 2 (Nrf2) in Spinal Cord Astrocytes:

Consequences for motor neuron survival. Journal of Biological Chemistry 280: 25571–25579.

52. Howland DS, Liu J, She Y, Goad B, Maragakis NJ, et al. (2002) Focal loss of the glutamate transporter EAAT2 in a transgenic rat model of SOD1 mutant-mediated amyotrophic lateral sclerosis (ALS). Proc Natl Acad Sci U S A 99: 1604–1609.

53. Cassina P, Peluffo H, Pehar M, Martinez-Palma L, Ressia As, et al. (2002) Peroxynitrite triggers a phenotypic transformation in spinal cord astrocytes that induces motor neuron apoptosis. Journal of Neuroscience Research 67: 21–29.

54. Gnaiger E (2007) Mitochondrial Pathways and Respiratory Control. ORO-BOROS MiPNet Publications, Innsbruck. 96 p.

When too much ATP is a bad thing: a pivotal role for P2X$_7$ receptors in motor neuron degeneration

Susan E. Browne

Neuropharmacology, Merck Research Labs, West Point, Pennsylvania, USA

Read the full article '*P2X7 receptor-induced death of motor neurons by a peroxynitrite/FAS-dependent pathway*' on page 382.

The P2X$_7$ purine receptor has come under intense scrutiny of late, amid claims that under conditions of tissue stress its activation may trigger numerous CNS pathologies. In fact, this ATP-gated ion channel is rapidly gaining a reputation as being thoroughly pervasive in its contributions to cellular dysfunction. A quick survey of the scientific literature reveals that in only the first 3 months of 2013, the P2X$_7$ receptor was cited as a critical player in the pathogenesis of Alzheimer's disease, epilepsy, tumor-genesis, CNS ischemic damage, depression, and autism, as well as peripheral neuropathic pain, rheumatoid arthritis, and glaucoma. Within the CNS this apparent fecundity arises, in large part, from the P2X$_7$ receptor's position as a gatekeeper between glia and neurons in inflammatory cascades, coupled with physiologic characteristics that set it apart from other ATP-sensing P2 receptors. While the role of the P2X$_7$ receptor subtype in neuroinflammation is well documented, evidence for direct cytotoxic actions on neurons has been sparse. In the current issue of the Journal of Neurochemistry, however, Gandelman and colleagues turn the spotlight back from glia to neurons as they demonstrate a direct role for P2X$_7$ receptors in motor neuron cell death pertinent to amyotrophic lateral sclerosis (ALS).

Extracellular nucleotides regulate numerous physiologic processes throughout the body via the activation of purinergic P1 (G-protein coupled, adenosine-preferring), P2X (ionotropic, ATP-preferring), and P2Y (G-protein coupled, ATP and metabolite-preferring) nucleotide receptors. The seven identified P2X receptor subtypes are differentially distributed throughout the CNS, where they contribute to the regulation of a diverse range of critical homeostatic and trophic processes in normal tissue, including inflammatory responses and microglial proliferation, phagocytosis, neurotransmission, and pain perception. In this regard, P2X$_7$ receptors are predominantly localized to microglia throughout the CNS, but are also found on astrocytes and oligodendrocytes, and pre-synaptically on neurons in the cerebral cortex, hippocampus, brainstem, spinal cord, and at neuromuscular junctions (Weisman *et al.* 2012). Accordingly, their normal CNS functions encompass the control of inflammatory processes (including microglial proliferation, cytokine release, and autolysosome generation), and modulating the release of neurotransmitters including GABA, glutamate, acetylcholine, and ATP (Volonté *et al.* 2012). P2X$_7$ receptors possess one particular trait, however, that set them apart from their P2X kin, namely the ability to switch between two open channel states depending on extracellular conditions during activation. Basal P2X$_7$ receptor activation leads to opening of membrane channels permeable to small cations (e.g., Ca^{2+}, K$^+$, Na$^+$). During prolonged exposure to high concentrations of ATP, for example following trauma or inflammation-induced cell damage or lysis, P2X$_7$ receptors show little change in current over several minutes, while other P2X receptors desensitize rapidly (in milliseconds to seconds). Instead, prolonged activation leads to opening of a dilated membrane pore permeable to molecules up to 900 Da, rendering the cell vulnerable to necrosis or apoptosis triggers or osmotic lysis. Abnormal fluctuations in local concentrations of ATP can effectively turn a P2X$_7$ receptor from a homeostatic regulator to a cell death trigger (Volonté *et al.* 2012).

As ATP is released in the CNS following both relatively minor inflammatory events, as well as major responses to trauma and ischemia, a complex balancing act is required to maintain the inflammatory machinery, including P2X$_7$ receptors, in neuroprotection mode. As a result, P2X$_7$ receptors have garnered a great deal of interest as potential therapeutic targets for disorders involving neuroinflammation. One example is ALS, where inflammatory responses and the astroglial environment appear to be key to deciding motor neuron fate. While the mechanism of neurodegener-

ation underlying muscle loss in ALS is still not clear, over the last few years there has been a realization that a special relationship exists between glial cells and motor neurons in the disease. In this regard, several of the prevalent hypotheses of disease etiology are intrinsically linked with astrocyte and microglial functions, including glutamate excitotoxicity, oxidative damage, energetic dysfunction, and decreased trophic support (Fig. 1). Microglial and astrocytic activation in the spinal cords of ALS patients is a hallmark of the disease, and is also prominent in transgenic mouse models expressing familial ALS gene mutations (most commonly Cu/Zn-superoxide dismutase (SOD1) mutations). As well as providing structural, metabolic, and trophic support to motor neurons, it is proposed that non-neuronal cells may be critical for motor neuron toxicity in ALS models (reviewed by Vargas and Johnson 2010). This concept initially arose from observations in SOD1 mutant mice that segregating mutant SOD1 expression into either neurons or astrocytes precluded motor neuron pathology.

Against this backdrop of increased neuroinflammation in ALS, findings of up-regulation of P2X$_7$ receptors in spinal cord microglia and astrocytes from ALS patients, and in SOD1 animal models, led to the hypothesis that ATP signaling may trigger cytotoxic events in astroglial cells that result in damage to proximal motor neurons. A mechanistic bridge between glial cell activation and motor neuron death was proposed in 2010, when Gandelman and colleagues reported that normal spinal cord astrocytes could initiate a neurotoxic phenotype in co-cultured wild type motor neurons when the astrocytes were repeatedly exposed to high ATP concentrations (Gandelman *et al.* 2010). This phenomenon involved release of diffusible factors from the astrocytes and induction of peroxynitrite-induced neuronal damage that was blocked by P2X$_7$ receptor-selective inhibitors. Furthermore, they found that P2X$_7$ receptors on astrocytes expressing mutant SOD1 from a familial ALS mouse model were basally active without the need for excessive ATP priming, and that P2X$_7$ receptor activation was required to maintain their toxic phenotype. A similar phenomenon was previously demonstrated in a cortical neuron/microglia co-culture (Volonté *et al.* 2012). Hence, it appears that ATP release in ALS spinal cord may, via activation of P2X$_7$ receptors, create the conditions necessary to transform astroglial cells from a trophic to a cytotoxic phenotype.

In the present issue, Gandelman and colleagues ask if ATP might also directly target motor neurons, as P2X$_7$ receptors are located on motor neuron axons in addition to surrounding astroglial cells (Gandelman *et al.* 2013) (Fig. 1). Using cultured wild type rat spinal cord motor neurons, in the absence of any glial cell support, the group demonstrate that a subset of motor neurons were susceptible to relatively low concentrations of the selective P2X$_7$ agonist 3-O-(4-benzoyl)-ATP. A 'peroxynitrite-fueled apoptotic cascade' ensued, involving activation of neuronal p38 MAPK, nitric

oxide synthase, and Fas signaling, resulting in neuronal death. The authors go on to show that Ca^{2+} influx following P2X$_7$ receptor activation underlies the nitric oxide synthase activation, and the subsequent cell death mechanism corresponds with the peroxynitrite/Fas death pathway previously identified in motor neuron death following mutant SOD1 expression or trophic factor deprivation. Together, the studies in mixed cultures and in primary motor neuron cultures suggest that P2X$_7$ receptor activation can mediate motor neuron damage both indirectly as a result of stimulation of astroglial cells, and directly via activation of neuronal receptors, with both routes involving activation of downstream signaling pathways associated with oxidative damage (Gandelman *et al.* 2010, 2013). Several questions remain unanswered, however, including how the consequences of an ALS-associated gene mutation might impact neuronal receptor activation, plus whether P2X$_7$ receptors on motor neurons contribute to cell death in intact ALS models *in vivo*. This latter point is particularly pertinent because, as Gandelman and colleagues describe, the natural endogenous agonist, ATP, can have opposing beneficial effects in situ as a result of actions of the ATP degradation product adenosine (Gandelman *et al.* 2013). In addition, P2X$_7$ receptor activation can induce expression of other purinergic receptor subtypes, including neuroprotective P2Y$_2$ receptors (reviewed by Weisman *et al.* 2012).

The observations of a neuronal role for P2X$_7$ receptors in a motor neuron degeneration model add to the rapidly accumulating evidence that P2X$_7$ receptor antagonists may be effective therapeutic targets for multiple neurodegenerative disorders, not limited to ALS. For example, in Huntington's disease mouse models expression of mutant huntingtin protein is linked with an up-regulation of P2X$_7$ receptors at presynaptic sites on cortico-striatal projection neurons (Díaz-Hernández *et al.* 2009). Treatment with a P2X$_7$ inhibitor abrogated behavioral deficits and neuronal apoptosis in the Huntington's disease mice. In Alzheimer's disease, the microglial P2X$_7$ receptor has taken center stage following reports that receptor expression is up-regulated in microglia around β-amyloid plaques and regulates amyloid precursor protein processing in brains of amyloid precursor protein over-expressing mice (Diaz-Hernandez *et al.* 2012). Furthermore, inhibition of P2X$_7$ is linked to increased α-secretase activity through inhibition of glycogen synthase kinase 3, which translated to a reduction in numbers of hippocampal amyloid plaques in a mouse model. Another recent study reports that silencing P2X$_7$ receptor expression increased microglial phagocytic activity, leading to increased β-amyloid clearance *in vitro* (Ni *et al.* 2013).

The P2X$_7$ receptors possess several features that make them reasonable candidates as drug targets, as North and Jarvis describe in a recent review (North and Jarvis 2013). These include their relatively restricted tissue distribution,
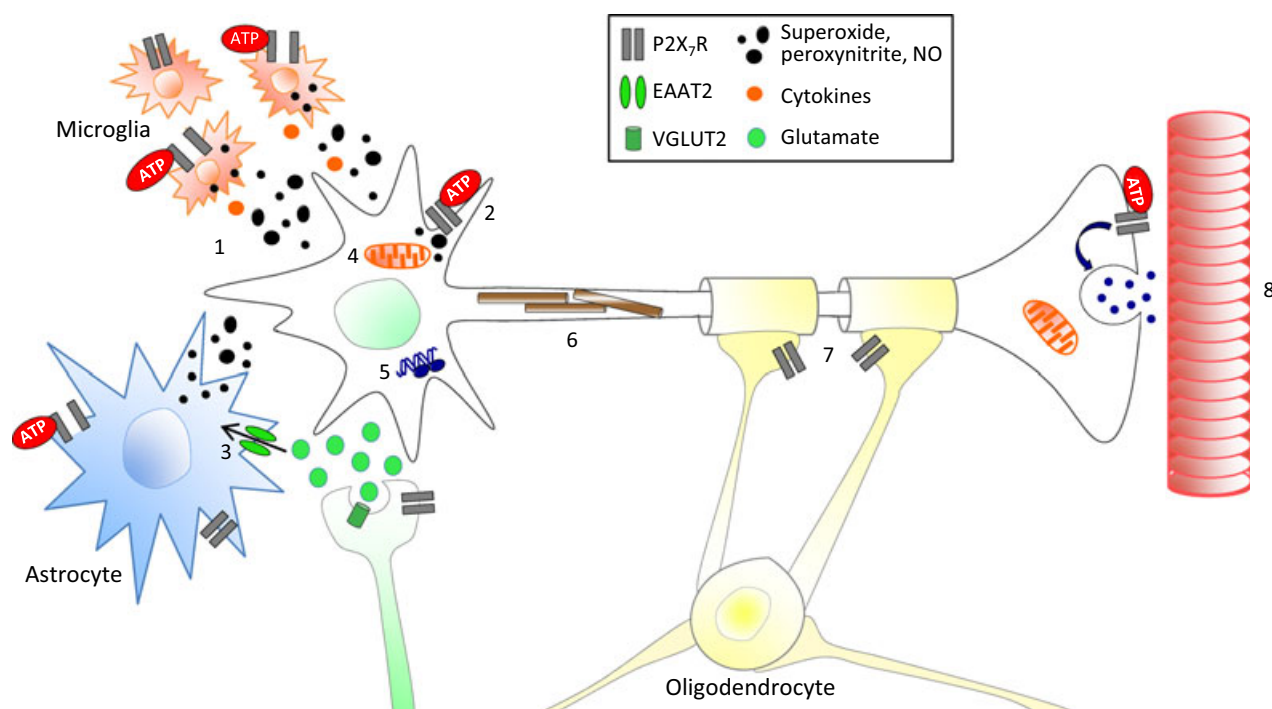
Fig. 1 Via activation of P2X$_7$ receptors at different cellular locations, ATP signaling has the potential to impact both spinal cord motor neuron activity, and survival. A schematic representation of P2X$_7$ receptor locations on motor neurons and their support cells, and potential associations with cell-damaging pathways implicated in amyotrophic lateral sclerosis pathogenesis including the following: (1) Cytokine release and oxidative damage following microglial and astrocyte activation, (2) Oxidative damage following neuronal receptor activation, (3) Glutamate-induced excitotoxicity, (4) Mitochondrial dysfunction and apoptosis, (5) RNA processing abnormalities, (6) Axonal trafficking defects, (7) Oligodendrocyte dysfunction, (8) Muscle atrophy. (Atkinson *et al.* 2004; Gandelman *et al.* 2010, 2013; Kang *et al.* 2013; Moores *et al.* 2005; Vargas and Johnson 2010).

and structural differentiation from other P2 receptors. With respect to this latter point, one characteristic feature of the P2X7 receptor that could be targeted is its long intracellular C-terminus 'tail', as disruption of this region has been shown to impact multiple properties of the receptor, including the capacity for large pore formation, activation of intracellular signaling pathways, and non-exocytotic glutamate release (Cervetto *et al.* 2013). Despite increasing interest in targeting P2X$_7$ receptors, drug development has been relatively slow because of a dearth of small molecule tools. The potential for successful drug development increased substantially, however, following the recent solution of the P2X$_4$ receptor atomic structure, opening the door for molecular modeling approaches. Currently, P2X$_7$ inhibitors are being tested preclinically in animal models of numerous CNS disorders, while antagonists have reached clinical trials for treatment of chronic inflammatory diseases, including rheumatoid arthritis, Crohn's disease, and pain.

In conclusion, in circumstances where neuroinflammation is present, P2X$_7$ receptor activation by ATP can play an early role in the propagation of cytotoxic insults, including oxidative damage cascades. This positioning of the P2X$_7$ receptor early in the ATP signaling pathway, plus its localization to multiple cell types, makes it an attractive target for drug manipulation with the potential to impact multiple CNS and peripheral disorders. The success of drug development efforts for CNS disorders, however, will be critically dependent on the ability to modulate the receptor's cytotoxic actions in specific tissues, while maintaining its normal physiologic activities elsewhere.

Conflict of interest

The author declares no competing financial interests.

References

Atkinson L., Batten T. F., Moores T. S., Varoqui H., Erickson J. D. and Deuchars J. (2004) Differential co-localisation of the P2X7 receptor subunit with vesicular glutamate transporters VGLUT1 and VGLUT2 in rat CNS. *Neuroscience* **123**, 761–768.

Cervetto C., Alloisio S., Frattaroli D., Mazzotta M. C., Milanese M., Gavazzo P., Passalacqua M., Nobile M., Maura G. and Marcoli M. (2013) The P2X7 receptor as a route for non-exocytotic glutamate release: dependence on the carboxyl tail. *J. Neurochem.* **124**, 821–831.

Diaz-Hernandez J. I., Gomez-Villafuertes R., León-Otegui M. *et al.* (2012) In vivo P2X7 inhibition reduces amyloid plaques in Alzheimer's disease through GSK3β and secretases. *Neurobiol. Aging* **33**, 1816–1828.

Díaz-Hernández M., Díez-Zaera M., Sánchez-Nogueiro J., Gómez-Villafuertes R., Canals J. M., Alberch J., Miras-Portugal M. T. and Lucas J. J. (2009) Altered P2X7-receptor level and function in mouse models of Huntington's disease and therapeutic efficacy of antagonist administration. *FASEB J.* **23**, 1893–1906.

Gandelman M., Peluffo H., Beckman J. S., Cassina P. and Barbeito L. (2010) Extracellular ATP and the P2X7 receptor in astrocyte-mediated motor neuron death: implications for amyotrophic lateral sclerosis. *J. Neuroinflammation* **7**, 33–42.

Gandelman M., Levy M., Cassina P., Barbeito L. and Beckman J. S. (2013) P2X7 ATP receptor-induced death of motor neurons by a peroxynitrite/FAS-dependent pathway. *J. Neurochem.* **126**, 382–388.

Kang S. H., Li Y., Fukaya M., Lorenzini I., Cleveland D. W., Ostrow L. W., Rothstein J. W. and Bergles D. E. (2013) Degeneration and impaired regeneration of gray matter oligodendrocytes in amyotrophic lateral sclerosis. *Nat. Neurosci.* **16**, 571–579.

Moores T. S., Hasdemir B., Vega-Riveroll L., Deuchars J. and Parson S. H. (2005) Properties of presynaptic P2X7-like receptors at the neuromuscular junction. *Brain Res.* **1034**, 40–50.

Ni J., Wang P., Zhang J., Chen W. and Gu L. (2013) Silencing of the $P2X_7$ receptor enhances amyloid-β phagocytosis by microglia. *Biochem. Biophys. Res. Commun.* **434**, 363–369.

North R. A. and Jarvis M. F. (2013) P2X Receptors as Drug Targets. *Mol. Pharmacol.* **83**, 759–769.

Vargas M. R. and Johnson J. A. (2010) Astrogliosis in amyotrophic lateral sclerosis: Role and therapeutic potential of astrocytes. *Neurotherapeutics* **7**, 471–481.

Volonté C., Apolloni S., Skaper S. D. and Burnstock G. (2012) P2X7 receptors: channels, pores and more. *CNS Neurol. Disord. Drug Targets* **11**, 705–721.

Weisman G. A., Camden J. M., Peterson T. S., Ajit D., Woods L. T. and Erb L. (2012) P2 receptors for extracellular nucleotides in the central nervous system: role of P2X7 and P2Y receptor interactions in neuroinflammation. *Mol. Neurobiol.* **46**, 96–113.
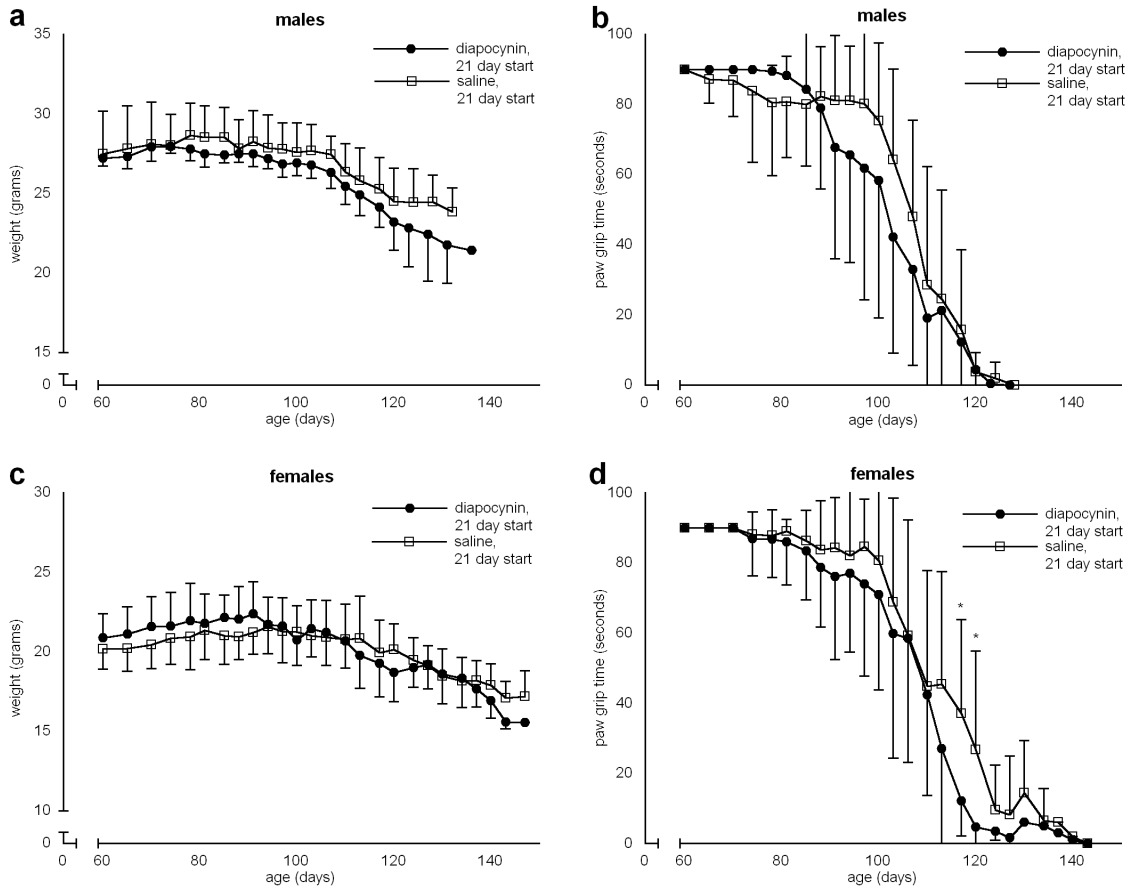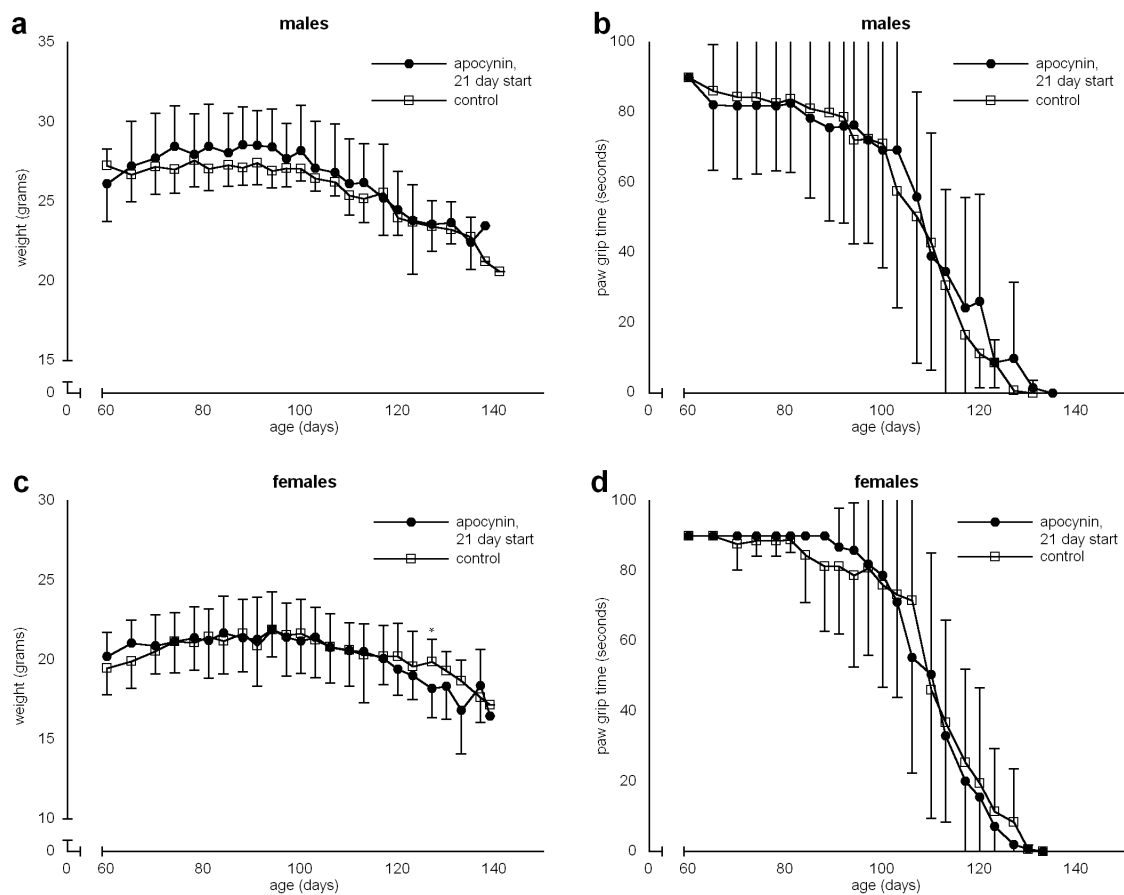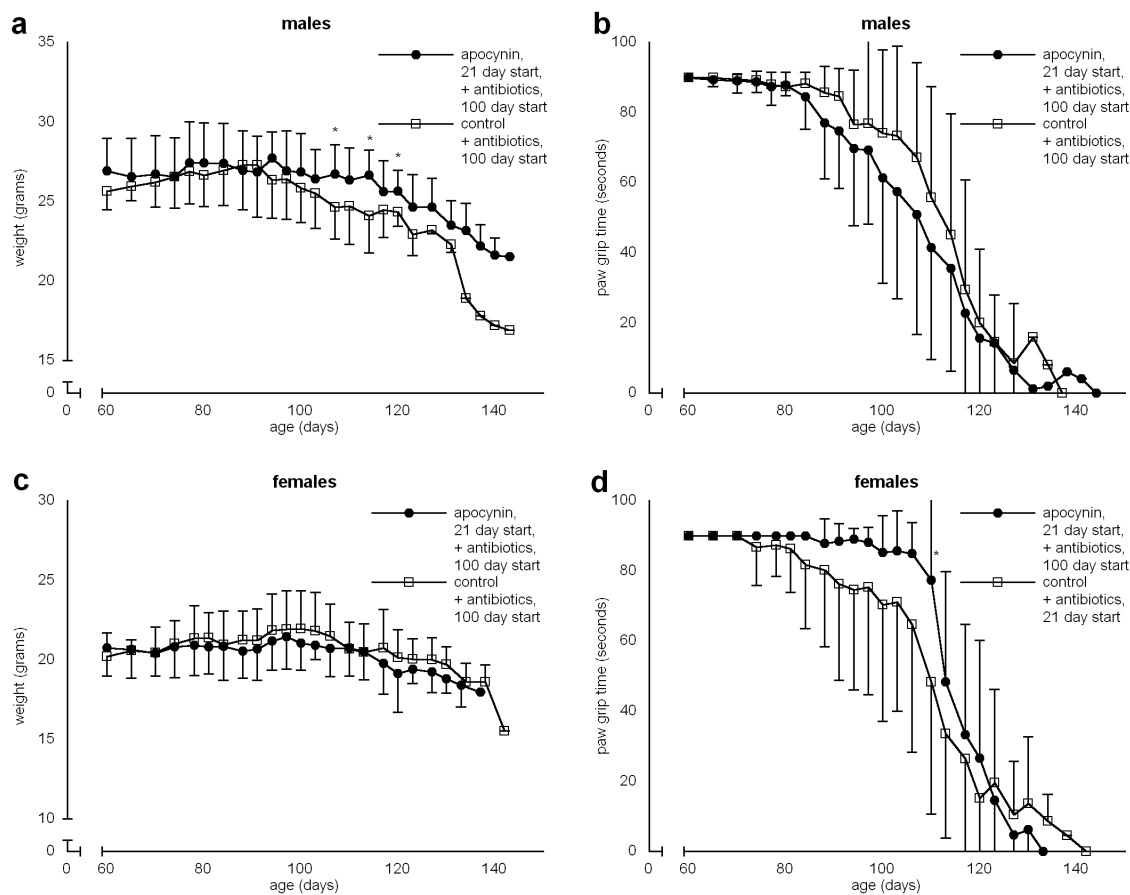
Supplementary Figure 1. Administration of 150 mg/kg/day diapocynin compared to saline control started at 21 days of age in G93A SOD1 ALS mice. a) Body weight loss in male mice (n=12). b) Paw grip endurance in male mice (n=12). c) Body weight loss in female mice (n=12). d) Paw grip endurance in female mice (n=12). Data represent mean ± SD; *statistically significant difference p<0.05.
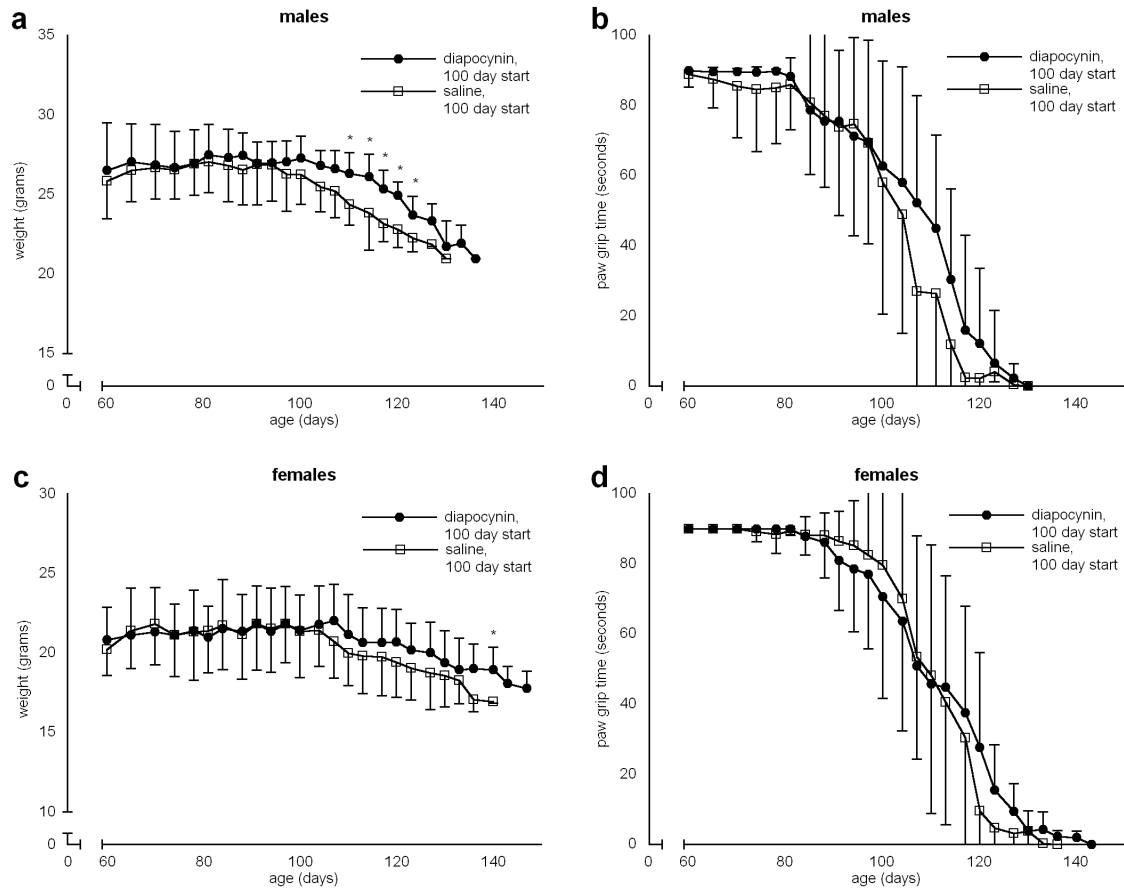
Supplementary Figure 2. Administration of 150 mg/kg/day diapocynin compared to saline control started at 100 days of age in G93A SOD1 ALS mice. a) Body weight loss in male mice (n=12). b) Paw grip endurance in male mice (n=12). c) Body weight loss in female mice (n=12). d) Paw grip endurance in female mice (n=12). Data represent mean ± SD; *statistically significant difference p<0.05.
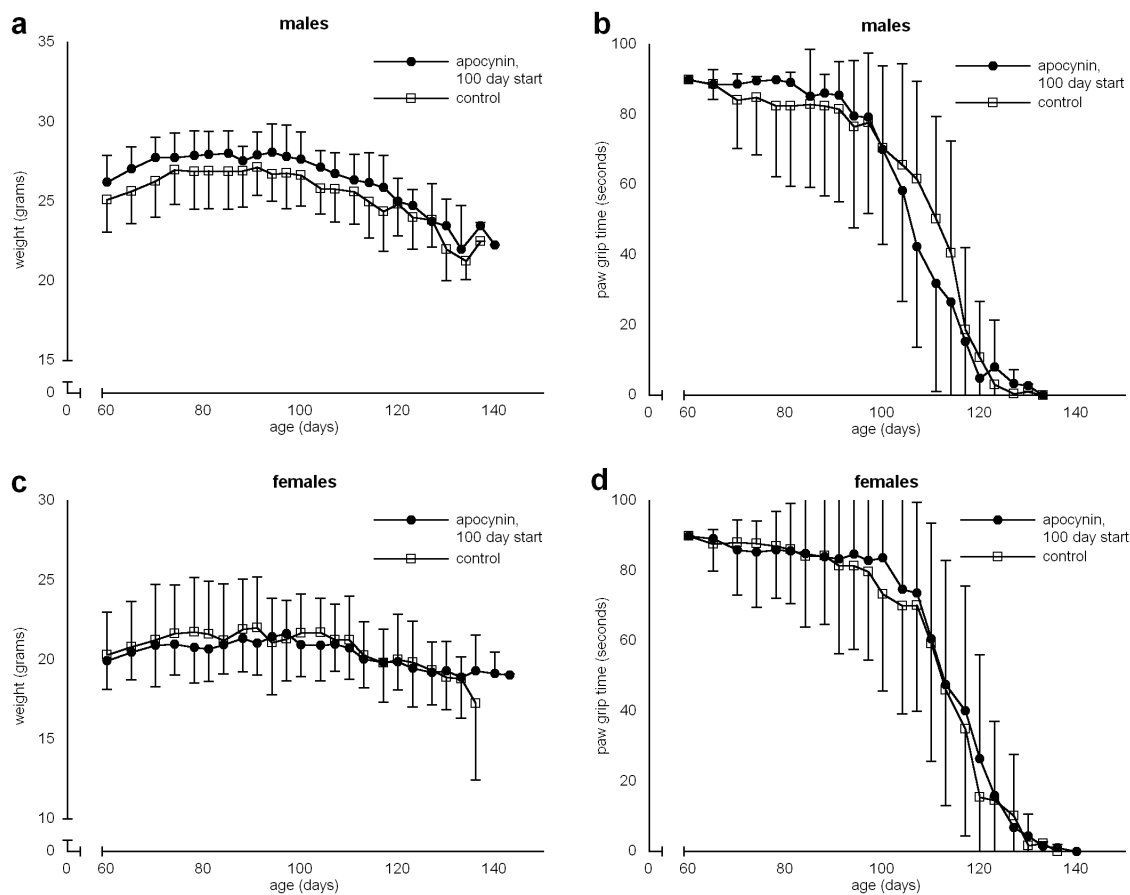
Supplementary Figure 3. Administration of 300 mg/kg/day apocynin compared to control started at 21 days of age in G93A SOD1 ALS mice. a) Body weight loss in male mice (n=12). b) Paw grip endurance in male mice (n=12). c) Body weight loss in female mice (n=12). d) Paw grip endurance in female mice (n=12). Data represent mean ± SD; *statistically significant difference p<0.05.

Supplementary Figure 4. Administration of 300 mg/kg/day apocynin started at 21 days of age plus antibiotics started at 100 days of age compared to control plus antibiotics at 100 days of age in G93A SOD1 ALS mice. a) Body weight loss in male mice (n=12). b) Paw grip endurance in male mice (n=12). c) Body weight loss in female mice (n=12). d) Paw grip endurance in female mice (n=12). Data represent mean ± SD; *statistically significant difference p<0.05.

Supplementary Figure 5. Administration of 300 mg/kg/day apocynin compared to control started at 100 days of age in G93A SOD1 ALS mice. a) Body weight loss in male mice (n=12). b) Paw grip endurance in male mice (n=12). c) Body weight loss in female mice (n=12). d) Paw grip endurance in female mice (n=12). Data represent mean ± SD.